NASA TECHNICAL NOTE

NASA TN D-2685

c. 1

NASA TN D-2685

SEALED-FOAM, CONSTRICTIVE-WRAPPED, EXTERNAL INSULATION SYSTEM FOR LIQUID-HYDROGEN TANKS OF BOOST VEHICLES

by Lewis Research Center Staff

Lewis Research Center
Cleveland, Ohio

NATIONAL AERONAUTICS AND SPACE ADMINISTRATION • WASHINGTON, D. C. • MARCH 1965

NASA TN D-2685

SEALED-FOAM, CONSTRICTIVE-WRAPPED, EXTERNAL INSULATION SYSTEM FOR LIQUID-HYDROGEN TANKS OF BOOST VEHICLES

By Lewis Research Center Staff

Lewis Research Center
Cleveland, Ohio

NATIONAL AERONAUTICS AND SPACE ADMINISTRATION

For sale by the Office of Technical Services, Department of Commerce,
Washington, D.C. 20230 -- Price $5.00

CONTENTS

SUMMARY

Thermal insulation is required for liquid-hydrogen tanks used on high-energy boost vehicles in order to keep boiloff losses to acceptable values. An investigation was conducted to determine a lightweight hydrogen tank insulation system that would provide adequate thermal insulation during ground hold conditions, and would be able to withstand the aerodynamic forces and heating encountered during the launch trajectory. The experimental investigation included tests of impact sensitivity of the insulation components in the presence of liquid oxygen, aerodynamic tests in which the heating and dynamic pressure conditions were more severe than during a typical launch trajectory, and measurements of the effective thermal conductivity of the insulation by means of (1) small samples, (2) heat-transfer measurements on subscale tanks filled with liquid hydrogen, and (3) heat-transfer measurements on a full-scale insulated Centaur tank filled with liquid hydrogen. The insulation system as finally developed consisted of 0.4-inch thick, 2-pound-per-cubic-foot-density polyurethane foam panels hermetically sealed within a covering of a foil laminate of Mylar and aluminum. A thin layer of fiber-glass cloth over the insulation provided protection from aerodynamic erosion during launch. The insulation was bonded to the tank wall using adhesive in a grid pattern, primarily to keep air from cryopumping behind the panels. The principal means of holding the insulation on the tank was a prestressed constrictive wrap of fiber-glass roving. This wrap was completely effective in holding the insulation in place under all aerodynamic test conditions including heating in a jet engine exhaust and a wind tunnel test at Mach numbers up to 2.0.

The results of the investigation indicated that the hazard resulting from impacting insulation panels that may contain liquid oxygen from cryopumped air was negligible, the thermal effectiveness of the insulation was as good as predicted based on evacuated foam tests, and the insulation, which weighed only 0.16 pound per square foot installed, could well withstand the environmental conditions expected during ground hold and launch.

CHAPTER I

INSULATION CONCEPT

by Paul T. Hacker and Jack B. Esgar

Lewis Research Center

There is a need for lightweight, low-thermal-conductivity insulation systems for the liquid-hydrogen tanks of rocket boost vehicles to minimize hydrogen fuel losses from boiloff. This report presents the results of an experimental investigation to develop and evaluate a nonjettisonable foam-type insulation system that approaches the minimum weight feasible for the heat-transfer and aerodynamic conditions encountered during ground hold and launch.

The use of liquid hydrogen as a propellant for either chemical or nuclear rockets for boost-type vehicles and advanced spacecraft is predicated upon its high theoretical performance as compared to other propellants. Liquid hydrogen has a very low boiling temperature, -423° F, and a very low density, which results in a high tank surface area per unit weight of propellant. This combination causes high boiloff losses from uninsulated tanks, as shown in reference 1, however, even small amounts of insulation that will prevent air condensation on the outside of the tank wall will reduce the boiloff rate by more than 90 percent. Hydrogen boiloff is normally vented overboard, but during the early phases of the boost trajectory within the atmosphere and at relatively low velocities it is hazardous to vent the highly combustible hydrogen. With vent valves closed, the insulation must be sufficient to prevent excessive pressure-rise rates within the tank.

Insulation, propellant losses, and increased tank wall thickness to accommodate higher pressures all result in a payload weight penalty that detracts from the theoretically high performance of liquid hydrogen. Thus, in the design of a rocket system for liquid hydrogen, tradeoff of all these factors plus the relative merits of jettisoning the insulation after leaving the atmosphere should be considered in order to minimize the weight penalty. To aid in optimization, it is therefore desirable to utilize an insulation material or system that has low weight and high thermal resistance.

A number of low-density materials with high thermal resistance exist (ref. 2), but experience has indicated that the major practical problem is the application of these insulation materials to tank walls in a manner that will achieve a reliable and predictable system. Insulation attachments, insulation penetrations (fill and vent lines and tank supports), and the techniques used to prevent condensation of air or water vapor in external insulations (or fuel permeation in internal insulations) have a large effect on reducing the overall thermal effectiveness of an insulation system as compared to the basic insulation material. The insulation system must also be capable of withstanding the

thermal environment produced by liquid hydrogen and the effects of launch, ground handling, aerodynamic loads and heating, and acceleration loads.

The published results of investigations of insulation systems for hydrogen tanks of boost vehicles are very limited (refs. 3 to 5). The systems presently in use or under development consist of reinforced polyurethane foam as an internal insulation in Saturn S-IV and S-IVB, as a nonjettisonable external insulation in Saturn S-II, and as a jettisonable external insulation in Centaur. The relative advantages and disadvantages of various types of insulation systems are discussed in the section Insulation Concepts. For any of the insulation types, a barrier is needed to keep the insulation from filling with gases that are condensable at liquid-hydrogen temperature, because the permeation of the insulation with liquid can drastically lower the insulation qualities - often by more than an order of magnitude (refs. 6 and 7). For internal insulation the barrier must be against liquid hydrogen, whereas for external insulation the barrier must be against air and water vapor that can cryopump into the insulation and condense. For external insulation systems the barrier need not be a physical seal but may be a helium-gas purge of the space between the insulation and the cold tank walls.

In the hydrogen tank insulation systems in use or under development in the Saturn and Centaur vehicles previously mentioned, hydrogen or helium gradually permeates the foam during ground hold conditions. Furthermore, in all of these systems the thermal conductivity of the insulation is variable with exposure time. Although the thermal conductivity of gas-filled foam is considerably lower than that for liquid-filled foam, it is desirable to avoid either condition. Only with a hermetically sealed system is it possible to obtain thermal conductivity for a complete insulation system that is consistent and is as low as the basic foam used in the system.

The present investigation was conducted to evaluate a system having some advantages relative to each of the previously mentioned systems. This new insulation system consists of low-density polyurethane foam that is covered and hermetically sealed with a thin-film laminate of Mylar and aluminum foil (called MAM in this report) to provide a positive barrier against gases or liquids that might lower thermal conductivity. The system utilizes an attachment method in which the insulation panels are bound to the tank with a prestressed wrap of fiber-glass roving and which therefore does not depend on adhesive bonds or the cohesive or shear strength of the insulation. The result is a very lightweight insulation system consistent with insulation effectiveness and durability. This insulation system utilizes many concepts developed in a previous NASA Lewis Research Center investigation of hermetically sealed foam insulation (ref. 8). Some preliminary results of the present investigation are presented in reference 5. The development of this insulation system is presented in the nine chapters of this report.

REVIEW OF BOOST-VEHICLE INSULATION SYSTEMS

Insulation Materials

Many types of insulating materials have been considered for the hydrogen

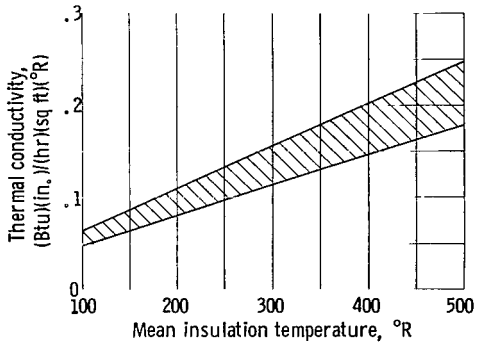

Figure I-1. - Thermal conductivity range of polyurethane foam as function of mean insulation temperature (ref. 2).

tanks of boost vehicles. Polyurethane and polystyrene foams have received the most serious consideration as insulation materials, with most emphasis on low-density polyurethane foam blown with either Freon or carbon dioxide. The thermal-conductivity range of polyurethane foams as a function of foam mean temperature (average for hot and cold surfaces) is shown in figure I-1. The lower portion of the range shown is generally obtained with low-density foams. With a density of about 2 pounds per cubic foot, foams have low thermal conductivity and sufficient structural strength for use in many systems. If additional strength is required, and additional weight can be tolerated, a polyurethane-foam-filled plastic or fiber-glass honeycomb can be used.

Corkboard is also a good insulator. It is less subject to internal air condensation from cryopumping than the foams are, and it can better withstand the effects of aerodynamic heating than foam insulations (ref. 6). Its primary disadvantage is that it is much heavier than foam-type insulation systems for the same thermal effectiveness (ref. 8). It may find use, however, for some vehicles - probably in combination with foam insulation.

Balsa wood has been considered as an insulator. It is less fragile than foams, but it is not as easily fabricated into large panels or into complex shapes, so that it has generally been discarded in favor of foams.

Evacuated powders provide excellent thermal protection, but their use in relatively thin insulation panels for boost vehicle tanks is fraught with complications resulting from the need for vacuum jackets, settling problems, and fragility.

Multiple reflective foils are excellent insulations if they are vacuum jacketed (refs. 9 to 11). This type of insulation system generally has not received serious consideration for boost vehicles up to the present time because it must maintain an internal vacuum to be effective, and it is so fragile that it may suffer damage during ground handling or from aerodynamic forces during launch. Because of its high effectiveness as an insulation, however, it is receiving serious consideration for long-time storage of cryogenic propellants in space vehicles (ref. 11).

Although it is not possible to obtain universal agreement on the best insulating material for thermal protection of hydrogen tanks during ground hold and the aerodynamic phase of the ascent trajectory, most of the advantages appear to lie with the foams. Foams were therefore selected as the basic insulation materials for this investigation.

Insulation Concepts

Internal foam insulation. - Figure I-2(a) illustrates a foam insulation

system placed on the inside of the tank wall. This general type of system is presently utilized on the Saturn S-IV and S-IVB stages. With internal insulation it is necessary to provide a seal to keep the liquid hydrogen out of the insulation. Substantial leaks that allow liquid to permeate the foam can degrade the insulating effectiveness by an order of magnitude. Even very small leaks are undesirable. If there were a leak, the hydrogen would vaporize, and the thermal conductivity of the insulation would approximate that of hydrogen gas, which is about 0.65 (Btu)(in.)/(hr)(sq ft)(^{o}R). The average value for low-density polyurethane foam is 0.11 (Btu)(in.)/(hr)(sq ft)(^{o}R) at a mean temperature of 250^{o} R, which is typical of that encountered for hydrogen tank insulation.

In addition to the need for a good seal against hydrogen, the insulation is required to withstand the compressive load imposed on it by tank pressurization, which in some cases may require the use of foam of higher density than would be desirable from weight and thermal conductivity considerations. There are also attachment problems that are made difficult by the low-temperature environment, the differential thermal contraction between the tank wall and the insulation, and the loads from slosh and acceleration.

If it is assumed that the previous problems can be solved, the primary advantages of internal insulation are (1) the tank wall affords protection for the insulation from aerodynamic forces; (2) internal insulation is less likely to be damaged during vehicle handling than external insulation; and (3) tank supports do not penetrate the insulation to produce heat shorts. The primary disadvantages to this type of insulation are (1) for some launch trajectories the tank wall may be heated and weakened excessively by aerodynamic friction heating; and (2) the insulation cannot be jettisoned after the boost vehicle leaves the atmosphere. Because the insulation cannot be jettisoned, the entire weight of the insulation is chargeable against payload. In addition, heat absorbed in the insulation from aerodynamic heating cannot be jettisoned. Therefore some of it is eventually transferred to the hydrogen, and added boiloff results (ch. II).

Externally purged foam insulation. - Figure I-2(b) illustrates an external insulation system in which a noncondensable purge gas (helium) is used to provide a barrier to stop condensable gases from cryopumping into and behind the insulation. Condensation of gases on the tank wall is undesirable since it greatly increases the heat transfer. The helium purge also gives assurance that liquid will not form or freeze in the insulation or between the tank wall and the insulation. A jettisonable system of this type is presently utilized on Centaur, and a nonjettisonable system is being considered for Saturn S-II.

The primary advantages of the purged external insulation system are (1) extreme care is not required to ensure against leaks occurring in the insulation system; (2) if the system is made jettisonable, only a small portion of its total weight is chargeable against payload; and (3) external insulation maintains low temperatures in the tank wall that result in higher strength. The primary disadvantage to this type of system is that the helium purge gas generally permeates the insulation and gives it a thermal conductivity that may

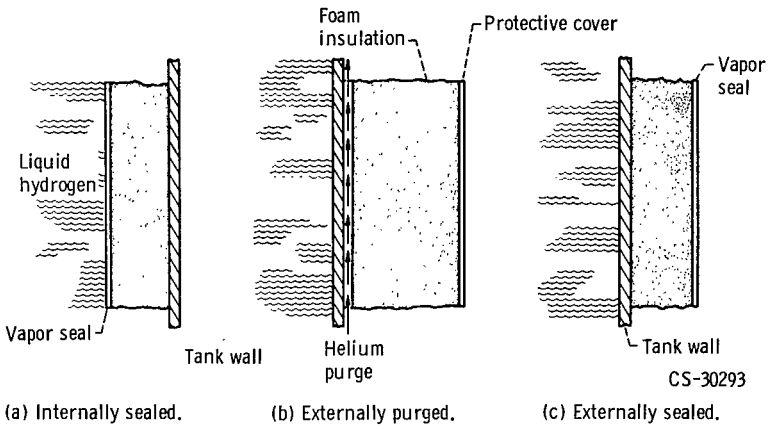

Figure I-2. - Basic types of foam insulation systems for liquid hydrogen tanks.

be as much as six times as high as that obtainable with foams not containing helium. A hermetic seal to keep the helium out of the foam insulation would therefore be beneficial. To obtain the same insulating effectiveness without the hermetic seal, helium-filled foam has to be thicker; consequently, weight is added to the system. A second disadvantage of this system is that purging adds complications at launch because of the requirement of supplying helium during ground hold, disconnecting it at launch, and providing adequate venting of the purge channels during the launch trajectory.

Externally sealed foam insulation. - As mentioned previously, there is a definite advantage to having a positive seal around the foam insulation to ensure that the basic conductivity of the foam will not be degraded by gas or liquid cryopumping into the foam. With an adequate seal, trapped gases within the foam are cryopumped to the cold boundary of the foam and cause the foam to be evacuated. Figure I-2(c) illustrates schematically the sealed foam concept. This is the insulation concept that has been developed at the NASA Lewis Research Center and is described in this report.

Sealed external insulation can be attached to the tank by bonding or by use of an external constrictive wrap of a lightweight, high-strength material. The constrictive wrap appears to be better than bonding for withstanding aerodynamic forces encountered during the launch trajectory because it holds the insulation in compression and thus makes it less subject to flutter or failure resulting from low cohesive or shear strength in the foam. The primary advantages of the sealed external insulation are (1) it is a self-contained, lightweight system that can be used with minimum complication; (2) it provides a predictable and the lowest possible thermal conductivity for an external foam-type insulation system; and (3) elimination of the need for jettisoning the insulation by making it very lightweight improves system reliability since at least one critical sequence in the launch operation is eliminated. The disadvantages of the system are (1) minimum-weight insulation is fragile and requires reasonable care during ground handling; and (2) in many cases even lightweight nonjettisonable insulation results in a greater payload weight penalty than a heavier jettisonable insulation.

CONSTRICTIVE-WRAP SEALED FOAM INSULATION SYSTEM

Evaluation and consideration of all of the types of insulation systems led to the conclusion that sealed foam attached to the tank by a constrictive wrap

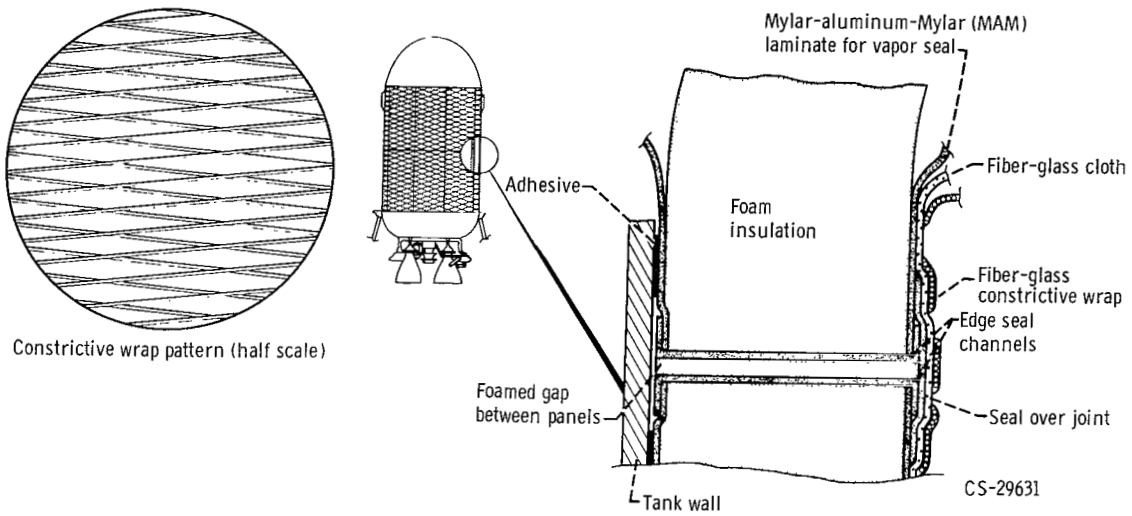

Figure I-3. - Lightweight externally sealed insulation system.

is a very promising type of insulation system. This system was therefore investigated, and the results are presented in this report. This insulation system, as illustrated schematically in figure I-3, consists of low-density and low-conductivity foam hermatically sealed by an impermeable foil laminate. The sealed foam is fabricated into panels that are bonded to the liquid hydrogen tank. A layer of fiber-glass cloth is placed over the outside of the panels to protect the foam from aerodynamic heating and erosion during launch. The protective cloth and panels are then held more securely to the tank by a constrictive overwrap of fiber-glass roving applied by a filament winding machine. Sufficient initial tension (prestress) is put into the roving during the winding process to maintain a compressive load on the insulation under all conditions anticipated during ground hold and launch. Compression of the insulation tightly against the tank walls should prevent flutter during launch. This insulation system is described in this section. Details of the insulation of a full-scale model Centaur tank are presented in chapter VII of this report.

Foam Insulation

Freon blown, rigid polyurethane foam with a density of 2 pounds per cubic foot was used as the primary insulation material. This foam has a closed cell structure, but is is not completely impermeable to gases that can slowly cryopump into the cells under cryogenic temperatures. Its main feature is low thermal conductivity, particularly at the cold mean temperatures encountered by insulation on liquid hydrogen tanks (fig. I-1). Based on information that was available at the initiation of this investigation, it appeared that a foam insulation thickness of 0.4 inch would result in approximately the same heat leak during ground hold that was being experienced on a heavier jettisonable insulation under development for the Centaur vehicle. The 0.4-inch-thick foam panels used for this system would be expected to show a thermal conductivity in the range 0.10 to 0.13 (Btu)(in.)/(hr)(sq ft)($^{\circ}$R) under ambient ground-hold conditions, which would give a mean temperature of about 250° R (fig. I-1).

Protection of the foam from erosion by the high-temperature windstream is required during launch. This protection is discussed in the section Surface Protection During Launch.

Sealing Material

The surfaces of the polyurethane foam are hermetically sealed by a thin film only 0.0015-inch thick. The film consists of a laminate of aluminum foil (0.0005 in.) with Mylar plastic film (0.0005 in.) on each side of the foil. The aluminum foil, having no measurable permeability, acts as the principal vapor barrier. The tough Mylar films supply strength to the laminate and prevent damage to the foil during fabrication and installation of the panels on the tank. This laminate is bonded to both surfaces of the foam with a thin coat of polyester adhesive. The bonded laminate adds considerable rigidity to the foam slabs and allows the foam panels to be formed into moderate contours without heat forming of the foam. The edges of the panel are covered with channels of Mylar and sealed with polyester adhesive. The laminate is also used in tape form to seal the space between panels (fig. I-3).

Attachment of Insulation to Tank

The insulation panels are bonded to the tank walls. This bond prevents air from cryopumping into any space that could exist between the panels and the tank walls and also holds the panels in place while the constrictive wrap of fiber-glass roving is wound around the tank. The wrap is applied with sufficient tension to provide a compressive load on the insulation panels under all conditions of ground hold and launch. The wrapping pattern is shown in figure I-3. The number of windings per linear inch was chosen to produce an initial compressive load in the insulation of 2 pounds per square inch. This compressive load was selected in a somewhat arbitrary manner so that reasonable assurance was obtained that the insulation would not flutter or come off because of aerodynamic forces during launch. Experience may show that a compressive load smaller than 2 pounds per square inch is adequate. The pretensioning strain (0.84 percent) was sufficient to accommodate the shrinkage of stainless-steel walls as they were cooled to liquid-hydrogen temperature, allow for fiber-glass expansion during aerodynamic heating, and allow for any deformation of the foam by compression and aerodynamic heating. The pretensioning is discussed further in chapters VII and VIII.

A possible disadvantage of the constrictive wrap is that the resulting compressive load acts as a collapsing force on the tank. There is steadily growing evidence, however, that cylinder buckling is not likely to occur from a constrictive load, particularly if the constrictive wrap is bonded to the tank. Unpublished results of tests conducted at the Lewis Research Center on a constrictive wrap applied to small thin-walled cylinders of steel have shown that buckling will not occur until the compressive stress in the steel is far in excess of the yield stress. In fact, usually it must be in excess of the tensile ultimate stress before the cylinder will buckle. In addition, the insulation panels themselves add rigidity to thin-walled tanks. It is likely, therefore,

that tanks with constrictive-wrap insulation are less likely to buckle than uninsulated tanks.

Surface Protection During Launch

Protection of the foam from aerodynamic heating and erosion could be supplied by the fiber-glass wrap if the entire area were covered. However, the amount of fiber glass used at 0.84-percent strain to produce the 2-pound-per-square-inch compressive load on the insulation produces a wrap pattern that is too open (about 1/4-in.-wide diamond pattern shown in fig. I-3) to provide adequate protection. The wrap was therefore supplemented by a fine-weave fiber-glass cloth placed under the wrap and over the outer Mylar aluminum sealing laminate, as illustrated in figure I-3. Style 106 fiber-glass cloth having a 0.003-inch thickness was used with an impregnation of Dow Corning Silicone A-4000 adhesive.

CONCLUDING REMARKS

The low thermal conductivities of lightweight foams such as polyurethane make them practical for insulation of the hydrogen tanks of boost vehicles. Their unreinforced strength is probably too low to withstand the aerodynamic forces and temperatures encountered during launch for external insulation. Therefore, the foams have to be reinforced or held in place by an external constrictive wrap. In order to capitalize on the low conductivity of the foam fully, it is necessary to seal out positively all gases that could cryopump or leak into the foam while the tank is filled with hydrogen. An insulation system has been developed that has a positive hermetic seal to ensure minimum thermal conductivity, and it achieves minimum weight because the insulation is held in place by a lightweight constrictive wrap rather than by reinforement. The details of the fabrication and testing of this insulation are presented in the remaining chapters of this report.

REFERENCES

1. Schaechter, Wolfgang: Heat Transfer to Uninsulated Missile Tanks Containing Liquid Hydrogen. Paper 753A, SAE, 1963.

2. Moeller, Calvin E., Loser, John B., Snyder, Warren E., and Hopkins, Vern: Thermophysical Properties of Thermal Insulating Materials. ASD-TDR-62-215, Midwest Res. Inst., July 1962.

3. McGrew, Jay L.: A Comparative Study of Airborne Liquid Hydrogen Tank Insulation. Advances in Cryogenic Eng., K. D. Timmerhaus, ed., Vol. 8, Plenum Press, Inc., 1963, pp. 387-392.

4. Miller, R. N., Bailey, C. D., Beall, R. T., and Freeman, S. M.: Foams and Plastic Films for Insulation Systems. Advances in Cryogenic Eng., K. D. Timmerhaus, ed., Vol. 8, Plenum Press, Inc., 1963, pp. 417-424.

5. Perkins, Porter J., Jr., and Esgar, Jack B.: A Lightweight Insulation System for Liquid Hydrogen Tanks of Boost Vehicles. AIAA Fifth Annual Structures and Materials Conf., Palm Springs (Calif.), Apr. 1-3, 1964, Pub. CP-8, AIAA, 1964, pp. 361-371.

6. Gray, Vernon H., Gelder, Thomas F., Cochran, Reeves P., and Goodykoontz, J. H.: Bonded and Sealed External Insulations for Liquid-Hydrogen-Fueled Rocket Tanks During Atmospheric Flight. NASA TN D-476, 1960.

7. Weiss, S., and Goodman, I. A.: Effect of Condensation on Conventionally Insulated Cryogenic Tanks. Advances in Cryogenic Eng., Vol. 5, K. D. Timmerhaus, ed., Plenum Press, Inc., 1960, pp. 157-161.

8. Perkins, Porter J. Jr.: Experimental Study Under Ground-Hold Conditions of Several Insulation Systems for Liquid-Hydrogen Fuel Tanks of Launch Vehicles. NASA TN D-2679, 1964.

9. Black, I. A., and Glaser, P. E.: Progress Report on Development of High-Efficiency Insulation. Advances in Cryogenic Eng., Vol. 6, K. D. Timmerhaus, ed., Plenum Press, Inc., 1961, pp. 32-41.

10. Perkins, Porter J., Colaluca, M. A., and Smith, L. S.: Preliminary Test Results on a Compressed Multi-Layer Insulation System for a Liquid-Hydrogen Fueled Rocket. Advances in Cryogenic Eng., Vol. 9, K. D. Timmerhaus, ed., Plenum Press, Inc., 1964, pp. 38-45.

11. Knoll, Richard H., and Oglebay, Jon C.: Lightweight Thermal Protection Systems for Space Vehicle Propellant Tanks. Paper 746C, SAE, 1963.

CHAPTER II

THERMAL CONDITIONS DURING TYPICAL BOOST TRAJECTORY

by William H. Roudebush

Lewis Research Center

In order to conduct a meaningful experimental investigation of the sealed wrapped insulation concept described in chapter I, it was necessary to know approximately the temperature and dynamic head that the insulation might encounter. For this purpose, a typical Atlas-Centaur trajectory was chosen, and a detailed aerodynamic heating calculation was carried out with the program described in reference 1. The calculated insulation temperatures provided a guide in the design of experiments on aerodynamic heating effects described in chapters V and VI. In addition, the calculated heating rates were used for making a gross comparison of the thermal performance of the sealed wrapped insulation with an insulation designed to be jettisoned.

ANALYSIS

A typical Atlas-Centaur trajectory was selected for the calculation. Figure II-1 shows the variation with time of the velocity, Mach number, altitude and dynamic pressure from launch to 675 seconds, at which time the Centaur is finished firing. From the altitude and velocity variations, it is possible to carry out a numerical computation of the temperatures throughout the insulation at each time and to determine the heat flow into the insulation and into the propellant.

In reference 1, the standard transient heat conduction equation is applied to the insulation. At the outer surface, heat is assumed to enter by convection from the hot boundary layer. The convective heat-transfer coefficient is obtained by means of the reference enthalpy method described in reference 2. Radiation of heat away from the outer surface and radiation to the outer surface from the Sun are also included. A set of algebraic equations is used to approximate the differential equations so that a numerical solution can be found.

The actual calculations are very extensive, and a computer program must be used. The program presented in reference 1 was used for the results of this chapter. The equations used in the program and the underlying assumptions are described in detail and the Fortran listing is given in that reference.

In applying the program to the present problem, the following assumptions were made:

(1) The heat flow is assumed to occur only in a direction normal to the tank wall.

(2) The heat radiated to the surface from the Sun is constant and equals 100 Btu per square foot per hour.

(3) The emissivity of the outer surface of the insulation is 0.8.

Two insulations were examined, a jettisonable insulation and the sealed wrapped insulation described in chapter I. The sealed wrapped insulation is a

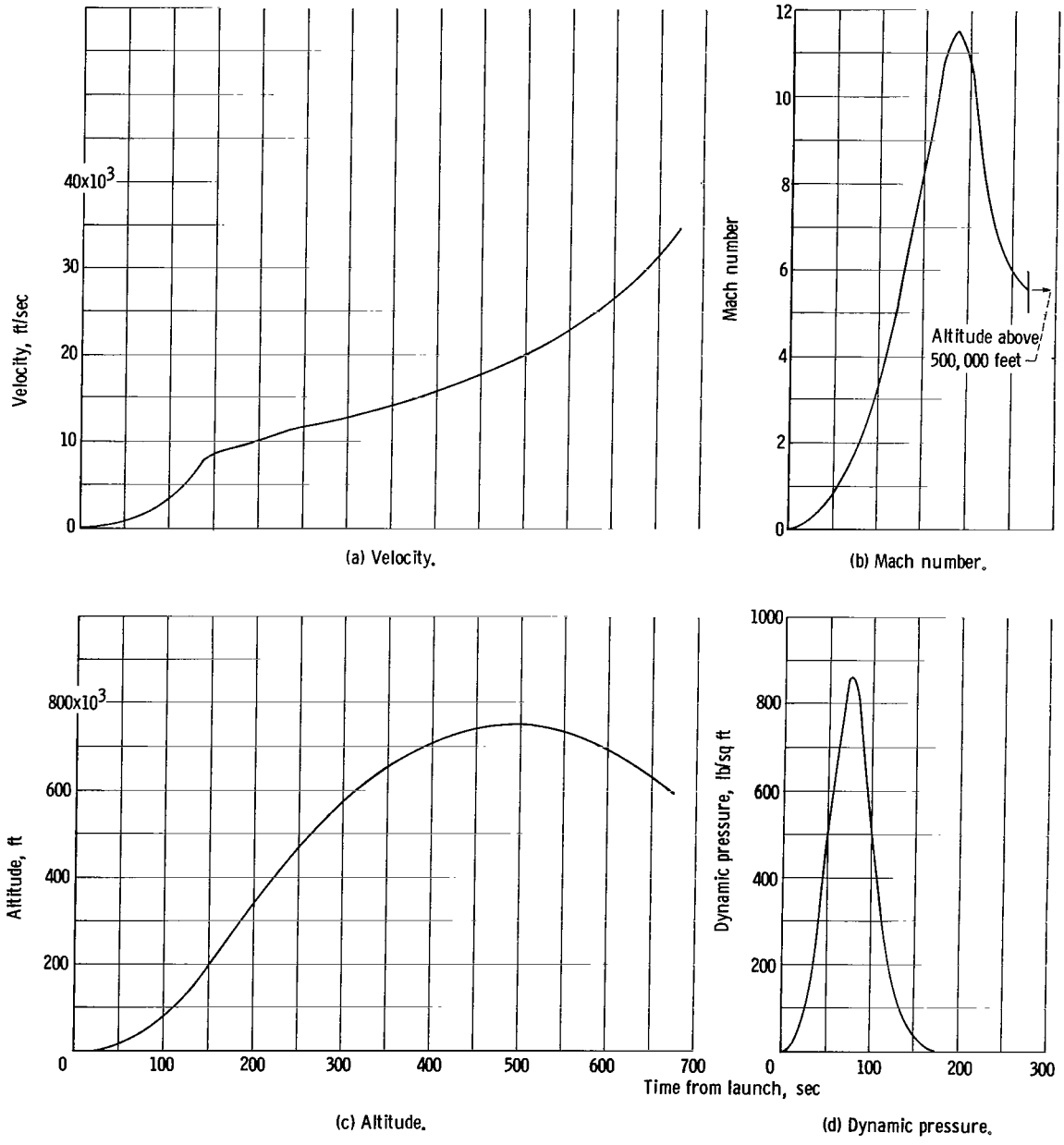

(a) Velocity.

(b) Mach number.

(c) Altitude.

(d) Dynamic pressure.

Figure II-1. - Typical Atlas-Centaur trajectory.

0.4-inch-thick foam panel covered with a laminate of aluminum and Mylar with a 0.0005-inch layer of Mylar on each side of a 0.0005-inch layer of aluminum. The laminate was assumed to have a density of 115 pounds per cubic foot, a specific heat of 0.25 Btu per pound per $^{\circ}R$, and a thermal conductivity of 1.548 Btu per square foot per hour per $^{\circ}R$ per inch. The foam core was assumed to have a density of 2 pounds per cubic foot, a specific heat of 0.4 Btu per pound per $^{\circ}R$, and a thermal conductivity varying with temperature according to the upper boundary of the region shown in figure I-1 (p. 3).

TABLE II-I. - SPECIFIC HEAT AND THERMAL CONDUCTIVITY OF FOAM CORE

Temperature, $^{\circ}R$	Specific heat, c_p, Btu/(lb)($^{\circ}R$)	Thermal conductivity, k, (Btu)(in.)/(sq ft)(hr)($^{\circ}R$)
40	0.283	0.037
160	-----	.147
180	-----	.162
220	.295	-----
360	.303	-----
500	.312	-----
760	-----	.503
1500	.378	-----

TABLE II-II. - SPECIFIC HEAT AND THERMAL CONDUCTIVITY OF FIBER-GLASS LAMINATE

Temperature, $^{\circ}R$	Specific heat, c_p, Btu/(lb)($^{\circ}R$)	Thermal conductivity, k, (Btu)(in.)/(sq ft)(hr)($^{\circ}R$)
400	0.2220	1.615
500	.2340	1.701
600	.2460	1.788
700	.2580	1.860
800	.2700	1.945
900	.2820	2.029
1000	.2940	2.122

The jettisonable insulation was taken to be a 1.0-inch-thick foam-filled honeycomb structure with faces of 0.015-inch fiber-glass laminate. The foam core was assumed to have a density of 4.2 pounds per cubic foot and specific heat and thermal conductivities as given in table II-I. The fiber-glass laminate was assumed to have a density of 120 pounds per cubic foot and specific heat and thermal conductivity as listed in table II-II. The tank wall was assumed to remain at liquid-hydrogen temperature so that no tank wall properties are required. The jettisonable insulation was assumed to be separated from the tank wall by a 0.1-inch helium-filled gap. A heat-transfer coefficient of 2.56 Btu per hour per square foot per $^{\circ}R$ was used for the heat flow across the helium gap. At 173 seconds, the insulation was assumed to be jettisoned.

In making calculations for both insulations, an initial wetted area of 485 square feet was used. A characteristic length of 10 feet was used in determining the Reynolds number for the aerodynamic heat-transfer coefficient.

RESULTS

Heating Rates

Figure II-2 shows heating rate incident on the outer surface of the sealed wrapped insulation due to aerodynamic heating plus an averaged radiant heat

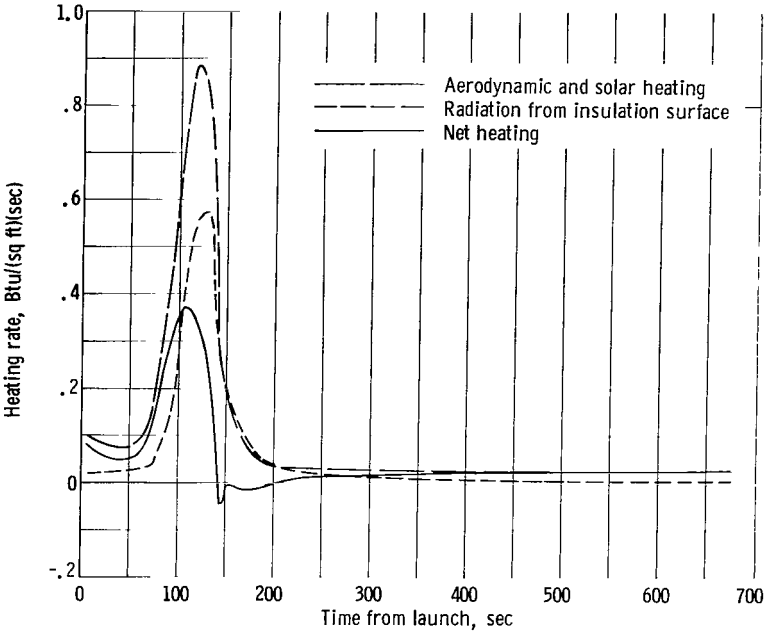

Figure II-2. - Aerodynamic and solar heating, radiant heat from insulation, and net heating rate.

from the Sun. Also shown is the heat radiated away from the surface of the insulation and the net heat (i.e., the difference of the two) that actually enters the insulation. It can be seen from figure II-2 that the aerodynamic heating rate peaks at about 120 seconds. The rate of heat radiation away from the insulation surface peaks slightly later.

Not all of the heat that actually enters the insulation gets through to the liquid hydrogen on the inside. Figure II-3 shows how the rate of heat entering the insulation compares with the rate of heat entering the propellant for the sealed wrapped insulation described in chapter I. Because of thermal lag, the heat flow rate to the propellant peaks somewhat later.

The total heat input to the hydrogen can be obtained by integrating the dashed curve in figure II-3 and multiplying by the average wetted area. When this is done, the total heat input from 0 to 675 seconds is about 13,300 Btu.

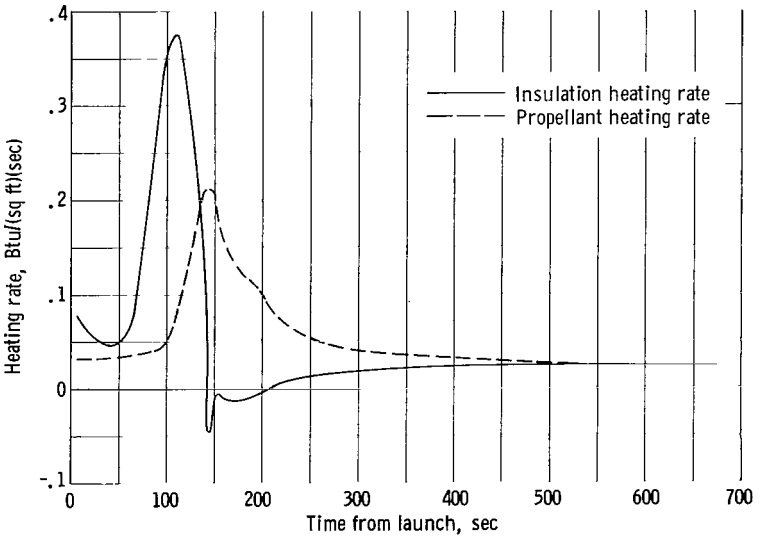

Figure II-3. - Heating rate to insulation and to propellant.

Temperature and Dynamic Head

In addition to the heating rate, the temperature of the insulation is significant because of the effect of temperature on the physical properties of the insulating material. Figure II-4 shows the variation of the temperature of the outer surface of the insulation during the first 675 seconds of flight. The curve peaks at 127 seconds and reaches a maximum value of slightly over 1100° R. The temperature is above 800° R for approximately 65 seconds.

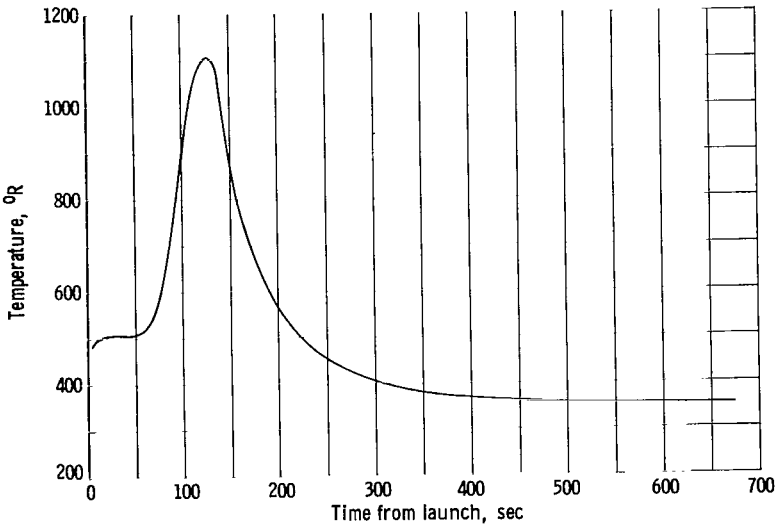

Figure II-4. - Surface temperature.

Dynamic pressure $(1/2)\rho V^2$ (where ρ is the local density and V is the freestream velocity), as well as temperature, is important in its effect on the durability of the insulation. These two variables taken from figures II-1(d) and II-4 are plotted against each other in figure II-5. The maximum values of temperature and dynamic pressure are substantially separated in time. The maximum dynamic pressure (860 lb/sq ft) occurs while the temperature is quite low, about 600° R. Fortunately, by the time maximum temperature is reached, the dynamic pressure is only about 17 percent of its maximum value.

Propellant Heating

A comparison of propellant heating rates for the two types of insulation systems is shown in figure II-6. The jettisonable insulation transmits very little heat to the propellant during the time it is in position. After jettison, the heat flow rate rises sharply as the bare tank wall is exposed but quickly diminishes in the increasingly rare atmosphere.

The total heat input, obtained from integration of the heating rate curve (fig. II-6), is significantly lower for the jettisonable insulation. This is shown in table II-III. The maximum boiloff that could occur with these heat inputs is about 33 pounds for the jettisonable insulation and 69 pounds for the sealed wrapped insulation.

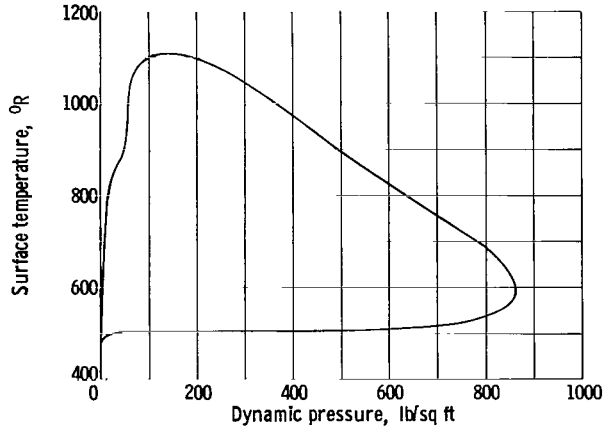

Figure II-5. - Surface temperature as function of dynamic pressure.

TABLE II-III. - HEAT INPUT

Time, sec	Insulation	
	Jettisonable	Sealed wrapped
	Heat input, Btu	
0 to 173	2198	7213
173 to 675	4265	6095
Total	6463	13,308

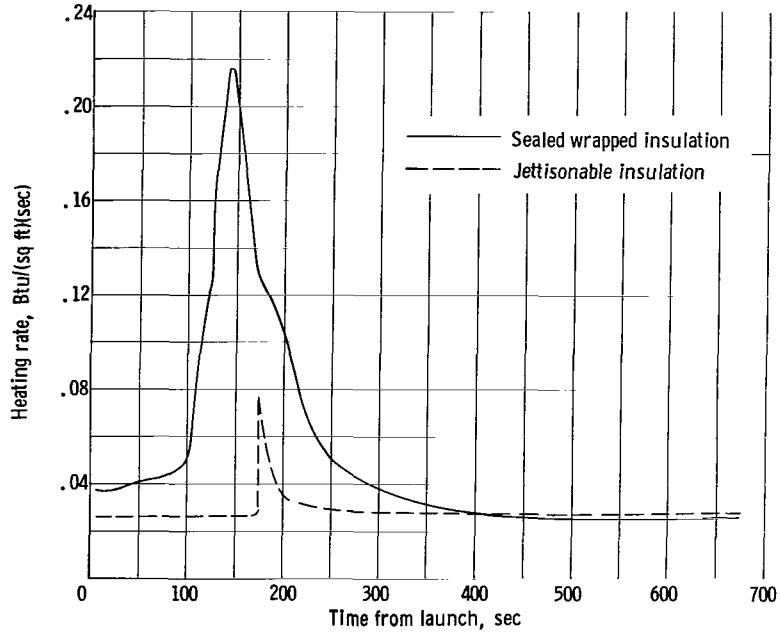

Figure II-6. - Propellant heating rates.

The comparison of the insulations in terms of the effect on payload is complicated. The heat input and consequent loss of fuel by vaporization is only a part of the effect the insulation has on payload. The difference involved in carrying the sealed wrapped insulation throughout the mission and jettisoning the other insulation early in the mission must also be analyzed. The analysis depends on the entire mission. A payload loss comparison is made in chapter IX for the two types of insulation.

SUMMARY OF RESULTS

The results of an analysis of thermal conditions during a typical boost trajectory can be briefly summarized as follows:

1. The maximum temperature to which the sealed wrapped insulation will be subjected is about 1100° R. It must sustain a temperature above 800° R for more than 1 minute.

2. The maximum dynamic pressure is 860 pounds per square foot. This value occurs when the surface temperature of the insulation has risen to about 600° R.

3. The sealed, wrapped, nonjettisonable insulation allows more than twice the amount of heat to get into the hydrogen during the first 675 seconds of flight than does the jettisonable insulation system. The maximum possible boil-off is about 69 pounds for the sealed, wrapped insulation and about 33 pounds for the jettisonable insulation.

REFERENCES

1. O'Neill, R. F., and Rozendaal, C. D.: The Variable-Boundary Transient Heat Conduction Program. Rep. AE62-0401, General Dynamics/Astronautics, May 1962.

2. Eckert, E. R. G.: Engineering Relations for Heat Transfer and Friction in High-Velocity Laminar and Turbulent Boundary-Layer Flow Over Surfaces with Constant Pressure and Temperature. Trans. ASME, vol. 78, no. 6, Aug. 1956, pp. 1273-1283.

CHAPTER III

THERMAL CONDUCTIVITY TESTS OF INSULATION SYSTEM

by Laurence J. Heidelberg

Lewis Research Center

The overall thermal performance of the insulation system depends upon the thermal conductivity of the basic foam and of the materials composing the joints between the panels and on the thermal contact resistance between the inside surfaces of the insulation panel and the tank wall. Thus, to determine the best design configuration, overall thermal conductivity measurements of several insulation test samples were made in a flat-plate thermal-conductivity apparatus. The test samples were designed to evaluate the effect on overall conductivity of (1) evacuation of the foam by either cryopumping or mechanical pumping, (2) various materials used as panel edge seals, (3) a typical panel joint, and (4) a lightweight low-conductivity, open-weave fiber-glass cloth used as a separator between the insulation panel and the tank wall to increase the thermal contact resistance.

Inasmuch as the insulation system is to be attached to the wall of the liquid-hydrogen tank by a constrictive wrap of prestressed nylon or fiber-glass yarn, the panels will constantly be under a compressive load. Since a compressive load on the insulation will affect the thermal contact resistance between the insulation and the tank wall, insulation samples were tested in the thermal-conductivity apparatus over a range of compressive loads.

All the test samples were fabricated by Goodyear Aerospace Corporation and were composed of polyurethane foam with a density of 2 pounds per cubic foot and were 0.4 inch thick. All tests were conducted with liquid-hydrogen temperature on the cold side of the thermal-conductivity apparatus and near-ambient temperature on the warm side, so that the mean temperature would approximate actual conditions.

APPARATUS AND PROCEDURE

Thermal-Conductivity Apparatus

The apparatus used was a Double-Guarded Cold Plate Thermal Conductivity Apparatus designed, built, and operated by Arthur D. Little, Incorporated, for the NASA Lewis Research Center under contract number NASw 615. The apparatus was designed and built primarily to determine an effective thermal conductivity of highly effective multifoil radiation-type insulation where the thermal contact resistance is of the same order of magnitude as that of the insulation.

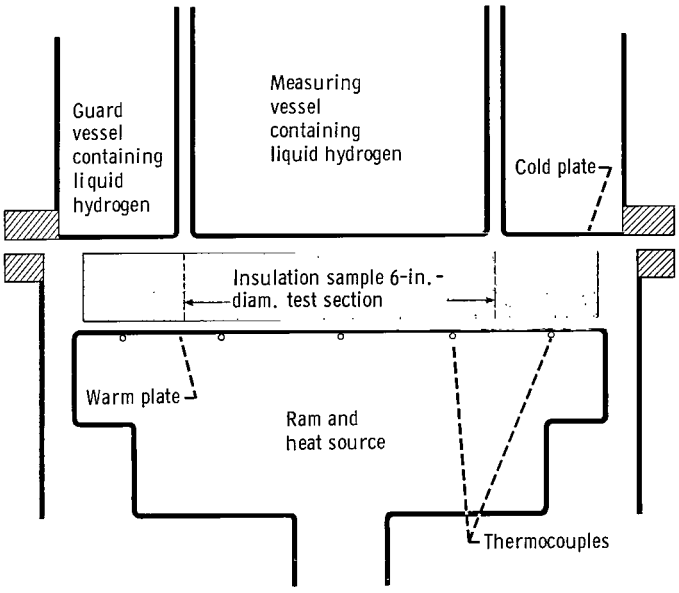

(a) Schematic of test sample area.

Figure III-1. - Double-guarded cold-plate thermal-conductivity apparatus.

For solid insulation of the type tested here, however, the thermal resistance of the contact is generally much larger than that of the solid and has more influence on the overall thermal conductivity. A schematic of the apparatus test section is shown in figure III-1(a), and a cross section of the entire assembly is shown in figure III-1(b). The measuring vessel, filled with liquid hydrogen, is enclosed by an annular guard vessel, also filled with liquid hydrogen. The guard vessel is used to prevent extraneous heat leaks to the measuring vessel and to establish one-dimensional heat transfer in the insulation sample at the 6-inch-diameter test section. The liquid-hydrogen guard vessel is surrounded by a liquid-nitrogen shield and vacuum jacket to reduce loss of liquid hydrogen from the guard vessel. The sample chamber is located between the lower end of the measuring vessel and a movable warm plate. The temperature of the warm plate was measured by thermocouples and was maintained constant by a controller. During the tests, the insulation test chamber could be evacuated or maintained at a controlled pressure. The movable warm plate was provided with a hydraulic jack by which the insulation samples could be subjected to a compressive load. The compressive load was measured by a pressure gage. Volume flow rate of gas generated by boiloff of liquid from the measuring vessel was measured by a gas meter. The instrumentation and the fluid flow system are shown schematically in figure III-2. A more detailed description of the thermal-conductivity apparatus and its operation is presented in reference 1.

Procedure

For the tests reported herein, the thermal-conductivity apparatus was operated in the following manner. The temperature of the warm plate was maintained at about 70° F to approximate insulation temperature conditions for a liquid-hydrogen-filled tank during ground hold. The insulation-sample chamber was evacuated, since the insulation system, when applied to a liquid-hydrogen tank, would be evacuated by cryopumping. The insulation test samples were subjected to two compressives loads, 2 and 15 pounds per square inch. The 2-pound-per-square-inch load corresponds to the compressive load imposed by the constrictive wrap, while the 15-pound-per-square-inch load corresponds to the situation when the sealed insulation is evacuated by cryopumping.

The thermal conductivity K of the insulation test sample was determined from

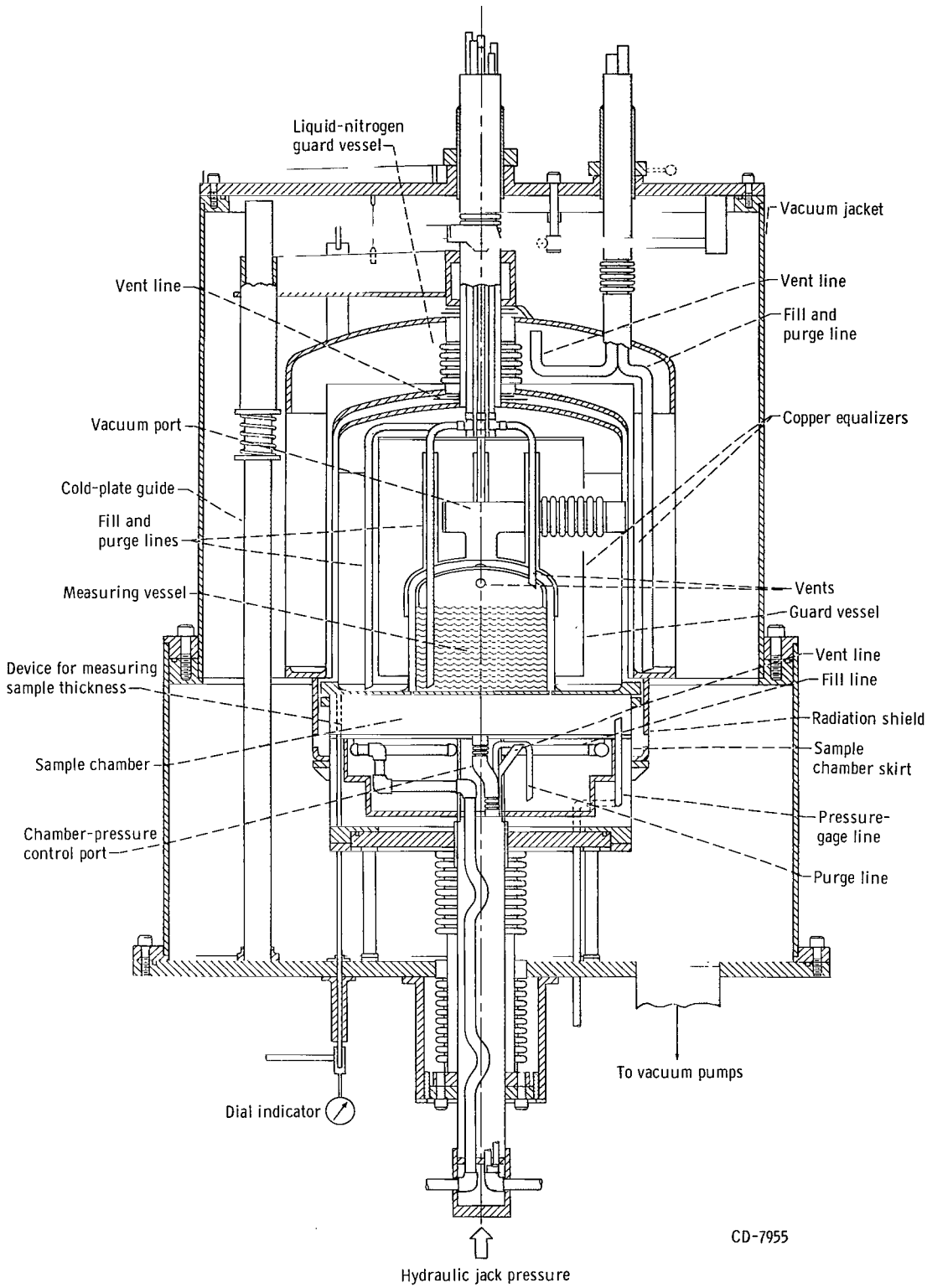

(b) Cross sectional view of complete apparatus.

Figure III-1. - Concluded. Double-guarded cold-plate thermal-conductivity apparatus.

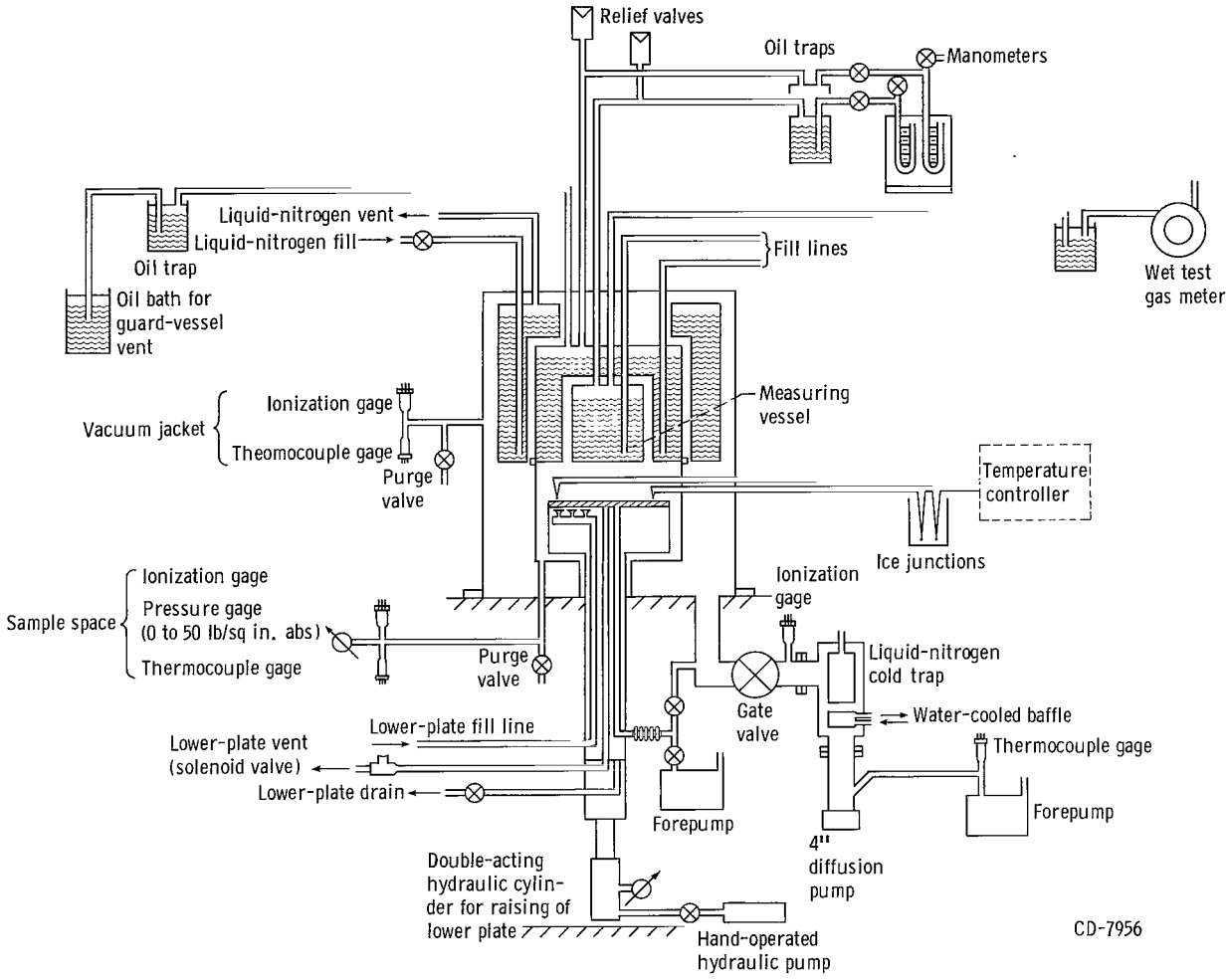

Figure III-2. - Schematic of instrumentation and fluid flow systems required for double-guarded cold-plate thermal-conductivity apparatus.

$$K = \frac{Q\ \Delta x}{A\ \Delta T} \tag{1}$$

where Q is the heat flow rate, Δx is the insulation thickness, A is the area of the test section, and ΔT is the temperature difference between the warm and cold plates (with the cold plate assumed to be at the temperature of the liquid in the measuring vessel). The heat flow rate Q is determined from

$$Q = \dot{m}\ h_{fg} \tag{2}$$

where $\dot{m}$ is the mass flow rate of the boiloff gas and h_{fg} is the heat of vaporization of liquid hydrogen.

The thermal conductivity K, as determined by equations (1) and (2), is an overall value that includes the effects of two thermal contact resistances (interfaces between the insulation sample and the constant-temperature plates) as

well as the thermal conductivity of the sealed-foam samples. Thermal contact resistance can be highly variable and can significantly influence the overall thermal conductivity of an insulation system. An overall thermal conductivity was determined for the insulation test samples in this study because it is more representative of the thermal performance of the insulations system as applied to a tank than the thermal conductivity of the foam itself.

INSULATION TEST SAMPLES

The samples were octagonal panels of closed-cell polyurethane foam 0.4 inch thick and 12 inches between opposite corners. The foam was Freon blown and had a density of about 2 pounds per cubic foot. A laminate of 3/4-mil Mylar, 1-mil aluminum, and 3/4-mil Mylar (hereinafter called MAM laminate) covered the panel surface (see fig. III-3(a)). Later in the program, a thinner laminate became available and was found to be satisfactory as a vapor barrier. Vitel PE 207 adhesive was used to attach the MAM laminate to the foam insulation and the edge channels to the MAM laminate face seals.

The following six samples were investigated:

Sample 1: A panel having edges covered with a MAM laminate channel and sealed to the top and bottom MAM laminate to encapsulate the foam completely (fig. III-3(a)).

Sample 1a: Sample 1 with the edges of the panel completely removed (see fig. III-3(b)). With this configuration the foam was vented to the sample chamber, where it could be evacuated to chamber pressure, and thus a comparison with a sealed sample was provided for the purpose of checking the effectiveness of cryopumping.

Sample 2: A panel like sample 1 except that a 2-mil Mylar channel was used on the edge instead of MAM laminate. This channel eliminated a direct heat short of the edge of the sample. Thus, when this sample was compared to sample 1, a check of the ability of the cold guards to prevent edge effects from appearing in the test section was provided. This sample also was used for comparison with tests of samples 2a, 2b, and 2c.

Sample 2a: Sample 2 with style 191 Fiberglas cloth (5 mil thick, 1/10- by 1/10-in. mesh) used as a separator between the cold plate and the sample.

Sample 2b: Sample 2 with a thicker, 15-mil resin-coated fiber-glass screen (1/8- by 1/8-in. mesh) between the cold plate and the sample.

Sample 2c: Sample 2 with a gap between the sample and the cold plate. Gap thicknesses of 0 to 10 mils and 30 to 40 mils were used.

Sample 3: A panel with a 2-mil Mylar edge channel and a 6-inch length of test joint running through the middle of the panel (see fig. III-3(c)). The purpose of this sample was to evaluate the thermal performance of a panel joint.

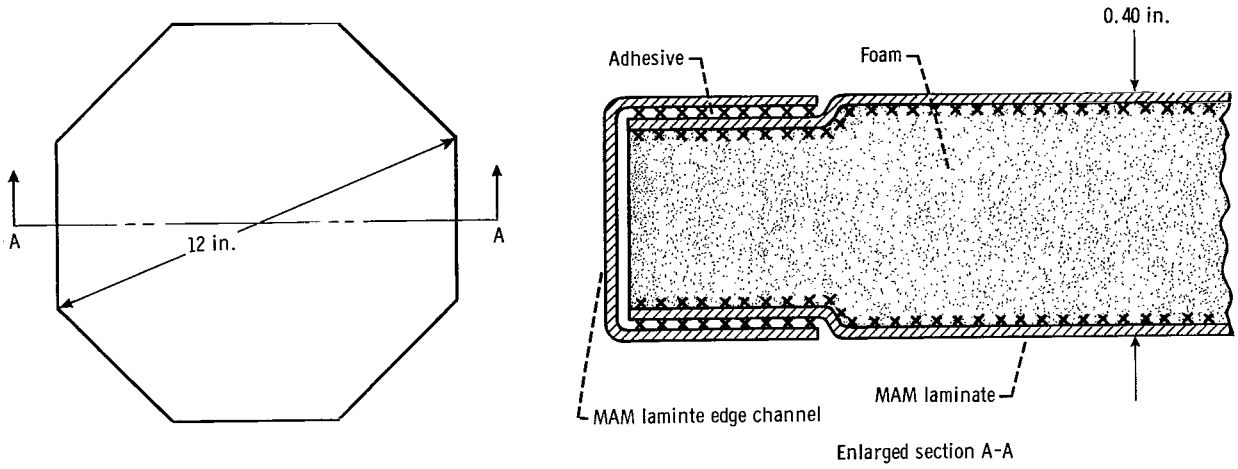

(a) Sample 1.

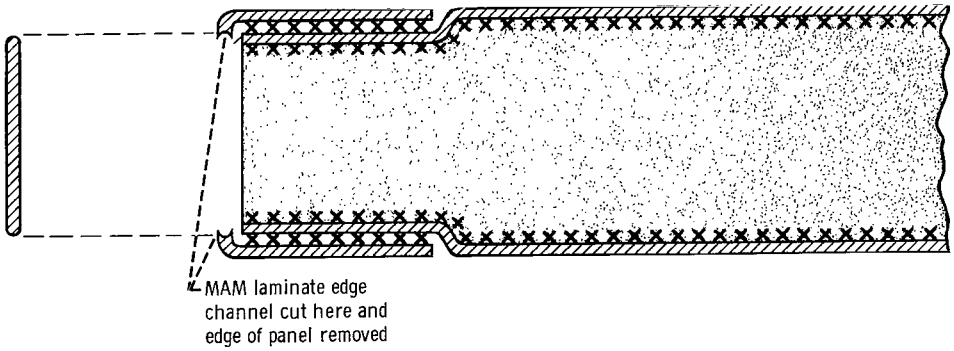

(b) Sample 1a.

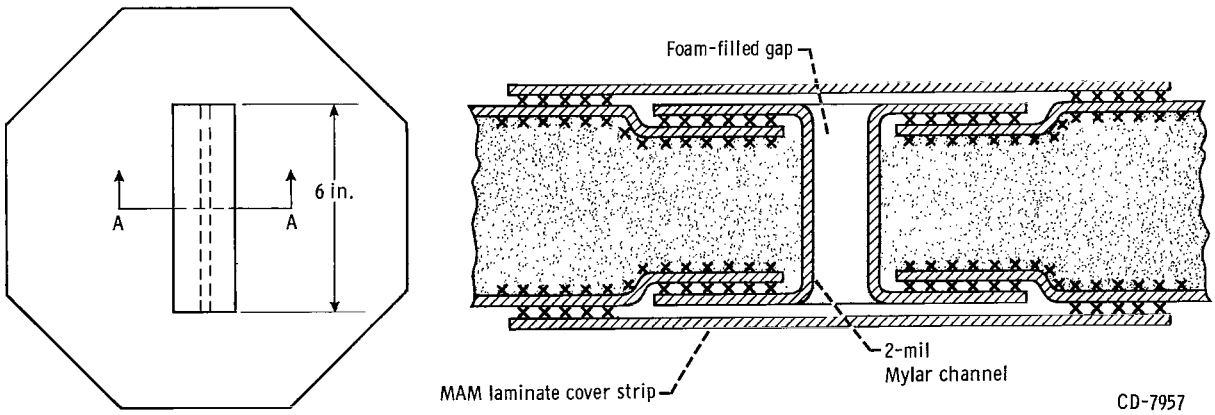

(c) Sample 3.

Figure III-3. - Insulation test samples.

TABLE III-I. - THERMAL CONDUCTIVITY OF INSULATION TEST SAMPLES

Run	Sample	Contact pressure, lb/sq in.	Warm plate temperature, °F	Overall thermal conductivity, $\frac{(Btu)(in.)}{(hr)(sq\ ft)(^{o}R)}$	Remarks
1	1	15	67	0.111	Chamber pressure, 10^{-5} torr
2	1	2	67	.171	Chamber pressure, 10^{-5} torr
3	1	15	68	.148	Chamber pressure, 10^{-5} torr
4	1	2	68	.142	Chamber pressure, 10^{-5} torr
5	1a	15	69	.160	Sample vented to chamber; chamber pressure, 2×10^{-5} torr
6	1a	15	67	.143	Sample vented to chamber; chamber pressure, 6×10^{-6} torr
7	2	2	70	.149	Chamber pressure, 8×10^{-6} torr
8	2	15	71	.143	Chamber pressure, 8×10^{-6} torr
9	2	2	72	.140	Chamber pressure, 8×10^{-6} torr
10	2a	2	71	.101	Chamber pressure, 1×10^{-5} torr; fiber-glass cloth separator
11	2a	15	72	.138	Chamber pressure, 1×10^{-5} torr; fiber-glass separator
12	2a	15	71	.135	Chamber pressure, 1×10^{-5} torr; fiber-glass cloth separator
13	2a	2	72	.118	Chamber pressure, 1×10^{-5} torr; fiber-glass cloth separator
14	2b	2	70	.106	Chamber pressure, 1×10^{-5} torr; fiber-glass screen separator
15	2b	15	70	.130	Chamber pressure, 1×10^{-5} torr; fiber-glass screen separator
16	2c	0	71	.015	30- to 40-mil gap between sample and cold plate
17	2c	0	72	.039	0 to 10-mil gap
18	3	2	70	.127	Questionable contact
19	3	15	71	.137	Questionable contact
20	3	2	69	.13	Questionable contact
21	3	15	70	.12	Questionable contact

RESULTS AND DISCUSSION

Twenty one measurements of the overall thermal conductivity of the six samples were made. Test conditions and results are summarized in table III-I. The results are not as conclusive as had been anticipated. Data scatter, presumably due to varying thermal contact resistance between the sample and the constant-temperature plates (warm and cold) tended to obscure the possible difference in thermal conductivities of the various samples. Variations in thermal contact between different samples is not the only problem. Nonuniform contact in a sample can cause the measured thermal conductivity to be too high or low. To assure uniform thermal contact, the test sample must be of uniform thickness, flat and have smooth surfaces. The surfaces of the MAM laminate-covered foam test samples are far from smooth (as can be seen in fig. III-4). The MAM laminates formed fairly deep dimples over the holes in the foam.

Although the data obtained on the test samples may not be representative of the basic thermal conductivity of foam plus two MAM sealing laminates, they are probably very representative of the overall thermal-conductivity values to

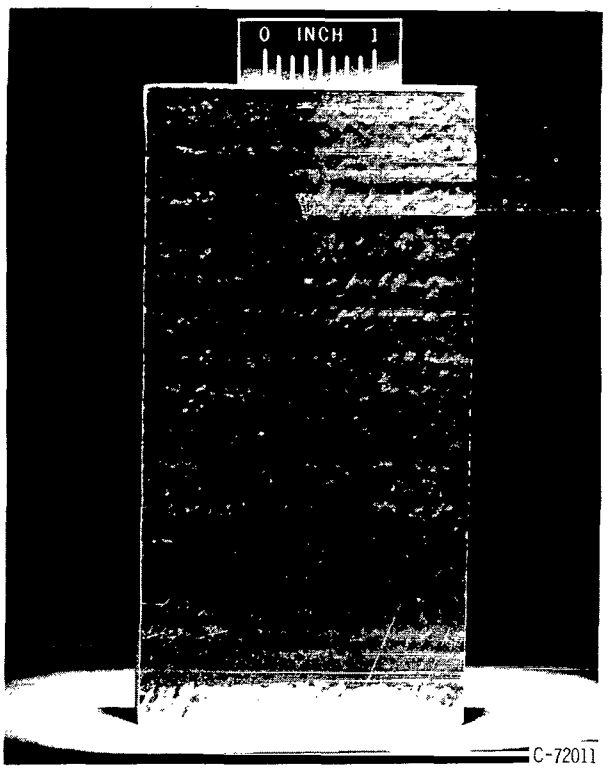

Figure III-4. - Sample of insulation panel showing roughness of MAM laminate surface.

be expected when the insulation panels are applied to a liquid-hydrogen tank. The physical situations of the insulation sample in the conductivity apparatus under a compressive load and the constrictive-wrap insulation on a propellant tank are very similar. The thermal contact resistance in both cases is variable.

The data for sample 1 (runs 1 to 4, table III-I) illustrate the variability of the overall thermal conductivity. The overall thermal conductivity of this sample was measured four times, twice at two different contact pressures, and the values ranged from 0.111 to 0.171 (Btu)(in.)/(hr)(sq ft)(^{o}R) with an average value of 0.143 (Btu)(in.)/(hr)(sq ft)(^{o}R) for an overall mean temperature of insulation of -178^{o} F. For all samples tested, a contact pressure of only 2 pounds per square inch did not produce thermal-conductivity values consistently different from those obtained with a contact pressure of 15 pounds per square inch.

Sample 1a was tested to evaluate, by comparison with sample 1, the effectiveness of cryopumping and mechanical evacuation on the thermal conductivity of the foam. The overall thermal conductivities measured, 0.160 and 0.143 (Btu)(in.)/(hr)(sq ft)(^{o}R) (runs 5 and 6, table III-I), are in the range of scatter of the data for sample 1, which indicates that the difference in thermal conductivity between cryopumped and mechanically evacuated foam is not significant.

Sample 2 was tested to determine the effectiveness of the cold guard in eliminating the effect of the thermal short produced by the MAM laminate used as an edge seal on sample 1. For sample 2 the edge seal was made of thin Mylar. Again the thermal-conductivity measurements for sample 2 (runs 7, 8, and 9, table III-I) are within the range of scatter for sample 1, and no definite conclusion can be drawn.

Various schemes to increase the thermal resistance between the insulation panel and the tank evaluated by testing samples 2a, 2b, and 2c. Sample 2a used a 5-mil-thick fiber-glass cloth (1/10- by 1/10-in. mesh) as a separator. For sample 2b, a 15-mil-thick resin-coated fiber-glass screen (1/8- by 1/8-in. mesh) was used, while for sample 2c, actual physical separation of the sample and the cold plate was used. The overall thermal-conductivity measurements for samples 2a and 2b compared to sample 2 indicate that the use of a fiber-glass material as a separator does decrease the overall thermal conductivity, but not appreciably. The thicker resin-coated material appeared to be slightly better than the plain fiber-glass cloth.

An indication of the increased reduction in overall thermal conductivity that can be obtained by the use of a separator between the panel and the cold surface is shown by runs 16 and 17 for sample 2c. For the case of a 30- to 40-mil gap between the sample and the cold plate, an overall thermal conductivity of 0.015 (Btu)(in.)/(hr)(sq ft)($^{\circ}$R), an order of magnitude reduction, was obtained.

Sample 3 (runs 18 to 21, table III-I) was intended to show the effect of a typical panel joint on the overall thermal conductivity. The measured values for these tests were, on an average, slightly less than those for other samples, which was not expected. These results were definitely caused by poor thermal contact between sample and cold plate. When the sample was removed after run 21 and inspected, it was found that the impression of the cold plate did not go completely around the sample, which indicated a variation in thickness. This variation in thickness could have been due to the two MAM laminate cover strips over the joint (fig. III-3(c)). In addition, the sample might have warped when the slot was cut in it.

CONCLUDING REMARKS

The average value of overall thermal conductivity for all runs where the insulation panels were placed directly in contact with the cold plate (runs 1 to 9) was 0.145 (Btu)(in.)/(hr)(sq ft)($^{\circ}$R) at a mean temperature of -178° F (282° R). This is probably the best indication of the overall thermal conductivity of an insulation system in which the foam panels are held against the cold tank wall by the pressure of a constrictive wrap. This value of thermal conductivity agrees very closely with that for the polyurethane foam (fig. I-1, p. 3).

An increase in compressive load from 2 to 15 pounds per square inch in all runs did not seem to affect the thermal conductivity of the foam or change the contact resistance between the insulation and the constant-temperature plates. The fiber-glass cloth and fiber-glass screen separators tested produced only a small reduction in overall thermal conductivity and probably are not worthwhile if consideration is given to the added complexity and weight. A reduction in overall thermal conductivity of an order of magnitude is possible if a gap between the cold wall and the insulation can be maintained.

REFERENCE

1. Anon.: Liquid Propellant Losses During Space Flight. Second Quarterly Prog. Rep. 63270-00-02, Arthur D. Little, Inc., May 1961.

CHAPTER IV

IMPACT SENSITIVITY OF FOAM INSULATION IN PRESENCE OF LIQUID OXYGEN

by Robert P. Dengler

Lewis Research Center

The concept or objective of the sealed panel insulation system described in chapter I is to prevent any air from being cryopumped into the insulation of a liquid-hydrogen tank during ground hold conditions. The impermeable foil laminate encapsulating the foamed polyurethane panel forms an excellent seal, but it must be conceded that a panel seal could be punctured or develop a leak. At the time of loading then, air or moisture would cryopump into the panel and condense within the insulation forming liquid air or possibly liquid oxygen. Besides decreasing the thermal effectiveness of the system, the presence of this liquid air or liquid oxygen may create a hazardous condition should the affected area be impacted accidentally.

The sensitivity to impact of certain materials in the presence of liquid oxygen was soon recognized after liquid oxygen came into common usage as a rocket propellant. Numerous drop-impact tests (ref. 1) were conducted at Marshall Space Flight Center on a large variety of materials to determine their compatibility or sensitivity to impact when submerged in liquid oxygen. Under the conditions of the tests, a majority of materials tested were impact sensitive in varying degrees. When reactions did take place, they varied from a barely audible noise or explosion and/or a barely detectable flash of light to a very violent reaction similar to the explosive and pyrophoric results of high-velocity impact tests on titanium tanks containing liquid oxygen described in reference 2. In general, reference 1 indicates that the two basic materials used in the insulation panels - Mylar and polyurethane - exhibit some sensitivity to impact when submerged in liquid oxygen. It was cautioned in reference 1, however, that these results "may not apply to other similar materials or to other products meeting the same specifications" and it was advised to test samples of the actual material or composite materials to determine whether or not a hazard would exist.

To resolve this uncertainty, a test program was initiated to determine whether explosions or fires could result from the impact of insulation-panel samples containing, or saturated with, liquid oxygen. The test apparatus involved a stainless-steel plummet that impacted a stainless-steel striker pin resting on top of a 2-inch-square sample of the insulation material immersed in liquid oxygen. Preliminary impact tests were made on 12 polyurethane foam insulation samples, and the general indications or results are briefly discussed and commented on in reference 3. Visual observations were made, and reactions from three of the tests were indicated by a small flash of light and

a barely audible noise. Forty additional tests were conducted in the present investigation on various forms of polyurethane foam samples to verify the indications or results of the preliminary tests and, in so doing, to obtain a better statistical sampling. Photographic equipment was employed in these tests to record any visible reaction resulting from the impact. The results of these tests are reported herein.

In the event of air being cryopumped into the insulation, the permeability and, therefore, the degree to which the air can spread throughout the foam insulation will determine the severity of the hazard that could exist. In view of this, permeability tests were also conducted and are reported herein.

APPARATUS AND PROCEDURE

Impact Tests

Test rig. - A rather simple apparatus based on the principles utilized in reference 1 was used to conduct impact-sensitivity tests on polyurethane foam insulation samples. Figure IV-1 shows the general arrangement or setup of the test rig. A 10-foot-long, 3-inch-diameter (outside diameter) stainless-steel tubing was used to guide a $9\frac{1}{4}$-pound stainless-steel plummet for impacting a 3/4-inch-diameter (5-in.-long) stainless-steel striker pin. The cylindrical plummet was $5\frac{1}{2}$ inches long and had a diameter of $2\frac{3}{4}$ inches, which allowed an annular gap of 1/16 inch between the plummet and the guide tube. The striker pin was resting on a test sample placed in a stainless-steel cup containing the liquid oxygen. The cup consisted of a 3-inch-long, $3\frac{1}{2}$-inch-diameter pipe welded to a 1/4-inch-thick, flat, stainless-steel plate. An inverted, U-shaped, stainless-steel strap was placed over the cup to act as a guide for positioning the striker pin, which was inserted through a hole in the strap. Both the strap and the cup were clamped to a 3-inch-thick steel base that rested on a concrete floor.

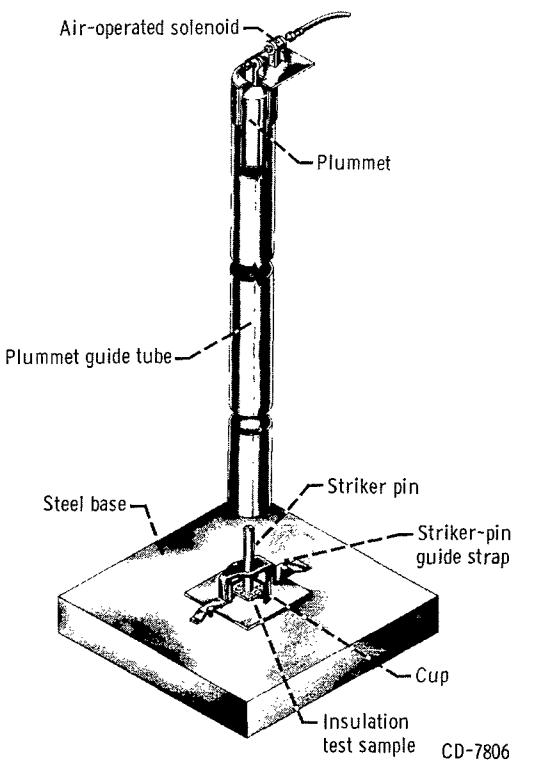

Figure IV-1. - Schematic of impact sensitivity test apparatus.

Release of the plummet from the top of the plummet guide tube would result in imparting an energy of 88 foot-pounds to the striker pin, which was resting on the test sample. An impact of this energy level was considered to be a very severe test. If this foam material is used as an external insulation for a cryogenic pro-

pellant tank, an impact of this magnitude during ground hold conditions on the launching pad appears rather remote.

The test apparatus previously described was used in a drop-test made on an 0.018-inch-thick stainless-steel sheet covering the test cup, which had previously been filled with water, to illustrate the severity of this impact test. The sheet of metal was essentially unrestrained, and the striker pin was placed to rest on top of the sheet. The thickness and the material of this test specimen is typical of that used in present-day propellant tanks for missile or space applications. (The tank wall for the Centaur vehicle is 0.014-in.-thick stainless steel.) The impact of the plummet caused the striker pin to become badly deformed and also penetrate the metal sheet.

Test samples. - All test samples were 2 inches square with a thickness or height of 0.4 inch when placed in the cup for testing. Tests were conducted on groups of insulation samples having the following forms:

(1) Basic foam. This group of samples consisted of a rigid foamed plastic (polyurethane) with a closed-cell structure.

(2) Composite foam. These samples consisted of polyurethane foam with Mylar-aluminum-Mylar (MAM) laminates glued to the top and bottom surfaces with Vitel PE 207 adhesive.

(3) Basic foam with adhesive residue. The MAM layers were stripped or removed from composite foam insulation to expose the adhesive for these test samples.

(4) Composite foam with longitudinal holes through foam. Three 1/16-inch-diameter holes were drilled lengthwise through the foam material to assure the presence of liquid oxygen within the samples.

(5) Composite foam with perpendicular holes through the samples. A number of 1/32-inch-diameter holes were made completely through the samples perpendicular to the MAM surfaces to assure the presence of liquid oxygen within the sample and directly beneath the striker pin.

(6) Basic foam with longitudinal holes. Three 1/16-inch-diameter holes were drilled lengthwise through the foam to provide an intimate contact between the liquid oxygen and the foam material.

A more detailed description of the polyurethane foam insulation system is given in chapters I, V, and VII of this report.

Photographic recording equipment. - A commercially available camera, using black and white film with an ASA rating of 3000, was mounted on a tripod for photographically recording any visible reaction resulting from impact tests. A 5/8-inch-thick Plexiglas shield approximately 7 feet square was placed between the test setup and the camera for protection.

Procedure. - The plummet, striker pin, guide strap, and cup were first

cleaned with acetone to remove any traces of grease or other foreign substance. A test sample was then placed in the cup, and all associated parts were properly located and clamped in place. The cup was then filled with liquid oxygen, and the sample was allowed to soak for at least 5 minutes. If the boiloff was excessive during that time, the cup was refilled and allowed to boiloff until the liquid level decreased and approached the upper surface of the test sample. With the plummet put in place, the camera was set at the largest aperture opening (f/4.5) for a time exposure. The room or test cell was darkened, and the camera shutter opened. With the level of liquid oxygen at or above the top surface of the test specimen, the plummet was dropped by activating an air-operated solenoid release mechanism. (In a few of the tests, the liquid was purposely allowed to boil off completely to present a gaseous oxygen environment at the time the plummet was released.) The camera shutter mechanism was left open for a few seconds after impact took place in order to photograph any and all of the reaction that might result.

Permeability Tests

Test rig. - A cylindrical metal vacuum chamber with a volume of approximately 2 cubic feet was used to conduct permeability tests on the polyurethane foam material. One flat end of the chamber contained a 1/2-inch-diameter hole drilled completely through the wall.

Procedure. - Plain polyurethane foam samples of the same dimensions as those used for the impact tests (2 in. square by 0.4 in. thick) were used to seal or cover the hole in the wall of the vacuum chamber. The foam sample was cemented to the outside of the tank wall carefully so that the portion of the foam sample covering the hole was kept free of cement. The sample was otherwise left exposed to the atmosphere. The vacuum chamber was evacuated for a period of 16 hours to decrease any effects of outgassing the foam material. At the end of this evacuation period, the vacuum pump was turned off and the pressure within the chamber was recorded. Pressure readings were recorded at various times over a period of 24 hours.

An air inleakage check of the vacuum chamber was made with a solid metal seal and a Teflon gasket covering the hole so that the system's inherent leakage rate could be determined. The same procedure for pump-down of evacuation of the chamber was followed as for the tests on the foam insulation samples. In addition, pressure readings within the vacuum chamber were recorded at times after cutoff of the vacuum pump identical to those for the foam sample tests. If the leakage rates from both these tests are known, the leakage rate attributed to the permeation of air through the thickness of foam and/or outgassing of the foam can then be determined.

RESULTS AND DISCUSSION

Impact Tests

Table IV-I lists the 40 impact tests conducted and gives a description of the test sample along with the type of environment (liquid or gaseous oxygen)

TABLE IV-I. - DROP-IMPACT TESTS ON POLYURETHANE FOAM INSULATION SAMPLES

Sample number	Group number	Sample description	Environment	Relative intensity of reaction
1	I	Plain polyurethane foam	Liquid oxygen	No visible reaction
2				Barely visible reaction
3				Barely visible reaction
4				No visible reaction
5				
6				
7				
8				
9			Gaseous oxygen	
10			Gaseous oxygen	
11	II	Polyurethane foam with MAM layers glued to top and bottom surfaces with Vitel PE 207 adhesive	Liquid oxygen	Very bright reaction with sustained combustion
12				No visible reaction
13				
14				
15				
16				
17				
18				
19			Gaseous oxygen	
20			Gaseous oxygen	
21	III	Polyurethane foam with MAM layers removed, but with some glue residue	Liquid oxygen	No visible reaction
22				No visible reaction
23				Plainly visible reaction
24				Relatively bright reaction
25				Plainly visible reaction
26				No visible reaction
27				No visible reaction
28				No visible reaction
29	IV	MAM-covered polyurethane foam with three longitudinally drilled holes under striker pin	Liquid oxygen	Relatively bright reaction
30				No visible reaction
31				Relatively bright reaction
32				No visible reaction
33	V	MAM-covered polyurethane foam with holes through sample perpendicular to MAM layers and directly under striker pin	Liquid oxygen	No visible reaction
34				No visible reaction
35				Barely visible reaction
36	VI	Plain polyurethane foam with three longitudinal holes through sample and under striker pin	Liquid oxygen	No visible reaction
37				Barely visible reaction
38				No visible reaction
39				No visible reaction
40				No visible reaction

for testing. Photographic records for all the impact tests were obtained as described in the APPARATUS AND PROCEDURE section. Of the 40 test photographs obtained, 10 revealed indications of reaction as a result of the impact. The relative intensity of the reaction is given in the last column of table IV-I and the relation is as follows in order of magnitude:

(1) No visible reaction

(2) A barely visible reaction

(3) A plainly visible reaction

(4) A relatively bright reaction

(5) A very bright reaction with sustained combustion

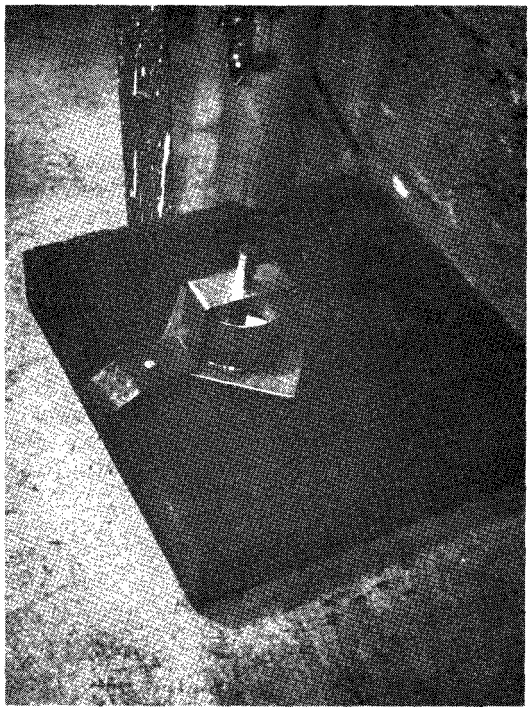

(a) Test impact area.

(b) Barely visible reaction.

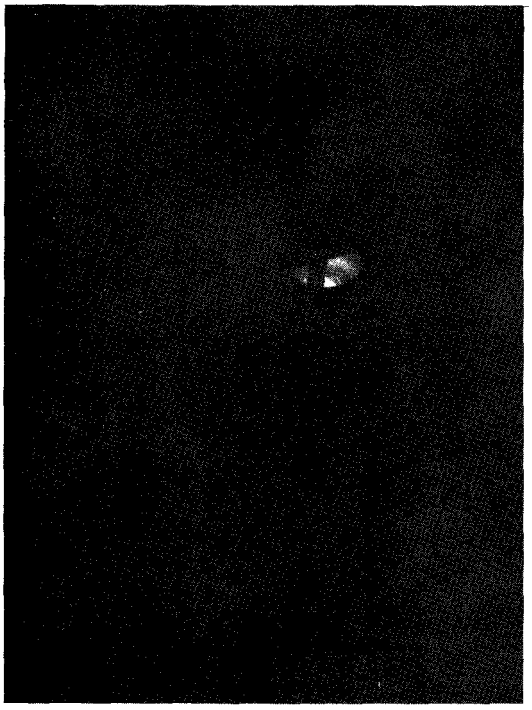

(c) Plainly visible reaction.

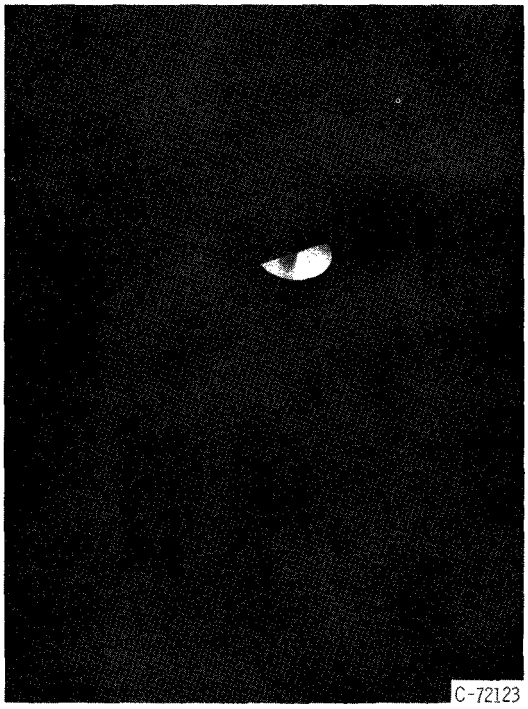

(d) Relatively bright reaction.

Figure IV-2. - Relative intensity of reactions from impact tests of polyurethane foam insulation samples submerged in liquid oxygen.

When a flash of light did result from an impact, it was generally accompanied by an audible noise or explosion.

Figure IV-2(a) is a photograph of the general impact test area and represents the approximate area covered by the camera during testing for recording the visible reactions such as those shown in the subsequent photographs of figure IV-2. The intensity of reaction is illustrated by the various degrees of illumination of the test cup or impact area in figures IV-2(b), (c), and (d), which are representative of barely visible, plainly visible, and relatively bright reactions, respectively. The illumination by the resultant flash is generally confined to the area of the test cup with the striker pin visible in some photographs along with the outline of the striker-pin positioning strap.

Group I (samples 1 to 10). - The test samples of this group consisted of plain polyurethane. Two of the 10 impacts from this group resulted in slight indications of reactivity; that is, a slight flash or emission of light resulted from the impact. Samples 2 and 3 exhibited reactivity and they both had a barely visible reaction. Even though a reaction had occurred, it was extremely small and any damage to the sample was limited effectively to the area under the striker pin.

Figure IV-3(a) shows both a typical sample from this group before impact and the results of impact on test sample 4. The after impact results shown in this figure are fairly typical of impact results on all samples in this group, including those of samples 2 and 3, which had indicated some sign of reactivity. Inspection of the samples after impact revealed that the foam was pulverized in the area where the striker pin was resting and subsequently impacted, but there were no signs of any sustained burning or ignition of the foam material. The damage that did occur was of a localized nature, and in some cases the polyurethane foam sample had split in two as shown in figure IV-3(a).

Group II (samples 11 to 20). - The samples of this group consisted of polyurethane foam with MAM attached to two surfaces with Vitel PE 207 adhesive. Of the 10 samples tested in this group, only one exhibited an indication of reaction; that one was sample 11. The impact of this test resulted in the most intensive reaction for all the samples tested and actually produced ignition and sustained combustion of a portion of the sample. The test photograph obtained for this impact was overexposed, that is, too much light was admitted through the camera lens so that the resulting picture was all white with no traces of a distinguishable image. Figure IV-3(b) shows a typical sample before impact and also shows the results of the impact on sample 15, which is fairly representative of the impact results of other samples in this group with the exception of sample 11. The results of impact on test sample 11 are shown in figure IV-3(c). The impact initiated ignition of the sample, and evidence of melted or burned MAM is revealed in the figure. Even though there was sustained combustion, not all of the polyurethane foam was consumed.

Group III (samples 21 to 28). - The samples of this group consisted of polyurethane foam with glue residue on top and bottom surfaces; that is, the

MAM layers were removed from samples similar to those of group II. Impact of test samples 23 to 25 indicated some reactivity with samples 23 and 25 having plainly visible reactions and sample 24 having a relatively bright reaction. Figure IV-3(d) shows a typical sample of this group before impact and also the results after impact on test sample 22, the after impact result being representative of impacts that did not produce an indication of reactivity. Figure IV-3(e) also shows a typical sample of this group before impact along with the impact results on sample 23. The results of the impact shown in this figure are fairly representative of the other two impacts of this group that resulted in indications of reactivity. It can be noticed from figure IV-3(e) that the impact resulted in more extensive pulverizing of the foam material than was evident in the previous tests of groups I and II, suggesting that an explosive force accompanied the flash of light that was emitted. Even though the damage to the three reacting specimens of this group was more obvious, there was still no evidence of ignition or sustained combustion of the parent material.

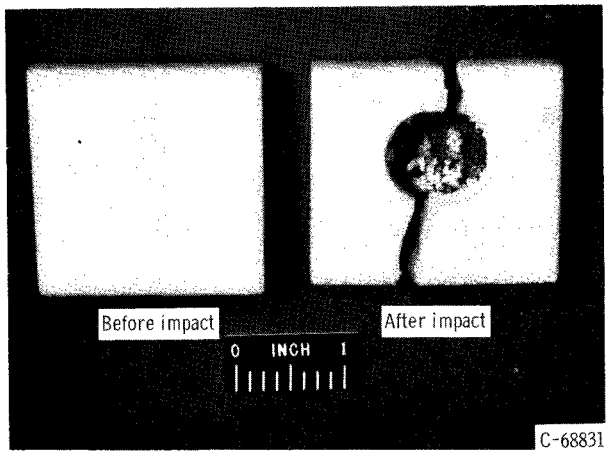

(a) Plain polyurethane foam. Sample number, 4.

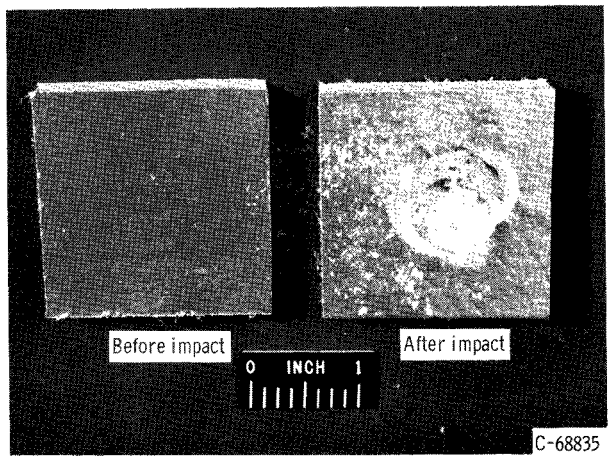

(b) Polyurethane foam with MAM glued to two surfaces. Sample number, 15.

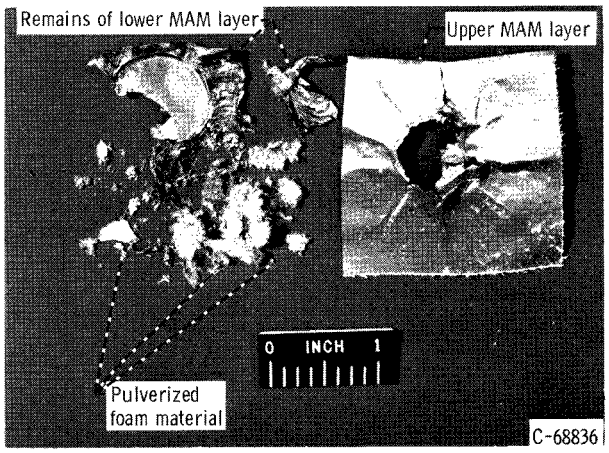

(c) Polyurethane foam with MAM glued to two surfaces. Sample number, 11.

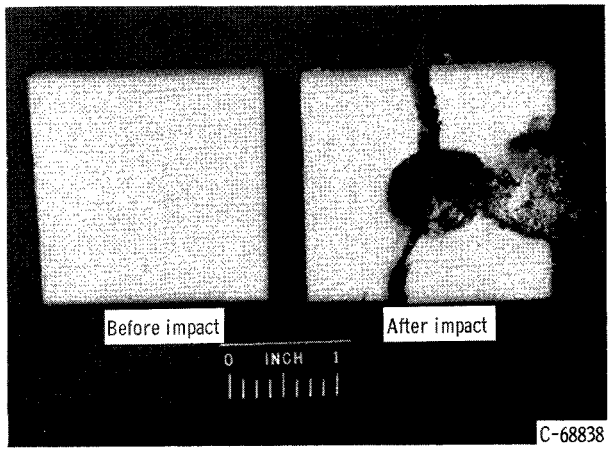

(d) Polyurethane foam with adhesive residue. Sample number, 22.

Figure IV-3. - Results of impacts on polyurethane foam insulation samples submerged in liquid oxygen.

Group IV (samples 29 to 32). - The samples of this group were similar to those of group II in that they consisted of polyurethane foam with MAM on the top and bottom surfaces. The samples for this group, however, had three 1/16-inch-diameter holes drilled through the foam lengthwise or longitudinally to provide assurance that liquid oxygen was within the sample. In this arrangement, the striker pin was placed directly over and perpendicular to the longitudinal holes. Two of the four impacts conducted resulted in an indication of reactivity; both of these impacts resulted in a relatively bright reaction. Figure IV-3(f) shows the result of impact on test sample 31 (a reacting sample), and it is obvious that practically all of the foam was pulverized by the impact and ensuing explosive force accompanying the reaction or flash of light. Despite the obvious damage that had been done to the samples of this group that exhibited reactivity, there was no evidence of sustained combustion resulting in burned material.

Group V (samples 33 to 35). - The test samples for this group consisted of

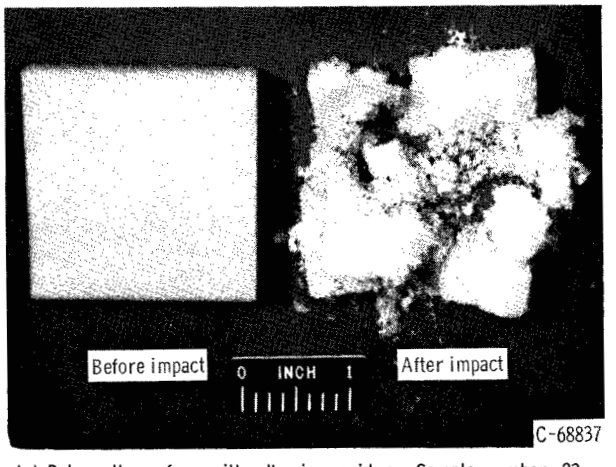

(e) Polyurethane foam with adhesive residue. Sample number, 23.

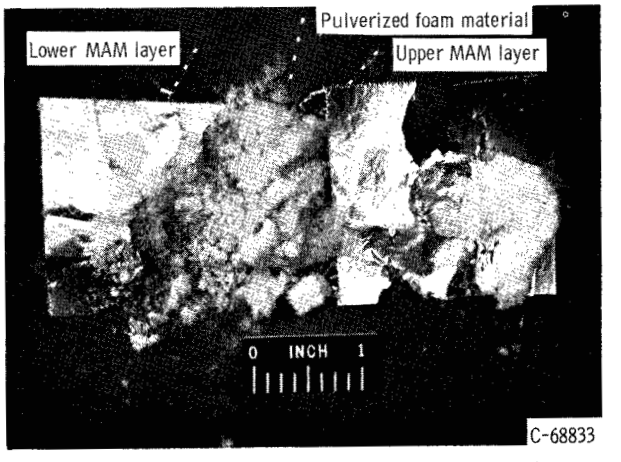

(f) Polyurethane foam with MAM glued to two surfaces and longitudinal holes in foam under striker pin. Sample number, 31.

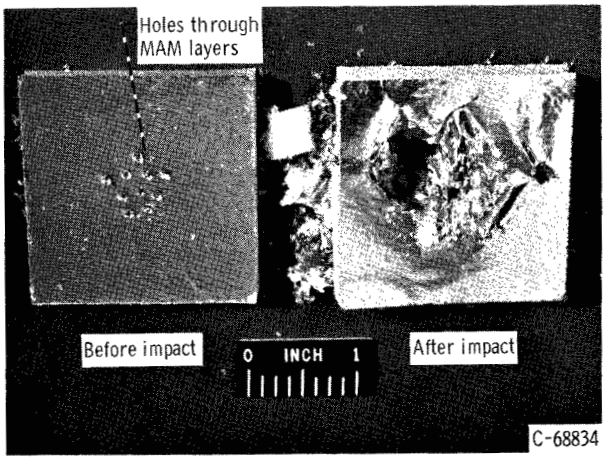

(g) Polyurethane foam with holes pierced through MAM. Sample number, 35.

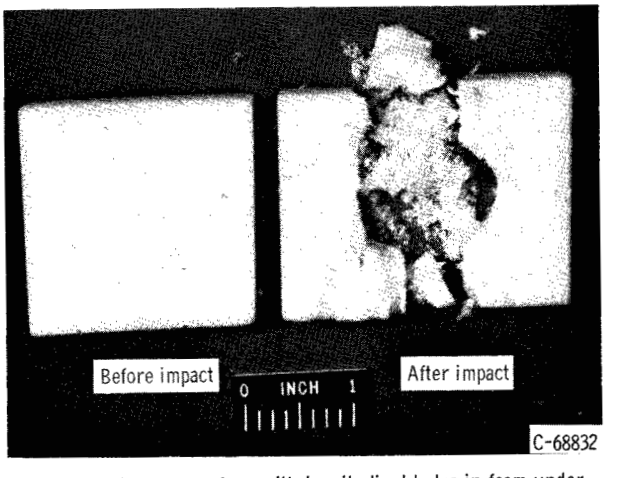

(h) Plain polyurethane foam with longitudinal holes in foam under striker pin. Sample number, 37.

Figure IV-3. - Concluded. Results of impacts on polyurethane foam insulation samples submerged in liquid oxygen.

polyurethane foam with MAM similar to those of group II but with holes pierced through the laminates to allow liquid oxygen to be in contact with the foam material directly under the striker pin. One of the impacts (sample 35) from this group resulted in a very weak flash or indication of reaction. Figure IV-3(g) shows a typical example before impact and also the result of the impact on test sample 35.

Group VI (samples 36 to 40). - Five impact tests were conducted on plain polyurethane foam samples with three 1/16-inch-diameter holes drilled lengthwise or longitudinally in the foam sample. As for tests of group IV, the striker pin was located over the holes at right angles for the subsequent impact. One of the impacts (sample 37) resulted in a slight flash; the results of this impact are shown in figure IV-3(h).

Impact test summary. - For the impact tests conducted on the various insulation samples, reactions occurred sporadically, and no apparent reason for this could be determined. From table IV-I, however, it can be seen that although reactions did occur for tests with only the basic foam material (three reactions out of 15 tests), the reaction in all cases was a barely visible reaction. A reaction of greater intensity (plainly visible or relatively bright reaction) is more likely to occur if the polyurethane foam has the glue residue on its surfaces and/or MAM covering it and with liquid oxygen in intimate contact within the sample. Therefore, it appears that the basic foam material itself is comparatively insensitive to an impact of the magnitude described herein. In only one instance did an impact result in sustained combustion; this one exception is unexplainable since the same procedure and precautions were followed for this test as for the others.

Permeability Tests

It was pointed out earlier that the possibility of the outer layer of MAM sustaining a puncture does exist and subsequent cryopumping of air into the foam insulation would take place. The degree to which the air would permeate or spread through the foam insulation to cause a larger area of impact sensitivity is not now known. Some preliminary tests, however, were conducted at room temperature to obtain an insight into the permeability characteristics of this closed-cell type of foam material.

As mentioned in the APPARATUS AND PROCEDURE section, the permeability tests of the foam samples involved an initial pump-down or evacuation period of 16 hours, after which the vacuum pump was turned off. The recorded vacuum chamber pressures taken at various times after the initial pump-down period and the known leakage rate inherent to the system were used to determine the rate of leakage through the foam and/or outgassing of the foam. At the end of 24 hours (after the pump-down period), the pressure rise attributed to the foam material was 537 microns of mercury. This corresponds to a leakage rate of 0.36 cubic centimeter of air per cubic centimeter of foam material per hour for a pressure differential of 1 atmosphere. This leakage rate was determined by assuming that the affected volume of foam material approximated a truncated cone over the hole with a half angle of 45° where the 1/2-inch-diameter hole was the smaller base of the truncated cone.

It is recognized that the conditions for this test, by no means, simulate the conditions that would exist if air were to be cryopumped into an encapsulated polyurethane foam insulation system applied to a tank filled with liquid hydrogen. Nevertheless, all factors being considered, it still seems apparent that air cryopumped into the foam material as a result of a developed leak would tend to localize at the area of the leak during ground hold and launch conditions and would, therefore, limit the area of impact sensitivity. In addition, the volume of air leaking in for 1 hour would be considerably less than the volume of foam affected.

CONCLUSIONS

The findings of this report indicate that the probability of a damaging liquid-oxygen foam insulation reaction occurring as the direct result of an accidental impact is extremely small during ground hold and launch conditions. This conclusion is based on the following reasons or reasonings:

1. The foam insulation panels are hermetically sealed with Mylar-aluminum-Mylar (MAM) laminates to prevent air from being cryopumped into and subsequently condensing within the foam insulation.

2. If a leak were to develop despite this effective sealing method, the high resistance to permeation of air through the foam material would restrict the cryopumping to a very localized area. With the area of impact sensitivity limited and small in comparison to the total area, it seems unlikely that an impact would occur in the affected region. In addition, since 80 percent of air is nitrogen, it is unlikely that the foam material would be in an oxygen-rich environment or submerged in liquid oxygen as were the test samples of this investigation.

3. In the event that an impact did occur in an area where a leak developed, the chances of a reaction occurring are small since only one out of every four foam samples tested indicated some reaction.

4. Even if a reaction should occur, it is highly unlikely that the damage would extend beyond the limits of the impacted region since a sustained reaction occurred in only one of the 40 tests on foam insulation samples.

5. It is highly improbable that a vehicle would sustain an impact of the magnitude investigated (88 ft-lb) during ground hold or launch conditions. An impact of this magnitude would most certainly damage the wall of a propellant tank of present-day space vehicles.

REFERENCES

1. Key, C. F., and Riehl, W. A.: Compatibility of Materials with Liquid Oxygen. NASA TM X-54611, 1963.

2. Dengler, Robert P.: An Experimental Investigation of Chemical Reaction Between Propellant Tank Material and Rocket Fuels or Oxidizers When Impacted by Small High-Velocity Projectiles. NASA TN D-1882, 1963.

3. Perkins, Porter J., Jr., and Esgar, Jack B.: A Lightweight Insulation System for Liquid Hydrogen Tanks of Boost Vehicles. AIAA Fifth Annual Structures and Materials Conf., Palm Springs (Calif.), Apr. 1-3, Pub. CP-8, AIAA, 1964, pp. 361-371.

CHAPTER V

FABRICATION AND TESTS OF INSULATED SUBSCALE TANKS

by Porter J. Perkins, Jr., Mario Colaluca, Frank P. Behning, and Francis Devos

Lewis Research Center

As a part of the development of the reported insulation system, four subscale tanks with full-scale cylindrical curvature (two combined circular segments with 4-ft arcs of 60-in. radius) were insulated and tested prior to the insulation of the full-scale tank. The purpose of this program was to develop and evaluate quickly and economically insulation techniques that would be applicable to the full-scale tank. To accomplish this program, thermal and structural performance data on the insulation system as applied to a tank were obtained under ground-hold and quasi-simulated launch conditions. Unfortunately, the true launch environment, including rate of change of altitude, aerodynamic forces, velocities, and surface temperatures, cannot be completely duplicated simultaneously in ground tests to produce the combined effects. Thus, certain launch conditions were combined but not necessarily duplicated in the proper time sequence.

This chapter of the report presents the details of the insulation fabrication for the circular-segment tanks, including the chronological development of the final insulation system that was applied to the full-scale tank. Test data are presented for (1) the equivalent thermal conductivity of the insulation systems during ground hold, (2) the structural effect of rapid drop in ambient pressure during launch, and (3) the effect of simulated surface heating during launch. These tests were conducted at the NASA Lewis Plum Brook Station on an outside tank test stand and in a vacuum chamber. The insulation systems were fabricated and applied to the the tanks at the Goodyear Aerospace Corp., Akron, Ohio, under Contract NAS3-3238 for the Lewis Research Center.

INSULATION SYSTEMS FABRICATION

Subscale Tank Design

In order to develop and evaluate the constrictive-wrap techniques and the materials for the insulation system (described in ch. I), a full-scale radius had to be used. This radius was necessary in order to duplicate the hoop tension in the wrap and the compressive load imposed on the tank through the insulation that would be experienced by the full-scale tank. A small-volume tank was obtained with full-scale cylindrical curvature on both sides by placing two

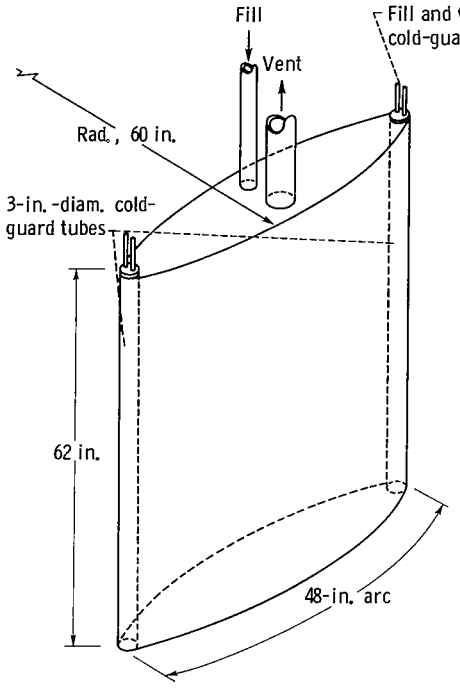

Figure V-1. - Circular-segment tank design used to develop insulation systems.

short circular segments back to back so that they formed a cross section resembling a symmetrically shaped wing.

A sketch of this tank design is shown in figure V-1. The edges were formed from 3-inch-diameter tubes having independent connections for filling with liquid hydrogen. These served as cold guards at the tank edges, where insulation panels under test could not extend. A vent line and a dip tube for filling the main tank extended from one end of the tank. These designs minimized heat leaks into the tank so that the thermal conductivity of the insulation panels could be measured with a reasonable degree of accuracy.

Four identical circular-segment tanks were fabricated of 16-gage stainless-steel with 48-inch-long arcs of 60-inch radius. The tanks were designed to stand on end and were about 62 inches high. The internal volume measured about 112 gallons. The width and the height were about the maximum size that would fit into the vacuum chamber used for quasi-simulated launch testing. Each tank was qualified by hydrostatic testing to 20 pounds per square inch gage, cold shocked with liquid nitrogen, and then tested for leaks.

Insulation Panel Design

A typical insulation panel configuration is shown in figure VII-2 (p. 100). This design utilized hermetically sealed foam insulation of 2-pound-per-cubic-foot density and 0.4-inch thickness. The primary insulation material, rigid polyurethane foam, is available in a variety of formulations. In the development program, consideration was given to two types of blowing agent used to produce a foam material. The physical properties listed in table V-I indicate the basic advantages and disadvantages of the two foam systems. On the basis of the lower thermal conductivity and the contractor's more extensive experience, Freon-blown foam was selected as the basic insulation material for the subscale and full-scale tanks.

The foam slabs were sealed on two faces with Mylar - aluminum-foil - Mylar laminate (hereinafter called MAM laminate). Two thicknesses of MAM laminate were used. The thicker material, 0.0024-inch thick (0.0007-in. Mylar - 0.001-in. aluminum - 0.0007-in. Mylar), was chosen for the first two systems because of its availability. On subsequent insulation systems, a thinner material, 0.0015-inch thick (0.0005-in. Mylar - 0.0005-in. aluminum - 0.0005 in. Mylar), was used to reduce the weight of the insulation panels. Face sheets of the laminate were bonded to the surfaces of the foam with a heat-sealable polyester resin (Vitel PE 207 - Goodyear Tire and Rubber Co.). Adhesives were ap-

TABLE V-I. - COMPARISON OF BLOWN POLYURETHANE FOAMS

Physical property		Freon-blown foam	Carbon dioxide-blown foam
Density, lb/cu ft		2.0	2.0
Thermal conductivity (at room temperature), (Btu)(in.)/(hr)(sq ft)(^{o}R)		0.14	0.22
Closed cells, percent		90	85
Tensile strength, psi		60	58
Compressive stress, psi	10-percent deformation	47	32
	30-percent deformation	45	28
	Yield point	46	30
Heat distortion temperature, ^{o}F		250	300

plied to the foam slabs by spraying and to the MAM laminate face sheets by a light brush coat. Bonding of MAM laminate to the foam was achieved under a vacuum bag with a hot iron (265^{o} F) applied over the surface. During bonding, the panel was held in a mold by the vacuum bag to shape the panel to the contour of the test tank. The bonded face sheets greatly increased the rigidity of the panel over that of the plain foam slab. The edges of the foam were sealed initially with preformed channels of MAM laminate and later of Mylar only. These channels were bonded to the face sheets with Vitel or Epon 828 and Versamid 125 resins using the corner fold illustrated in figure VII-2 (p. 100).

The achievement of a vapor-tight seal over the foam was checked by submerging the sealed panels in a bath of liquid nitrogen for a period of 5 minutes and then upon removal from the bath visually inspecting the panels for leaks. A complete description of the quality-control procedures is presented in chapter VII.

Constrictive-Wrap Design

It was necessary to have a constrictive-wrap material capable of withstanding a prestrain of approximately 0.8 percent during wrapping of the insulation. This amount of prestrain ensured a constrictive load on the insulation under all conditions, which included thermal contraction of the tank during cooldown, deformation of the insulation, and thermal expansion of the wrap from aerodynamic heating during launch. The constrictive-wrap materials under consideration at the time of fabrication of the subscale tanks were Nylon HT-1 fiber yarn (E. I. duPont de Nemours & Co.) and Fiberglas S/HTS roving (Owens-Corning Fiberglas Corp.). A more detailed description of the selection of wrap materials is presented in chapter VII.

Although the Fiberglas S/HTS roving resulted in a lighter constrictive-wrap material than HT-1 Nylon, strand breakage was encountered during the initial phase of the investigation when attempts were made to wind with a prestrain of 0.8 percent. As a result, the first three insulation systems inves-

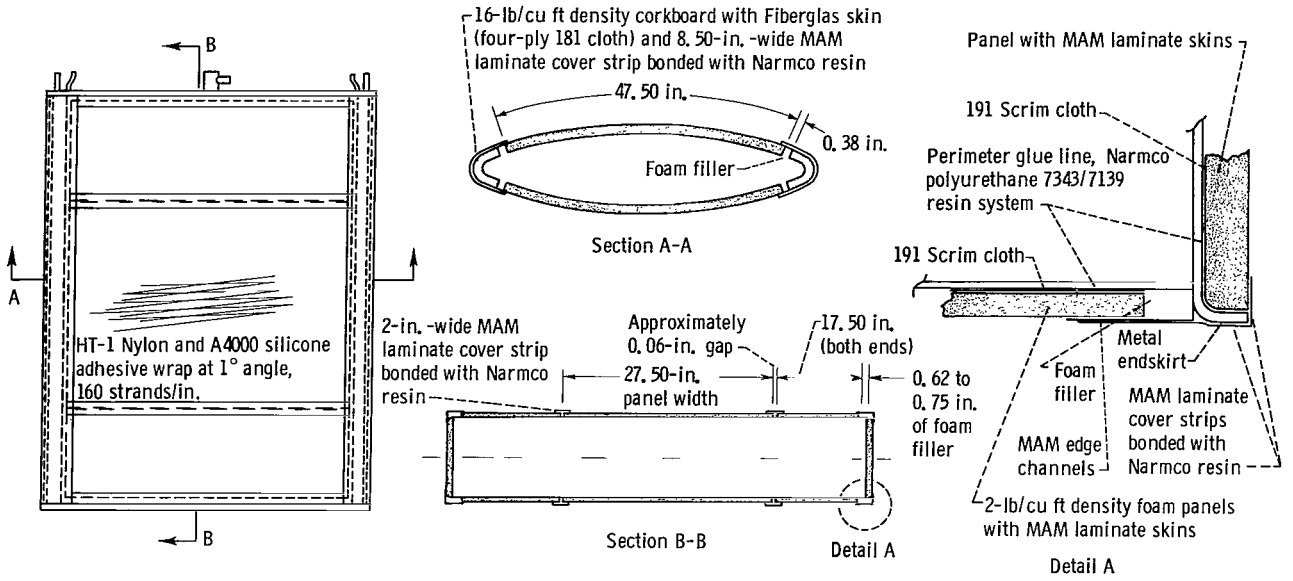

Figure V-2. - Fabrication details for insulation system 1. (Three panels on one side had tank edge channels bonded with Vitel PE 207 resin and on other side with Epon 828 and Versamid 125 resin system.)

tigated used HT-1 Nylon for the constrictive wrap because of its greater strain capability.

A large-size filament winding machine was used to apply the constrictive wrap on all circular-segment tanks. The wrap was bonded to itself with Dow Corning Silicone A-4000 resin at crossover points and to the outer surface of the insulation during winding. The resin was applied by passing the strands through a liquid bath preceding contact with the insulation surface.

Insulation of Circular-Segment Tanks

Four circular-segment tanks were insulated by the Goodyear Aerospace Corporation, and test insulation panels were applied to both sides of each tank. All tanks were also insulated at the top and the bottom, except for the metal end skirts (fig. V-2), with sealed polyurethane foam. The edges of the tanks were insulated with corkboard covered with another layer of fiber-glass laminate (see fig. V-2). Corkboard was required to take the high compressive loads of the constrictive wrap caused by the small radius around the edges. Insulation systems on the side panels were varied for the four tanks as to materials, size, and application techniques. The fabrication details for each of the four insulation systems are described in the following sections and summarized in table V-II.

System 1. - Fabrication details for this system are shown in figure V-2. Three panels were used on each side of the tank. Multiple panels instead of single panels on each side were selected primarily to increase the amount of panel edge seals and panel joints, which were suspected of being the most likely sources of leaks in the vacuum jacket. All the panels were of identical construction except that the edge channels on the panels on one side of the

TABLE V-II. - SUMMARY OF INSULATION FABRICATION PARAMETERS FOR CIRCULAR-SEGMENT TANKS

Parameter	Insulation system			
	1	2	3	4
Panel size and number	Two 27.5 by 42.5 in. Four 17.5 by 42.5 in.	Two 37.5 by 62.5 in. Two 9.75 by 62.5 in.	Two 37.5 by 62.5 in. Two 9.75 by 62.5 in.	Two 37.5 by 62.5 in. Two 9.75 by 62.5 in.
Polyurethane foam density, lb/cu ft	1.8 to 2	1.8 to 2	1.8 to 2	1.8 to 2
Face sheets on foam	0.0024-in.-thick MAM laminate	0.0024-in.-thick MAM laminate	0.0015-in.-thick MAM laminate	0.0015-in.-thick MAM laminate
Edge seal channels	0.0024-in.-thick MAM laminate	0.002-in.-thick Mylar	0.002-in.-thick Mylar	0.002-in.-thick Mylar
Protuberances	None	None	One large One small	None
Adhesives for bonding -				
MAM laminate face sheets to foam	Vitel PE 207	Vitel PE 207	Vitel PE 207	Vitel PE 207
Channels to face sheets	Three panels, Vitel PE 207 Three panels, Epon 828 and Versamid 125	Two panels, Vitel PE 207 Two panels, Epon 828 and Versamid 125	Three panels, Vitel PE 207 One panel, Epon 828 and Versamid 125	All panels, Vitel PE 207
Panels to tank	Narmco 7343/7139 perimeter bond	Narmco 7343/7139 perimeter bond	Vitel PE 207 and Narmco 7343/7139, 100 percent area bond	Vitel PE 207 and Narmco 7343/7139, 11- by 15-in. grid pattern plus perimeter bond
Doubler or cover strips	Narmco 7343/7139	Narmco 7343/7139	Narmco 7343/7139	Narmco 7343/7139
Protuberances	None	None	Z-sections, Vitel PE 207 Caps - Epon 828/Versamid 125	None
Constrictive wrap	HT-1 Nylon at 1°, 160 strands/in., 0.75-lb/strand tension, 1.25-percent strain	HT-1 Nylon at 6°, 160 strands/in., 0.75-lb/strand tension, 1.25-percent strain	HT-1 Nylon at 6°, 160 strands/in., 0.75-lb/strand tension, 1.25-percent strain	Eight-strand fiber glass preimpregnated roving at 6°, 64 strands/in., 2-lb/strand tension, 0.88-percent strain
Constrictive-wrap matrix	Silicone A-4000 adhesive	Silicone A-4000 adhesive	Silicone A-4000 adhesive	Silicone A-4000 adhesive
Filler strips at panel joints	None	0.25-in.-thick, 2-lb/cu ft polyurethane foam	0.25-in.-thick, 2-lb/cu ft polyurethane foam	0.25-in.-thick, 2-lb/cu ft polyurethane foam

tank were bonded with an Epon 828 and Versamid 125 resin system, while those on the other side were bonded with Vitel PE 207. A perimeter glue line of Narmco 7343/7139 adhesive around the edges of each panel between panel and tank was used to seal against cryopumping of air into the space between the tank wall and the panels. This space could be eliminated entirely by a full panel area bond, but a perimeter bond reduces the weight of adhesive involved.

At the time of fabrication of this system, it was felt that a lower overall heat inflow to the liquid hydrogen could be achieved with a separator material between the tank wall and the panels, as a result of an increased contact resistance between the insulation and the tank wall. For a preliminary evaluation, a thin layer of Owens Corning type 191 glass scrim cloth was used as the separator material on this system. When thermal-conductivity apparatus tests (see ch. III) showed that little could be gained from the separator material, the separator was omitted in subsequent insulation systems.

The panels were installed on the tank with only a small gap between adjacent panels, but with much wider spaces at the panel edges adjacent to the tank end flanges and the corkboard insulation on the tank edges (fig. V-2). These wide spaces were filled with foam, but the gap between panels was left void. All joints between panels and between panels and other surfaces were sealed by cover strips of MAM laminate and adhesive.

The constrictive-wrap material was selected on the basis of ease of application, as mentioned earlier. Nylon yarn was used at a load of 0.75 pound per strand, which corresponds to a strain of 1.25 percent. This gave a wrap density of 160 strands per inch, wound at a helical angle of 1°. A 20-strand yarn was used for the winding, which required eight forward and reverse helical circuits. Typical application of a wrap is shown in figure V-3. The silicone resin (Dow Corning Silicone A-4000) applied during the winding was chosen because of its favorable high-temperature properties and room-temperature curing ability.

System 2. - Fabrication details for this system were about the same as those given in figure V-2 except that the insulation panel sizes were somewhat different (see table V-II). The circular-segment tanks could accommodate the full size panel width that was established for the full-scale Centaur tank but only about two-thirds of the length (see ch. VII). Two panels were therefore bonded to each side of the tank; one was the full width of a Centaur panel, and the other was a narrow fill-in strip. Joints between the insulation panels were filled with 1/4-inch-wide polyurethane foam strips and covered with the MAM sealing laminate.

It was felt that a slight heat short from the external surface to the tank wall, caused by the high-conducting aluminum foil in the MAM sealing laminate, existed along the panel edges in system 1. As a result, the edge channels used for system 2 were formed of Mylar only. Permeability characteristics of the edge-channel material are not as critical as those of the face sheet, since in the application of the panels to the tank MAM laminate cover strips were placed over all panel-to-panel joints and panel-to-tank joints. These cover strips acted as an additional seal. The Mylar edge channels proved to be an effective seal in the short-duration liquid-nitrogen checkout tests.

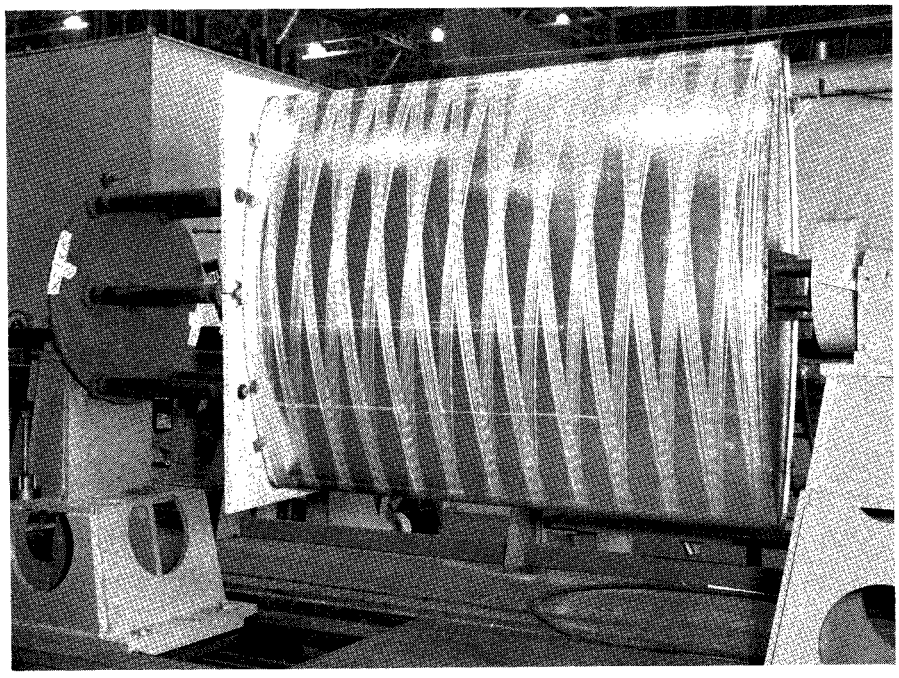

(a) Partial wrap.

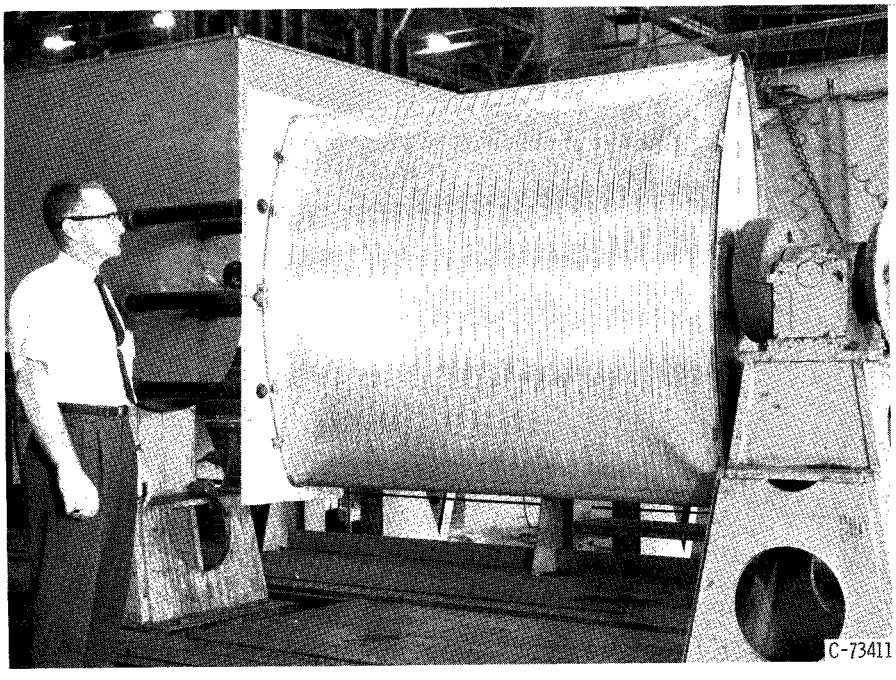

(b) Completed wrap.

Figure V-3. - Application of constrictive wrap on circular-segment tank by large filament winding machine. Insulation system 2.

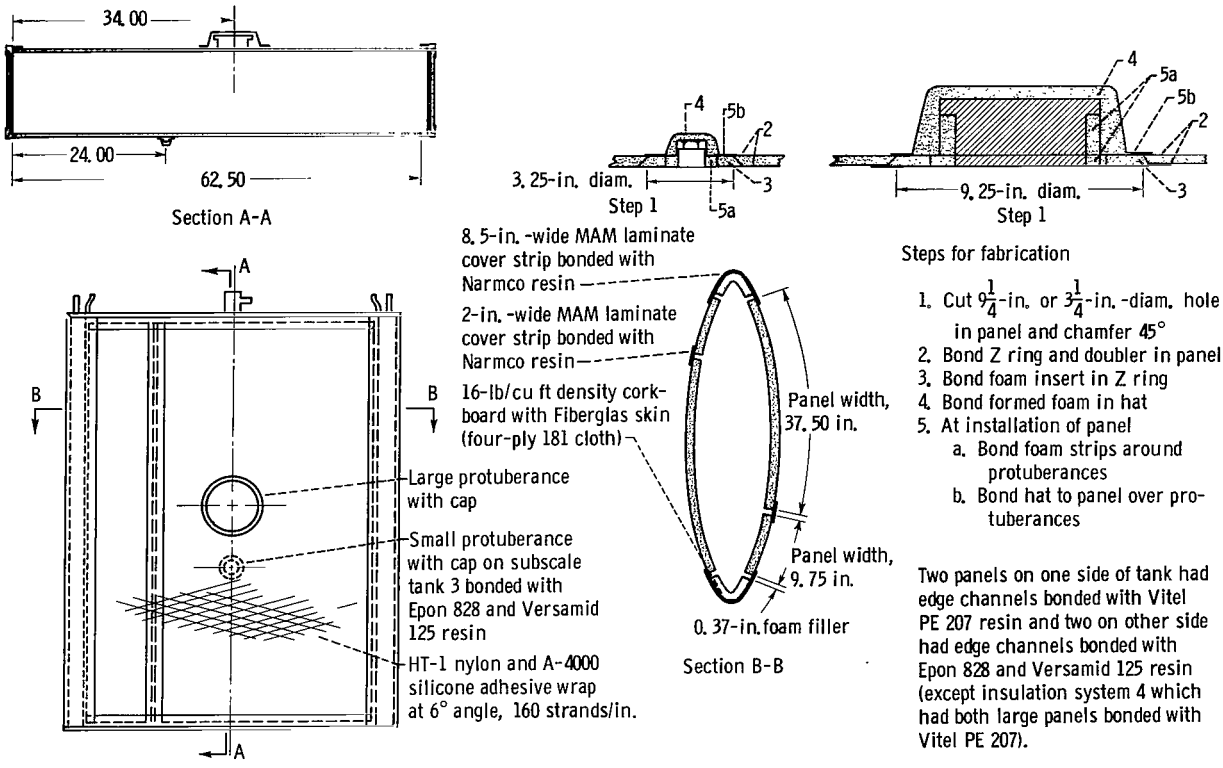

Figure V-4. - Fabrication details for insulation system 3.

The constrictive-wrap and binder materials were the same as for system 1. The wrap angle, however, was increased from 1° to 6°. The wrap angle was altered on this tank in anticipation of a problem that would be encountered on insulation system 3, which would include typical tank protuberances that penetrate through the insulation panel. Protuberances interrupt the winding pattern and cause areas of insulation on each side (circumferentially) of the protuberance that are unsupported. Increasing the wrap angle reduces the unsupported area.

System 3. - Fabrication details for this system are shown in figure V-4. The main objective in the fabrication and testing of this system was to determine the fabrication problems and thermal effects of typical tank protuberances through an insulation panel. A small protuberance simulating one of a large number of instrumentation fittings on the Centaur tank was placed on one side of the tank. A large protuberance simulating fill and drain lines on the Centaur tank was placed on the opposite side of the tank. Fabrication details of the insulation system for these protuberances are shown in figure V-4, along with the steps in fabrication. The Z and hat sections used around the protuberances were spun for an aluminum-Mylar-aluminum laminate 0.005 inch thick. Photographs of these protuberances on the tank after completion of the insulation are shown in figure V-5.

Panel size was the same as for system 2. The panel sealing laminate was changed from the 0.0024-inch-thick film to the thinner film (0.0015 in.).

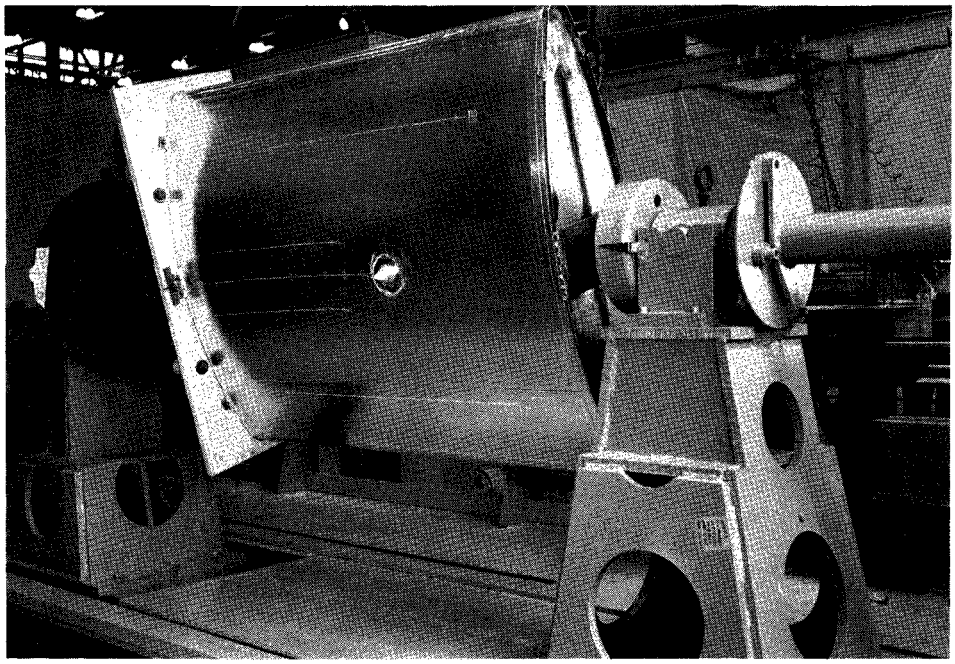

(a) Small protuberance.

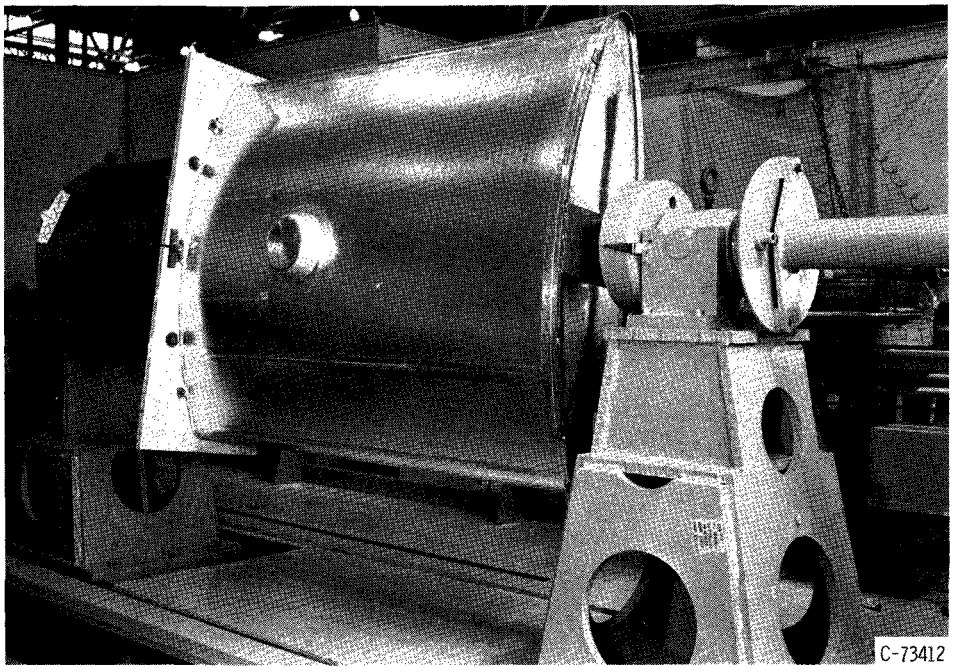

(b) Large protuberance.

Figure V-5. - Insulated protuberances through insulation panels. Insulation system 3.

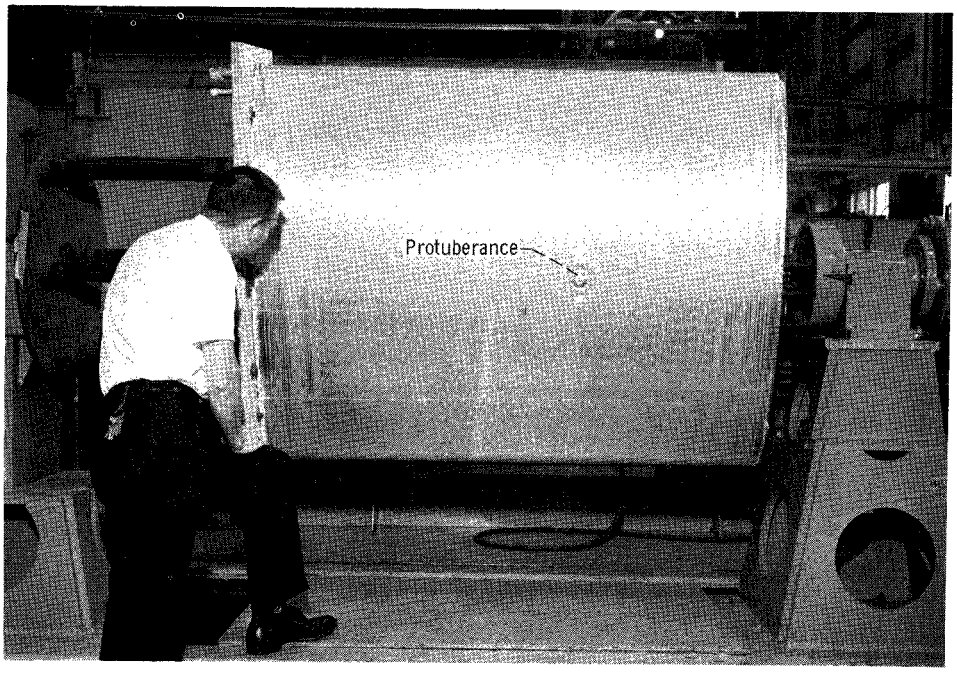

(a) Plan view.

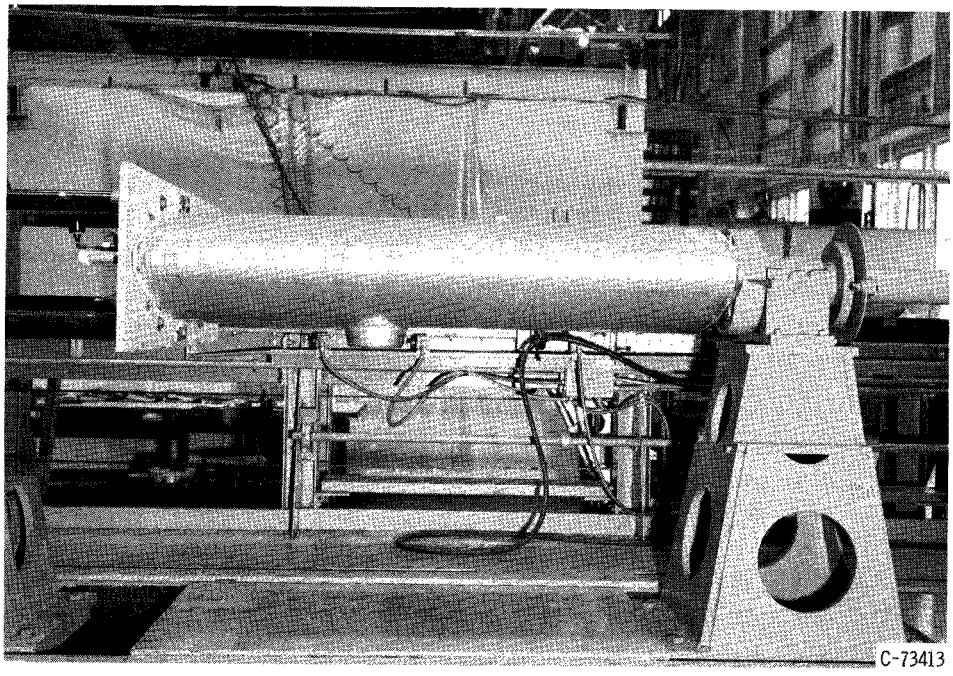

(b) Edge view.

Figure V-6. - Wrap pattern around protuberances. Insulation system 3.

Tests with previous system 2 (to be discussed later) revealed a leak in the perimeter bond around one of the panels. Therefore, 100 percent bond area of the panels to the tank was used.

The constrictive-wrap material and the procedure were unchanged from system 2. Triangular-islands of unsupported insulation were left by the interference of the protuberance, as shown in figure V-6. A technique to eliminate the unsupported areas is discussed in chapter VI, but it was not necessary to use the technique here because the system was not subjected to aerodynamic forces.

System 4. - Fabrication details for this system were essentially as shown in figure V-4 for system 3, but there were no protuberances. The main difference between this system and the previous systems was the use of fiber glass for the constrictive wrap. The strand breakage problem was overcome by using an epoxy-resin-preimpregnated glass roving (see ch. VII). The untreated roving had been breaking because of damage to the filament in the roving caused by pulleys and other rubbing surfaces on the winding machine. The preimpregnated material protected the filaments and eliminated fraying of the roving when individual filaments occasionally failed. The wrap was applied with 0.84 percent strain and with an eight-strand roving at 64 strands per inch.

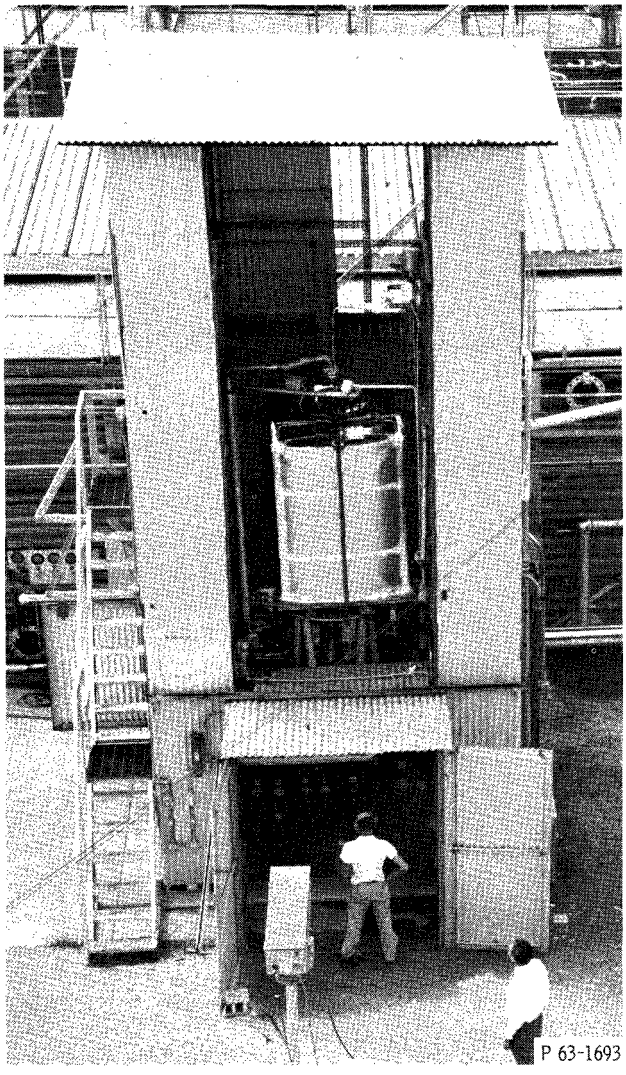

Figure V-7. - Circular-segment tank mounted in atmospheric test facility for ground-hold testing. Insulation system 1, immediately after test.

This system represented the final selection of materials, fabrication, and quality control techniques that was to be used for the full-scale Centaur tank insulation application.

APPARATUS AND PROCEDURE

Test Facilities

Two test facilities, an atmospheric test stand and a vacuum chamber, were used to evaluate the insulation systems on the circular segment tanks.

Atmospheric test stand. - The insulated circular-segment tanks were initially tested in the atmospheric test stand shown in figure V-7 (described in ref. 1). The liquid-hydrogen flow system used in the atmospheric test stand was the same as

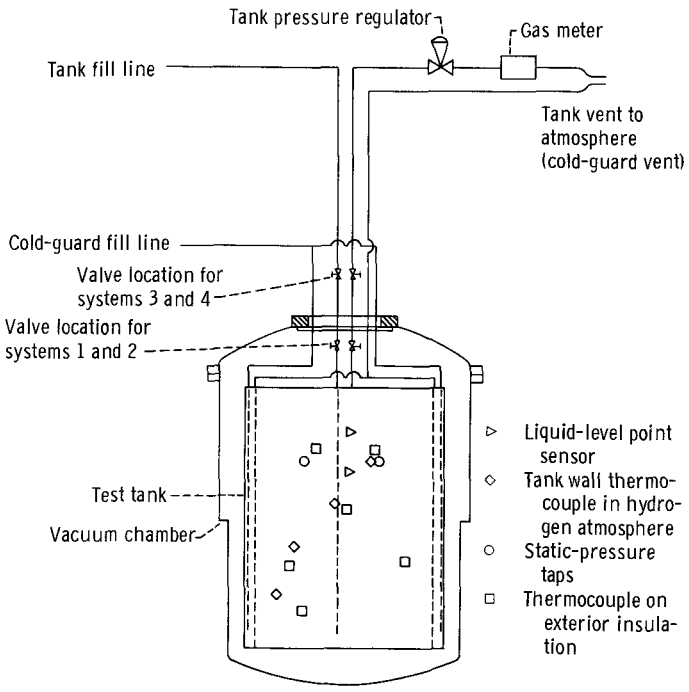

Figure V-8. - Diagram of flow system and instrumentation used for testing of insulation systems on circular-segment tanks in vacuum chamber.

that for the vacuum-chamber facility. These tests simulated ground-hold conditions where structural performance and equivalent thermal conductivity of the various insulation systems were determined. Test operations were conducted from a remote area for safety.

Vacuum chamber. - Following the tests in the atmospheric test stand, the test tanks were installed in a vacuum chamber (shown in fig. V-8) to observe the effects of quasi-simulated launch conditions. A mechanical vacuum pump provided a drop in pressure, while aerodynamic heating of one side of the insulation surface was simulated by infrared heating lamps. Aerodynamic forces that are present during launch were not simulated. The results of simulated heating with aerodynamic forces are presented in chapter VI.

Forty infrared quartz tubes having a power input of 30 kilowatts were mounted on an aluminum reflector contoured to conform to the tank radius. The arrangement of the heating lamps on the reflector is shown in figure V-9. The surface to be heated was painted black to increase its absorptivity.

A comparison of the simulated and computed (ch. II) pressure changes and surface-temperature changes (aerodynamic heating) for a typical launch trajectory is shown in figure V-10. The chamber pressure reduction was uncontrolled and did not quite match the calculated profile. The simulated surface-temperature profile was well matched to the calculated profile by use of manual off-on operation of the infrared lamps while the surface temperature was monitored.

The liquid-hydrogen flow system used is shown in figure V-8. Note the location of the two cryogenic valves in the vacuum chamber. These valves were required to maintain a pressure of 5 pounds per square inch gage, which prevented buckling of the tank walls. Early in the investigation it was believed buckling could possibly occur from the stresses imposed on the tank walls by the constrictive wrap.

Just prior to the tests reported herein, the vacuum-chamber facility had undergone extensive modifications in height and vacuum capabilities to accommodate another test program. The facility was further modified for this test program by the incorporation of the infrared heating lamps. Such extensive modifications would normally require a checkout of the facility before it was

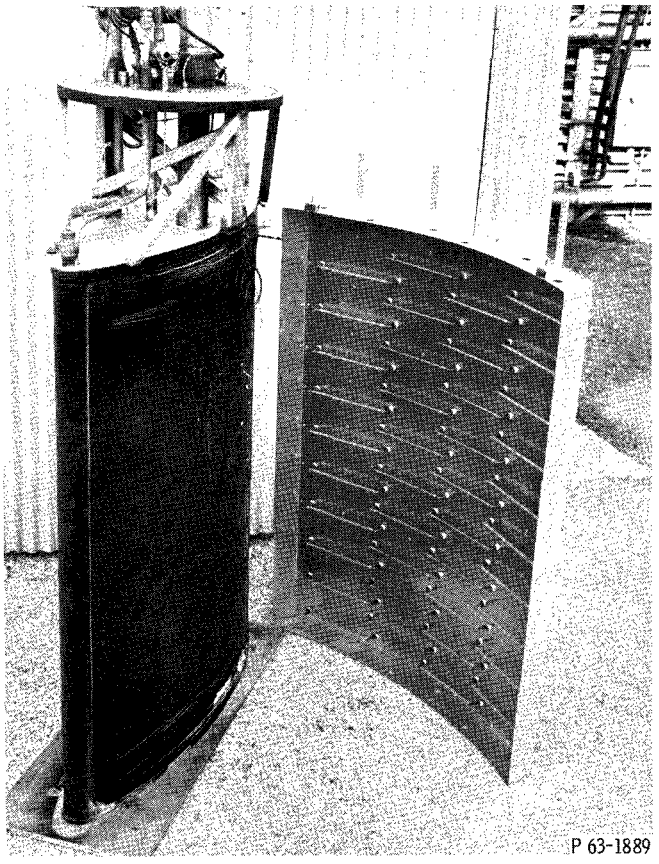

Figure V-9. - Infrared heating lamp assembly for simulating aerodynamic heating of insulation surface on circular-segment tanks. (Insulation surface painted black)

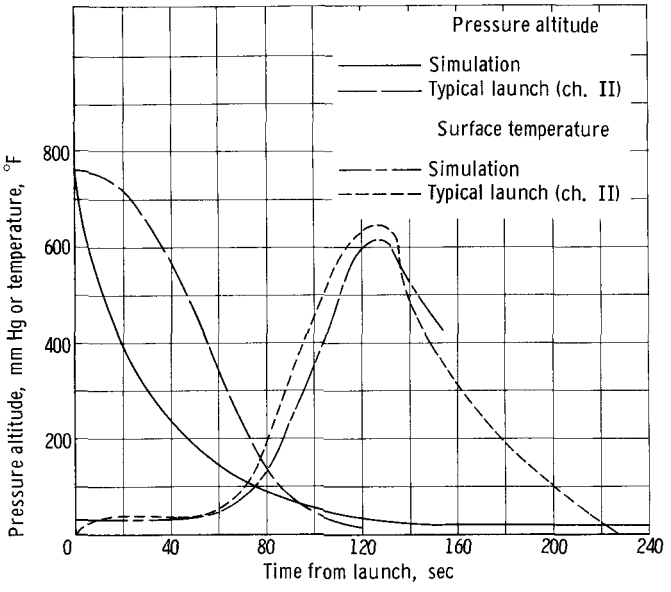

Figure V-10. - Typical launch simulation of pressure altitude and surface temperature in vacuum chamber used to test insulation on circular-segment tanks.

used for testing. A complete checkout would have required the use of an instrumented, insulated tank filled with liquid hydrogen. An insulated tank other than the circular-segment test tanks was not immediately available, so the capabilities and operation of the facilities were checked with the insulated circular-segment test tanks. This approach was deemed necessary because of a heavy test schedule for the facility. This procedure resulted in some problems in evaluating the constrictive-wrap insulation systems and produced changes in the test procedure for each circular-segment test tank.

Instrumentation

The circular-segment tanks were instrumented to determine the structural and thermal performance of the insulation systems. Total flow of boiloff gas was read from a gas meter in the vent line (fig. V-8), while the flow rate was determined at fixed time intervals by use of the gas meter and a stopwatch. During the surface heating tests in the vacuum chamber, the rapid changes of flow rate were recorded by a movie camera that photographed the rotating dials on the meter. Gas temperature at the meter, used in the calculation of the mass flow rate, was measured with a copper-constantan thermocouple.

Surface temperatures were measured on the outside of the insulation and on the inside walls of the tank with copper-constantan thermocouples. The number and the location of thermocouples varied from tank to tank depending on the insulation configuration and the results of previous tests. The number of thermocouples on the outer insulation surface varied from 5

to 10. Typical locations are shown on figure V-8. Epoxy adhesive with a cover patch of MAM laminate was used to attach the thermocouple to the insulation.

On insulation systems 2, 3, and 4, static-pressure taps (two on each side) were installed on the outer surface of the tank side walls with leads running to the top through the inside of the tanks (fig. V-8). These taps were used to determine if any leakage of air into the area between the tank walls and the insulation panels occurred from cryopumping.

Liquid levels near the full point were indicated by hot-wire point sensors mounted through the vent tube with a support extending into the top of the tank (fig. V-8). This level was used as a starting point for the boiloff period.

Test Procedure

Ground-hold thermal tests. - Tanks mounted on the atmospheric test stand were filled with liquid hydrogen, and were allowed to stabilize at a constant pressure to eliminate transient effects before any thermal data were taken. Initially, it also was planned to fill the cold guard tubes at the edges with liquid hydrogen, but because of their small volume and high heat leak, this was found to be impossible. However, a constant flow of liquid and gas maintained a temperature near the saturation temperature of liquid hydrogen at the edges, to eliminate any significant heat leak through the edges into the main tank.

Following the stabilization period, the liquid hydrogen was allowed to boil off at constant pressure until the tank was empty. The volume flow rate of boiloff gas was recorded at 5-minute intervals during the approximately 2 hours required for the tank to boil dry. Visual inspection of the insulation was made immediately following the end of the boiloff period.

Simulated launch tests in vacuum chamber. - Before filling a tank in the vacuum chamber with liquid hydrogen, considerable purging of the chamber with gaseous nitrogen was performed to ensure against the presence of a combustible mixture, in case a hydrogen leak should occur. Considerable care was exercised when purging the vacuum tank because of the unknown effects of pressure excursions on the insulated test tank. An increase in external pressure along with the load imposed by the constrictive wrap might collapse the tank, while a decrease in external pressure might rupture the insulation system prematurely. Purging was accomplished by alternately increasing the pressure slightly with gaseous nitrogen and venting to amospheric pressure several times. Purging of the test tank was accomplished by several cycles of pressurization to 15 pounds per square inch gage with helium and venting to 5 pounds per square inch gage. A 5-pound-per-square-inch-gage minimum pressure was maintained to ensure that the tank did not collapse because of the constrictive wrap. After the tank was filled with liquid hydrogen, the system was allowed to come to thermal equilibrium before tests were conducted. Following this period, the launch sequence of pressure drop and surface heating was performed. The volume flow rate of boiloff gas was measured by a gas meter and was recorded during these tests through the use of a motion picture camera. Visual inspection of the insulation could not be made until the tank was removed from the chamber several hours following the tests.

THERMAL PERFORMANCE DATA REDUCTION

The thermal performance of the insulation system was measured in terms of an equivalent thermal conductivity K_{equiv}. The method used to obtain K_{equiv} from the boiloff tests is basically that presented in reference 2 and is outlined in this section.

A heat balance on the volume of liquid in the tank indicates that the total heat input to the liquid hydrogen Q_T is the sum of the heat inputs through the insulation panel Q_I and the insulated tank ends Q_{ext} or

$$Q_T = Q_I + Q_{ext} \tag{1}$$

where

Q_T total heat input to liquid hydrogen as determined from boiloff data, Btu/hr

Q_I heat input to liquid hydrogen through insulation side panels, Btu/hr

Q_{ext} extraneous heat leaks through ends of tank, Btu/hr

If it is assumed that

(1) The heat transfer across the insulation is one dimensional

(2) The heat transfer across the bottom lid of the tank is constant

(3) The ullage gas recovers all the heat transferred through the insulation above the liquid

the heat input through the side walls is given by the one-dimensional Fourier law as

$$Q_I = \frac{K_{equiv} A_I (T_I - T_c)}{\Delta x} \tag{2}$$

where

K_{equiv} equivalent thermal conductivity of insulation system, (Btu)(in.)/(hr)(sq ft)(^{o}R)

A_I sidewall wetted surface area, sq ft

T_I outside insulation skin temperature, ^{o}R

T_c temperature of saturated liquid hydrogen, ^{o}R

Δx thickness of insulation system, in.

Substituting equation (2) into equation (1) gives

$$Q_T = \frac{K_{equiv} A_I (T_I - T_c)}{\Delta x} + Q_{ext} \tag{3}$$

For steady-state conditions, the temperature difference across the insulation $T_I - T_c$ is constant, and since the insulation thickness Δx is also constant, equation (3) is the equation of a straight line, that is,

$$Q_T = C_1 A_I + Q_{ext} \tag{4}$$

where C_1, the slope of the line, is

$$C_1 = \frac{K_{equiv} (T_I - T_c)}{\Delta x} \tag{5}$$

The total heat input to the liquid hydrogen Q_T is given by the product of the mass flow rate boiled off at the liquid-vapor interface and the heat of vaporization of the liquid. If it is assumed that steady-state conditions exist between the liquid-gas interface and the gas meter, then the mass flow rate is the product of the volume flow rate at the gas meter and the density of the gas at the meter. The density of the gas is determined from the gas temperature at the meter by assuming the ideal gas equation of state at a pressure of 1 atmosphere. The assumption of steady-state conditions in the volume between the liquid-gas interface and the gas meter requires that the total mass of gas in the volume remain constant with time. Changes in gas pressure and/or gas temperature, unless they compensate each other, produce a change in total mass in the volume and thus an erroneous value of the heat flow rate to the

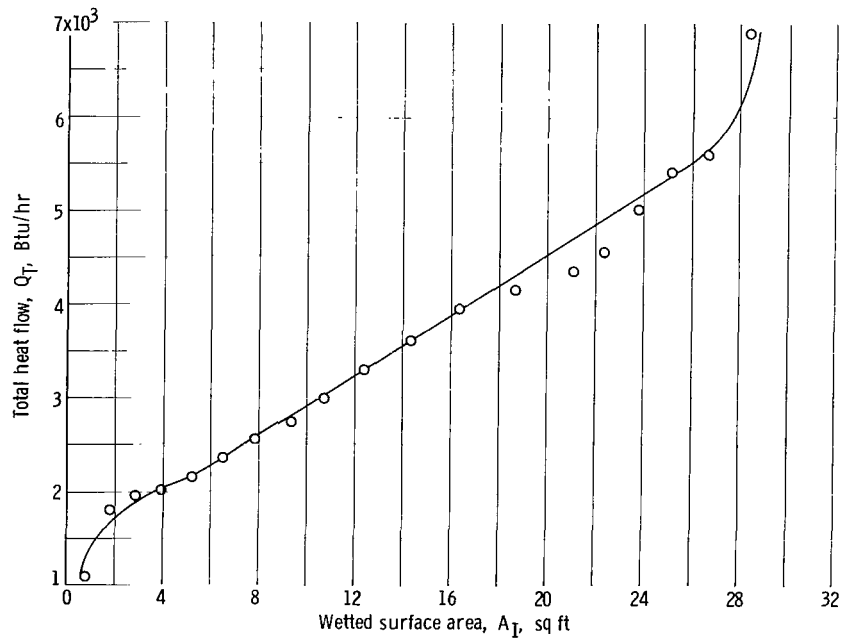

Figure V-11. - Typical results of ground-hold thermal performance test. (Insulation system 2, test B.) Temperature difference, 450° F; equivalent thermal conductivity of system, 0.14 (Btu)(in.)/(hr)(sq ft)(°R); slope of line C_1, 160 Btu/(hr)(sq ft).

liquid. For a constant gas temperature, an increase in gas pressure because of an increase in atmospheric pressure results in an indicated value of heat flow to the liquid that is too low, and vice versa.

From equation (4), it can be seen that, if Q_T, as determined from the boiloff data, is plotted against A_I, which is a function of the cumulative volume boiled off, the result is a straight line, and the equivalent thermal conductivity K_{equiv} can be determined from the measured slope of the line C_1 and equation (5).

Figure V-11 is a plot obtained from the data on system 2 illustrating the linear relation between total heat flow Q_T and wetted area A_I.

RESULTS AND DISCUSSION

The results of the ground hold and quasi-simulated launch tests are summarized in table V-III. Also included in this table are the distinguishing features of the individual insulation systems and variations in the test procedures.

Insulation System 1

The first system consisted of three small insulation panels on each side of the tank with no foam fillers between panels and with a nylon constrictive wrap wound at a 1^o helix angle. The panel edge channels were of 0.0024-inch-thick MAM laminate.

The heat flux to the liquid hydrogen during ground-hold tests of this system was 200 Btu per hour per square foot. The average outside insulation skin temperature was 47^o F. The equivalent thermal conductivity for the system was 0.17 (Btu)(in.)/(hr)(sq ft)(^{o}R). This value of equivalent thermal conductivity is slightly higher than the average value of 0.14 (Btu)(in.)/(hr)(sq ft)(^{o}R) measured in the thermal-conductivity apparatus (see ch. III). This may be due in part to the high heat shorts caused by the MAM-laminate edge channels, as is indicated in figure V-7 (p. 51) by the frost deposits over the panel joints.

A visual observation immediately following the test revealed that one of the panels had blistered in a small area because of a gas pressure buildup between the polyurethane foam and the outer sealing laminate. Pressure in the blister relieved itself after a short time. No evidence of a leak between the outer tank wall and inner sealing laminate was observed during the ground-hold test.

After the ground-hold test, insulation system 1 was installed in the vacuum tank with the nonblistered side of the tank facing the infrared lights. When the tank was filled with liquid hydrogen, a hydrogen leak into the vacuum chamber was detected, and the test was aborted. The leak was presumed to be in the cryogenic valves located inside the vacuum chamber (see fig. V-8, p. 52). The tank was then filled with liquid nitrogen and the test completed. The test

TABLE V-III. - SUMMARY OF RESULTS OF GROUND-HOLD AND QUASI-SIMULATED LAUNCH TESTS

Insulation system	Significant features of insulation system	Type of test (a)	Thermal performance: Heat flux, Btu/(hr)(sq ft)	Thermal performance: Average outside insulation temperature, °F	Thermal performance: Equivalent thermal conductivity, (Btu)(in.)/(hr)(sq ft)(°R)	Sealing performance: Within panel	Sealing performance: Behind panel	Heating effects	Remarks
1	Nylon constrictive wrap at 1° helix angle; three small panels per tank side; no foam filler strips in gap between panels; panel edge channels of 0.0024-in.-thick MAM; perimeter bond of panels	A - Ground hold with liquid hydrogen	200	47	0.17	One panel blistered	Satisfactory	None	----------
		B - Simulated launch with liquid nitrogen	---	--	----	No detrimental effects noted on unheated side due to depressurization; blister did not grow in size		Outside MAM laminate and constrictive wrap ruptured under unknown temperature (fig. V-12); temperature estimated above 700° F	----------
2	Nylon constrictive wrap at 6° helix angle; one large and one small panel on each side of tank; foam filler strips between panels; panel edge channels of 0.002-in.-thick Mylar; perimeter bond of panels	A - Ground hold with liquid hydrogen	150	30	0.13	One panel blistered	One panel bulged away from tank during warmup	None	----------
		B - Ground hold with liquid hydrogen	160	50	0.14	No additional blisters or increase in size	Bulging did not reoccur	None	----------
		C - Simulated launch with liquid nitrogen	---	--	---	No effects of depressurization noted		Nylon constrictive wrap ruptured under unknown temperature (fig. V-14); MAM laminate unaffected	----------
		D - Simulated launch with liquid nitrogen; heat applied to reverse side of tank from test C	---	--	----	No effects of depressurization, even in area where wrap was destroyed in test C		Nylon wrap frayed in one small spot (fig. V-15); maximum insulation temperature 650° F	----------
3	Nylon constrictive wrap at 6° helix angle; panel sizes same as in system 2; two protuberances, one large, one small, on opposite sides of tank; thinner MAM laminate (0.0015 in.) than used in previous systems; 100 percent adhesive bond between panels and tank	A - Ground hold with liquid hydrogen	165 to 185	27	0.15	One panel blistered; pressure did not relieve itself; blister punctured and patched (figs. V-16 and V-17)	Satisfactory	None	One panel damaged and repaired before testing; repair satisfactory
		B - Simulated launch with liquid hydrogen	---	--	----	Patched blister redeveloped and enlarged (fig. V-18); no other effects of depressurization noted		Maximum temperature, 620° F; no damage to constrictive wrap; MAM laminate developed several small horizontal slits	Areas unsupported by wrap near protuberances showed no damage
4	Same as system 3 except no protuberances, constrictive wrap was fiber glass at a helix angle of 6°, and perimeter plus grid pattern was used to bond panels to tank walls	A - Ground hold with liquid hydrogen	165	30	0.12	One panel blistered	Satisfactory	None	----------
		B - Simulated launch with liquid hydrogen	---	--	----	No effects on unheated side due to depressurization		Maximum temperature, 620° F; fiber-glass wrap in excellent condition; MAM laminate developed 13-in. long by 1/32-in. wide vertical slit in large panel; MAM laminate separated from foam and bulged out between wrap near bottom of tank but not ruptured (fig. V-20)	----------
		C - Simulated launch with liquid hydrogen; heat applied to reverse side of tank from test B	---	--	----	No obvious effects due to depressurization		Maximum temperature, 835° F; fiber-glass wrap in excellent condition; MAM laminate ruptured in small areas near bottom of tank (fig. V-21(a)); foam expanded and bulged out between wrap (fig. V-21(b)); adhesive under cover strips melted	----------
		D - Ground hold with liquid hydrogen	315	-10	0.31	Seal destroyed in test C		None	Seals on panels damaged during previous tests

[a] In chronological order.

Figure V-12. - Insulation system 1 after being subjected to simulated launch tests. Maximum surface temperatures unknown.

was only partially successful. Most of the lamps in the two center rows (fig. V-9, p. 53) failed to operate. Unfortunately, all the insulation skin thermocouples including the one for the heating control, were located in this unheated region. As a result, a large portion of the insulation surface was subjected to a high unknown temperature, which caused the nylon constrictive wrap and outer MAM laminate seal to rupture as shown in figure V-12. In two small areas, upper and lower left corners of tank, the foam cracked and separated from the MAM laminate and fell out. Visual inspection of the unheated side, especially the blister that developed during the ground-hold test, indicated that rapid depressurization did not affect the insulation. Thermal performance of the insulation was not determined for this test, since liquid nitrogen was used in place of liquid hydrogen.

In order to determine the temperature limit of the nylon con-

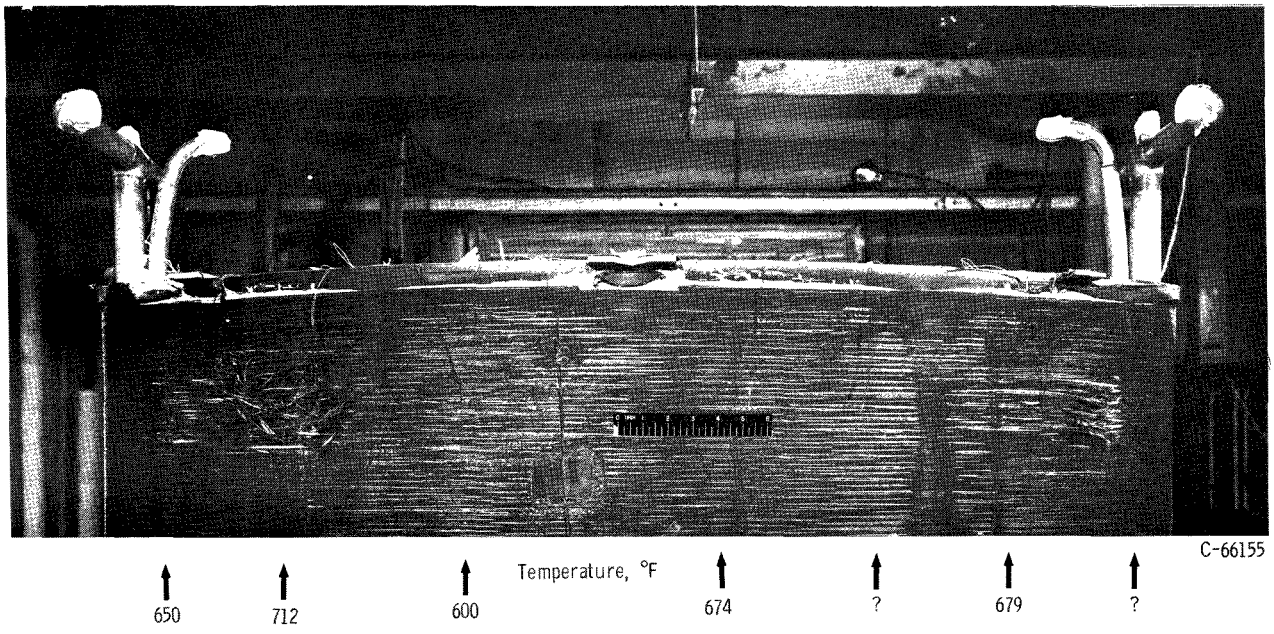

Figure V-13. - Results of small patch tests to determine nylon-constrictive-wrap rupture temperature. Insulation system 1.

strictive wrap, heating tests on 1-square-foot sections of the good side of the test tank were made later under atmospheric conditions. The results of the tests are shown in figure V-13. The nylon constrictive wrap ruptured in the temperature range from 675° to 700° F.

Insulation System 2

Insulation system 2 consisted of one large and one small panel on each side of the tank with foam filler strips between panels. The nylon constrictive wrap was wound at a 6° helix angle. The edge channels for system 2 were 0.002-inch-thick Mylar.

Two ground-hold tests (A and B, table V-III) were run with system 2 to investigate any cyclic effects on the insulation system from repeated fills. Heat flux to the liquid hydrogen during test A was 150 Btu per hour per square foot. The average outside insulation skin temperature was 30° F, and the equivalent thermal conductivity was found to be 0.13 (Btu)(in.)/(sq ft)(°R).

Inspection of the insulation after completion of test A revealed a blistered area in one of the large panels, and as the tank warmed up, one of the panels bulged out from the tank wall, which indicated that gas had been cryopumped into the space between the insulation panel and tank wall. The blister covered an area of about 1 square foot and appeared to be somewhat different from the blister that occurred on insulation system 1. The blister on system 1 felt as though it was gas filled, while the one on system 2 had the feel of being filled with crushed ice. When the pressure behind the bulged panel was relieved through the pressure tap on the tank side wall, the nylon constrictive wrap forced the panel back solidly against the tank wall with no apparent damage to the panel. As a result of this leak, a full adhesive bond between the insulation panel and the tank wall was used on insulation system 3.

After the tank had completely warmed up following test A, it was refilled with liquid hydrogen and another boiloff test B was conducted. The heat flux to the liquid during test B was 160 Btu per hour per square foot. The average outside insulation skin temperature was 50° F, and the equivalent thermal conductivity was 0.14 (Btu)(in.)/(hr)(sq ft)(°R). No additional blistering was observed following test B, and the bulge did not reoccur. Since the heat flux and the equivalent thermal conductivity from both tests were in general agreement, it was concluded that the observed damage to the panels (blistering and bulging) due to leakage during the first fill and warmup cycle had little effect on ground-hold thermal performance. The equivalent thermal conductivity for this insulation system is slightly lower than that for system 1. This may be a result of the use of Mylar as edge channels or of the change in panel configuration, which resulted in less panel joint length on system 2.

Insulation system 2 was subjected to two simulated launch tests (C and D, table V-III) with liquid nitrogen as the test liquid. During the first test (C), the insulation outer surface thermocouple system failed, and the insulation was subjected to an unknown high temperature. As with insulation system 1, the nylon wrap was ruptured as shown in figure V-14. The MAM laminate was wrinkled but remained intact, and the bond between the MAM laminate and the

Figure V-14. - Damage inflicted during first quasi-simulated launch test of insulation system 2. Maximum surface temperature unknown.

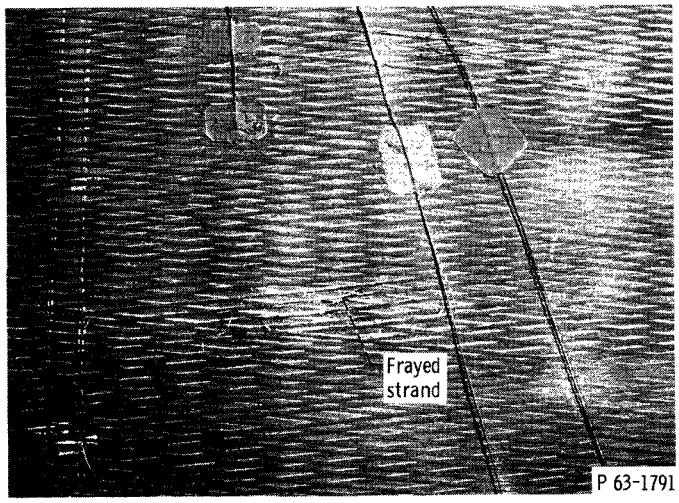

Figure V-15. - Second test side of insulation system 2 after being subjected to quasi-simulated launch tests.

foam was apparently not affected by the heat and decompression. The unheated side of the tank did not show any effect of the decompression either.

For test D, the tank was turned so that the undamaged insulation side of the tank was exposed to the infrared heating lamps. The maximum recorded insulation outer skin temperature for this test was 650° F. Damage to the insulation was very slight. The nylon yarn frayed in one small section, as shown in figure V-15. There was no apparent damage to the outer MAM laminate seal. No detrimental effects due to decompression were observed, even in the areas that were severely damaged during the first heating test.

After completion of tests on system 2, the insulation system was dissected. In the areas where the nylon constrictive wrap was undamaged, the yarns retained some tension, as was indicated by separation of the ends when they were cut. This was also observed on other tanks. Inspection of the blistered area showed that the bond between the foam and both MAM laminates had

failed, and the foam had warped and cracked.

Insulation System 3

The materials and the panel size in system 3 were identical to those in system 2, except that the sealing MAM laminate was reduced in thickness from 0.0024 to 0.0015 inch. In addition, two protuberances that penetrated the insulation panels were added, one on each side of the tank, and a 100 percent area adhesive bond was employed between panels and tank walls.

During installation of the tank for the ground-hold test, a small hole was inadvertently placed in the outer MAM laminate skin in the large panel on one side. Before testing, this hole was repaired in the field. The repair was made by cutting and peeling back some of the nylon constrictive wrap while other yarns were separated in a longitudinal direction to expose the hole in the MAM laminate. The hole in the MAM laminate was covered with a patch of MAM laminate and sealed with Vitel PE 207 adhesive. The severed nylon yarns were tied off to adjacent wrap strands and adhesive was applied to the area to prevent slipping of knots. The repaired area is shown in figures V-16 and V-17.

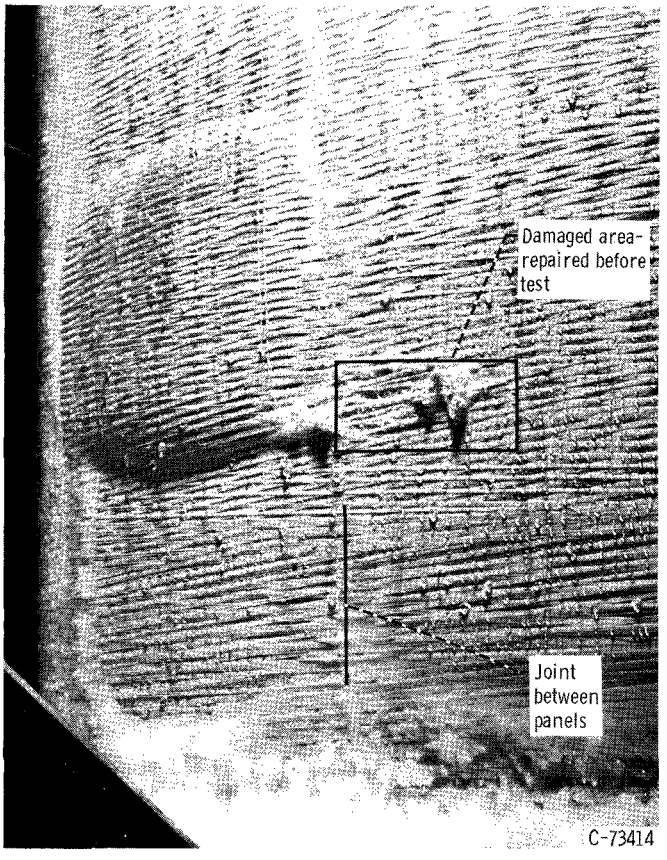

Figure V-16. - Panel blister caused by small leak into panel during ground-hold test. Insulation system 3, shown before pressure was relieved.

The boiloff data for the ground-hold test for system 3 exhibited some scatter for an unknown reason. Heat flux to the liquid varied from 165 to 185 Btu per hour per square foot. The average outside insulation temperature was 27° F, which gave an equivalent thermal conductivity of about 0.15 (Btu)(in.)/(hr)(sq ft)(°R).

Again one panel developed a blister during the warmup period immediately after the ground-hold test, as shown in figure V-16. The blister was in the small panel and was located next to the area in the large panel that had been repaired before the test. Pressure in the blister did not automatically relieve itself as the insulation warmed up, which indicated that the leak only occurred at cold temperature. The pressure was relieved by puncturing the MAM laminate. This puncture was repaired by a MAM laminate patch and Vitel PE 207 adhesive before the quasi-simulated launch test in the vacuum facility was made. The leak itself was not found. When the pressure in the

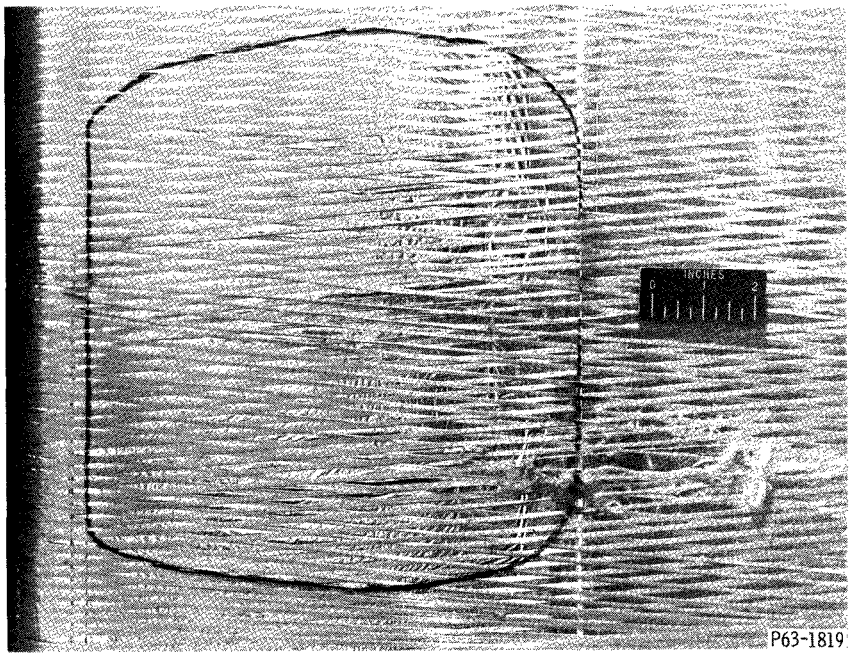

Figure V-17. - Panel blister after pressure was relieved by puncturing outer MAM laminate. Patch over puncture is in center of outlined area; insulation system 3.

blister was relieved the tension in the nylon wrap forced the MAM laminate back solidly against the foam, as shown in figure V-17. The area that was repaired prior to the tests did not exhibit any change after the test. This indicates that satisfactory field repairs can be made to the insulation system.

Bulging of panels similar to that which occurred on system 2 was not observed. The 100 percent area adhesive bond between panels and tank wall appeared to be effective in preventing cryopumping of air behind the panels.

Insulation system 3 was the first tank to use liquid hydrogen for both the ground-hold and the quasi-simulated launch tests. The maximum insulation outer surface temperature recorded during the simulated launch test was 620° F on the black painted surface. A thermocouple located on the outer surface of the protuberance that had not been painted black recorded a maximum temperature of 520° F. This temperature difference of 100° F results from the low value of absorptivity of the MAM laminate in its natural state.

Inspection of the heated side did not reveal any obvious damage to the nylon constrictive wrap. The MAM laminate on the heated side, however, had several small horizontal slits. This had not occurred on system 2, which was subjected to a slightly higher temperature (650° F). System 2 used a thicker MAM laminate (0.0024 in.) than system 3 (0.0015 in.).

The blister that developed during the ground hold test (figs. V-16 and V-17) was on the cold side during the simulated launch test. It became larger during the test. The increase in size is shown by the dark line in figure V-18. Enlargement of the blister is a further indication that the leak occurs only at cold temperatures.

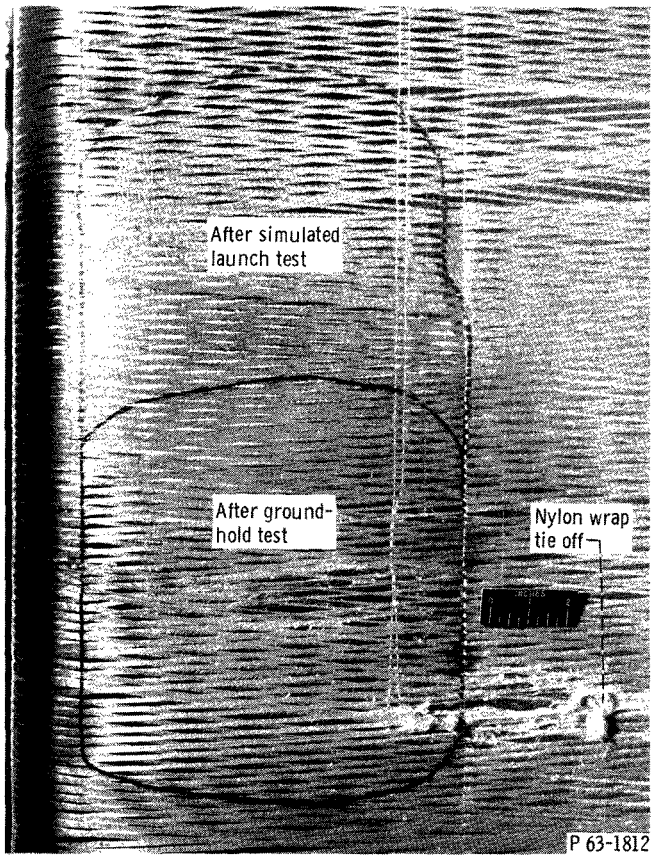

Figure V-18. - Increase in blister size after quasi-simulated launch test. Insulation system 3.

Insulation System 4

Insulation system 4 employed the same panel size and configuration as system 2. The thinner (0.0015-in.-thick) MAM sealing laminate was used in system 4. The constrictive wrap was fiber glass wound at a 6° helix angle. The 100 percent area bond between panels and tank walls of system 3 was replaced for system 4 with a perimeter and grid pattern (table V-II, p. 45).

Two ground hold boil-off tests (A and D, table V-III, p. 58) were made, one before the system was subjected to heating and the other following two heating cycles. The heat flux to the liquid hydrogen in test A was 165 Btu per hour per square foot. The average outside insulation skin temperature was 30° F, which gave an equivalent thermal conductivity of 0.12 (Btu)(in.)/(hr)(sq ft)(°R).

As with the previous three systems, one panel developed a blister during the test, but since there was no evidence of a leak into the area behind the panels, the perimeter and grid pattern of adhesive was considered successful. The blister occurred in one of the small panels. An attempt to find the leak on this tank was made before it was subjected to a simulated launch test. A hole was punctured through the outer MAM laminate in the vicinity of the blister. A vacuum tap flanged fitting was placed over the hole and secured with adhesive. A helium mass-spectrometer leak detector was attached to the fitting, and the insulation panel was surveyed with a jet of helium gas while the tank was at ambient temperature conditions. The leak was not located. The vacuum tap was then sealed for further tests.

Insulation system 4 was subjected to two quasi-simulated launch tests (B and C, table V-III); the first simulated the calculated insulation surface temperatures for a typical trajectory on one side of the tank (fig. V-10, p. 53), and the second simulated a much hotter trajectory on the other side of the circular-segment tank. The temperature histories for the two tests are shown in figure V-19. The maximum surface temperature measured during the first simulation (test B) was 620° F. The physical appearance of the insulation after the test is shown in figure V-20. The glass constrictive wrap was in excellent condition. The adhesive bond between the foam and the MAM laminate failed in some small areas near the bottom of the tank. The MAM laminate pushed out between the wrap but did not rupture. The outer MAM laminate on the large panel split

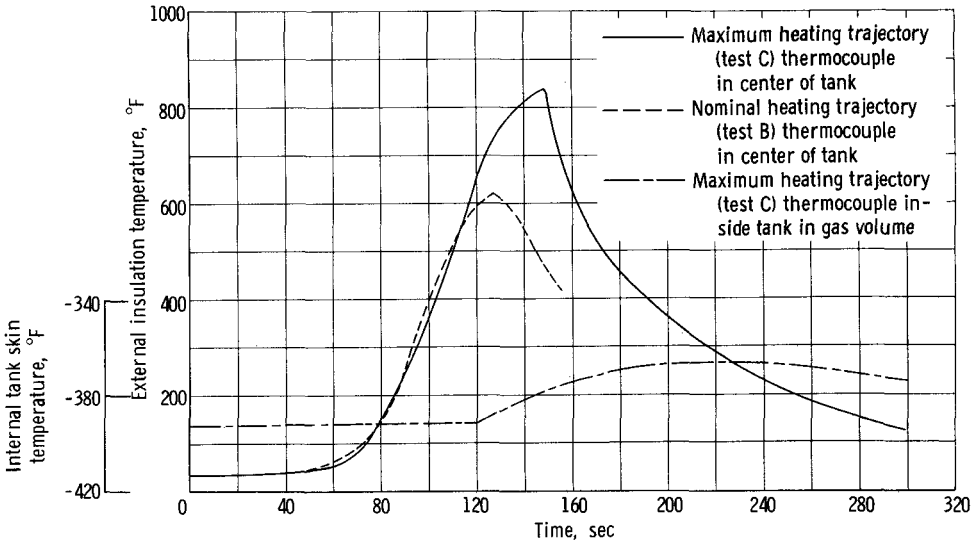

Figure V-19. - Surface temperatures plotted against time for simulated aerodynamic heating of insulation system 4.

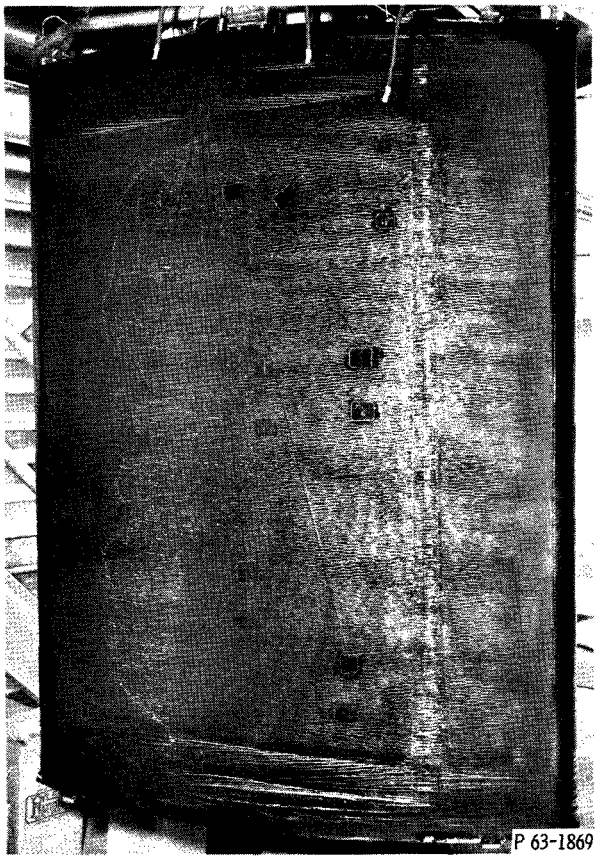

Figure V-20. - First side of insulation system 4 after being subjected to simulated launch surface temperature of 620° F.

near the tank midsection and along a line parallel to and near to the MAM laminate cover strip over the joint between the large and small panels. The length of the split was about 13 inches and its width was about 1/32 inch. No effects of rapid depressurization could be discerned.

Upon completion of a detailed examination of the physical condition of the insulation after test B, the tank was reinstalled in the vacuum chamber with the undamaged side of the tank oriented towards the heating lamps. This side was then subjected to a simulated launch (test C) to determine the effectiveness of the constrictive fiber-glass wrap at a higher temperature. The highest measured temperature for this test was 835° F (fig. V-19). The appearance of the tank after the test is shown in figure V-21(a). At this higher temperature a large portion of the black paint was removed, and the exposed Mylar was straw colored. The fiber-glass wrap, however, was not damaged. The adhesive used on the joint cover strip and the fiber-glass wrap softened and foamed up to form globules along the wrap and joint, as is shown in figure V-21(b). Damage

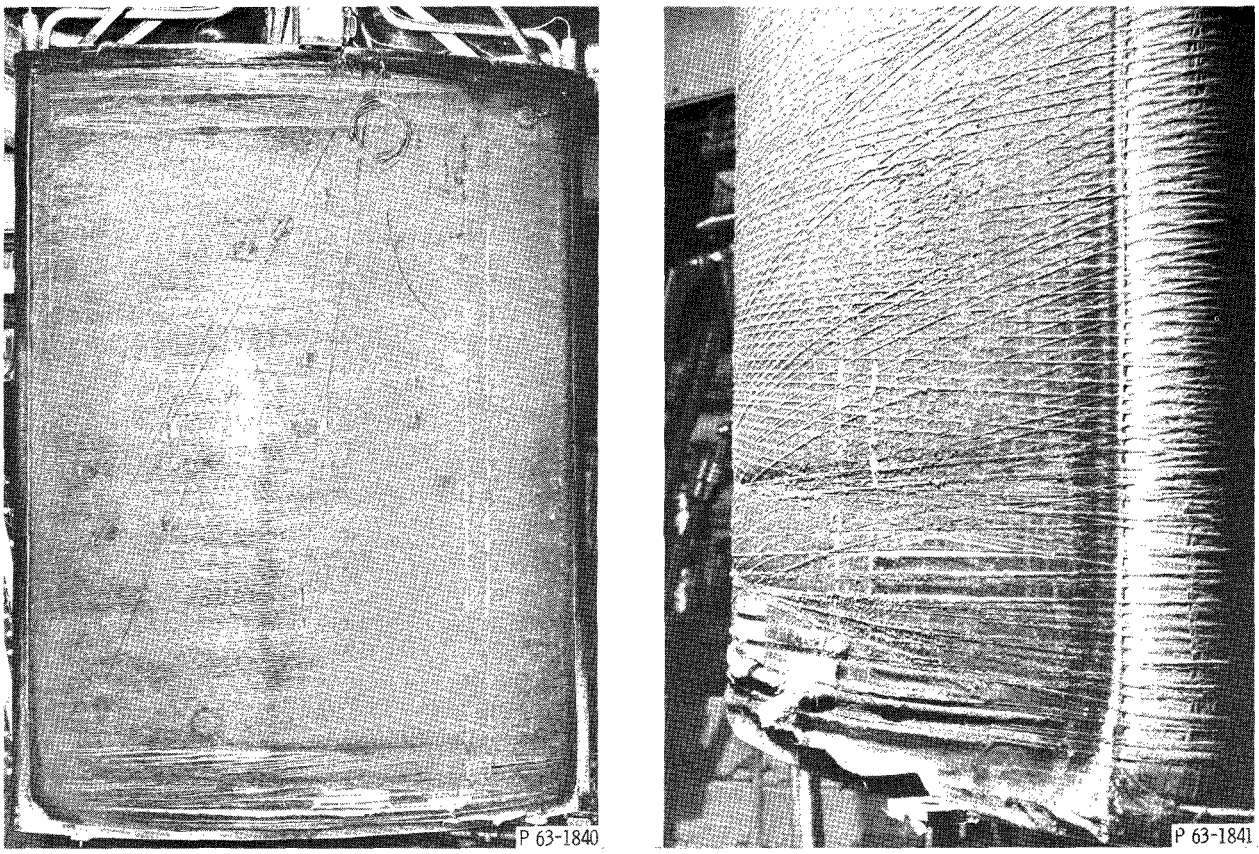

(a) Front view.

(b) Side view. Note expansion of foam and it being held in by fiber-glass constrictive wrap.

Figure V-21. - Second side of insulation system 4 after being subjected to simulated launch surface temperature of 835° F.

to the MAM laminate was confined mainly to the bottom of the tank, as noted for test B of system 4. In this case, however, damage was more pronounced. The bond between the MAM laminate and the foam failed again, and, in addition, the MAM laminate ruptured in two small areas. Failure of the insulation system along the bottom edge was probably the combined result of two factors. First, the constrictive wrap, because of inherent characteristics, has a more open pattern near the ends of the tank. Thus, the panels are not supported as much in these areas. Second, although both ends of the tank suffer from the first deficiency, the bottom received more damage because it was probably heated to a higher temperature than either the top or other areas where temperatures were measured. The excess heating was produced by a slightly unsymmetrical location of the infrared heating lamps on the reflector. The lamps in the bottom row (fig. V-9, p. 53) were slightly closer to the boxed end of the reflector than those at the top. Thus, reflection from the ends concentrated more heat energy per unit area at the bottom of the tank than at the top. Similar damage was not observed on the nylon-wrapped tanks, probably because of the fact that the wrap pattern was not as open for the nylon system. The fiber-glass system required only 64 strands per inch compared to 120 strands per inch of nylon to achieve the same compressive load on the insulation panels (table V-II, p. 45).

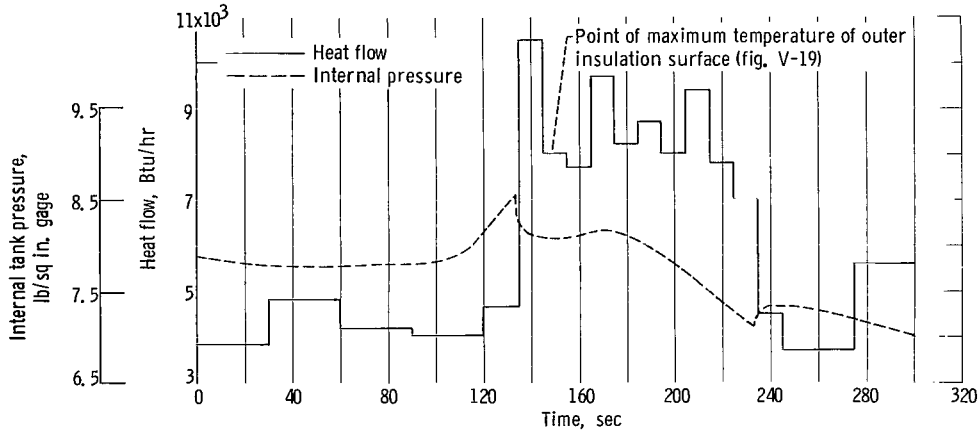

Figure V-22. - Heat flow and internal tank pressure during quasi-simulated launch test of insulation system 4 (table V-III, test C).

In addition to the MAM laminate separating from the foam and rupturing, the excessively high temperature also caused the foam to swell and bulge out beyond the fiber-glass constrictive wrap, as is shown in figure V-21(b). The fiber-glass wrap, however, was not damaged.

Approximate values of the heat flow rates to the liquid hydrogen during the second high-temperature simulated launch were determined from periodic measurements of liquid boiloff. These heat flow results, as a function of time, are shown in figure V-22. The corresponding outer-insulation skin temperatures are shown in figure V-19 (test C).

The heat flow rate measurements shown are approximate because the changes in tank pressure also shown in figure V-22 were not taken into consideration when calculating the heat flow rate from the boiloff-vent gas flow rate. An explanation for the tank pressure changes, especially the rapid changes at 133 and 233 seconds, cannot be given. The effect of pressure changes on the determination of heat flow rate to the liquid by the method used herein is discussed in the THERMAL PERFORMANCE DATA REDUCTION section. The data are presented, however, to indicate the magnitude of the change in heat flow rate with an increase in outer-insulation temperature and to indicate the time lag of the heat flow behind the outer-insulation temperature. The heat flow rates to the liquid during the first part of the simulated launch were between 3800 and 4800 Btu per hour and were slightly lower than those measured with full tanks in the ground-hold boiloff tests (fig. V-11, p. 56). The high heat flow rate starting at 135 seconds was due primarily to the sudden decrease in pressure occurring at 133 seconds. The heat flow rates indicated just prior to that time are probably too low because of the slow increase in tank pressure. The heat flow rate to the liquid remained high (approx. 8500 Btu/hr) for a considerable period of time after the outer insulation skin temperature had reached its peak value of 835° F at 149 seconds and cooled off. This high heat flow rate was partially due to the slow decrease in pressure during this period, while the remainder was caused by the temperature lag in the insulation as a result of its heat capacity. The magnitude of this temperature lag is indicated by the temperature curve shown in figure V-19 for a thermocouple located on the inside of the tank wall and

and above the liquid. This temperature peaked about 90 seconds after the maximum outer skin temperature. The peak temperature was about -367° F. This temperature time lag of the insulation is greater than that which was computed in chapter II for a typical launch trajectory. The sudden decrease in heat flow rate at 235 seconds, shown in figure V-22, was the result of the sudden pressure rise at 233 seconds.

After the system was subjected to the two quasi-simulated launch tests (tests B and C, table V-III) described previously, it was subjected to another ground-hold boiloff test (test D, table V-III). The heat flux was about 315 Btu per hour per square foot. The outside insulation skin temperature was -10° F, which gave an equivalent thermal conductivity of 0.31 (Btu)(in.)/(hr)(sq ft)(°R). Although this test has no practical significance, since an insulation system for a boost vehicle will not have to function under ground-hold conditions after being subjected to aerodynamic heating, it does indicate that the insulation, especially the outer MAM sealing laminate, can be moderately damaged without producing a catastrophic failure.

SUMMARY OF RESULTS

The results of the evaluation of the insulation system using subscale tanks in ground-hold and quasi-simulated launch conditions can be summarized as follows:

1. Changes in design and construction (panel bonding, protuberances, and panel edge seals) had little effect on the thermal performance within the accuracy of the measurements.

2. The thermal performance of the insulation measured in tank tests was essentially the same as that measured in the thermal conductivity apparatus.

3. Both HT-1 Nylon and S/HTS Fiberglas were found satisfactory for the constrictive wrap; however, the fiber glass has the capability of operating at higher temperatures.

4. A perimeter plus grid pattern of bonding the insulation panels to the tank was found to be as satisfactory as a full bond area in preventing cryopumping of air behind the panels.

5. A hermetically sealed foam panel insulation system withstood the external pressure decay associated with a launch trajectory without being damaged.

6. In all tests conducted, some leaks were found in the hermetic seals of the insulation panels. The effects of these leaks were localized, and within the accuracy of the measurements, the leaks had little or no effect on the insulation system thermal performance.

REFERENCES

1. Perkins, Porter J., Jr.: Experimental Study Under Ground Hold Conditions of Several Insulation Systems for Liquid-Hydrogen Fuel Tanks of Launch Vehicles. NASA TN D-2679, 1965.

2. Brown, Edmund H., and Arnett, R. W.: Insulation for Liquid Oxygen Tanks. Rep. 5A229, NBS, Feb. 29, 1956.

CHAPTER VI

AERODYNAMIC HEATING TESTS OF SEVERAL VARIATIONS OF INSULATION SYSTEM

by Reeves P. Cochran, Volodymyr O. Bazarko, and Robert W. Cubbison

Lewis Research Center

Insulation systems for boost vehicles must provide adequate thermal protection for both ground hold and the launch trajectory. One of the prime considerations during launch is to maintain the structural integrity of the insulation system during the time that high aerodynamic heating rates and high dynamic pressures are being encountered. This chapter describes the results of tests conducted to evaluate the ability of the lightweight constrictive-wrap sealed-foam insulation system to withstand conditions similar to those encountered during launch.

Aerodynamic heating tests were conducted on several variations of the insulation system in the subsonic exhaust jet of a turbojet engine and in transonic and supersonic (up to Mach 2) airstreams in the Lewis Research Center 8- by 6-foot supersonic wind tunnel. The maximum temperatures and dynamic pressures encountered in these tests exceeded those of the assumed typical launch trajectory, although the airflow velocities were usually below trajectory conditions. Specimens of the insulation were mounted on liquid-nitrogen-filled model tanks and exposed to gas or air temperatures up to 840° F and dynamic pressures up to 1300 pounds per square foot. Eight specimens were investigated. Four variations of the insulation system and two methods of handling the constrictive wrap around external protuberances were included.

DESCRIPTION OF INSULATION SYSTEM VARIATIONS INVESTIGATED

The basic lightweight constrictive-wrap insulation system is described in chapter I. Specimens of several variations of this system were tested. These variations represent a progressive development of the insulation system based on the results of successive aerodynamic heating tests. In all of these variations, the core and sealant materials described in chapter I were used in making the sealed insulation panels. The differences among the several variations investigated were in the nature of the exposed (outer) surface of the insulation, in the treatment of the seam areas between adjacent panels, and in the materials and wrapping methods for the constrictive wrap. Detailed descriptions of these variations in the insulation system are given in the following sections.

Mylar-Aluminum-Laminate (MAM) Covering

The insulating component of this system consists of a polyurethane foam core encapsulated in a sealant covering of the 0.0015-inch-thick Mylar-aluminum laminate (MAM) discussed in previous chapters. Sealed panels of this type are bonded adhesively to the propellant tank and further supported by a pretensioned constrictive wrap of fiber-glass or nylon filaments to form the basic insulation system. A cross-sectional schematic view of this basic system is shown in figure VI-1(a). The space between adjacent panels (seam area) is filled with a polyurethane-foam filler, which is sealed with a MAM cover strip bonded to the foam filler and to the two panels. All the variations of the insulation system considered herein are essentially adaptations and improvements of this basic system.

Glass-Cloth Protective Layer

The MAM sealant covering has a published temperature limitation of approximately 500° F. To provide a better temperature- and erosion-resistant covering for the foam insulation, a layer of glass cloth can be added to the basic insulation system. There are two possible locations for this glass-cloth layer. It can be placed within the sealed panel (between the foam and the MAM sealant coat, as shown in figure VI-1(b)), or it can be used as an outer coating for the sealed panels, as shown on figure VI-1(c). In the internal location the glass cloth would provide protection to the foam even if the MAM sealant covering were destroyed, and, since it would be adjacent to the foam, the glass cloth would not be dislodged if the MAM covering deteriorated. This arrangement does not, however, provide continuous protection in the seam areas between adjacent panels. With the glass-cloth layer as an outer covering for the insulation, (external location) protection for the foam insulation is continuous.

Combination of Sealed and Unsealed Panels

Application of heat to the polyurethane foam core of the insulation will cause the release of trapped gas. When released within a sealed panel in the insulation system, this gas can cause the outer surface (MAM laminate, glass cloth, and constrictive wrap) to bulge. To determine whether a completely-sealed-foam panel is the most advantageous, a combination of sealed- and unsealed-foam panels, such as shown in figure VI-1(d) was investigated. With this combination, the unsealed-foam can release gas through the glass cloth (which is permeable) while the sealed foam underneath is still at a temperature sufficiently low to prevent release of gas. With the proper ratio of thicknesses between sealed and unsealed panels, no cryopumping of air into the unsealed panel will occur during holding time on the launch pad.

Glass-Cloth Reinforcement in Unconstricted Area Around Protuberances

The 6° helix angle wrapping pattern (described in ch. VII) used for the

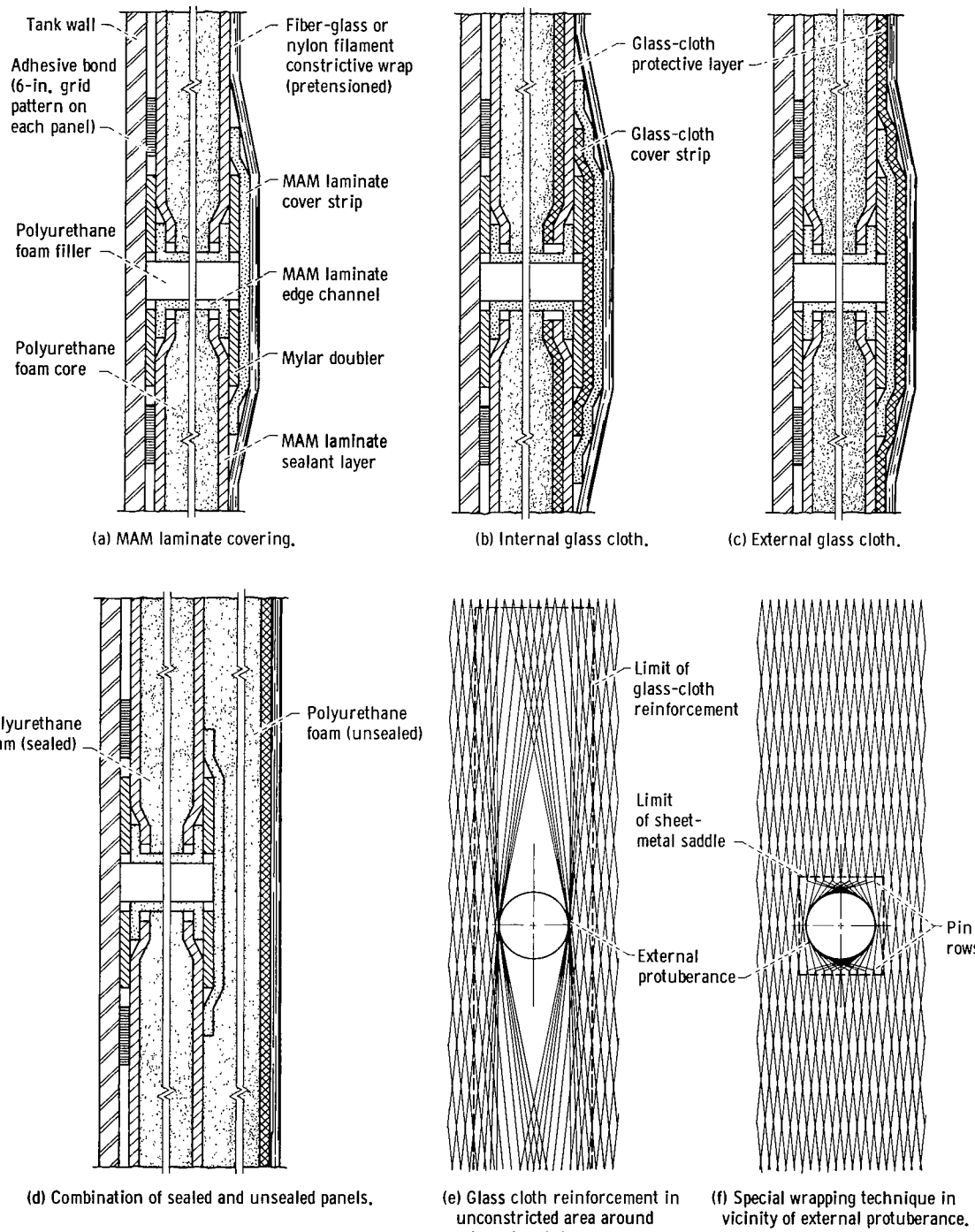

(a) MAM laminate covering.

(b) Internal glass cloth.

(c) External glass cloth.

(d) Combination of sealed and unsealed panels.

(e) Glass cloth reinforcement in unconstricted area around external protuberance.

(f) Special wrapping technique in vicinity of external protuberance.

Figure VI-1. - Variations of lightweight constrictive-wrap insulation system. (schematic view, not to scale.)

constrictive wrap is interrupted by the presence of external protuberances on the propellant tank. Protuberances can cause unconstricted areas such as shown in figure VI-1(e). One way to protect such an area is to add a layer of heavy glass cloth prior to wrapping so that the reinforcing glass cloth is anchored around the edges of the unconstricted area by the filaments of the wrap as shown in figure VI-1(e).

Special Wrapping Technique Around Protuberance

To avoid large-scale interruption of the constrictive-wrap pattern due to external protuberances, the special wrapping technique illustrated in figure VI-1(f) can be used. This technique has also been described in reference 1. A row of pins spaced to match the wrapping pattern is provided on two opposing sides of the protuberance. The pins are mounted on a sheet-metal saddle to maintain the proper spacing. Each filament of the wrap that would otherwise pass over the protuberance is bent around a pin in one of the rows, passed around the side of the protuberance, and then bent around a corresponding pin in the opposite row, and thereby returned to the original helical path.

APPARATUS AND PROCEDURE

Simultaneous duplication of the flight Mach number and temperatures and pressures imposed on the insulation in a complete launch trajectory is very difficult to achieve in ground tests. Therefore, some simulation of actual conditions must be used. It is believed that the insulation surface temperature and the dynamic pressure in the airstream are the most important environmental factors affecting insulation durability; however, standing shock waves generated at supersonic velocities by protuberances may also affect the insulation. To evaluate the effects of these factors, test specimens of the variations of the insulation system previously described were mounted on liquid-nitrogen-filled model tanks and exposed to the environments of the exhaust gas stream of a turbojet engine and the transonic-supersonic airstream (Mach 0.5 to Mach 2) of a wind tunnel. The apparatus for the subsonic and the transonic-supersonic tests are shown in figures VI-2 and VI-3, respectively. Figure VI-4 shows a general comparison of the gas and air temperature and dynamic pressure conditions available in the engine jetstream and the wind tunnel with the predicted insulation surface conditions of the typical launch trajectory from chapter II.

Subsonic Aerodynamic Heating Tests

Test setup. - A turbojet engine mounted in an airplane was used to generate a hot gas stream for the subsonic aerodynamic heating tests (see fig. VI-2(a)). A wheeled stand, carrying a model tank on which specimens of the insulation system were mounted, was positioned on a guide rail behind the engine exhaust nozzle in line with the jetstream. Variations in gas temperature and pressure for the tests were obtained by varying the distance between the tank and the engine exhaust nozzle. An instrument and observation station

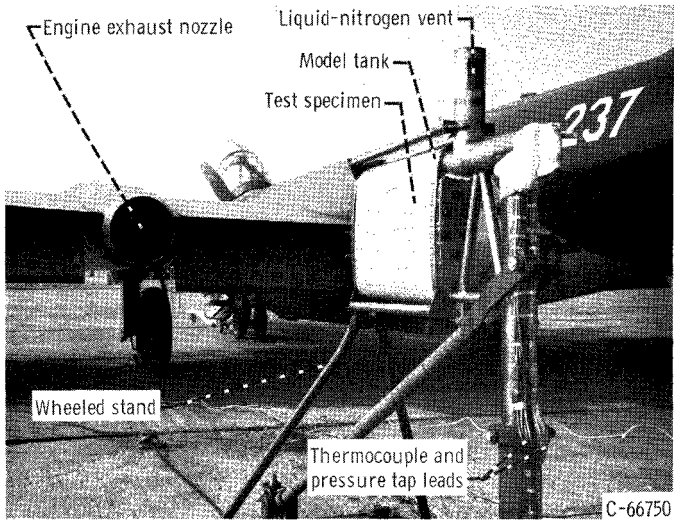

(a) Test setup using exhaust jetstream of turbojet engine.

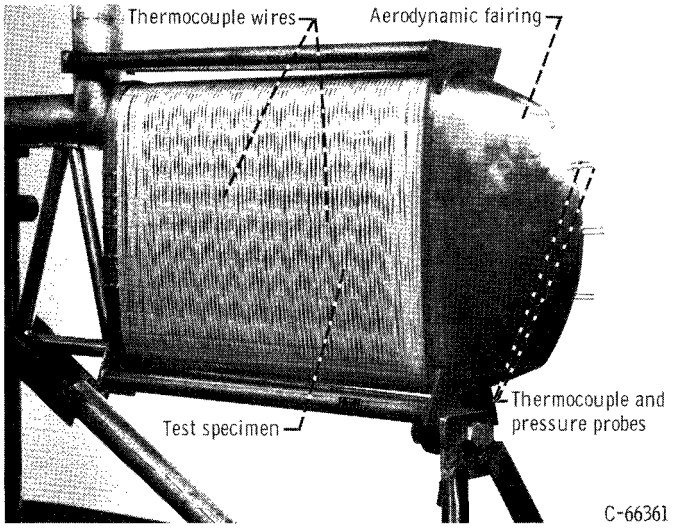

(b) Model tank.

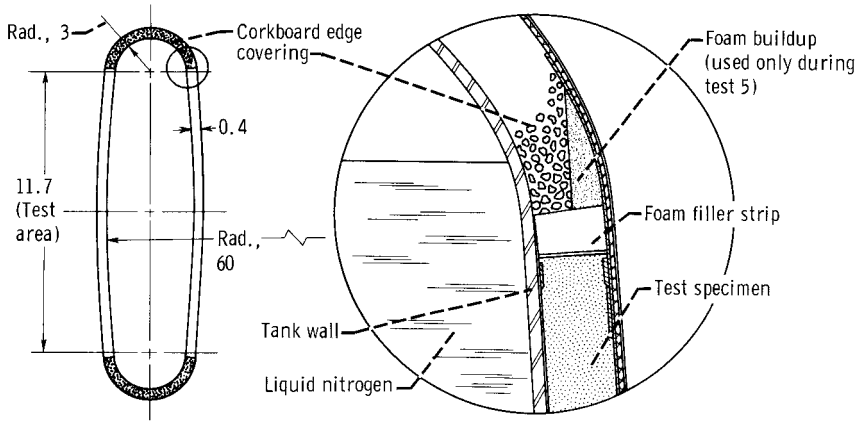

(c) Cross section of test tank and details of insulation mounting. (Dimensions in inches.)

Figure VI-2. - Apparatus for subsonic aerodynamic heating tests.

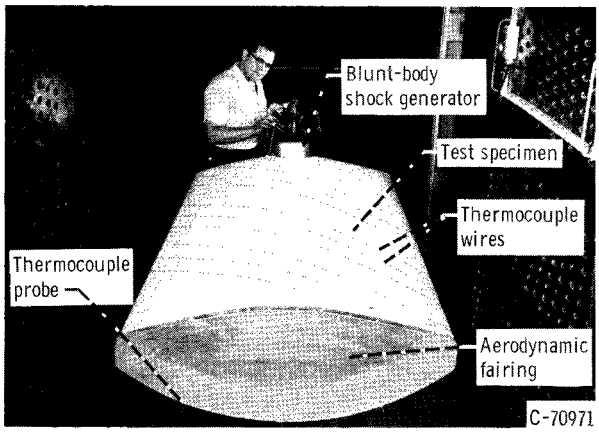

(a) Model tank with blunt-body shock generator installed in wind tunnel.

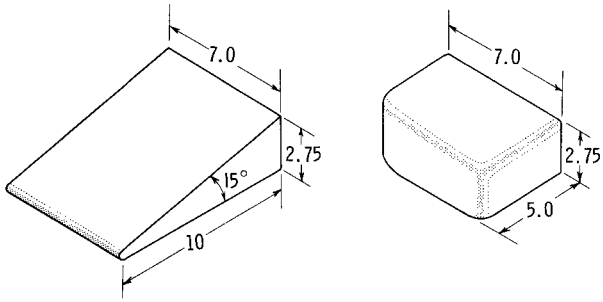

(b-1) 15° Wedge.

(b-2) Blunt body.

(b) Shock generators. (Dimensions in inches.)

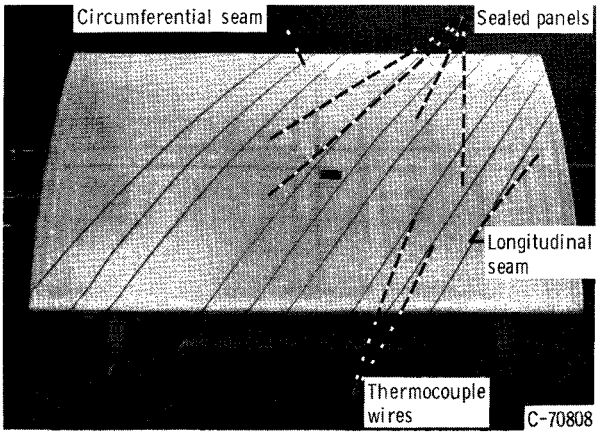

(c) Insulation specimen 7 mounted on lower surface of model tank.

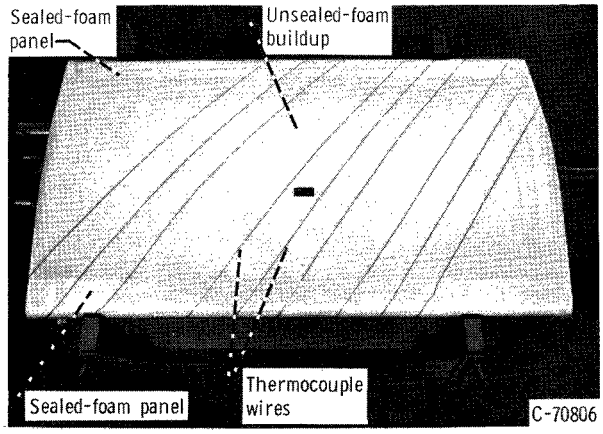

(d) Insulation specimen 8 mounted on upper surface of model tank.

Figure VI-3. - Apparatus for transonic-supersonic aerodynamic heating tests.

was located a safe distance from the test site. Flexible extensions on the instrument lead systems connected the model tank to recording instruments at this station.

Model tank. - The model tank for the subsonic tests is shown in figure VI-2(b). This tank had a 60-inch radius of curvature on the sides (fig. VI-2(c)) to match that of the liquid-hydrogen tank of the Centaur vehicle. Corkboard insulation of the same thickness as the test specimens was used on the small-radius portions at the top and bottom of the tank to withstand the large crushing load generated by the tensioned filament wrap in the small-radius turn.

Specimens of the several variations of the insulation system were installed successively on the tank. The insulated tank was mounted on a wheeled stand, which could be adjusted in height and horizontal location to position the tank correctly in the jetstream. An aerodynamic fairing for the forward end of the tank (fig. VI-2(b)) was an integral part of the test stand. A large vent (seen at the top of the vertical mast in fig. VI-2(a)) was provided for the test tank to accommodate rapid boiloff of the liquid nitrogen should the insulation

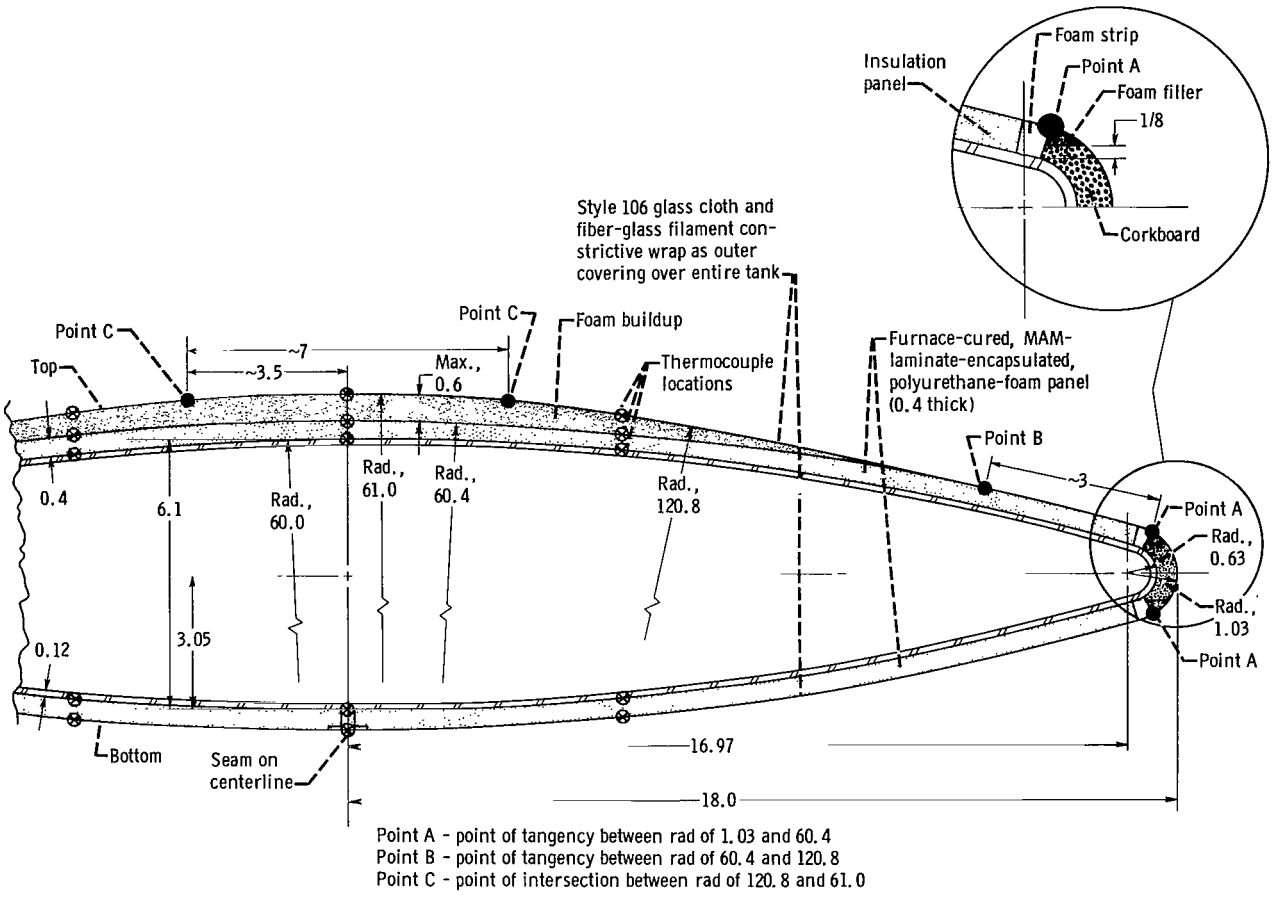

(e) Insulation details. (Dimensions in inches.)

Figure VI-3. - Concluded. Apparatus for transonic - supersonic aerodynamic heating tests.

experience a catastrophic failure while under the influence of the jetstream environment.

The model tank was equipped with temperature and pressure instrumentation to measure conditions in the jetstream, on the surface of the insulation, between layers of insulation (for the combination sealed and unsealed case only), and in the liquid-nitrogen compartment. Three total-temperature probes and three total-pressure probes were mounted on the leading edge of the aerodynamic fairing at the forward end of the test tank (see fig. VI-2(b)). The thermocouples used to measure outer insulation surface temperatures were installed under the constrictive wrap in varying patterns. All thermocouples were connected to appropriate recording potentiometers, and the pressures were measured on gages or manometer tubes.

Test specimens. - The test specimens for the subsonic aerodynamic heating tests were samples of the insulation system which, in materials and configuration, duplicated the variations proposed in figure VI-1. The total thickness

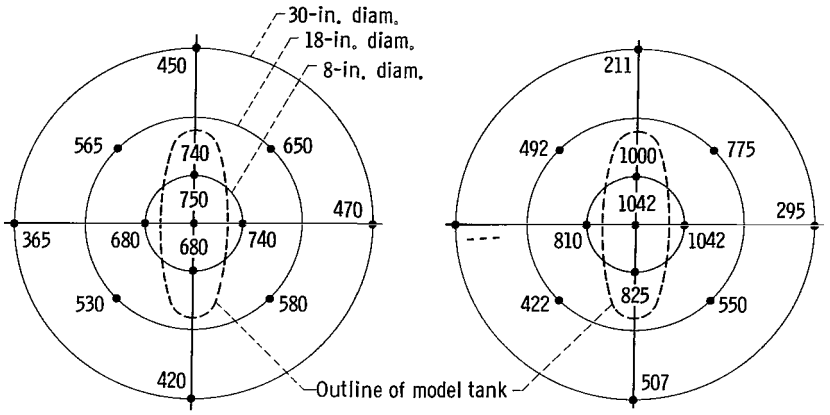

(a-1) Gas total-temperature survey. (Temperatures in ^{o}F.)

(a-2) Gas dynamic pressure survey. (Pressures in lb/sq ft.)

(a) Sample survey point measured with instrumented rake in engine exhaust jetstream.

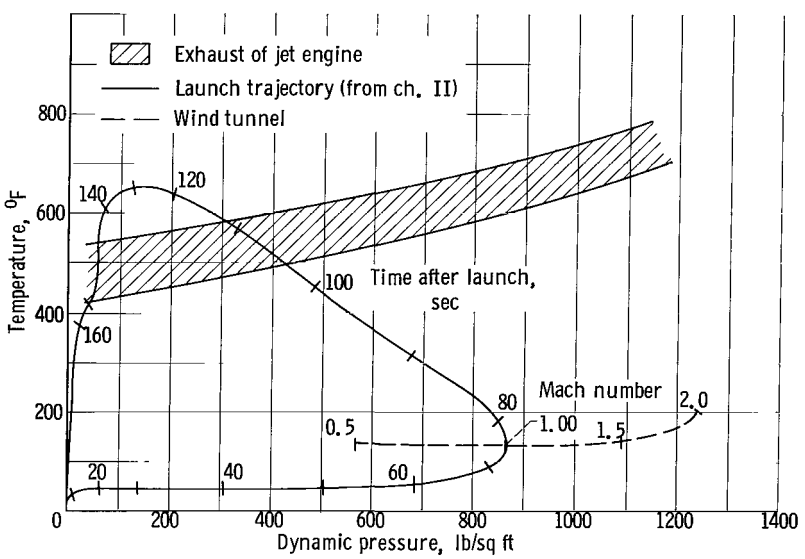

(b) Comparison of conditions in engine jetstream and wind tunnel with predicted insulation surface conditions for typical launch trajectory from chapter II.

Figure VI-4. - Temperature and dynamic pressure conditions in test environments and in typical launch trajectory.

of each specimen was 0.4 inch. The test specimens are described as specimens 1 to 6 in table VI-I and are pictured individually in figures VI-5(a) to VI-10(a). The sealed-foam panels of the test specimens were bonded with an adhesive resin to the 60-inch-radius sides of the test tank. The test area was approximately 20.0 inches long, 11.7 inches wide, and 0.4 inch thick. The specimens installed in this area were made either as two equal size panels with a central longitudinal seam or as a single panel. The panels were installed with a foam filler strip at the top and bottom edges to form a seam between the panel and the corkboard (see fig. VI-2(c)). Depending on the specimen being tested, the joints between the corkboard and the insulation panel were covered in the same manner as the joints shown in figures VI-1(a) to (d). A constrictive wrap of

TABLE VI-I. - DESCRIPTION OF TEST SPECIMENS

Specimen	Name	Description (a)	Shown in figures -
b_1	MAM-laminate covering	Polyurethane-foam core encapsulated in MAM-laminate sealant covering; central longitudinal seam; high-strength-plastic constrictive wrap	VI-1(a) and VI-5(a)
b_2	Internal glass cloth	Polyurethane-foam core with layer of style 106 glass cloth bonded to outer face; core encapsulated in MAM-laminate sealant covering; single panel; fiber-glass-filament constrictive wrap; glass-cloth cover strip over seam not included	VI-1(b) and VI-6(a)
b_3	External glass cloth	Polyurethane-foam core encapsulated in MAM-laminate sealant covering; single panel; outer surface of sealed panel covered with layer of style 106 glass cloth; fiber-glass-filament constrictive wrap; glass cloth not extended over seam area, terminated at panel edge	VI-1(c) and VI-7(a)
b_4	External glass cloth with unconstricted area	Polyurethane-foam core encapsulated in MAM-laminate sealant covering; outer surface of sealed panel covered with layer of style 106 glass cloth; central logitudinal seam; unconstricted circumferential area 2 in. wide in center of tank reinforced with layer of 0.007-in.-thick glass cloth; remainder of specimen constricted with fiber-glass-filament wrap	VI-1(c), VI-1(e), and VI-8(a)
b_5	Combination of sealed- and unsealed-foam layers with special wrap adaptation	0.25-in.-thick polyurethane foam encapsulated in MAM-laminate sealant covering as inner layer; 0.15-in.-thick polyurethane foam (unsealed) as outer layer; outer surface of unsealed foam covered with style 106 glass cloth; sheet-metal saddle with pin strip adjacent to external protuberance to redirect filaments of wrap; fiber-glass-filament constrictive wrap	VI-1(d), VI-1(f), and VI-9(a)
b_6	External glass cloth with special wrap adaptation	Polyurethane-foam core encapsulated in MAM-laminate sealant covering; outer surface of sealed panel covered with layer of style 106 glass cloth; sheet-metal saddle with pin strip surrounding external protuberance to redirect filaments of wrap; fiber-glass-filament constrictive wrap	VI-1(c), VI-1(f), and VI-10(a)
c_7	External glass cloth	Four equal panels, each consisting of 0.4-in.-thick furnace-cured polyurethane-foam core encapsulated in MAM laminate sealant covering; outer surface of sealed panel covered with layer of style 106 glass cloth; fiber-glass-filament constrictive wrap	VI-1(c) and VI-3(c)
c_8	External glass cloth with unsealed-foam buildup	Single panel of furnace-cured polyurethane-foam core encapsulated in MAM-laminate sealant covering; unsealed buildup of foam to simulate faired covering over external plumbing or wiring; outer surface covered with layer of style 106 glass cloth; fiber-glass-filament constrictive wrap	VI-1(d) and VI-3(d)

[a]Unless otherwise noted, foam core was 0.4 in. thick. MAM-laminate sealant covering is composed of three layers, 0.0005-in.-thick plastic, 0.0005-in.-thick aluminum, and 0.0005-in.-thick plastic.

[b]Subsonic aerodynamic heating tests (engine jetstream).

[c]Transonic-supersonic aerodynamic heating tests (wind tunnel).

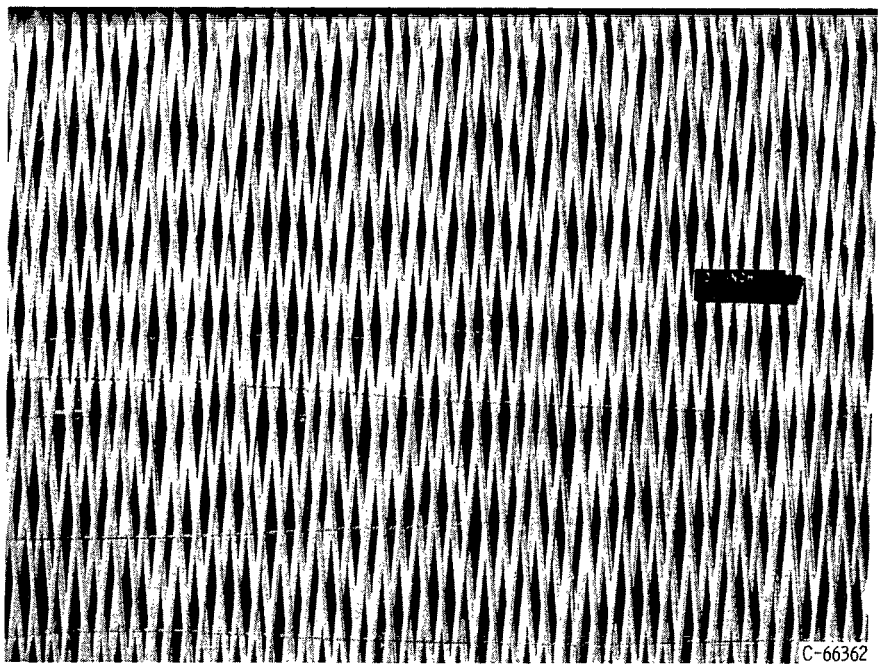

(a) Prior to test.

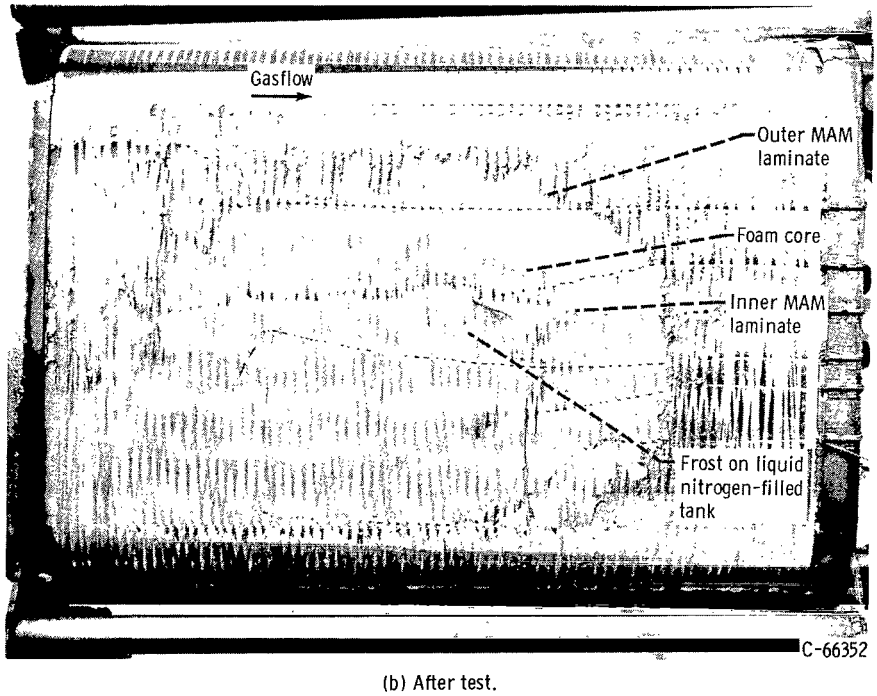

(b) After test.

Figure VI-5. - Effect of heating test 1 on insulation specimen 1 (MAM-laminate-covered foam with high-strength-plastic constrictive wrap).

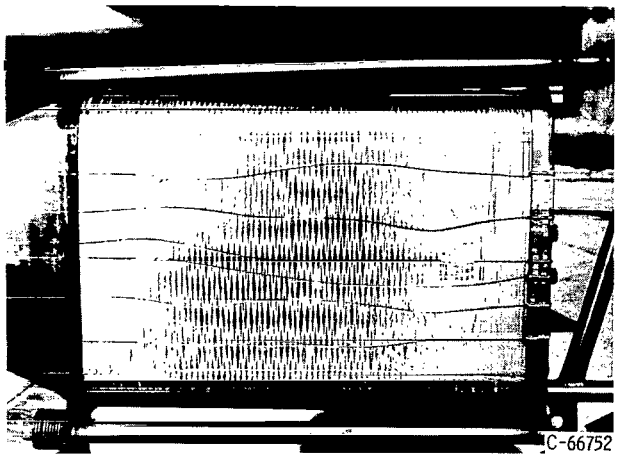

(a) Prior to tests.

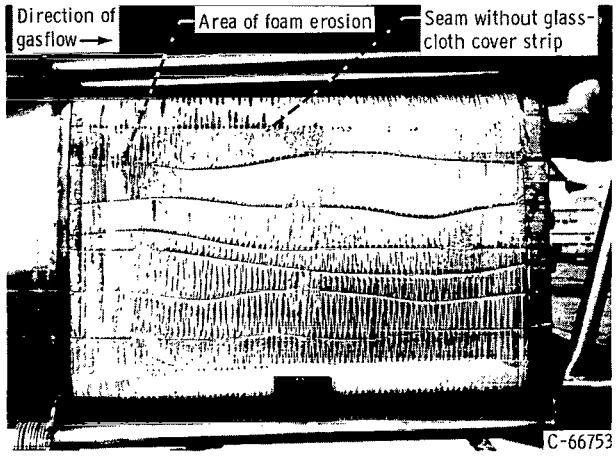

(b) After test 2.

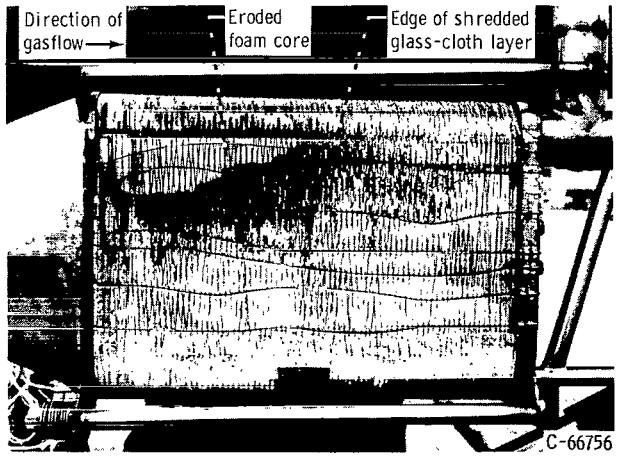

(c) After test 3.

Figure VI-6. - Effect of heating tests 2 and 3 on insulation specimen 2 (internal glass-cloth protective layer with fiber-glass constrictive wrap).

either nylon or fiber-glass filament was applied in a filament winding machine to complete the test specimen.

Test procedure. - An initial survey of the jetstream was made with an instrumented rake to determine simultaneously temperatures and pressures. This rake was mounted on a wheeled stand similar to that which carried the model tank. Gas temperatures and dynamic pressures measured at a sample survey point are shown in figure VI-4(a). A study of this figure will show that the rake was not exactly centered in the jetstream during this survey point. The "eye" of the jetstream was slightly above and to the right of the center of the rake. Small misalinements such as this were unavoidable during tests with the model tank also. The survey showed that there were gradients in both temperature and pressure from the center of the jetstream outward. However, the high-temperature and -pressure zone in the jetstream was sufficiently large to cover most of the model tank (see outline of tank in fig. VI-4(a)). The general range of conditions in the jetstream is shown in figure VI-4(b). From this survey, a distance behind the engine exhaust nozzle was chosen at which the desired conditions, or the closest approximation to the desired conditions, could be obtained. This choice of test conditions was based on the maximum temperatures and pressures measured in the jetstream.

Prior to a test on an insulation specimen, the wheeled stand (carrying the model tank) was positioned over the guide rail about 40 feet from the engine exhaust nozzle. Connections to the recording instruments were made, and the tank was filled with liquid nitrogen and allowed to stand for a sufficient interval of time to assure that the presence of the cryogenic fluid was felt by the insulation. When all pretest preparations were

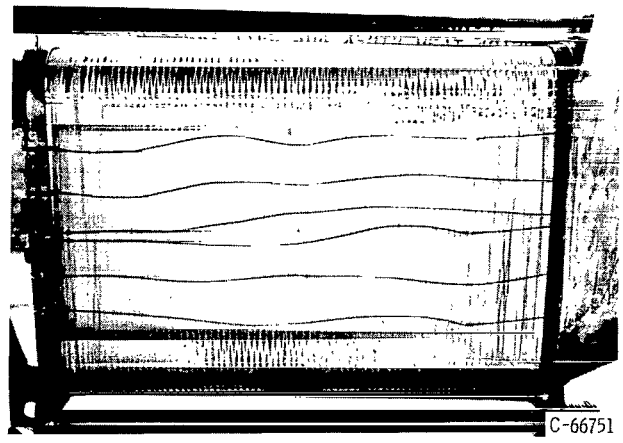

(a) Prior to tests.

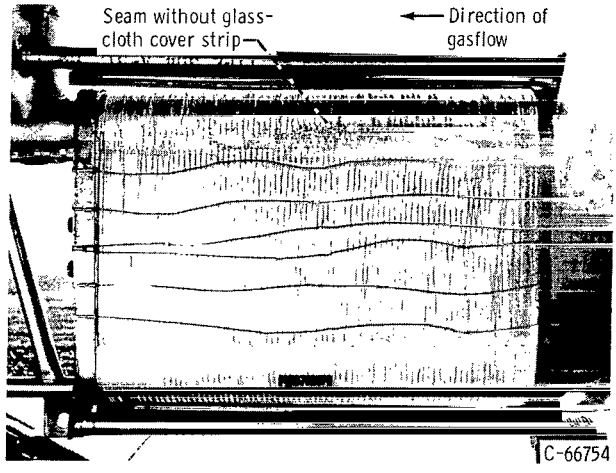

(b) After test 2.

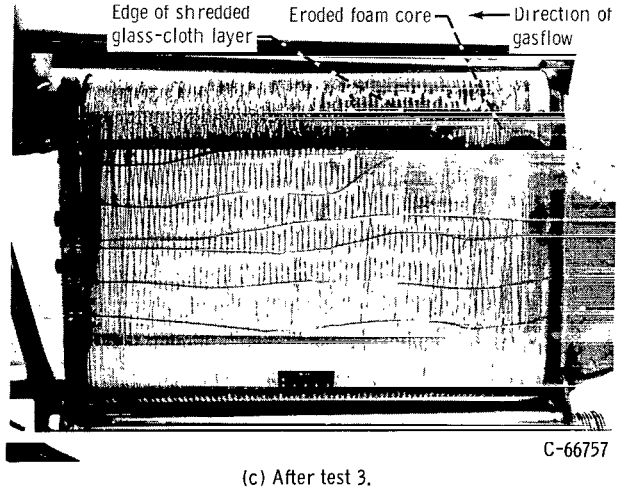

(c) After test 3.

Figure VI-7. - Effect of heating tests 2 and 3 on insulation specimen 3 (external glass-cloth protective layer with fiber-glass constrictive wrap).

completed, the engine was started and brought to idle conditions for operational checks. Then the tank was moved forward to the predetermined test position (12 to 15 ft from the engine exhaust nozzle), and the engine was accelerated to the speed that resulted in the desired temperatures and pressures. During the test, personnel at the observation station monitored the recording instruments, observed the test visually, and recorded the test operation on high-speed motion-picture cameras. At the end of the test, the engine was shut down abruptly to avoid further exposure of the insulation specimen to the jetstream environment.

All heating tests except the last one were of 40-second duration. This 40-second time interval approximated the time interval in the launch trajectory between the maximum dynamic pressure and the maximum temperature (see fig. VI-4(b)). The last subsonic heating test was conducted as a three-phase test with step increases in temperature and dynamic pressure between phases. These changes in jetstream conditions were accomplished by varying engine speed. Total time in this test was over twice as long (82 sec) as in the previous tests, although the time at maximum temperature and dynamic pressure was only about half as long (~17 sec). This latter test was considered to be more representative of the temperature and dynamic pressure profile of the launch trajectory shown in figure VI-4(b) than the single-phase tests.

Transonic-Supersonic Aerodynamic Heating Tests

Test setup. - The transonic-supersonic aerodynamic heating tests on specimens of the insulation system were conducted in the Lewis 8- by 6-foot supersonic wind tunnel. A view

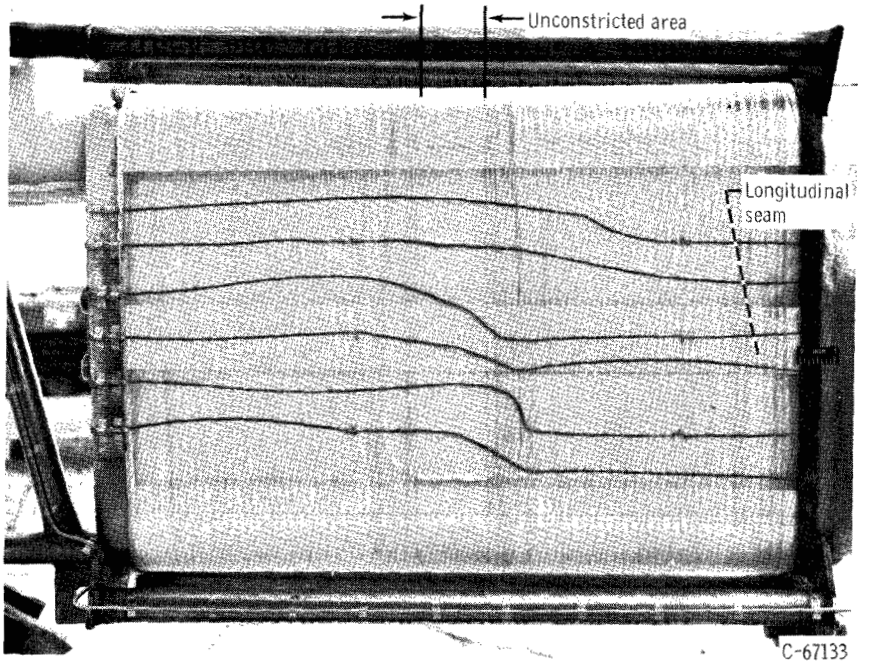

(a) Prior to test.

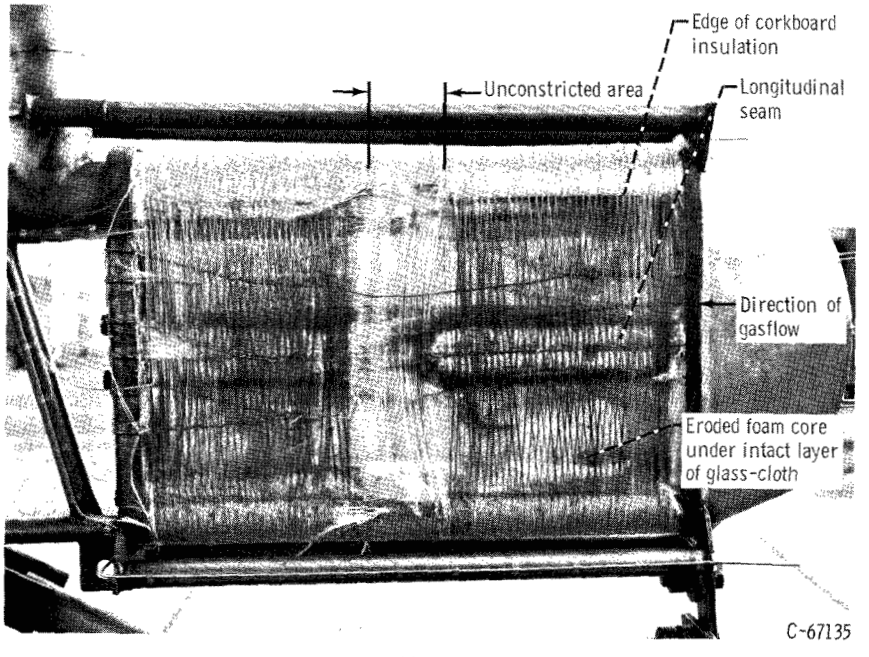

(b) After test.

Figure VI-8. - Effect of heating test 4 on insulation specimen 4 (external glass-cloth protective layer with fiber-glass constrictive wrap; circumferential unconstricted band reinforced with layer of heavy glass cloth).

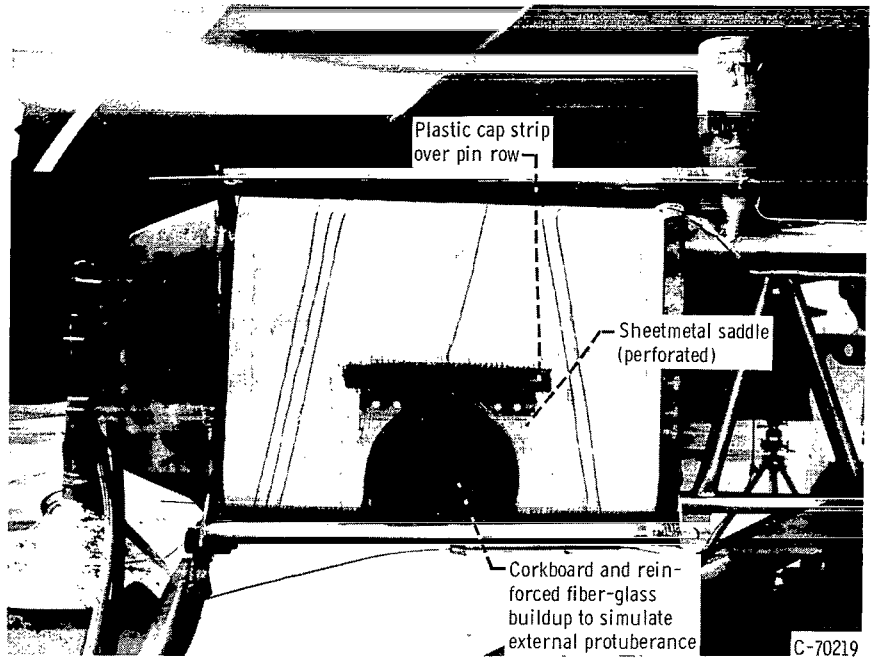

(a) Prior to test.

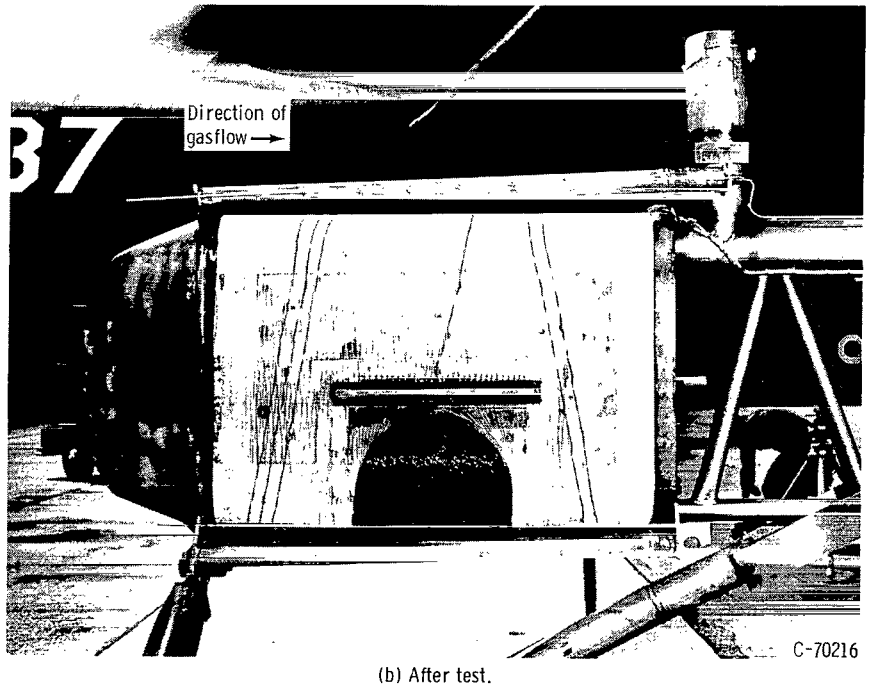

(b) After test.

Figure VI-9. - Effect of heating test 5 on insulation specimen 5 (combination of sealed- and unsealed-foam layers with external glass-cloth and fiber-glass constrictive wrap; special adaption of wrap in vicinity of protuberance).

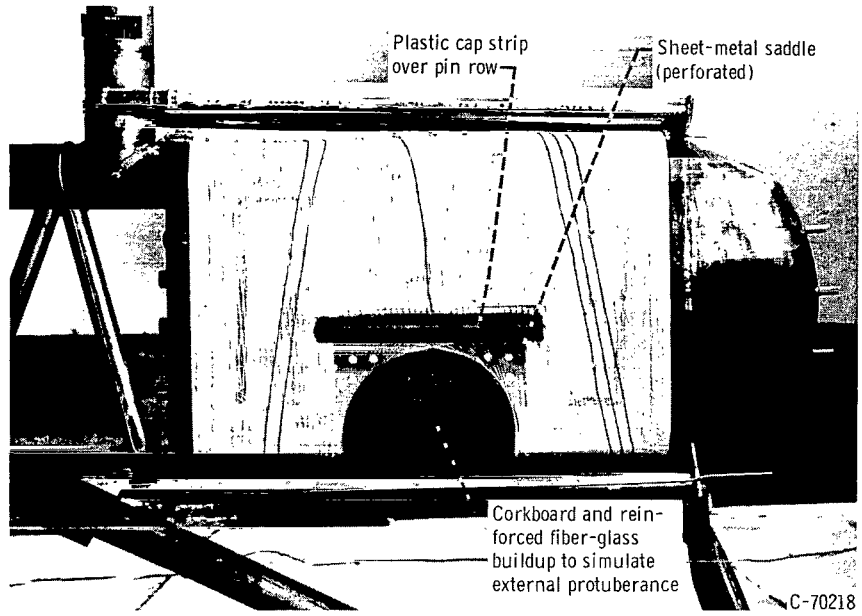

(a) Prior to test.

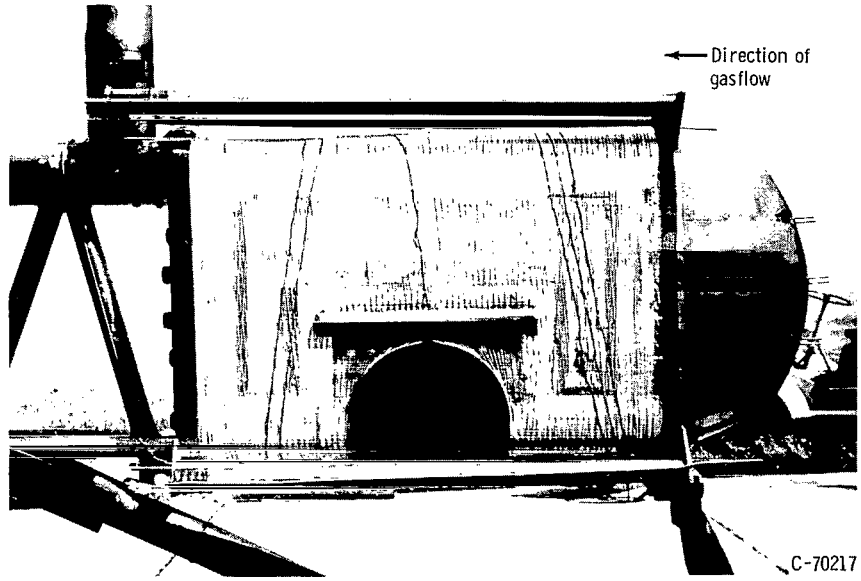

(b) After test.

Figure VI-10. - Effect of heating test 5 on insulation specimen 6 (external glass-cloth protective layer with fiber-glass constrictive wrap; special adaption of wrap in vicinity of protuberance).

of the model tank sting-mounted at zero angle of attack in the transonic test section of this wind tunnel is shown in figure VI-3(a). A retractable shock generator was mounted on top of the tank to simulate the presence of a large external protuberance. Two shock generator configurations - a 15° wedge and a blunt body - were used during these tests. Schematic diagrams of these configurations are shown in figure VI-3(b). Liquid nitrogen was supplied to the model tank through insulated lines, and gaseous boiloff was vented outside the tunnel.

Model tank. - The model tank for these tests was similar in cross section to the subsonic tank previously described, but of larger dimension (figs. VI-3(a) and (e)). The chord of this tank was 3 feet, the length 5 feet, and the thickness about 7 inches. The radius of curvature of the sides of the tank was 60 inches to match that of the Centaur vehicle. Corkboard insulation of the same thickness as the test specimens was used on the small-radius edges of the tank to withstand the large crushing loads generated by the tensioned filament wrap at reduced radius. An aerodynamic fairing of fiber-glass-reinforced plastic was attached to the forward end of the tank.

Test specimens. - Two specimens of the insulation system were installed on the tank for exposure to the wind tunnel environment. Specimen 7 (fig. VI-3(c) and table VI-I) was fabricated as shown in figure VI-1(c) and installed on the lower surface of the tank. Specimen 8 (fig. VI-3(d) and table VI-I), installed on the upper surface of the tank, was similar in construction to the variation shown in figure VI-1(d). Details of the specimen installation are shown in figure VI-3(e). The sealed panels on both specimens were 0.4 inch thick. The unsealed-foam buildup on specimen 8 simulated a fairing necessary to include an external wiring or conduit tunnel under the constrictive wrap without forming concave surfaces on the insulation. The maximum thickness of this unsealed-foam buildup was 0.6 inch. The materials and methods of fabrication used on specimens 7 and 8 were the same as those used on the panel portions of specimens 5 and 6, respectively, with one exception. The polyurethane foam for specimens 7 and 8 was furnace-cured at 150° F for 4 hours, 230° F for 8 hours, and 300° F for 8 hours. Trapped gas and constituents of the foam that are volatile at temperatures up to 300° F were thus eliminated prior to sealing with MAM laminate.

Thermocouples were installed in representative locations on the test specimens to measure temperatures during test operations. Thermocouples were bonded to the glass-cloth outer layer (under the constrictive wrap) in the patterns shown in figures VI-3(c) and (d). Between the sealed and unsealed layers of foam on specimen 8, the pattern of figure VI-3(d) was duplicated again. Thermocouples were bonded to the outside of the metallic skin of the tank on both sides in patterns matching those in figures VI-3(c) and (d). Total temperature in the airstream was measured with three thermocouple probes on the forward edge of the aerodynamic fairing, as shown in figure VI-3(a). All these thermocouples, plus other thermocouples and pressure tubes that are standard tunnel instrumentation, were connected to the automatic data recording system of the facility.

Test procedure. - Prior to the beginning of the transonic-supersonic tests, the tank and the associated plumbing system were filled with liquid nitrogen.

TABLE VI-II. - DESCRIPTION OF AERODYNAMIC HEATING TESTS

Test	Specimen	Test conditions				Results	Shown in figures VI-11 and -
		Maximum gas temperature, °F	Maximum insulation temperature, °F	Maximum dynamic pressure, lb/sq ft	Approximate time at test conditions		
g_1	1	590	550	720	40 sec	Outer MAM laminate sealant covering destroyed over approximately three-fourths of test area; foam eroded away where exposed; inner sealant covering destroyed over approximately one-fourth of test area; high-strength-plastic-filament constrictive wrap intact without visible signs of damage	VI-5(b)
g_2	2	600	560	648	40 sec	Outer MAM laminate sealant covering partially destroyed; underlying glass cloth intact; foam core eroded away in local edge area; fiber-glass wrap intact; absence of glass-cloth protection over seam area contributed to damage sustained in this and next test	VI-6(b)
	3	600	530	648	40 sec	Some heat damage to outer glass-cloth layer and melting of underlying MAM laminate sealant covering; fiber-glass constrictive wrap intact; absence of glass-cloth protection over seam area contributed to damage sustained in this and next test	VI-7(b)
g_3	2	665	620	792	40 sec	Damage area from test 2 greatly enlarged; glass cloth shredded locally along edge because of fluttering; appreciable foam erosion where exposed; fiber-glass wrap intact	VI-6(c)
	3	665	580	792	40 sec	Damage area from test 2 enlarged; glass cloth intact but damaged; some local erosion of foam under edge of glass cloth; fiber-glass wrap intact	VI-7(c)
g_4	4	840	690	1150	40 sec	Planned test conditions greatly exceeded; unconstricted band of style 128 glass cloth completely destroyed; style 106 glass cloth intact but damaged from heat and flutter; foam thickness reduced by about 70 percent except in seam area; seam area intact with only slight thickness reduction; fiber-glass wrap intact with loss of a few strands	VI-8(b)
g_5	5	685	[a]600	952	[b]17 sec	Special adaption to wrap, fiber-glass wrap, and style 106 glass cloth all intact; pronounced shrinkage in 0.15-in.-thick unsealed layer in local areas	VI-9(b)
	6	685	[c]615	952	[b]17 sec	Special adaption to wrap, fiber-glass wrap, and style 106 glass cloth all intact; very little shrinkage	VI-10(b)
h_6	7 / [e]8	221	205	1306	[d]1.5 hr	Specimen in excellent condition at end of test; no damage visually apparent	
h_7	7 / [f]8	224	212	1277	[d]1.5 hr	Specimen in excellent condition at end of test; only slight local shrinkage visually apparent	

[a]Estimated.
[b]At maximum conditions (total test time, 82 sec).
[c]Measured.
[d]At Mach 0.5 to 2.
[e]15° Wedge shock generator used above specimen.
[f]Blunt shock generator used above specimen.
[g]Subsonic aerodynamic heating tests (engine jetstream).
[h]Transonic-supersonic aerodynamic heating tests (wind tunnel).

During the test, a sufficient flow of liquid nitrogen was maintained to assure that the tank was full at all times. Testing was begun at the minimum Mach number (~0.5) and progressed stepwise to the maximum Mach number (~2). At each test point, temperatures and pressures on the tank and in the tunnel were recorded both without and with the shock generator extended over a portion of the insulation. Color motion pictures of the insulation in the area influenced by the shock generator were obtained at all test conditions. Continuous television surveillance of the tank was maintained from two locations.

RESULTS AND DISCUSSION

Although the environmental conditions of the aerodynamic heating tests

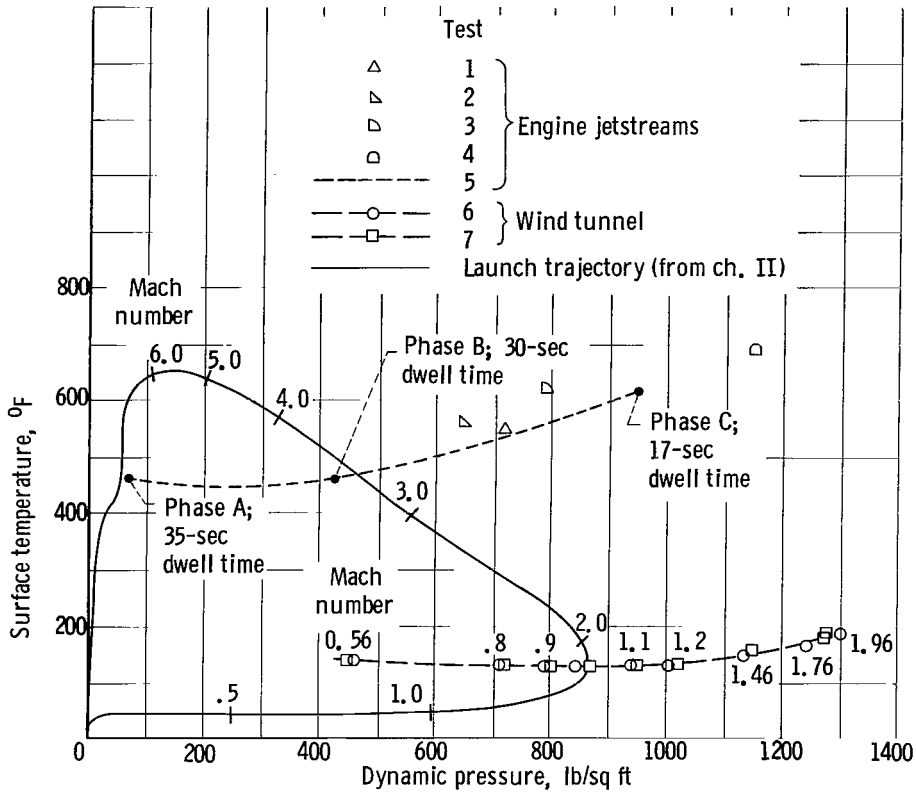

Figure VI-11. - Dynamic pressure and surface temperature on test specimens in aerodynamic heating tests.

were only rough approximations of the conditions predicted in chapter II of this report for the typical boost trajectory, the results of these tests should be indicative of the gross effects of the actual trajectory conditions on the insulation system. In general, these tests on several variations of the constrictive-wrap, sealed-foam external insulation system showed that such a system could be adapted to withstand temperature and dynamic pressure conditions similar to the operational conditions of the boost trajectory. The results of the tests are discussed in detail in this section; a brief summarization of the tests is given in table VI-II, and the test conditions are shown graphically in figure VI-11.

Subsonic Aerodynamic Heating Tests

MAM-covered specimen. - The MAM-laminate-covered specimen (specimen 1, fig. VI-5(a) and table VI-I) was tested at a position in the engine jetstream where the maximum gas temperature was 590° F and the maximum dynamic pressure was 720 pounds per square foot (test 1, table VI-II). The maximum temperature measured on the surface of the insulation during exposure at these jetstream conditions was 550° F. Time of exposure at these conditions was 40 seconds. From figure VI-11 it can be seen that this test resulted in exposure at conditions simultaneously approaching the maximum values of surface temperature and dynamic pressure for the launch trajectory. The test exposure time of

40 seconds was approximately equal to the time interval between peak values of pressure and temperature shown in figure VI-4.

A large blister formed under the MAM-laminate layer near the middle of the specimen early in the test. This blister was due to the formation of gas within the sealed panel as the foam core decomposed upon heating. The blister could be observed visually, and its formation was recorded by the high-speed motion-picture camera. Inspection of the film showed that the blister receded after a few seconds without catastrophic rupturing of the outer laminate. After the recession of this blister, melting of the laminate layer was observed at a spot about 5 inches from the forward edge and slightly below the horizontal centerline. (Starting with this initial breakdown, the outer MAM laminate melted and was blown away from about three-fourths of the test surface (see fig. VI-5(b)). The underlying foam was eroded away over approximately the same area. About one-fourth of the inner layer of MAM laminate melted and was blown away, as can be seen in the lower-left corner in figure VI-5(b). At the end of the test, the nylon constrictive wrap was still intact, and no damage to the wrap was visually apparent.

Obviously from the results of this test, the MAM laminate does not have sufficient heat and erosion resistance to withstand the anticipated launch conditions. Once the protective coating of laminate was destroyed, the foam insulation was eroded away by the jetstream. A more durable protective coating is needed for the insulation. This need led to the next step in the development of the insulation system, namely, the introduction of a protective layer of fiber-glass cloth.

The initial test on specimen 1 indicated that the nylon-filament constrictive wrap was capable of withstanding the conditions that partially simulated the typical launch trajectory conditions predicted in chapter II and shown in figure VI-4(b). Because of the inherently greater strength and temperature potential of fiber-glass filaments, however, the remainder of the test specimens were prepared with fiber-glass constrictive wraps.

Glass-cloth-protected specimens. - Specimens of glass-cloth-protected sealed foam of the types shown in figures VI-6(a) and VI-7(a) were tested simultaneously on opposite sides of the subsonic test tank. The specimen with glass cloth enclosed within the sealed foam (specimen 2, table VI-I) is shown in figure VI-6(a); the specimen with glass cloth as an outer covering (specimen 3, table VI-I) is shown in figure VI-7(a). Each specimen was a single panel. These specimens were constructed as shown in the schematic diagrams of figures VI-1(b) and (c) except that there were no glass-cloth cover strips or protective layers over the seam areas (foam filler) adjacent to the corkboard edge coverings.

The specimens were subjected to two consecutive simulated aerodynamic heating tests. During the first of these tests, the gas temperature was 600° F, and the gas dynamic pressure was 648 pounds per square foot (test 2, table VI-II and fig. VI-11). The maximum insulation surface temperatures measured on the specimens under these gas conditions were 560° F for the internal glass-cloth specimen (fig. VI-6) and 530° F for the external glass-cloth specimen (fig. VI-7). This difference in measured surface temperatures most prob-

ably resulted from the test tank not being exactly centered in the jetstream. The length of time at test conditions was 40 seconds. The conditions of these two specimens at the conclusion of this test are shown in figures VI-6(b) and VI-7(b). As can be noted from the damage patterns shown in these figures, the centerline of the jetstream was above the centerline of the test tank. On the side with the internal glass-cloth layer (fig. VI-6(b)), the MAM-laminate sealant layer, cover strip, and edge channel and the plastic doubler (see fig. VI-1(a)) melted and were blown away in a small area at the upper corner on the forward (left) section. Loss of these outer coatings exposed the edge of the underlying glass cloth and left an opening through which the jetstream eroded the foam insulation. This erosion of the foam was confined to the localized area on the specimen shown in figure VI-6(b). Although the MAM-laminate sealant layer was strengthened by the underlying glass cloth, the interruption of the glass-cloth layer at the panel edge created a potential trouble spot that would not have been remedied even if a glass-cloth cover strip over the seam had been used.

On the test specimen with the external glass-cloth layer (specimen 3, fig. VI-7(b)), the MAM-laminate cover strip covering the seam melted, and the foam filler was eroded away. However, the style 106 glass-cloth covering the test panel was still intact, although loss of some of the silicone resin is obvious from the change in surface appearance. There was no erosion of the underlying foam, but slight shrinkage due to heat was apparent. Some melting of the MAM-laminate layer, which was beneath the glass cloth on this specimen, was apparent but without adverse effect to the insulation system. Destruction of the MAM-laminate layer was not considered catastrophic on either of these specimens because the purpose of this layer was to provide a seal for the insulation during prelaunch time. It is not an essential part of the thermal-insulation function of the system after launch has taken place. No damage was apparent to the fiber-glass constrictive wrap on either side as a result of the exposure to the jetstream in this test.

Without any repairs being made, the two glass-cloth-protected specimens were subjected to a second aerodynamic heating test during which the gas temperature was 665° F and the gas dynamic pressure was 792 pounds per square foot (test 3, table VI-II and fig. VI-11). The maximum insulation surface temperatures measured on the specimens under these gas conditions were 620° F on the internal glass-cloth specimen (fig. VI-6) and 580° F on the external glass-cloth specimen (fig. VI-7). This difference in measured temperatures also was due probably to the test tank not being located exactly in the center of the jetstream. The length of time at these conditions was 40 seconds. The conditions of the test specimens at the conclusion of this test are shown in figures VI-6(c) and VI-7(c). The damage areas that resulted from the previous test were enlarged during this test. On the internal glass-cloth specimen (specimen 2), the eroded area spread to most of the upper forward (left) quandrant, as outlined roughly by the damage pattern on the MAM-laminate layer (fig. VI-6(c)). The exposed edge of the glass-cloth layer in this area was shredded by the action of the jetstream. On the external glass-cloth specimen (specimen 3) where loss of the MAM-laminate cover strip exposed the edge of the glass-cloth layer (because the glass cloth did not extend over the seam area on this specimen), severe buffeting by the jetstream caused the glass cloth to be shredded. Erosion of the foam occurred in the edge region where the glass-

cloth protective covering was lost. There was further melting of the silicone resin in the glass cloth, as evidenced by the change in appearance of the insulation surface. The fiber-glass constrictive wrap was intact over both specimens and was without apparent damage at the end of the test.

From the results of the tests on these glass-cloth-protected specimens it is evident that the seam areas will be critical spots if proper protection is not provided. It can also be concluded that the external glass-cloth layer, with the possibility of continuous coverage across the seam area, is preferable to the internal glass-cloth layer, where seam area protection can be had only by splicing an added glass-cloth strip over the seam. Another specimen of the external glass-cloth variation (made as shown in fig. VI-1(c)) was tested in the engine jetstream to prove the reliability of a properly protected seam. The specimen (specimen 4) is shown in figure VI-8(a) and described in table VI-I. The unconstricted area in the center of this specimen is considered in the section Specimen with Glass-cloth Reinforcement in Unconstricted Area. This specimen was subjected to a gas temperature of 840° F and a dynamic pressure of 1150 pounds per square foot for 35 seconds in the jetstream (test 4, table VI-II, and fig. VI-11). The test conditions had been planned to duplicate the conditions of the last previous test (test 3); but, due to an error in positioning the test tank, these conditions were greatly exceeded. The maximum insulation surface temperature measured during this test was 690° F.

The effects of the test conditions on specimen 4 can be seen in figure VI-8(b). The central longitudinal seam was still intact except in the unconstricted area. Overlapping of the various component layers of the insulation system in the seam area provided a better heat barrier above the foam core than was present in the remainder of the panel. As a result, the seam area shrank very little in thickness because of heat, and the constrictive wrap remained taut over the seam. In the area between the central longitudinal seam and the corkboard insulation, the foam core was reduced to an average thickness of about 1/8 inch. The relatively rigid edges on the corkboard at the top and bottom of the tank did not shrink when heated. These corkboard edges plus the central seam provide anchor points for the glass-cloth layer and the fiber-glass constrictive wrap. The high-speed motion pictures showed that severe buffeting of the glass cloth and the wrap occurred above the panel in the areas between the seam and the corkboard edges during the test. This buffeting obviously impinged on the panel and probably contributed to the destruction of the foam core. (The high edge of the corkboard edge covering was cut back and replaced with a wedge-shaped foam buildup (see fig. VI-2(c)) for subsequent testing. This foam buildup shrank with the test specimen and thereby avoided the bridging of the filaments of the constrictive wrap between nonrepresentative high points.) A few strands of the fiber-glass-filament constrictive wrap were observed (in the motion pictures) to fail during this test. The glass-cloth layer covering the panel was still intact, however, despite the severe buffeting encountered.

From this test, where the temperature and dynamic pressure were far in excess of the design conditions (although the gas flow was subsonic), it can be concluded that seam areas can be properly protected. The test results also indicate that the constrictive wrap must remain taut on the surface of the panel to maintain the integrity of the insulation system.

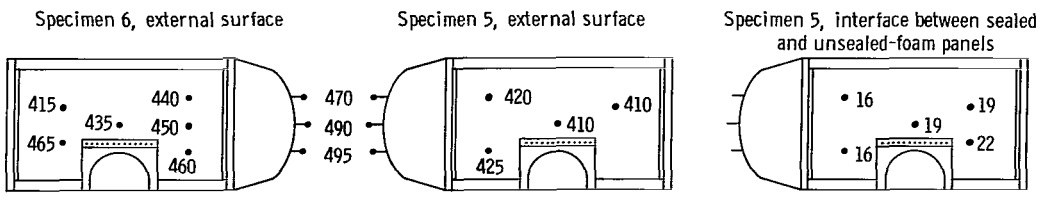

(a) Phase A; maximum dynamic pressure, 64 pounds per square foot.

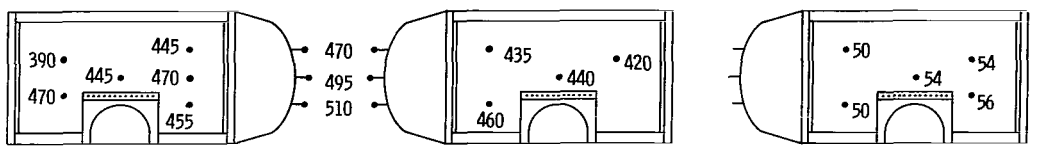

(b) Phase B; maximum dynamic pressure, 423 pounds per square foot.

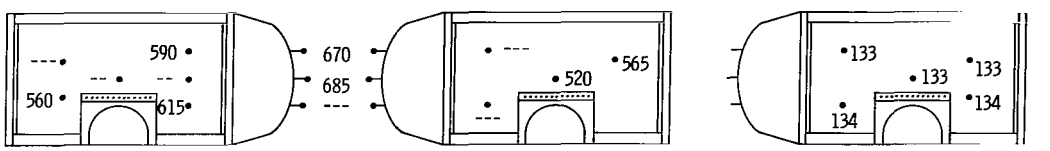

(c) Phase C; maximum dynamic pressure, 952 pounds per square foot.

Figure VI-12. - Insulation temperatures measured on specimens 5 and 6 during test 5. (All temperatures in ^{o}F.)

Combination (sealed- and unsealed-foam) specimen. - Motion pictures and visual observations of previous tests showed that gas blisters or bubbles sometimes formed on the surface of the sealed-foam insulation panels because of expansion of trapped gases. The gas pressure that caused these blisters was sometimes sufficiently strong to raise the constrictive wrap appreciably. The variation of the insulation system with a combination of sealed- and unsealed-foam layers (fig. VI-1(d)) was devised to avoid this problem. A comparative test was made on opposite sides of the model tank between a specimen of the combination system and a specimen of the external glass-cloth system of figure VI-1(c). The two specimens had the same overall thickness (0.4 in.) with the combination specimen consisting of 0.25 inch of sealed foam and 0.15 inch of unsealed foam. Specimens are shown in figures VI-9(a) and VI-10(a) and described in table VI-I as specimens 5 and 6, respectively. The protuberances and special patterns on the constrictive wrap that are a part of these specimens are considered in the section Special wrapping technique.

The test specimens of figures VI-9 and VI-10 were subjected to a range of jetstream gas temperatures up to 685° F and dynamic pressures up to 952 pounds per square foot for a total test time of about 82 seconds (test 5). The detailed conditions of the test are listed in table VI-II and shown in figure VI-11. Insulation temperatures measured during the three phases of test 5 are shown in figure VI-12. The 17-second time interval for phase C (fig. VI-11) was not sufficient to complete a full set of temperature measurements during this phase. The maximum insulation outer-surface temperature was 615° F on the external glass-cloth specimen; the maximum temperature on the combination layer specimen was estimated to be about 600° F on the basis of comparing thermocouple readings at lower temperature levels during this test. The maximum temperature measured at the interface between the sealed-and unsealed layers of foam was 134° F. Figures VI-9(b) and VI-10(b) show the effects of the test

conditions on the specimens. The fiber-glass constrictive wrap and the glass-cloth covering on both specimens were intact after the test. The layer of unsealed foam on the combination specimen (specimen 5, fig. VI-9(b)) shrank in thickness appreciably while the underlying sealed foam layer was not dimensionally affected by the test environment. The exposed sealed foam panel on specimen 6 (fig. VI-10(b)) showed a very slight shrinkage due to heat. The edges of the corkboard insulation were provided with foam buildups (see fig. VI-2(c)) during this test so that the bridging and subsequent vibration of the glass-cloth layer and constrictive wrap that occurred during test 4 were not encountered during this test. The wrap remained taut over both specimens 5 and 6 throughout the test.

The overall performance of the single-sealed panel was better than the combination of sealed and unsealed panels in this test. The choice of relative thicknesses for the sealed and unsealed layers on the combination specimen was arbitrary. A relatively thicker unsealed layer may be more desirable from a structural standpoint, but some shrinkage of the layer is unavoidable. Any combination of sealed and unsealed layers must also be evaluated for thermal insulation performance. For the conditions of the typical launch trajectory shown in figure VI-11, where the time at high temperatures is very short, the bubbling of the insulation surface probably will not be a serious problem. Preliminary tests on samples of polyurethane foam that were oven cured at about 300° F for approximately 4 hours prior to encapsulation in the MAM-laminate sealant covering indicated that much of the tendency to bubble can be avoided by removing the low-temperature volatiles before sealing the foam. It can be concluded from this test that the single sealed-foam panel with an external glass-cloth protective layer is the best of the insulation system variations tested for this particular application.

Specimen with glass-cloth reinforcement in unconstricted area. - Specimen 4, containing an unconstricted area that was reinforced with a 0.007-inch-thick layer of glass cloth, is shown in figure VI-8(a). This specimen was subjected to a gas temperature of 840° F and a dynamic pressure of 1150 pounds per square foot for 35 seconds (test 4, table VI-II, and fig. VI-11). These conditions greatly exceeded the planned test conditions, as explained previously, but the complete breakdown of the unconstricted glass cloth (as shown in fig. VI-8(b)) indicated that this insulation system variation would be only marginal at best under conditions of lower temperature and dynamic pressure. As a result of the successful test on the special wrapping technique described in the next section, no further consideration was given to unconstricted areas on the insulation system.

Special wrapping technique. - Two test specimens that incorporated the special wrapping technique shown schematically in figure VI-1(f) are pictured in figures VI-9(a) and VI-10(a) (specimens 5 and 6). The parts pertaining to the special wrapping technique on these two specimens are identical, although the surrounding parts of the insulation system are different, as previously described. These specimens have a cap strip covering the row of pins about which the filaments of the constrictive wrap bend. This cap strip shields the high-stress point at the bend in the filaments from the effects of aerodynamic heating and anchors the filaments to the level of the insulation surface to avoid any displacement due to bubble formation.

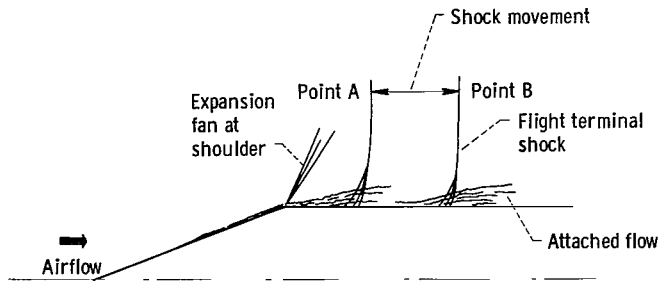

(a) Attached flow pattern showing upstream and downstream extremes of shock location.

(b) Flow pattern after breakdown occurring when shock moves forward to point A.

Figure VI-13. - Schematic of alternating attached and detached flow pattern occurring at cone shoulder at onset of transonic flight.

Specimens 5 and 6 were subjected to the jetstream environment of test 5, table VI-II (see also fig. VI-11). The condition of the specimens at the conclusion of this test is shown in figures VI-9(b) and VI-10(b).

The maximum temperatures measured on specimens 5 and 6 during test 5 are shown in figure VI-12. There was no apparent damage to any part of the constrictive wrap or the special parts for rerouting the wrap as a result of the test. It can be concluded that this method of eliminating unconstricted areas of insulation in the vicinity of external protuberances is practical for the environmental condition of this test, which simulated typical launch conditions except for high Mach number flow.

Transonic-Supersonic Aerodynamic Heating Tests

Glass-cloth-protected sealed-foam specimen. - Subsonic aerodynamic heating tests on the external glass-cloth-protected variation of the insulation system (fig. VI-1(c)) have shown this to be a very promising configuration. Wind tunnel tests on a larger specimen of this variation (specimen 7, table VI-I and figs. VI-1(c) and VI-3(b)) were made at airflow conditions up to about Mach 2 to determine the effects of transonic and supersonic flow on the insulation. These tests were conducted in the Lewis 8- by 6-foot supersonic wind tunnel and are designated tests 6 and 7 in table VI-II. As shown in figure VI-11, the values of temperature and dynamic pressure attained in the wind tunnel exceeded those that occurred along the assumed launch trajectory at corresponding Mach numbers up to about Mach 2. The maximum value of dynamic pressure was approximately 50 percent higher in the wind tunnel than for the flight trajectory. The point of intersection of the curves for the wind tunnel and the flight trajectory is in the transonic range near Mach 1.0 for the wind tunnel and in the supersonic range near Mach 1.9 for the flight trajectory. In the transonic region, peak-to-peak static-pressure fluctuations as large as 40 to 50 percent of free-stream dynamic pressure can occur. These pressure fluctuations are a result of the transonic phenomenon of a terminal shock moving down the tank. First indications of this shock occur at moderately high subsonic Mach numbers, where flow expansion about the cone shoulder produces local sonic velocities (see fig. VI-13). The onset of this expansion phenomenon is characterized by a rapid oscillation between attached and separated subsonic flow at the shoulders (fig. VI-13). An area of large pressure oscillations (from shoulder to point B) which may adversely affect the insulation results from this flow mechanism. As the flight Mach number increases, this expansion produces a supersonic velocity distribution with attendant low static pressures along the tank. Theo-

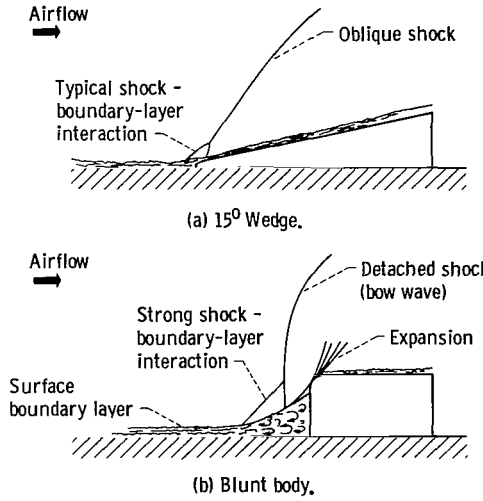

Figure VI-14. - Waveforms generated in supersonic stream by shock generators.

retically, an isentropic recovery to local free-stream static pressure would be predicted. In the actual case, however, recovery occurs through a normal shock. This shock moves downstream on the tank and decreases in strength as the Mach number increases. At Mach 1.0 for a flight vehicle this shock would be perhaps 8 vehicle diameters downstream of the cone shoulder. In the tunnel, however, the downstream movement of the shock is retarded (compared to the flight condition) because of blockage effects of the model tank in the transonic tunnel. This, in turn, subjects the insulation to a stronger shock in the tunnel at a given location downstream of the cone shoulder than would be encountered at the flight trajectory.

In addition to the intensified shock waves resulting from the wind tunnel testing, the time of exposure in the wind tunnel was far in excess of that encountered in the flight trajectory. The accumulated test time in the wind tunnel at airflow conditions between Mach 0.5 and Mach 2 was about 3 hours. Time of exposure in the flight trajectory is of the order of a few minutes (see fig. VI-4(b)). Consequently, for the Mach number range covered, the wind tunnel investigation subjected the insulation to a more severe durability test from the standpoint of shock strength and exposure time than would be prescribed by the assumed trajectory conditions (figs. VI-4(b) and VI-11).

Visual inspection of specimen 7 after tests 6 and 7 showed only slight shrinkage in the insulation system. Maximum insulation surface temperatures of about 212° F and maximum dynamic pressures of about 1300 pounds per square foot were endured in these two tests. It appears that the buffet loads associated with transonic flow conditions did not have an adverse effect on any part of specimen 7.

Unsealed-foam buildup. - On the basis of the results of the subsonic test on a combination of sealed and unsealed layers of foam, the use of an unsealed-foam buildup to permit the inclusion of external plumbing or wiring under the constrictive wrap seemed to be logical. Specimen 8, which incorporated such a buildup, was tested in the supersonic wind tunnel simultaneously with specimen 7 to determine the resistance of the unsealed foam to supersonic flow conditions with and without the influence of standing shock waves. The 15° wedge shock generator (shown in fig. VI-3(b)) was used in test 6, and the blunt body shock generator (also shown in fig. VI-3(b)) was used in test 7 to generate shocks similar to those that would result from large external protuberances on the tank. Sketches of the centerline flow patterns that would be expected for these shock generators in a supersonic stream are shown in figure VI-14. The 15° wedge produced a relatively mild oblique shock-boundary-layer interaction compared to that caused by a strong detached or bow wave produced by the blunt body. These interaction regions (especially that caused by the bow wave) are

characterized by high turbulence and large pressure fluctuations that could be detrimental to the constrictive wrap and the foam insulation.

In addition to the shocks from these generators, specimen 8 was also subjected to the same overall flow conditions discussed in detail in connection with specimen 7.

Visual inspection of specimen 8 after tests 6 and 7 showed only slight local shrinkage in the insulation. Maximum insulation surface temperatures of about 212° F and maximum dynamic pressures of about 1300 pounds per square foot were attained during these tests. The accumulated test time at airflow conditions between Mach 0.5 and Mach 2 was about 3 hours. Exposure to these conditions with the added shocks from the shock generators did not have an adverse effect on the unsealed-foam buildup or on any other part of specimen 8. Color motion pictures of the area around the shock generator did not indicate any difficulties during the actual exposure to supersonic airflow conditions.

CONCLUSIONS

From the results of aerodynamic heating tests on specimens of the lightweight, constrictive-wrap sealed-foam insulation system for cryogenic propellant tanks of boost vehicles, the following conclusions can be drawn:

1. This type of insulation system can be adapted to withstand environmental conditions similar to those predicted for a typical launch trajectory by incorporating a heat- and erosion-resistant protective coating of glass cloth over the sealant coating of the foam panels and under the constrictive wrap. Specimens of the insulation system satisfactorily withstood the environment of a subsonic gas stream from a turbojet engine for periods of time representative of the critical part of a typical launch trajectory. Insulation temperatures as high as 615° F and dynamic pressures as high as 952 pounds per square foot were encountered during these exposures. Similar specimens withstood supersonic wind tunnel environments up to Mach 2 with superimposed standing shock waves from external protuberances. A maximum insulation temperature of 212° F and a maximum dynamic pressure of 1306 pounds per square foot were produced in the wind tunnel environment.

2. Special adaptations to the constrictive-wrap technique must be used to avoid large unconstricted areas on the insulation due to the presence of external protuberances on the propellant tank. One such adaptation, which involves redirecting the wrap over two rows of pins, was successfully demonstrated in the course of these tests.

3. Both nylon and fiber-glass filaments could be used for the constrictive wrap. Fiber glass was investigated more thoroughly in this series of tests because of its greater inherent strength and high-temperature potential.

REFERENCE

1. Perkins, Porter J., Jr., and Esgar, Jack B.: A Lightweight Insulation System for Liquid Hydrogen Tanks of Boost Vehicles. AIAA Fifth Annual Structures and Materials Conf., Palm Springs (Calif.), Apr. 1-3, Pub. CP-8, AIAA, 1964, pp. 361-371.

CHAPTER VII

DESIGN, FABRICATION, AND APPLICATION OF INSULATION SYSTEM TO FULL-SCALE TANK

by Porter J. Perkins, Jr., Clem B. Shriver,* and Ralph A. Burkley*

Lewis Research Center

This chapter presents the details of the lightweight insulation system design, fabrication, installation, and weight breakdown for the full-scale Centaur tank. The full-scale insulation design, tooling, and fabrication were conducted concurrently with other development phases involving materials testing and application and tests of subscale tanks. Application of the system to the full-scale tank was started only after material and application techniques had been finally determined from the subscale tank tests discussed in chapter V.

This work was performed by the Goodyear Aerospace Corporation at Akron, Ohio under Contract NAS3-3238 for the NASA Lewis Research Center.

INSULATION SYSTEM DESIGN

Full-Scale Centaur Tank Design

The propellants for the Centaur launch vehicle are stored in a two-compartment tank 10 feet in diameter with an overall length of 25 feet (fig. VII-1). The compartments are separated by a double-walled internal bulkhead filled with fiber-glass insulation and evacuated. Liquid hydrogen is stored in the larger top compartment, and warmer liquid oxygen is stored in the bottom compartment. The flight-vehicle tank is a pressure-stabilized structure with thin walls of stainless steel (0.014 in. thick) fabricated with lapped joints. The tank used for this program, however, was constructed for ground testing only and, although the same as the flight configuration generally, it was of much heavier wall construction (0.040 in. thick). This test tank had fill, drain, and vent connections and a number of brackets attached to the outside walls that were typical of the flight vehicle. However, a number of other protuberances from the side walls existed on the test tank for special instrumentation connections which were not on the flight version. The experimental insulation system reported herein was applied to the cylindrical side walls of the liquid-hydrogen tank. This cylindrical area measured approximately 485 square feet (10 ft in diameter and $15\frac{1}{2}$ ft high between top and bottom transition flanges,

*Goodyear Aerospace Corporation, Akron, Ohio.

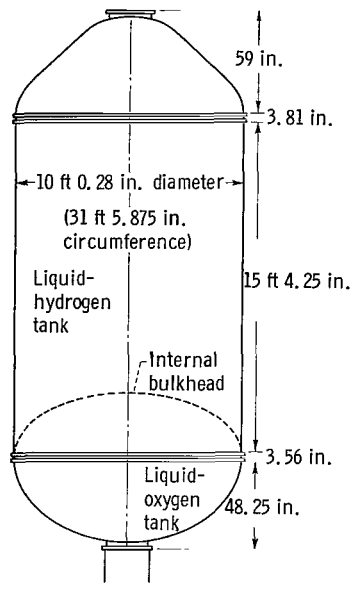

Figure VII-1. - Outline dimensions of full-scale Centaur tank used for installation of insulation system.

see fig. VII-1). The top dome also required insulation for the liquid-hydrogen testing but was not treated as part of the experimental system.

Insulation Panel Design

The final design of the full-scale insulation panels was determined on the basis of test results on insulation systems 1 and 2 as applied to subscale circular segment tanks (see ch. V) and on the basis of thermal-conductivity measurements made on small test panels (see ch. III). The elements of this design are shown in figure VII-2. Mylar and aluminum foil laminate (MAM) sealed top and bottom surfaces of polyurethane foam with a nominal density of 2.0 pounds per cubic foot cut 0.4 inch thick. The MAM laminate consisted of 0.0005-inch-thick layers of Mylar bonded to both sides of 0.0005-inch-thick aluminum foil. Preformed channels of 0.002-inch-thick Mylar sealed the edges of the foam with about a 0.62-inch overlap on top and bottom surfaces. The panels were formed to the 60-inch-radius curvature of the tank.

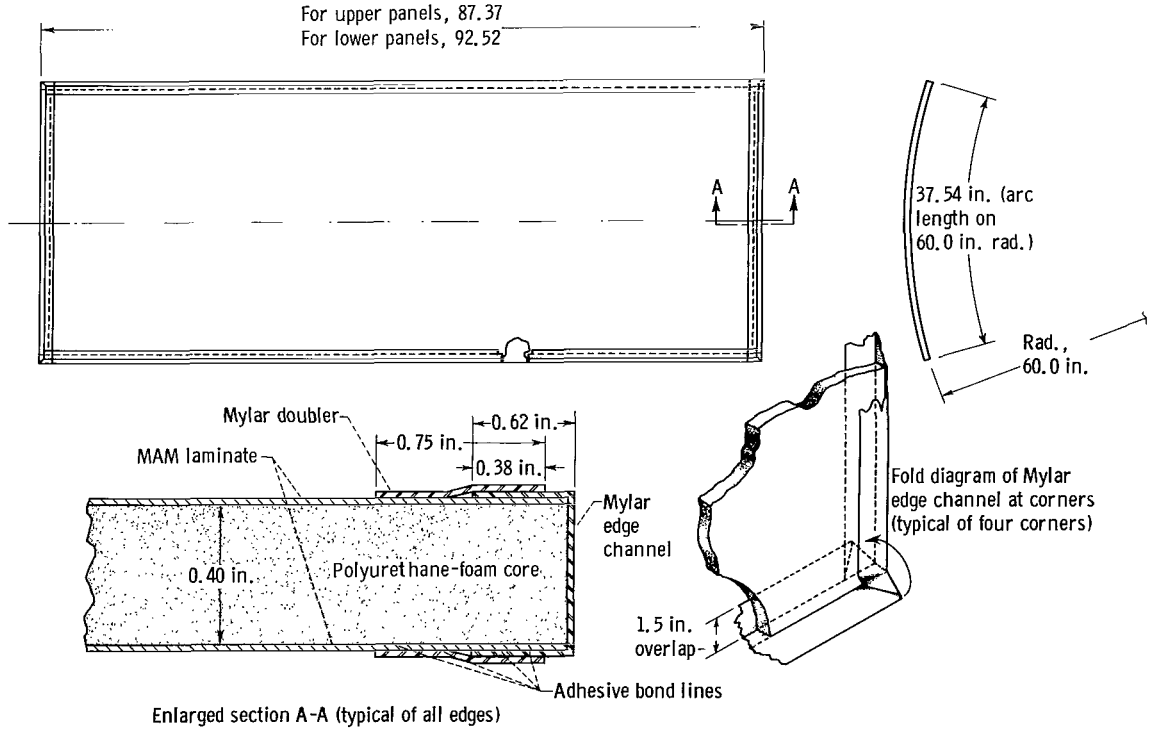

Figure VII-2. - Insulation panel details.

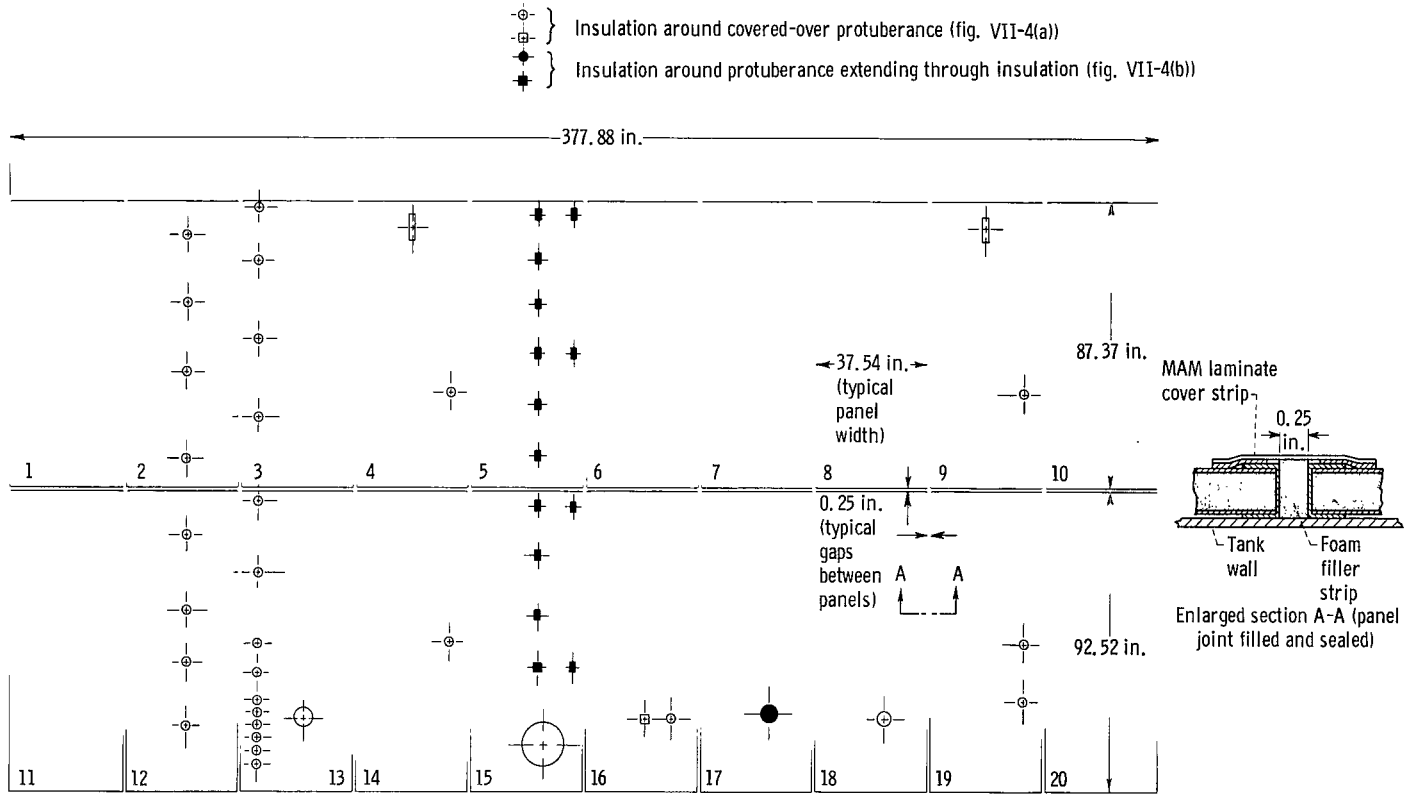

Figure VII-3. - Flat pattern layout of Centaur tank insulation panels.

To establish a basis for defining insulation panel sizes, a flat layout of the cylindrical portion of the Centaur test tank was developed from actual dimensions taken from the tank. Figures VII-3 and VII-4 illustrate the number and type of protuberances that were present. The number of insulation panels selected for the full-scale Centaur insulation system was 20. This number was based upon (1) availability and size of MAM sealing laminate, (2) perimeter dimensions of the panels, and (3) panel locations with respect to protuberances. The MAM laminate was available only in 38-inch-wide rolls, which, to eliminate splicing and reduce possible leak sources, limited panel size to less than this width. Because joints between panels were partial heat shorts and presented possible sources of air leaks into and behind the panels, the total length of joints around the tank was reduced by utilizing panels as large as possible. Thus, with a fixed width the panels were made as long as practical for handling purposes. A final consideration was to locate protuberance cutouts well within the area of the panel to avoid the difficulties of sealing at or near the edge of a panel. Thus, two panel sizes were used, as indicated in the design of the typical insulation panel shown in figure VII-2. To facilitate fabrication, detailed metal templates were developed for each insulation panel.

Design of Insulation of Protuberances

As indicated previously, the external surface of the test tank was not a smooth circular cylinder. The fill line connections, instrumentation connections, and support brackets (for support of the wiring harness, etc.) that must penetrate or pass through the insulation panels complicated the fabrication, installation, and sealing of the insulation system. There were basically two types of protuberances to be considered, as shown in figure VII-4: (1) small protuberances that could be covered with insulation; (2) protuberances, such as fill lines and brackets, that extended through the insulation. These protuberances extended from the surface of the tank and required sealed clearance holes to be cut through the insulation panels. Sealing of the foam around the perimeter of these holes was accomplished with a preformed section of Mylar with a flattened out Z-shaped cross section, as shown in figure VII-4. Foam placed in this cutout section insulated the area next to the protruding part.

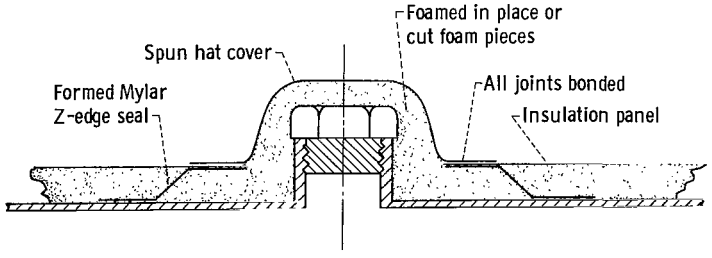

(a) Covered-over protuberance.

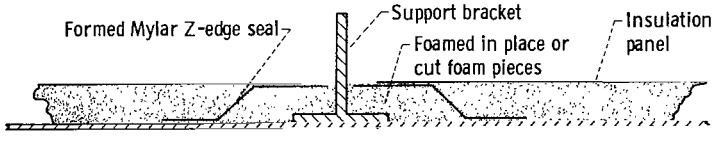

(b) Protuberance extending through insulation.

Figure VII-4. - Insulation around protuberances.

If the protuberance could be covered over as it is in figure VII-4(a), an impermeable hat section spun from 0.005-inch-thick aluminum-Mylar-aluminum laminate was added over the foam to provide a final seal. If the protuberance extended through the insulation, a gas-tight seal

TABLE VII-I. - CONSTRICTIVE-WRAP MATERIAL PROPERTIES

Property of single strand	HT-1 Nylon	S/HTS Fiberglas	Steel wire
Specific gravity	1.38	2.485	7.82
Weight, g/yd	0.021	0.031	0.128
Ultimate tensile strength, psi	100,000	400,000	530,000
Ultimate elongation, percent	10.8	3.2	2.15
Maximum elastic strain, percent	1.5	3.2	1.7
Modulus of elasticity, psi	500,000	12,500,000	30,000,000

was not obtained, and the small area around the protuberance was allowed to cryopump air. Air could not get into the insulation panel because of the peripheral Z-section seal around the cutout mentioned previously. Thirteen of the 20 insulation panels required cutouts for 1 to 11 protuberances.

Constrictive-Wrap Design

Constrictive wrapping, established as the primary method of attachment of the insulation panels to the test tank, required that prestressed strands be wound over the insulation in a helical pattern to provide a 2-pound-per-square-inch normal compression load on the insulation. The 2-pound-per-square-inch compressive load was chosen on a somewhat arbitrary basis, although this value was used on the jettisonable insulation developed for Centaur. Less compression could probably be used on this nonjettisoned insulation because there are no trapped gases behind the insulation to push it off, as is the case with the jettisonable purged system. A 6° helix was chosen to provide a large number of crossover points to hold the wrap together while leaving as little open area between strands as possible. Materials considered for the wrap were du Pont HT-1 Nylon fiber yarn, high-strength steel wire, and Owens-Corning S/HTS Fiberglas roving. After development effort on subscale tanks (chs. V and VI) proved S/HTS Fiberglas to be desirable, this material was chosen for the full-scale test tank wrap.

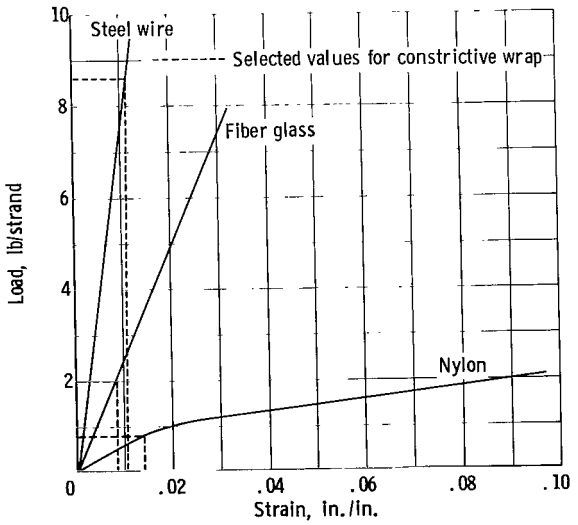

Figure VII-5. - Load-strain curves for constrictive-wrap materials.

The following discussion is a review of the various requirements and considerations leading up to the selection of the final wrap material.

A comparison of properties of the candidate materials is given in table VII-I. The load-strain relation for a strand of each material is given in figure VII-5.

The Centaur tank has a radius R of 60 inches; therefore, the required tension load T in the constrictive wrap

TABLE VII-II. - FACTORS AFFECTING INITIAL PRESTRAIN OF CONSTRICTIVE-WRAP MATERIALS

Material	Tank contraction, percent	Maximum foam deformation, percent	Expansion of constrictive wrap, percent	Minimum final residual strain, percent	Required initial prestrain, percent
HT-1 Nylon	0.25	0.20	0.75	0.20	1.40
Steel wire	.25	.20	.38	.20	1.03
S/HTS Fiberglas	.25	.20	.19	.20	.84

TABLE VII-III. - SUMMARY OF CONSTRICTIVE-WRAP MATERIAL DATA

Material	Load per strand, lb	Strand width, in.	Strands per inch	Strand crushing stress, psi	Strand weight, lb	Binder weight, lb	Total weight, lb
HT-1 Nylon	0.80	[a]0.005	150	2.67	18.00	6.53	24.53
Steel wire	8.70	.006	15	24.2	8.17	.49	8.66
S/HTS Fiberglas	2.00	[a].008	60	4.17	7.94	1.96	9.90

[a]Values based on total roving width divided by number of strands in roving.

to provide a 2-pound-per-square-inch compression load P on the insulation is

$$T = PR = 2 \times 60 = 120 \text{ lb/in.}$$

The wrapping strain must be sufficient to keep a positive compression load on the panels during all conditions encountered during ground hold and launch. Factors considered include thermal contraction of the tank during cooldown to liquid-hydrogen temperature, deformation of the panels from the constrictive-wrap load, possible foam shrinkage during aerodynamic heating, and thermal expansion of the constrictive-wrap material during aerodynamic heating to a maximum temperature of about 625° F. This thermal expansion is a function of the wrap material. Table VII-II shows the possible values for these factors, which, when summed up, provide the required initial prestrain in the wrap material.

From table VII-II and the load-strain curves given in figure VII-5, the load per strand, strand width, strands per inch, crushing stress of the strands on the insulation, and total weights for the materials considered were calculated and are summarized in table VII-III.

The weight data in table VII-III favor S/HTS Fiberglas over HT-1 Nylon for the constrictive wrap. Although the weight of steel wire is somewhat less than

that of S/HTS Fiberglas, the higher crushing stress under the steel wires would be a disadvantage because of greater localized crushing and deformation of the foam insulation. The superior physical properties of fiber-glass roving (no creep under load, high strength-to-weight ratio, and excellent low- and high-temperature characteristics) also strongly favor its use as a constrictive-wrap material. In the earlier phases of the program, strand breakage during winding at the required pretensioning (2.0 lb/strand) precluded the use of S/HTS Fiberglas. (The normal winding tension used for filament-wound fiber-glass rocket motor cases is only 0.75 lb/strand.) Laboratory tests with single fiber-glass strands, however, demonstrated that a static load of 2.5 pounds can be carried almost indefinitely (3 months) without failure by an uncoated strand of S/HTS Fiberglas, which indicated that the application of a fiber-glass constrictive wrap pretensioned to 2 pounds per strand should be feasible. Therefore, continued effort was exerted to develop a winding technique that eliminated the strand breakage problem.

The winding procedure finally developed consisted of winding eight-strand epoxy-preimpregnated S/HTS Fiberglas roving by a modified procedure for applying additional resin to the roving. This procedure was developed during the subscale tank program (ch. V) in insulation system 4. Use of a preimpregnated roving was required to eliminate snarling that resulted from occasional single-filament breakage under the high winding tension. It was not possible to cure the epoxy in the preimpregnated roving at room temperature; therefore, a temperature-resistant silicone resin that could be cured at room temperature, was also applied to provide fiber adherence to other fibers at crossover points In conventional winding procedures, resin is applied to the fiber-glass roving before it passes over the final distributor-head pulley guiding it onto the tank that is being wrapped. Under the load of 2 pounds per strand used in this procedure, occasional loose filaments that had been wetted with resin would snag on the pulley. Once snagged, the roving would split apart and fail by overwrapping about the pulley. To prevent this problem, a new silicone-resin impregnation device was designed and built that applied the resin after the roving had passed over the distributor-head pulley. Thus, the roving was impregnated with resin, wiped, and deposited as a constrictive wrap over the insulation without interference from pulleys normally employed in winding.

TABLE VII-IV. - TENSILE STRENGTH OF FIBER-GLASS-IMPREGNATED ROVING

Specimen	Ultimate tensile strength, lb
1	37.3
2	50.8
3	43.4
4	49.3
5	55.8
6	47.0
Average	47.2

To qualify the eight-strand S/HTS Fiberglas-impregnated roving selected for the constrictive wrap for the full-scale Centaur tank, strand tensile tests of the eight-strand roving in preimpregnated form were conducted. The results of these tests are given in table VII-IV. The results showed that the strength of the selected roving (ultimate tensile strength, 47.2 lb) was well above the required wrapping tension of 16 pounds.

These tests were conducted in accordance with the strand test procedures used to qualify epoxy-preimpregnated fiber-glass roving material in rocket motor case programs, with the exception that the impregnated roving was not preloaded and cured to simulate a cured composite material.

The average tensile strength per strand of roving when fully cured is about 9 pounds. In the qualification tests, in which the preimpregnated resin was in an uncured state, only two-thirds of its ultimate strength is apparent. This is understandable because the resin in the preimpregnated state has only a fraction of its ultimate cured strength. It is known that a preimpregnated resin will improve in strength with time and impart a higher interfilament shear strength within the preimpregnated roving and thus further enhance the tensile strength of the constrictive-wrap material.

FABRICATION OF INSULATION PANELS

The insulation panels were constructed from the following elements, as shown in figure VII-2 (p. 100):

(1) Polyurethane foam slabs

(2) MAM-laminate face sheets

(3) Mylar edge channels

(4) Mylar doubler strips

(5) Goodyear Vitel PE 207 adhesive

Techniques developed during subscale tank panel fabrication were employed in the construction of the full-scale tank insulation panels. The major problems in panel fabrication were

(1) Sealing Mylar channels at corner folds

(2) Accurately locating cutouts to match protuberance locations on the tank

(3) Sizing the cutouts to match the Z-section seal members

(4) Bonding Z-sections, doubler, and channels of lightweight Mylar without incurring wrinkles that would be potential leak sources

To ensure reliability of the final product, a system of quality-control procedures and careful workmanship was followed throughout the fabrication processes.

Fabrication Procedures

Foam slabs 0.4 inch thick were cut from Freon-blown polyurethane-foam blocks that were foamed in place in a steel block mold 10 inches deep by 42 inches wide by 99 inches long. The foam formulation is given in table VII-V. The measured foam density in the slabs ranged from 1.8 to 2.0 pounds per cubic foot. Slicing of the blocks into 0.4-inch-thick slabs was accomplished on a large bandsaw that had a hydraulically controlled feed table which moved the foam block

TABLE VII-V. - FOAM FORMULA

Compound	Parts by weight
Plaskon 6 foam resin	100.0
Dabco LV-33 catalyst	.6
Union Carbide L5310 silicone surfactant	1.5
Glidden RCR5043 isocyanate prepolymer	111.0
Freon R-11 fluorocarbon blowing agent	30.0

past a bandsaw blade set 0.400 inch from a 32-inch-high by 48-inch-long backup plate. With this setup, a thickness tolerance of ±0.008 inch was achieved over the entire area of the slab.

In the process of sealing the foam insulation slabs, the 0.0015-inch MAM sealing laminate was bonded to the foam panels with a heat-sealable polyester resin (Vitel PE 207, Goodyear Tire and Rubber Company). The foam surfaces were spray-coated, and the face sheet materials were precleaned with methylethyl ketone and brush coated lightly with resin and allowed to dry at least 2 hours. The foam slab was placed on a convex wooden die to form the 60-inch radius of curvature and covered with one of the MAM sealing laminate face sheets placed with the adhesive side toward the foam. A vacuum bag was applied, and the face sheet was heat sealed to the foam slab by ironing with a hand iron set at 265° F. The foam slab and the convex face sheet were then placed in a concave wooden die having a 60.4-inch radius of curvature, and the second face sheet was applied with the adhesive side toward the foam. A vacuum bag was applied, and the face sheet was heat sealed to the foam slab by ironing with a curved-shoe hand iron set at 265° F. The face-sealed foam slab was placed on a trim fixture and trimmed to final size with a razor-type knife guided by metal straight-edge bars clamped to each side of the slab.

The edges of the face-sealed foam slabs were sealed by bonding premolded 0.002-inch-thick Mylar channels to the perimeter of the slab. The Mylar channels were premolded by vacuum forming on steel molds and heat set at 275° F for 45 minutes. Before bonding to the edges, the Mylar channels were rough trimmed to length, and channel legs were finish trimmed to a width of 0.62 inch. The inside surfaces of the channels and the perimeter of the face sheets of the foam slabs were precleaned with methylethyl ketone, brush coated with resin, and allowed to dry. The channels were then assembled onto the edges of the foam slab. Two opposite channels were finish trimmed to the length of the foam panel. The other two opposite channels extended beyond the length of the panel at each end. The excess lengths were carefully folded over as shown in figure VII-2 (p. 100) to form the corner seal. The assembly was vacuum bagged, and the channels were heat sealed to the face sheets by using a 265° F hand iron. The channel-to-face-sheet bond was further reinforced and sealed with 0.75-inch-wide, 0.001-inch-thick Mylar doubler strips centered along the edge of the channel (fig. VII-2). The doubler strips were applied in the same manner as the channels. To further ensure that the insulation panel was leak tight, the corners and all edges were double-dipped in a bath of Vitel PE 207 resin to a depth sufficient to coat all edges and doublers. Earlier development work on subscale panels had shown that doubler strips and dipped edges reduced the possibility of leaks.

The fabrication procedures just outlined are for the fabrication of a typical full-scale Centaur insulation panel without protuberance cutouts. In this program all panels were fabricated and leak tested (in a manner to be discussed later) before protuberance cutouts were made and then subsequently retested after cutouts were sealed. Protuberance cutouts were located by detailed metal templates previously developed from the flat panel layout of the Centaur tank (fig. VII-3, p. 101). Beveled cutouts were hand cut at each protuberance location to match the preformed Mylar Z-section perimeter seal as shown in

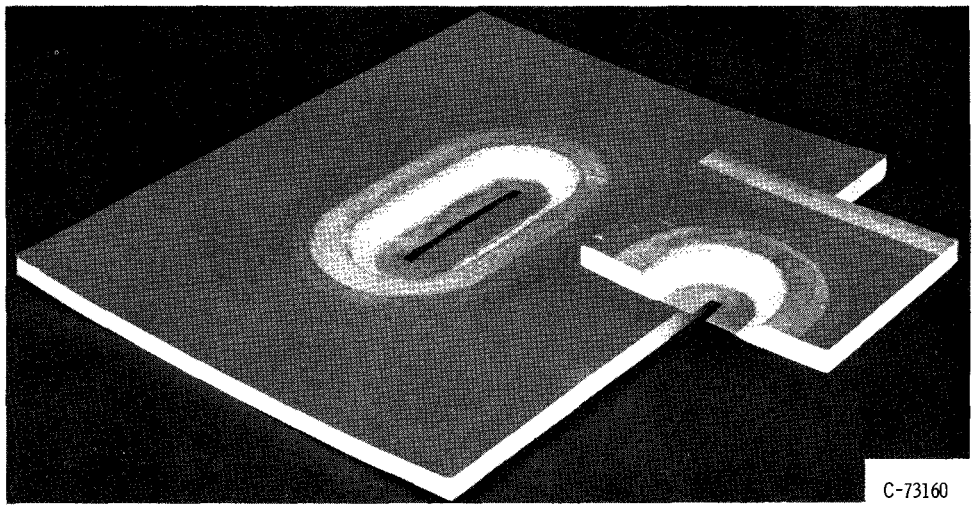

Figure VII-6. - Method of sealing protuberance cutouts in insulation panels using preformed Mylar Z-section and perimeter seal.

figure VII-6. The Z-section and all bonding surfaces of the Z-section, doublers, and face sheets around the perimeter of the panel cutout were coated with Vitel PE 207 resin and dried. The Z-section and doublers were then assembled into the panel cutout and held secure by vacuum bag pressure while the bond was sealed by ironing with a hand iron set at 265° F.

Quality Control

Two key steps in the processing of each panel were carefully controlled, since assurance of vacuum tight panels was required.

First, rolls of the MAM laminate were visually inspected over a backlighted glass table, and the frequency of pinhole light leaks was noted. Samples were cut from the pinhole areas and tested for leakage in a Dow-cell gas-diffusion test apparatus. Since no leakage was noted, it was concluded that the pinhole light leaks were holes in the aluminum foil only, and that the backup layers of Mylar sealed the pinholes in the aluminum foil.

Second, qualification of the completed insulation panels for the full-scale Centaur test tank included the following test procedures:

(1) Visual inspection. All panels were inspected for possible leak areas along the bonded edge channels on the surface, and all questionable areas were repaired with a patch of MAM sealing laminate and an overwipe of Vitel PE 207 resin.

(2) Leak test by liquid-nitrogen submergence. All sealed panels were leak tested for vacuum tightness prior to bonding to the tank. A method of leak testing was developed that somewhat duplicated the sealing requirements under actual conditions. The cryopumped vacuum normally obtained when the panels are attached to a liquid-hydrogen-filled tank was at least partially duplicated by immersing the panels in a bath of liquid nitrogen for 5 minutes. The cooling

caused the contained gases to contract or condense with a resultant decrease in internal pressure. If a leak of small size existed anywhere in the seal material, some nitrogen was drawn into the panel. Upon removal from the nitrogen bath, the panel warmed up, and the entrapped liquid nitrogen vaporized rapidly but could not escape through the small hole at a rapid enough rate to keep the internal pressure from building up to the point where a blister would appear in the laminate covering on the panel. Larger holes are not easily detected by this method since the warmed-up gases are able to escape without producing significant pressure. These larger leak sources, however, can be found by careful visual inspection of the panel after removal from the liquid nitrogen. A small trail of vapor can usually be seen emerging through the larger hole in the covering.

Three panels were disqualified during the leak testing in liquid nitrogen. Twenty three panels were built to obtain the twenty that qualified for use on the Centaur tank.

INSTALLATION OF INSULATION SYSTEM

For mobility and accessibility during installation of the insulation system, a multipurpose frame was used to support the full-scale Centaur test tank. The frame held the tank in a horizontal position for storage and transporting from fabrication area to test site. The frame also contained trunion bearings for raising the tank to an upright position for testing at the test site. The tank was supported in the frame by tubular spiders which were attached to transition flanges on the tank near each end. The tubular spiders were removable from the base of the frame. When detached from the frame, these spiders served as supports for mounting the tank in a filament winding machine.

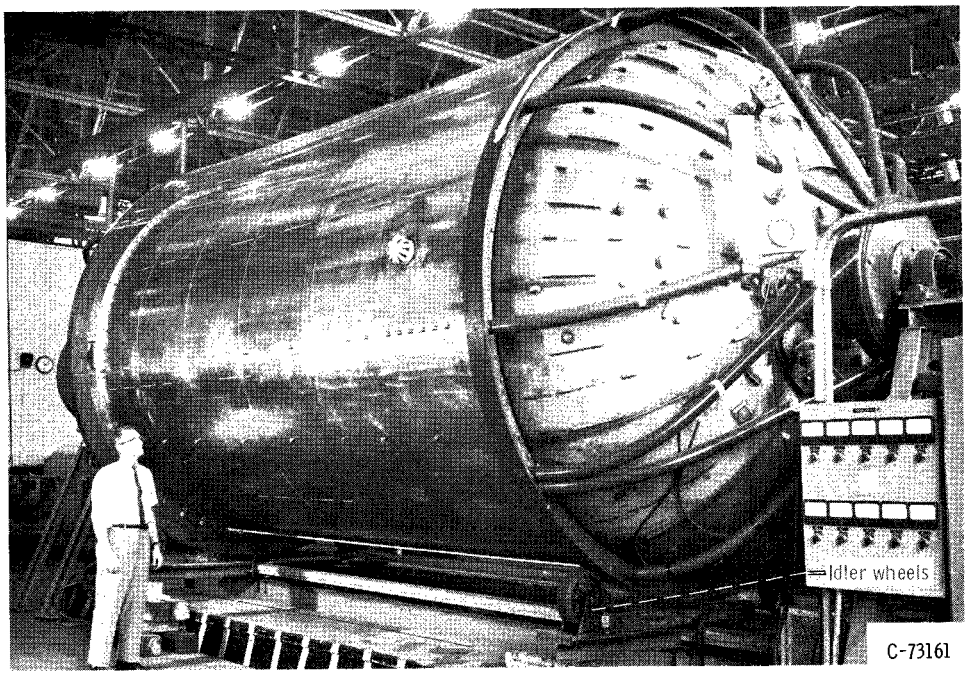

Figure VII-7. - Centaur test vehicle in filament winding machine.

Bonding of Panels to Tank

For accessibility during installation of the insulation panels, the full-scale Centaur test tank was installed in a horizontal filament winding machine as shown in figure VII-7.

After passing the leak test, the insulation panels were bonded and sealed to the tank exterior wall with a low-temperature polyurethane adhesive, Narmco 7343/7139. Figure VII-8 shows the panel-to-tank bonding resin being applied to the back side of an insulation panel after it was cleaned with methylethyl ketone. A pressure gun was used to lay a bead of the Narmco 7343/7139 resin around the perimeter of the panel and across a 6-inch-square glue line grid pattern. Each of the protuberance cutouts has its own perimeter glue line that intersects the grid pattern as required. The grid-pattern method of bonding held weight to a minimum and yet affected a satisfactory bond that provided a sectioned sealed airspace between the panel and the tank wall. Before the panels were bonded, the tank was wiped clean with toluene and thoroughly

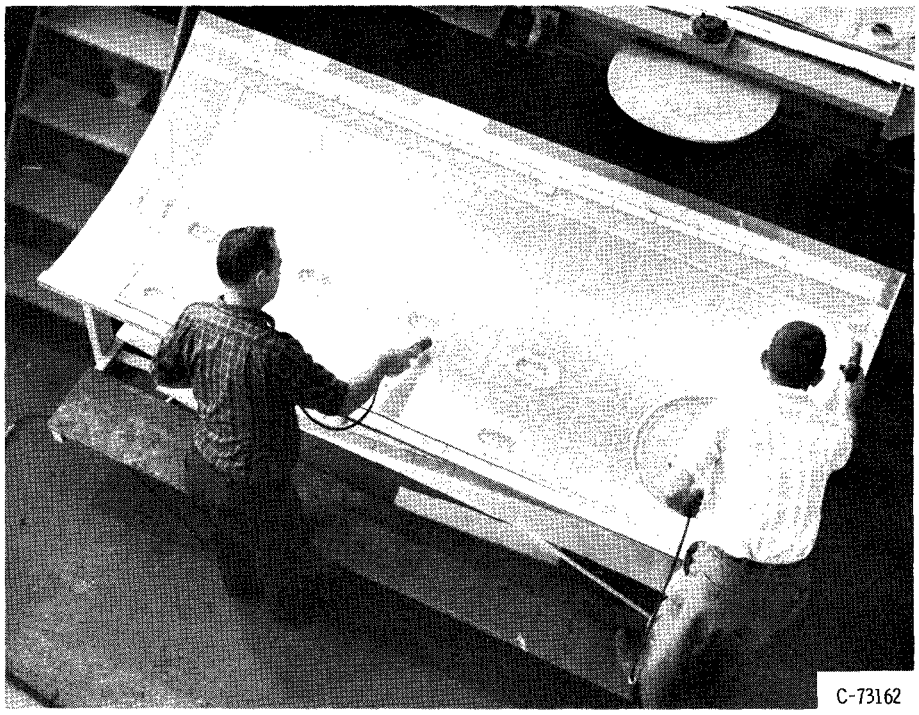

Figure VII-8. - Application of panel-to-tank bonding resin grid pattern.

scrubbed with methylethyl ketone. A light brush coat of Vitel PE 207 resin was then applied to serve as a primer on the tank surface.

Figure VII-9 shows the insulation panels being placed on the tank. At the left are panels just fitted to the tank. At the right are panels previously bonded to the tank and still under the vacuum bag used to hold the panels tightly to the tank while the adhesive between the panels and the tank cured at room temperature. The insulation panels were bonded to the tank in a sequence of seven groups of two to four panels per group. The number of panels per group was selected on the basis of the time required to prepare the panels for

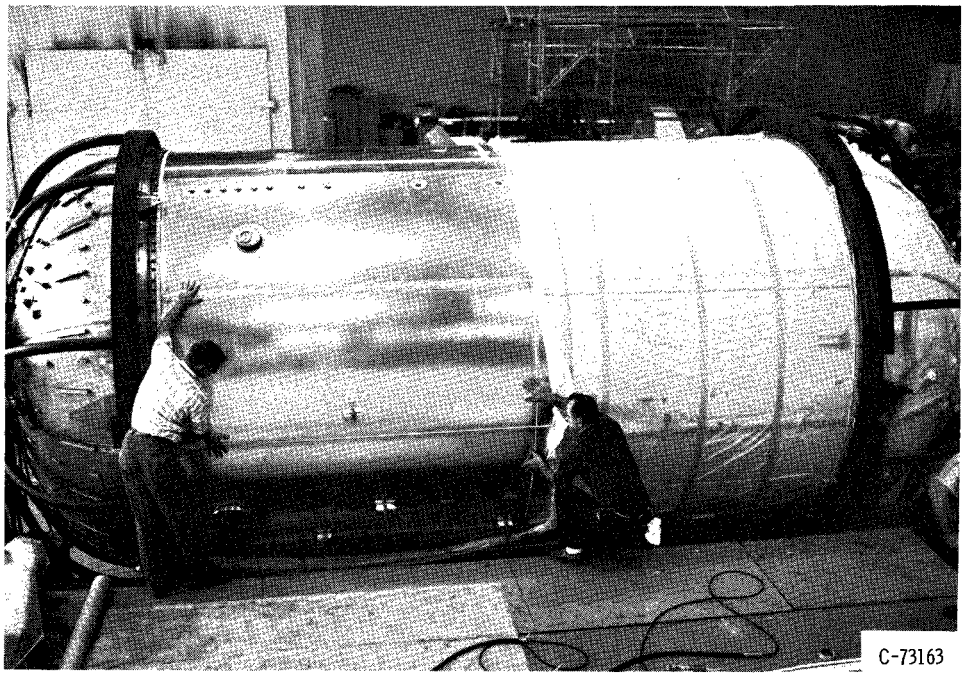

Figure VII-9. - Application of insulation panels to full-scale Centaur tank.

bonding and to cure the adhesive. There was a definite time limitation to obtain optimum bonding results because of the pot life of the Narmco 7343/7139 resin mixture.

Panel Joints

Joints between adjacent panels were filled with a 2.0-pound-per-cubic-foot polyurethane foam and cut and fitted in place as the panels were located on the tank (see fig. VII-3, p. 101). These filler strips were bonded in place with the Narmco 7343/7139 resin mixture. The nominal width of the filler strips was 1/4 inch; however, some changes in width were made to accommodate variations in panel-joint gap due to panel size and tank diameter tolerances. The foam filler strips were sanded flush with outer top surfaces of the panel, and MAM-laminate cover strips were bonded over the panel joints. The MAM-laminate cover strips, being about 2 inches wide, bridged the foam-filled gap between panels and sealed the gap against air penetration.

Protuberance Covers

The majority of protuberances on the Centaur test tank were covered with foam insulation, and a vapor-tight cover of spun aluminum-Mylar-aluminum laminate (0.005 in. thick) was added over the foam to provide the final seal, as shown in figure VII-4 (p. 102). These covers were bonded and sealed to the insulation panel with Narmco 7343/7139 resin mixture. A vacuum-bag pressure was employed to seat the protuberance covers while the resin was cured at room temperature. The final assembly for all types of protuberances is shown in figure VII-10.

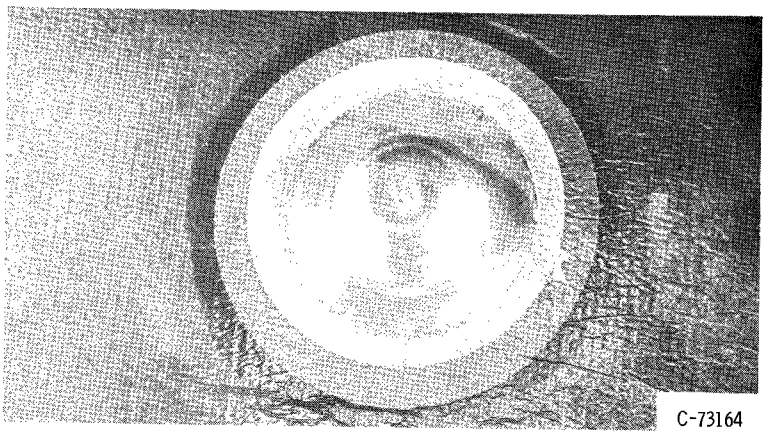

C-73164

(a) Small protuberance cap.

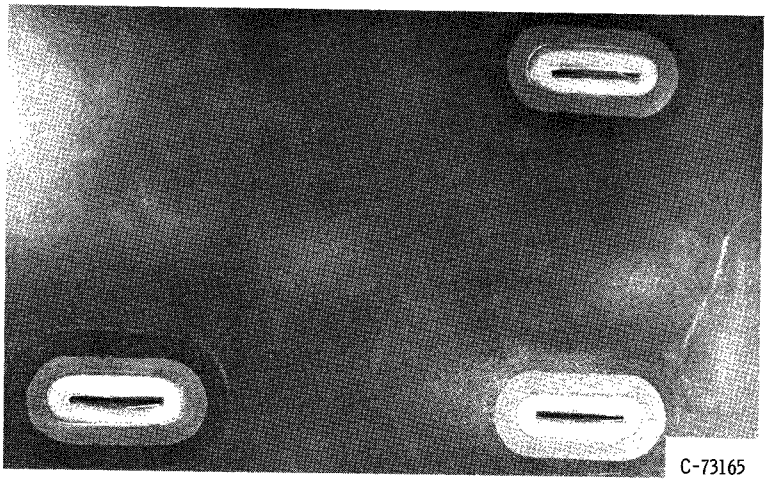

C-73165

(b) Wiring harness bracket cutout.

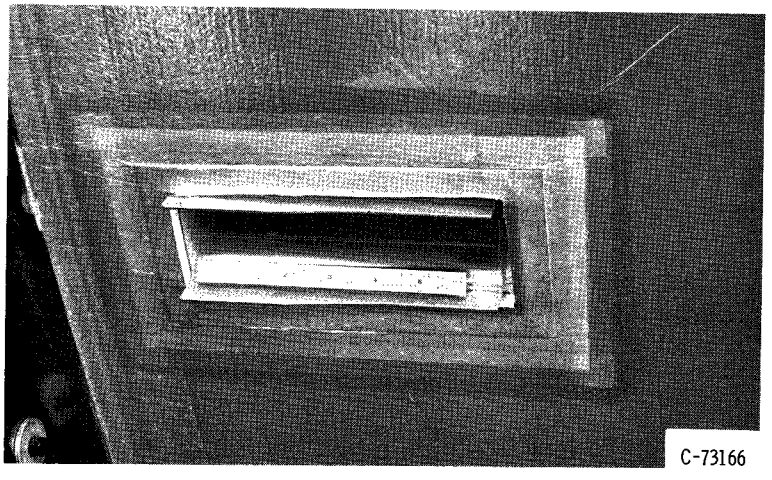

C-73166

(c) Hinge bracket cutout.

Figure VII-10. - Final assembly of sealed insulation over and around various types of protuberances.

Heat Protection Layer

Prior to the application of the constrictive wrap, the exterior surfaces of the insulation panels were covered with a heat protection layer of style 106 Fiberglas cloth impregnated and bonded with Silicone A-4000 resin (see ch. VI). The cloth was 38 inches wide and was applied in a series of single-layer circumferential wraps overlapping each other approximately $1\frac{1}{2}$ inches. The cloth was cut out around protuberance covers. The resin was catalyzed for a room-temperature cure of 8-hour duration.

Constrictive Wrap

The constrictive wrap was applied to the Centaur test tank by a horizontal filament winding machine (fig. VII-7, p. 109). Modifications were made to the machine mandrel drive shaft and the mandrel support stands to permit the installation of the 10-foot-diameter, 25-foot-long Centaur tank in the machine. The centerline of the mandrel shaft was offset from the drive-shaft centerline and raised from a 4-foot to a 6-foot swing by the installation of new support stanchions for the mandrel (tank) shaft bearings. To reduce bending loads in the forward and rear support spiders and attendent mandrel shafts, a pair of idler wheels was installed on the base of the machine at each spider ring, as shown in figure VII-7. A chain and sprocket arrangement coupled the relocated mandrel shaft and the existing drive shaft from the prime mover of the machine.

The application of the fiber-glass roving constrictive wrap was accomplished by utilizing the spool wrap setup on the filament winding machine. Figure VII-11 shows the application of the constrictive wrap. The entire wrapping

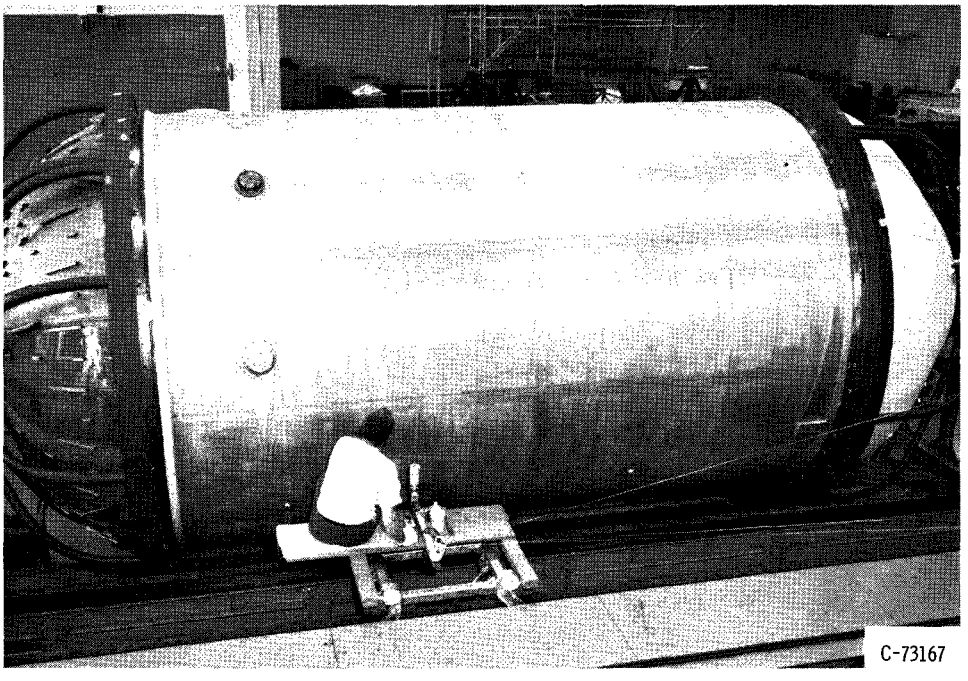

Figure VII-11. - Application of fiber-glass roving constrictive wrap to full-scale Centaur tank.

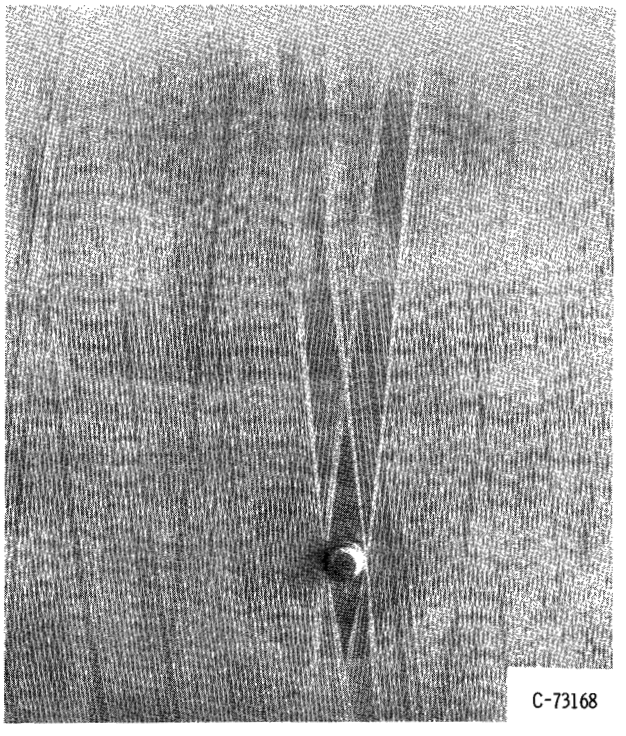

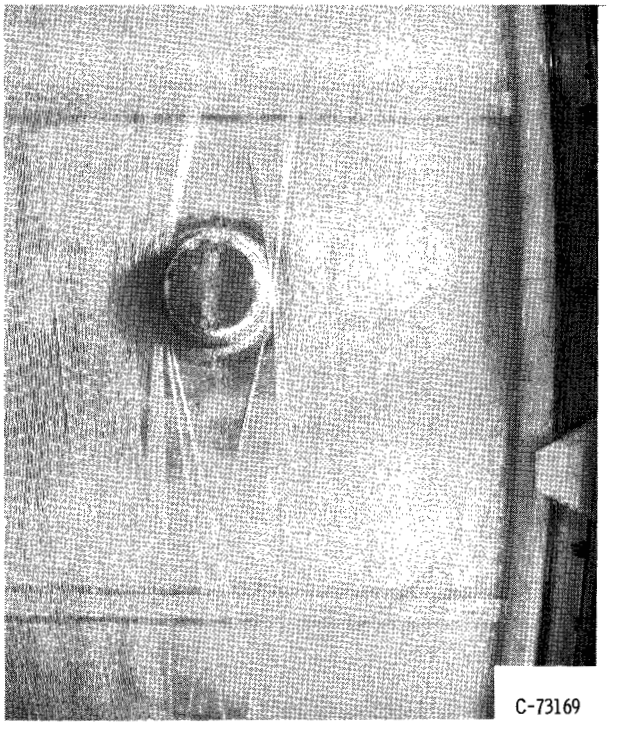

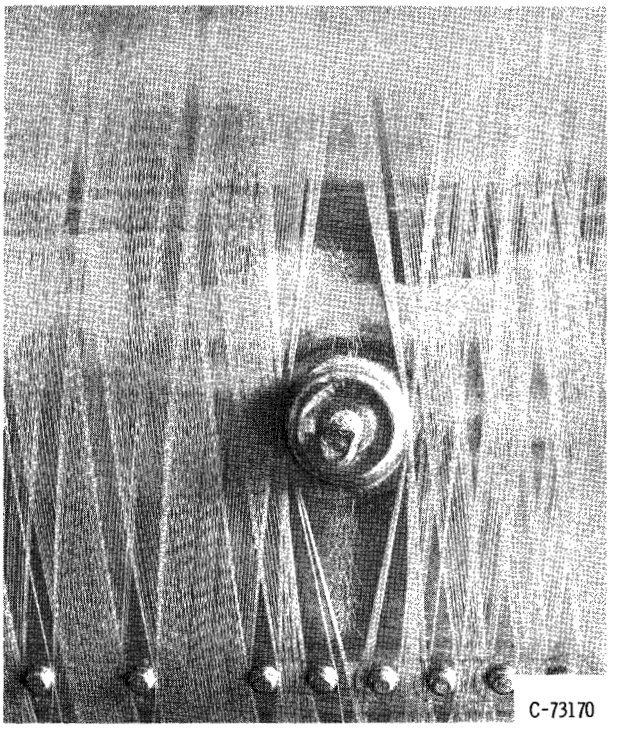

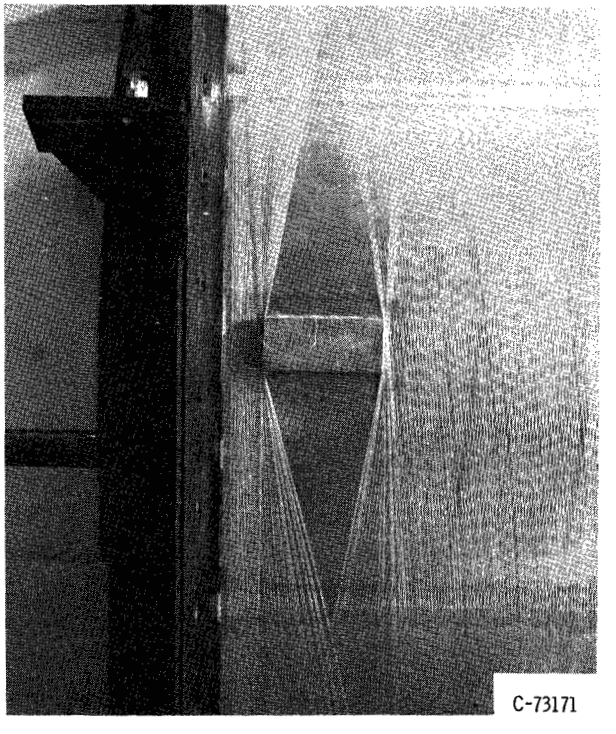

Figure VII-12. - Displacement of helical wrap by protuberances.

operation, including monitoring the wrapping speed control and the resin-impregnation device, was commanded by an operator riding on the carriage of the filament winding machine. Three rovings of eight-strand S/HTS Fiberglas preimpregnated epoxy roving were fed through the silicone resin impregnation device mounted on the carriage in order to eliminate strand breakage. During the wrapping process the rovings were manually displaced, by the operator, from their normal 6° wrap angle to a greater angle as required to clear protuberance covers (fig. VII-12). The rovings were tensioned to 2 pounds per strand to provide a 0.84 percent strain in the fiber-glass roving. Spacing was provided to give a 2-pound-per-square-inch compressive load. The complete wrap required 504 mandrel revolutions. An overnight room-temperature cure of the silicone A-4000 resin completed the application of the constrictive wrap.

Insulation of Forward Dome

The forward dome of the full-scale Centaur test tank was insulated to minimize heat leak when testing with liquid hydrogen. For expediency and economic

TABLE VII-VI. - WEIGHT DATA FOR INSULATION SYSTEM AS APPLIED TO CENTAUR TEST TANK

Material and thickness in inches	Unit weight	Estimated total weight, lb	Actual weight, lb
Panels			
Foam (0.4)	2 lb/cu ft	31.46	
Mylar-aluminum-Mylar (0.0005-0.0005-0.0005)	0.014 lb/sq ft	13.21	
Mylar channels (0.002)	.014 lb/sq ft	.85	
Mylar doublers (0.002)	.014 lb/sq ft	.85	
Resin	.05 lb/cu in.	2.40	
Subtotal		48.67	50.50
Panel gap joint			
Foam filler strips (0.4)	2 lb/cu ft	.77	[a].77
Mylar-aluminum-Mylar cover strips	.014 lb/sq ft	.50	.71
Subtotal		1.27	1.48
Panel bonding system			
Vitel PE 207 resin primer on tank	.05 lb/cu in.	2.60	1.75
Polyurethane resin (grid pattern seal)	.05 lb/cu in.	3.18	5.60
Subtotal		5.78	7.35
Glass-cloth overlay			
Glass cloth (0.0015)	.0059 lb/sq ft	4.50	3.0
Vitel PE 207 resin binder	.05 lb/cu in.	2.60	1.75
Subtotal		7.10	4.75
Constrictive-wrap system			
S/HTS Fiberglas (60 ends/in.)	$.228 \times 10^{-4}$ lb/ft	7.94	11.38
Epoxy-preimpregnated resin	.05 lb/cu in.	1.96	
Silicone binder	.05 lb/cu in.	1.96	3.25
Subtotal		11.86	14.63
Total weight of system		74.68	[a]78.71

[a]Based on estimated weight for panel gap foam-filler strips.

considerations, the dome was insulated with unsealed foam panels of 2.0-pound-per-cubic-foot polyurethane foam $1\frac{1}{4}$ inches thick. These panels were covered only with a helium-purge envelope made of 0.0024-inch-thick MAM laminate.

INSULATION SYSTEM WEIGHT

Table VII-VI lists the estimated design weights and the final actual weights of the components of the insulation system as applied to the full-scale Centaur tank. Estimated weights are based on component sizes and material densities (2.0 lb/cu ft for the foam). Actual weights were obtained by keeping an accurate tally of all the components and materials that were installed on the tank. The total actual weight exceeded the estimated weight by only about 5 percent. This weight comparison indicates that, with careful control of fabrication techniques, the installed insulation system can be held very close to the lightweight design. The average unit weight for the approximately 485 square feet of cylinder surface of about 0.16 pound per square foot makes this system the lightest external insulation system for liquid-hydrogen rocket tanks known to the authors.

SUMMARY OF RESULTS

The results of designing, fabricating, and applying the sealed-foam constrictive-wrap insulation system to a full-scale liquid-hydrogen tank can be summarized as follows:

1. A hermetically sealed polyurethane foam insulation system was developed that was suitable for installation on full-scale cylindrical hydrogen tanks in the form of large panels. The method of sealing the panels permitted protuberances to extend through the insulation by means of sealed cutouts in the insulation panels.

2. The panels are held to the cylindrical tank by means of a pretensioned constrictive wrap. Comparison of high-strength steel wire, HT-1 Nylon, and S/HTS Fiberglas as wrap materials showed that S/HTS Fiberglas was the best material for the purpose. Special wrapping techniques were developed for applying the constrictive wrap of S/HTS Fiberglas at a pretension of 2 pounds per strand.

3. The installed weight of the entire insulation system was 0.16 pound per square foot, including the polyurethane foam 0.4 inch thick, the hermetic sealing material, a glass-cloth layer for protection from aerodynamic forces and heating, and a constrictive wrap of S/HTS Fiberglas to hold the insulation in place.

CHAPTER VIII

FULL-SCALE-TANK GROUND-HOLD TESTS

by Howard F. Calvert, Porter J. Perkins, Jr.,
William C. Morgan, and Mario A. Colaluca

Lewis Research Center

The lightweight insulation system fully described in the preceding chapters was applied to a full-scale Centaur vehicle tank. The tank consisted of two compartments, one for liquid oxygen (which was filled with liquid nitrogen for these tests) and one for liquid hydrogen. The data obtained in this investigation were restricted to the insulation on the cylindrical section of the hydrogen tank. Two long-time ground-hold tests were conducted at the Plum Brook Station to investigate the insulation-system conductivity by measurement of boiloff rates and to determine the pressure rise rate with vent valves closed. The insulation was inspected after the completion of the investigation to determine any degradation that may have taken place. The detailed inspection of the insulation after the test is fully described in the appendix.

APPARATUS AND INSTRUMENTATION

Test Tank

The propellant-tank assembly utilized in the full-scale investigation reported herein was a heavy-weight model of the Centaur vehicle, which is a pressure-stabilized structure consisting of a straight cylindrical center section with two domed ends. Figure VIII-1 shows a sketch of this tank. The wall thickness of the tank was 0.040 inch, whereas the wall thickness of flight models of Centaur is 0.014 inch. The straight section was approximately $15\frac{1}{2}$ feet long and 10 feet in diameter, and the top and bottom domes were approximately 5 and 4 feet high, respectively. An intermediate bulkhead was located at the junction of the lower dome with the straight section to form a 3000-gallon liquid-oxygen tank at the bottom, and a 9400-gallon (1250 cu ft) liquid-hydrogen tank in the upper section. The top dome and the straight cylindrical section were fabricated from cold-reduced AISI 301 stainless-steel sheet with spot-welded lap joints. Spot-welded doublers were utilized around all openings. The bottom dome was fabricated by using butt-welded gores.

The tank contained numerous protuberances or pressure fittings and brackets, which made the installation of the panel insulation system difficult (ch. VII). This tank had been a ground-test research vehicle and therefore had

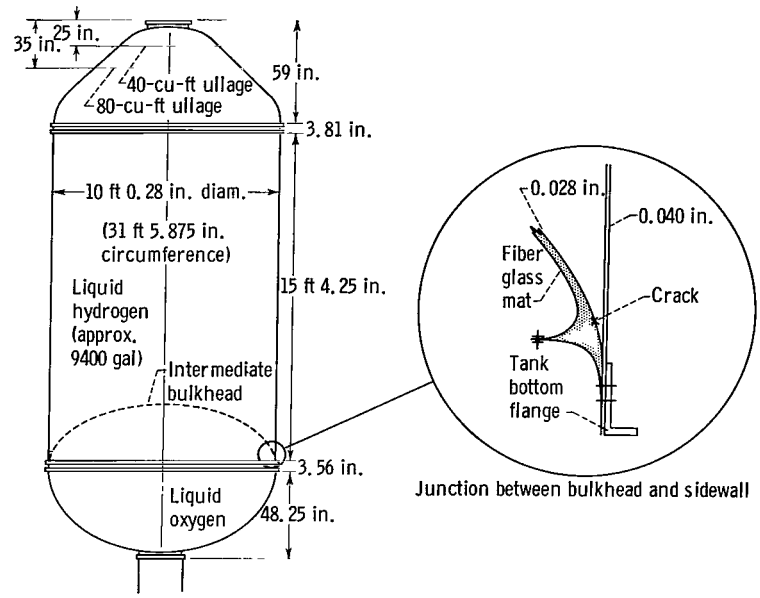

Figure VIII-1. - Schematic view of Centaur tank.

required more positions for measuring temperature, pressure, and liquid level than a production flight tank.

Figure VIII-1 shows a schematic cross-sectional view of the intermediate bulkhead and its junction with the outside wall. The bulkhead was formed by two closely spaced domes, the intervening space being filled with a fiber-glass mat.

Normally a vacuum is held in the bulkhead to assist in providing a satisfactory insulation between the liquid oxygen and the liquid hydrogen; however, during previous tests the intermediate bulkhead pressure approached atmospheric pressure during the detanking of the liquid hydrogen, which indicated a leak. The loss of vacuum would result in a high heat leak and in excessive loss of liquid hydrogen from boiloff.

At attempt was made to locate and repair the leak before the installation of the lightweight insulation system. Standard leak detection techniques were utilized to determine that the leak was in the area of the junction of the bulkhead (inset in fig. VIII-1). The location made it physically impossible to see the crack; however, the leak rate indicated the size of the crack to be small. A long hypodermic-type needle was used to inject a room-temperature curing polyurethane resin in the area of the crack. A vacuum was held in the bulkhead so that the resin would be pulled into the crack and form a seal. This technique sealed the crack so that the tank could be used for this investigation.

Test Stand

Figure VIII-2 is a picture of the test facility at the Plum Brook Station

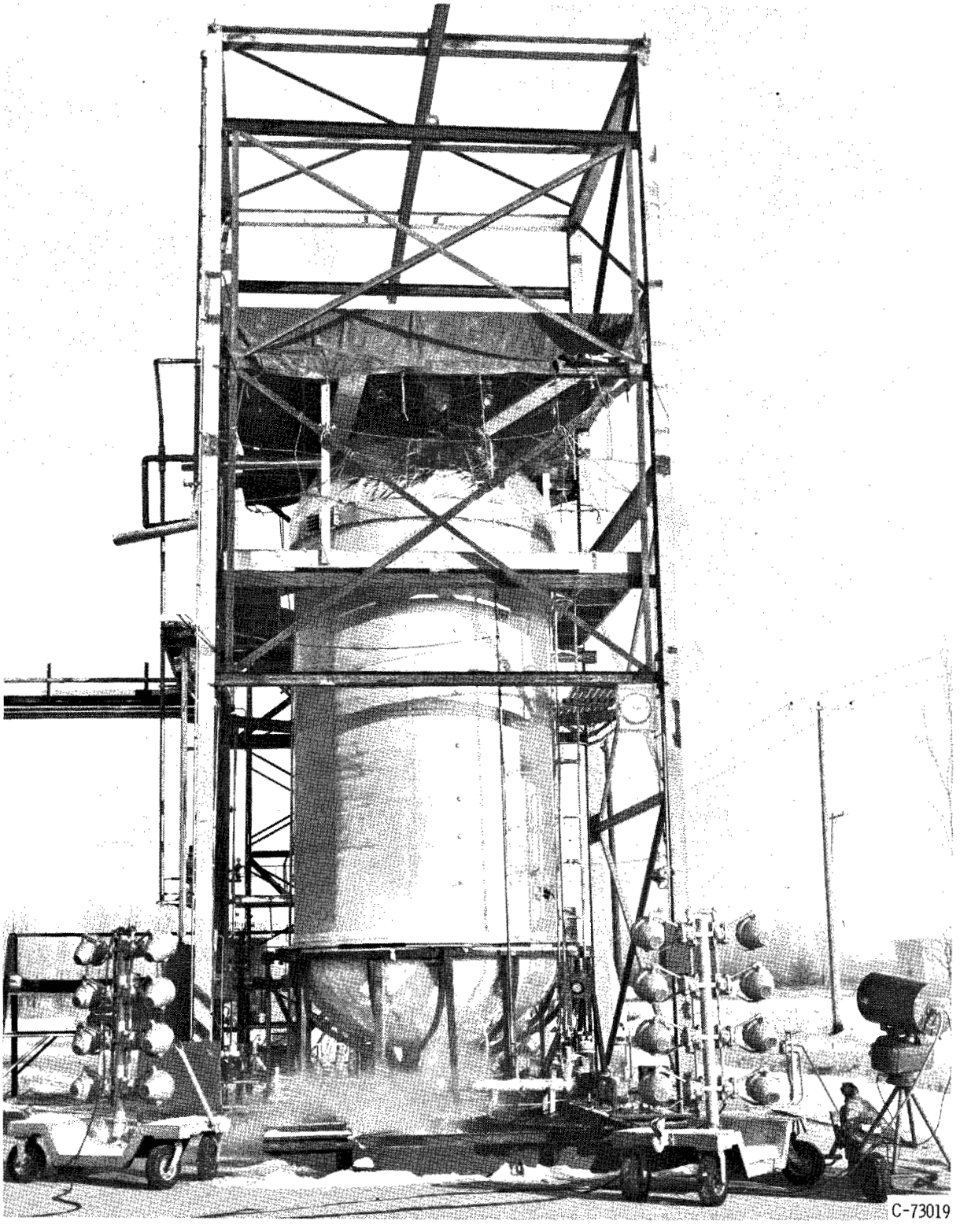

Figure VIII-2. - Centaur tank in test stand.

used for this investigation. The test stand consisted of inner and outer frames mounted on a concrete pad located beside an existing test facility that supplied gas, liquid hydrogen, liquid nitrogen, and electricity. The inner frame supporting the test vehicle was mounted in trunnion bearings on a stand that permitted the tank to be held in the horizontal position for transporting or the vertical position, as shown, for testing. The working platform, canvas weather protection, system piping, and instrumentation were supported by the outer frame. The tests were controlled remotely from the control room for this facility.

Two vent systems were used for the hydrogen boiloff gas. One vent contained a pressure-control valve and an orifice-type volume flow-rate measuring system. The pressure-control valve was a flight valve that maintained a constant tank pressure of approximately 6 pounds per square inch gage. The orifice system was used to measure the volume flow of hydrogen gas from boiloff. The second vent was a safety bypass system containing a remotely controlled fully open or closed valve.

Instrumentation

Three systems were used to measure the level of the liquid hydrogen. They were a hot-wire system, a differential-pressure gage, and a capacitance probe. A fourth system consisting of copper-constantan thermocouples mounted on the inside of the tank wall was used as an approximate-level indicator. The redundancy in the systems helped ensure accurate measurements of the level of liquid hydrogen. Liquid hydrogen is extremely lightweight and low in temperature (-423° F), the gas to liquid interface is difficult to determine, and the liquid may be boiling continually.

Eleven hot-wire liquid-level indicators were spaced on a vertical line so as to determine the level of liquid hydrogen during the fill and boiloff tests. The level was monitored and recorded by the use of a strip-chart recorder and indicating lights.

A differential-pressure transducer was installed at the same level as the lowest hot wire to measure the head of liquid hydrogen. The output of the pressure transducer was recorded on a strip-chart recorder.

A capacitance-type liquid-level probe was mounted through the top flange of the tank and extended approximately 16 feet down into the tank. The output was recorded on a strip-chart recorder. This probe was operative for the second run only.

Copper-constantan thermocouples were mounted on the inside wall of the tank at six vertical locations. Two thermocouples were located at each station 180° from each other. Thermocouples were also attached to the outside of the insulation at stations directly opposite the thermocouples on the inside surface of the tank. The method of attachment was the same as that described in chapter V for the subscale tanks. It consisted of attaching the thermocouples with an epoxy adhesive and a cover patch of MAM (Mylar-aluminum-Mylar) laminate.

The orifice run used for measuring hydrogen-gas vent rates contained three temperature-measuring stations. The temperature at the orifice was measured with a platinum resistor, whereas the temperatures upstream and downstream were measured with copper-constantan thermocouple probes. All temperatures were indicated and recorded on strip-chart recorders. The platinum resistor was read out on a null-balance system.

Television and Photographic System

Three television cameras were used to monitor remotely the visual appearance and efficiency of the insulation system. Two cameras were mounted 180° apart in a fixed position to present an overall view of the test. The third camera was a pan and tilt, full-control camera system used to monitor, with closeup views of the system (1) vents, piping, and connections for indications of leaks, (2) operation of the automatic liquid-nitrogen fill system for the liquid-oxygen tank, and (3) conditions of the insulation system such as frost formation. A 70-millimeter remote-control sequence-framing camera was used to record the insulation system condition with time.

TEST PROCEDURE

Two fill and boiloff tests were conducted on the test tank 34 days apart. These tests, in which the upper tank was filled with liquid hydrogen, were conducted in a manner to determine the thermal conductivity and integrity of the insulation under ground-hold conditions, and to determine the pressure-rise rate of the insulated tank with vent valves closed. The primary purpose of the second test was to determine if the first fill test had degraded the effectiveness of the insulation.

The same general test procedure was used for both parts of the investigation.

Before the fill tests were conducted, the liquid-hydrogen and liquid-oxygen tanks were filled with dry nitrogen gas at pressures of approximately 6 and 10 pounds per square inch gage, respectively, to maintain pressure stabilization of the structure. At the beginning of the fill tests the liquid-oxygen tank and its flow system were purged, and the tank was filled approximately one-half full of liquid nitrogen and automatically held at this level with a pressure of approximately 20 pounds per square inch gage throughout the duration of the test. Liquid nitrogen was used because it is much safer to handle than liquid oxygen, and still it provides a satisfactory temperature environment. The boiling point of liquid nitrogen is close to that of liquid oxygen.

The liquid-hydrogen tank and its flow system were purged of gaseous nitrogen with hydrogen gas, and the tank was filled with liquid hydrogen. All the liquid-level detecting systems were monitored to check out the instrumentation and the tank filling characteristics. Two types of ground-hold tests were conducted, that is, pressure-buildup and boiloff-rate tests. During the pressure-buildup tests, the valves in both vent lines were closed, and the pressure-rise

rate was measured. After the pressure reached 12 pounds per square inch gage, the valves were opened and the tank was vented down to the operating pressure of 6 pounds per square inch gage. The time required for this pressure buildup was measured to determine the pressure-buildup rate. This procedure was repeated at 40- and 80-cubic-foot ullage-liquid levels. Boiloff-rate tests were run continuously after the level had dropped to the cylindrical section until the tank was approximately one-fourth full. The hydrogen gas was vented through the orifice system, and the data were recorded for calculating the gas flow. Simultaneously, the data from the hot-wire system, the differential-pressure gage, and the capacitance probe were recorded on strip-chart recorders. A record was also made of the time when each light in the hot-wire probe system went out.

When the boiloff-rate tests were completed, the liquid hydrogen was flowed back into the supply Dewars, and the full-scale Centaur model tank was slowly warmed up to ambient temperature. Photographs were taken throughout the tests and the warmup period. After the ground-hold tests were completed, the tank was completely depressurized to determine if it would buckle from the constrictive load of the fiber-glass wrap over the insulation. A close physical examination was also conducted during warmup and 54 days after the final test. The insulation was cut away, section by section, closely examined, and photographed.

TEST CONDITIONS

The investigation reported herein was conducted in an open-air facility where the lightweight insulation system was exposed to the weather. Table VIII-I lists the weather conditions, barometric pressure, temperature, relative humidity, wind velocity, and moisture content of air. During the first phase of the investigation, the tank contained liquid hydrogen for approximately 25 hours, whereas, in the second phase, the tank contained liquid hydrogen for approximately 11 hours.

TABLE VIII-I. - WEATHER CONDITIONS

Time	Barometric pressure, in. Hg		Temperature, °F		Wind velocity, knots		Relative humidity, percent		Moisture content of air, grains/lb dry air	
	12/21/63	1/23/64	12/21/63	1/23/64	12/21/63	1/23/64	12/21/63	1/23/64	12/21/63	1/23/64
8:00 a.m.	29.39	29.10	4	43	SW. 8	SE. 5	59	89	10	35
12:00 m.	29.43	29.40	10	49	SW. 8	SSE. 8	63	74	10	37
4:00 p.m.	29.465	28.88	16	55	SW. 8	SSE. 12	56	62	10	37

EXPERIMENTAL DATA REDUCTION

Basically, the method used to reduce the boiloff data obtained from the full-scale ground-hold tests was that outlined in the THERMAL PERFORMANCE AND

DATA REDUCTION section of chapter V (p. 55). This method assumes one-dimensional, steady-state heat transfer and utilizes a modified form of the basic Fourier conduction equation:

$$Q_T = \frac{K_{equiv} A_I (T_I - T_c)}{\Delta x} + Q_{ext}$$

where

A_I sidewall wetted surface area, sq ft

K_{equiv} equivalent thermal conductivity of insulation system, (Btu)(in.)/(hr)(sq ft)(^oR)

Q_{ext} extraneous heat leaks through ends of tank, Btu/hr

Q_T total heat input to liquid hydrogen, Btu/hr

T_c tank wall temperature (assumed to be 37° R)

T_I outside insulation skin temperature, ^oR

Δx thickness of insulation system, in.

The total heat flow, measured by the boiloff rate, was plotted against the product of wetted surface area and temperature difference across the insulation. It can be seen from equation (1) that, if the end heat loss is constant, the slope of the plot of Q_T against $A_I(T_I - T_c)$ is $K_{equiv}/\Delta x$, from which an equivalent thermal conductivity can be determined. The data obtained by this method differed slightly from the data for the ground-hold tests of the sub-scale tanks, which are presented as total heat flow plotted against only the wetted surface area. The inclusion of the temperature difference as part of the independent variable was necessary to account for the progressively decreasing insulation skin temperatures caused by the frost layer that developed on the system during the longer full-scale tests.

RESULTS AND DISCUSSION

Ground-hold tests on the insulated full-scale Centaur tank consisted of two liquid-hydrogen fill and pressure-rise and boiloff runs conducted 34 days apart. The first test run was at a rather cold ambient temperature near 10° F, whereas milder temperatures around 50° F existed during the second run (table VIII-I). The principal reason for a second test was to determine the possible detrimental effects on the insulation of a second cooldown and warmup cycle.

During the second test, the leak in the intermediate bulkhead reoccurred and destroyed the vacuum insulation between the liquid hydrogen and the liquid nitrogen. The resulting heat flow into the liquid hydrogen increased the total heat inflow (insulation, bulkhead, etc.) over that of the first test.

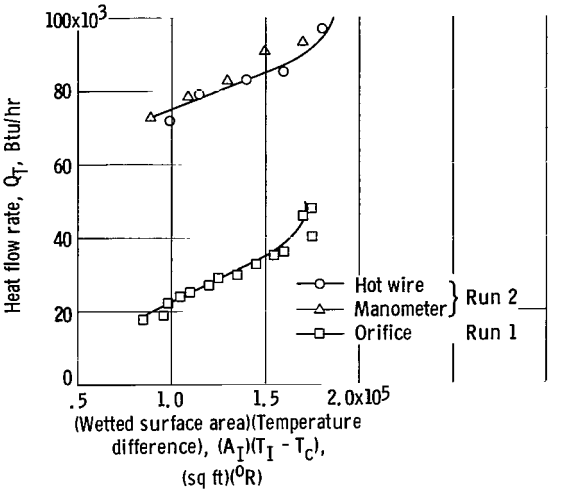

Figure VIII-3. - Heat flow to liquid hydrogen in full-scale tank.

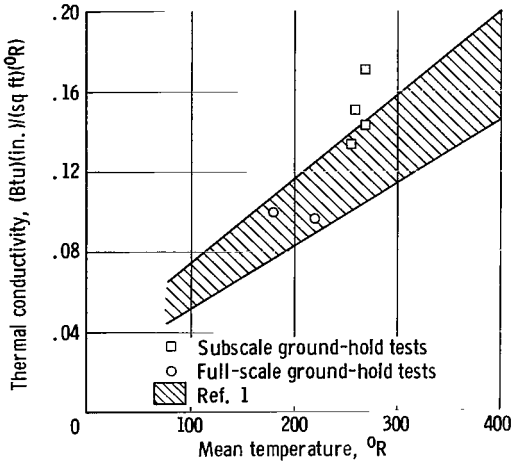

Figure VIII-4. - Thermal conductivity as function of mean temperature for polyurethane foam.

TABLE VIII-II. - RESULTS OF GROUND-HOLD TESTS

Run	Equivalent thermal conductivity, K_{equiv}, $\frac{(Btu)(in.)}{(hr)(sq\ ft)(^oR)}$	Average temperature difference across insulation, $T_I - T_c$, ^oR	Mean temperature of insulation, T_m, ^oR
Full scale			
1	0.096	360	219 to 225
2	.10	280	160 to 203
Subscale			
1	.17	470	273
2(a)	.13	453	265
2(b)	.14	473	275
3	.15	450	263
4(a)	.12	453	265
4(b)	[a]0.291 to 0.322	433	245

[a]Data taken after insulation was subjected to heating (see ch. V).

Thermal Performance of Insulation System

Thermal conductivity. - Equivalent thermal conductivities of 0.096 and 0.100 $\frac{(Btu)(in.)}{(hr)(sq\ ft)(^oR)}$ at an average mean temperature T_m of about 200° R were determined from the slope of the curves in figure VIII-3. The greater bulkhead heat leak and the lower temperature difference across the insulation (see table VIII-II) experienced during the second test shifted the position of the plot of Q_T against $A_I(T_I - T_c)$ by increasing Q_T and decreasing $A_I\ \Delta T$. The thicker frost formation during the second test decreased the temperature difference across the insulation. This does not, however, affect the determination of K_{equiv}, which is a function only of the slope of these

curves. These results are consistent with those reported in the literature for polyurethane foam (see fig. VIII-4). Also evident from figure VIII-4 is the fact that K_{equiv} for the full-scale system is from 30 to 40 percent lower than K_{equiv} as determined from the subscale tests (see table VIII-II). The lower mean temperatures of the full-scale tank tests account for a significant portion of the difference in thermal conductivities measured in full-scale and subscale tests. The fact, however, that most of the thermal conductivities measured in subscale tests fall above the curves from reference 1 indicates that heat leaks through the seam area were causing high values of equivalent thermal conductivity. In the full-scale tank tests with larger insulation panels, the seam areas were a smaller portion of the overall insulated area. As a result, the equivalent thermal conductivities are lower and agree better with thermal conductivities that have been obtained for the foam alone.

Rate of pressure rise. - Prior to the boiloff period of each test run, the pressure-rise rate in an unvented tank was determined by closing the vent valve until the pressure reached 12 pounds per square inch gage. These data are of interest since the Centaur launch procedure requires that the vent be closed for a period of time during the launch. The pressure-rise rates were recorded at two ullage volumes of approximately 40 and 80 cubic feet (fig. VIII-1) at the beginning of each thermal test run. Pressure-rise rates of about 2.36 pounds per square inch per minute at an ullage volume of about 40 cubic feet and 2.2 pounds per square inch per minute at an ullage volume of about 80 cubic feet were measured during the first test. A higher pressure-rise rate (3.9 lb/(sq in.)(min) at a 40-cu-ft ullage) was recorded during the second test. This higher rate in the second test was ascribed to the high heat leak through the intermediate bulkhead that resulted from the loss of vacuum previously described.

Photographic Test Data

Photographs were taken of the test throughout both phases of the investigation. The following discussion describes photographs taken during the second ground-fill test of the investigation because it was more indicative of the actual application where the tank would be loaded with liquid hydrogen more than once. Also, it permitted the observation of the blistered areas that occurred during the first run and the way in which they responded to the second test. It should be noted that the tests described herein were more severe than in an actual launch vehicle on the launch pad because there the vehicle is filled with liquid hydrogen, but not held in this condition for long periods of time as was the tank in this investigation. During the first run the tank was held with liquid hydrogen for approximately 25 hours, and during the second test it was held for approximately 11 hours. The characteristics of the frost formation, such as thickness buildup with time or local areas of excessive buildup, would be indicative of the insulation performance. The weather conditions that influenced frost buildup during the test are indicated in table VIII-I.

Figure VIII-5(a) is a photograph taken before the liquid-hydrogen tank was filled. The liquid-hydrogen flow for cooldown and filling the tank was started at 10:25 a.m., and at noon the tank was full. Figure VIII-5(b) shows the tank approximately 10 minutes after the start of liquid-hydrogen flow. The frost shown around the lower flange was caused by the liquid nitrogen in the liquid-oxygen tank. The liquid-oxygen tank had been filled approximately one-half full

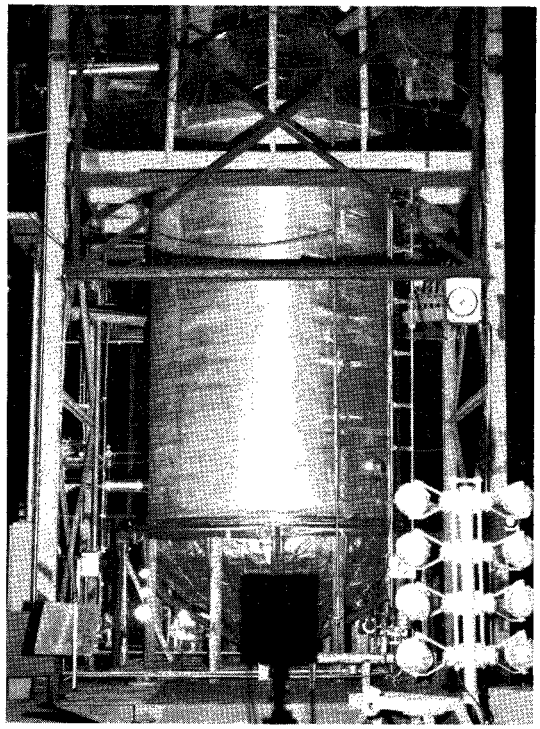

(a) 8:05 a.m.

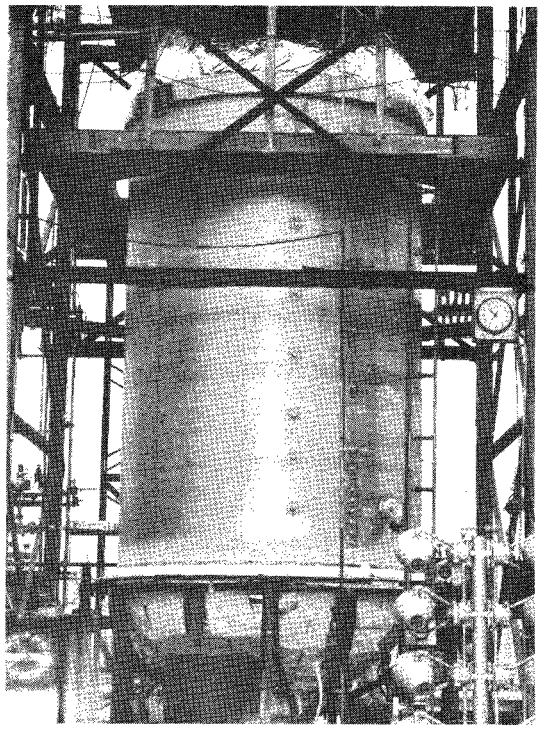

(b) 10:36 a.m.

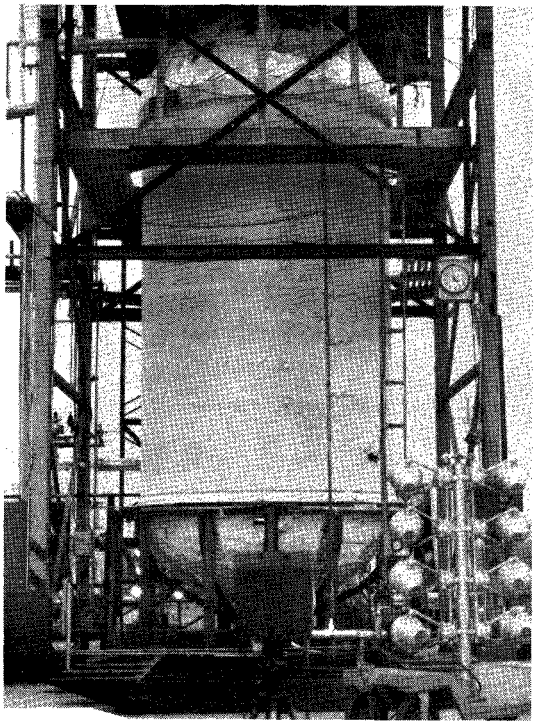

(c) 11:53 a.m.

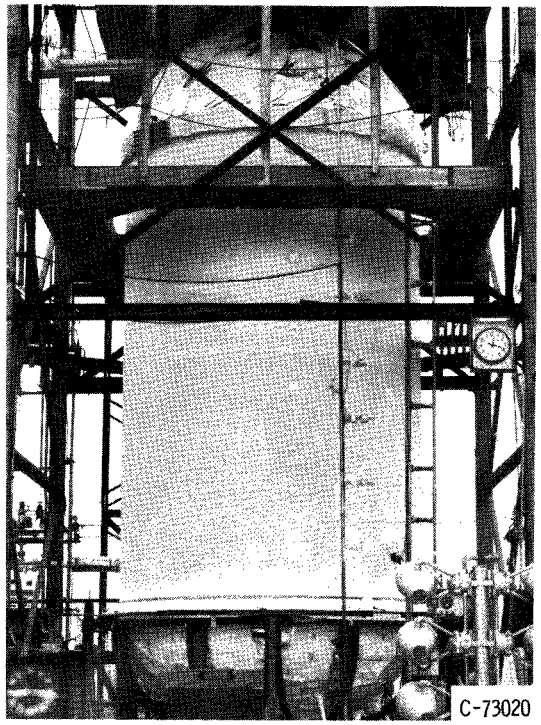

(d) 12:18 p.m.

Figure VIII-5. - Centaur tank before and after filling with liquid hydrogen during second fill test.

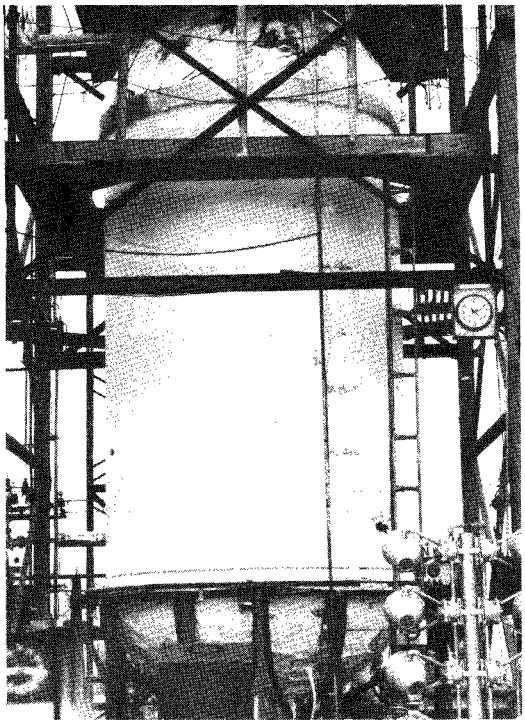

(e) 2:23 p.m.

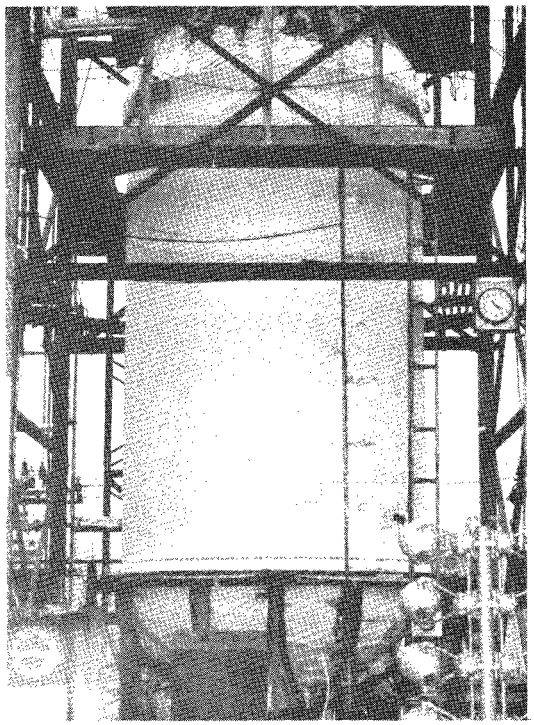

(f) 3:54 p.m.

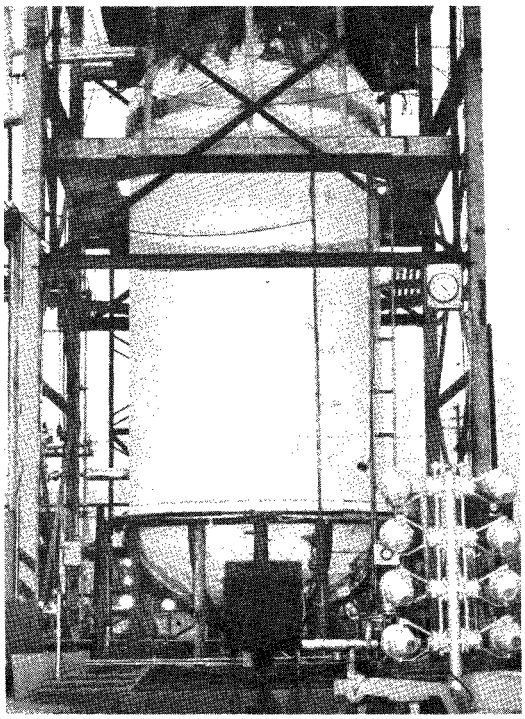

(g) 4:25 p.m.

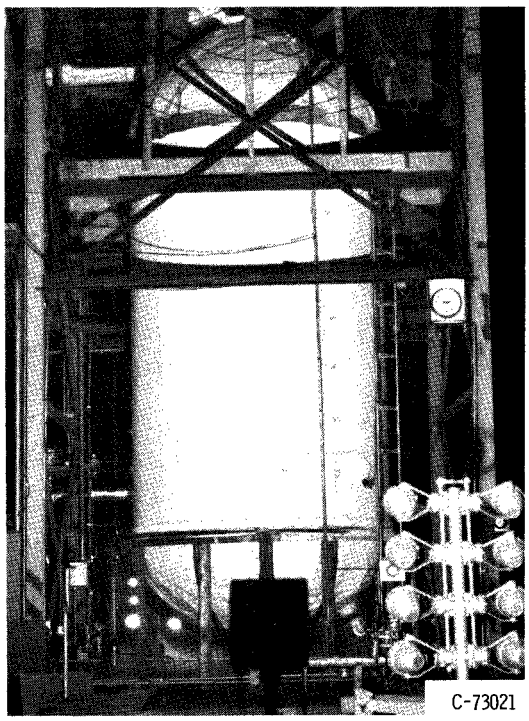

(h) 9:43 p.m.

Figure VIII-5. - Concluded. Centaur tank before and after filling with liquid hydrogen during second fill test.

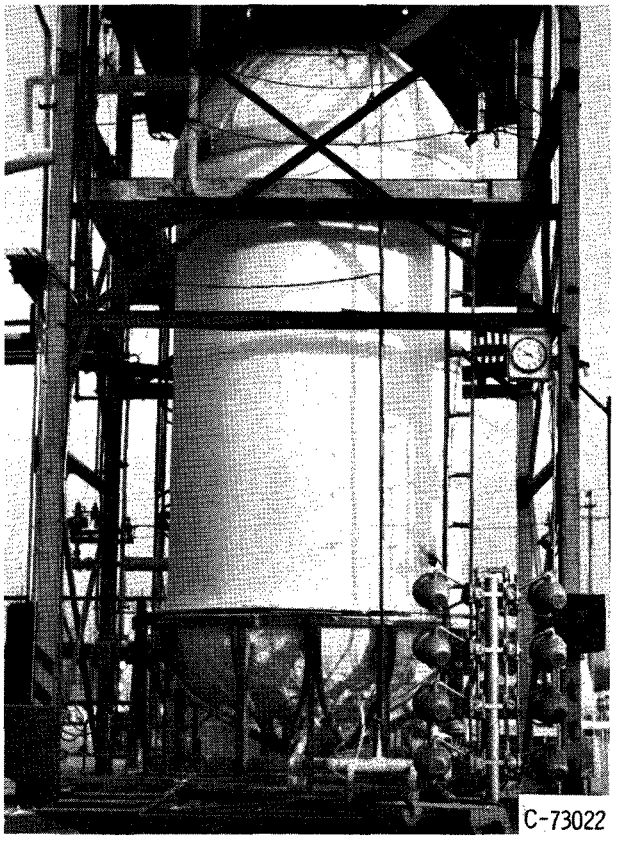

Figure VIII-6. - Frost formation during first fill test.

and stabilized, and the automatic control had been set for operation before the liquid hydrogen was introduced into the tank. Figure VIII-5(c) shows the tank and insulation when the tank was full. A light coat of frost covered the entire insulation system; however, it should be noted that the frost was heaviest at the bottom flange. Figure VIII-5(d) shows the frost approximately 1/2 hour later. Lines of heavier frost outlined the boundary of the insulation panels and areas of greater initial heat input. The frost was extremely thin because the filament winding was still evident. The next four photographs (figs. VIII-5(e) to (h)) indicates the frost buildup with time. At 4:25 p.m. (fig. VIII-5(g)) it was difficult to detect the boundary lines of the panels. It required approximately 5 hours for the frost to reach a thickness through which the filament winding and panel outline patterns could not be detected. At this time frost was estimated to be approximately 1/8 to 3/16 inch thick. Figure VIII-6 is a photograph of the frost during the first phase of this investigation. The photograph was taken approximately $17\frac{1}{2}$ hours after the tank had been filled. The frost buildup appeared to be approximately the same as in the second fill test, approximately 10 hours after the tank was full (fig. VIII-5(h)). Longer time was required for the frost buildup in the first test because of atmospheric conditions such as the lower humidity and moisture content shown in table VIII-I. Therefore, it was concluded that no noticeable changes had occurred in the insulation system between the two tests.

At 10:08 p.m. on the second fill test, the liquid hydrogen had boiled away until the tank was one-fourth full. The test was ended, and the remaining liquid hydrogen was flowed back into the supply Dewars. The tank was empty at 10:40 p.m. When the tank warmed up, sections of frost fell off, as shown by the photographs in figure VIII-7. This frost fell off because of movement of local areas of insulation that was triggered by the air that was cryopumped into the insulation during the cooldown or hold tests. After the liquid hydrogen was expelled from the tank, and as the insulation was permitted to warm up, the cryopumped air expanded and pushed either the MAM laminate and glass cloth away from the foam or local sections of the panel away from the side of the

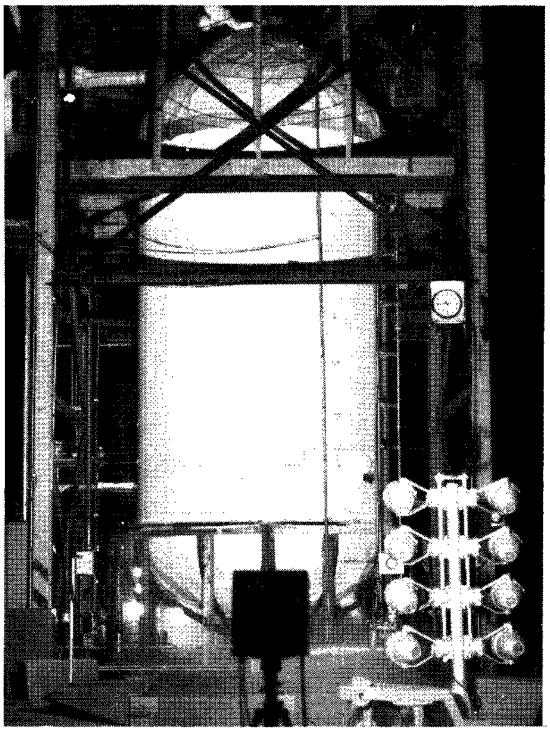

(a) 10:45 p. m.

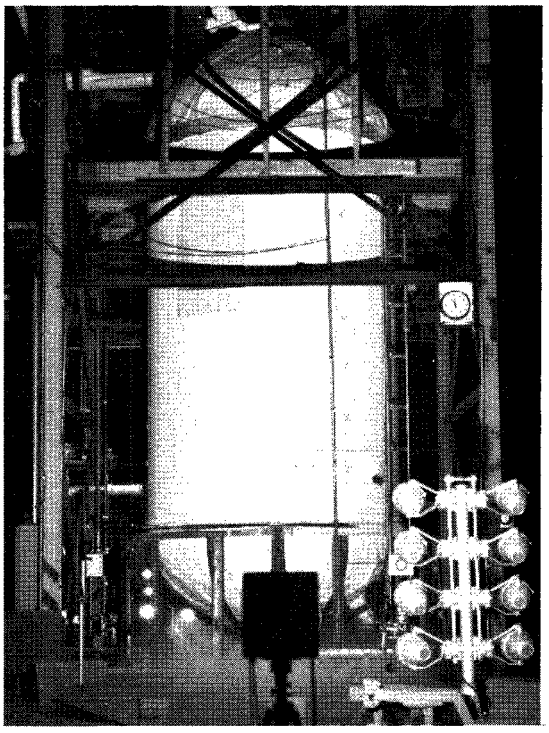

(b) 11:00 p. m.

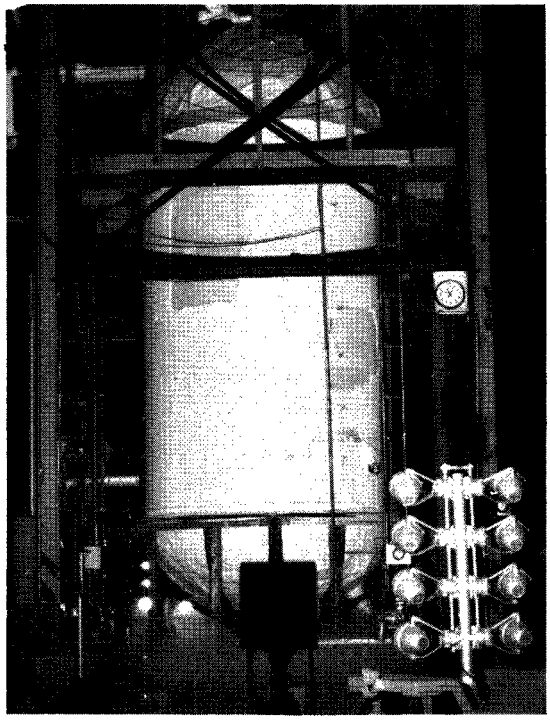

(c) 11:06 p. m.

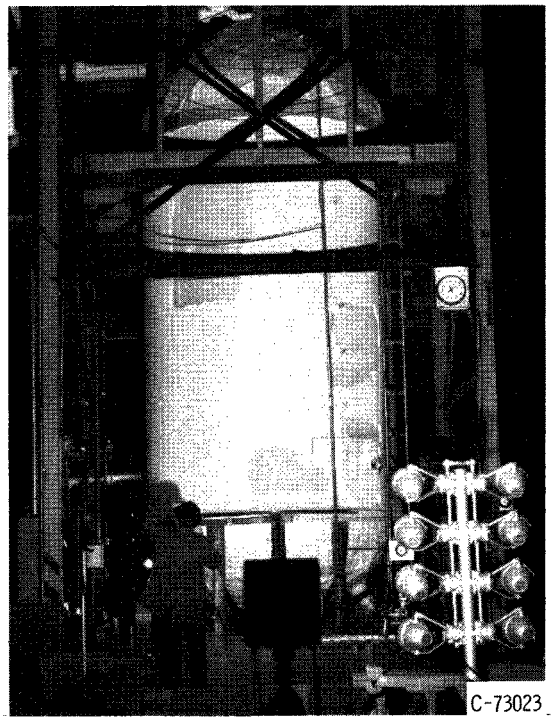

(d) 11:09 p. m.

Figure VIII-7. - Frost falloff as insulation warmed up.

tank. Generally, the area of the insulation that blistered was only a fraction of the frost-falloff area. For example, a 16-square-inch blistered area of insulation resulted in a frost-falloff area of approximately 600 square inches. This was caused by the low adhesive forces between the frost and the insulation.

After the tests were completed, a close examination was made of all the areas that showed blistering. Results of this examination are discussed in the appendix. The insulation was cut apart layer by layer and examined and photographed. Some of the areas that occurred during the first run exhibited little movement during the second test, and they appeared to have healed themselves. One area was repaired after the first run and showed no movement during the second test. A majority of these areas occurred close to the protuberances, and the leaks were in the seals around the protuberances.

The problems that were experienced indicated the requirement for a more rigorous procedure for testing of panels before their application to the tank. An improved adhesive-application system would be required for improving the adherence of insulation panels to a tank such as described herein. Special attention must be given to the surfaces around the protuberances and the doublers so that the air cannot be cryopumped between the insulation and the tank. In some of these areas, the adhesive must be applied to the tank as well as the panels before the panel application. The new filament winding technique for placing the winding around protuberances described in chapter VI would also greatly aid in improving the system.

Tank Depressurization

The Centaur-launch-vehicle tanks are pressure-stabilized structures, and therefore, structural stability is maintained by an internal pressure. For these vessels, a minimum internal pressure of approximately 6 pounds per square inch gage is specified. If the pressure is reduced to atmospheric, the tank must be put into stretch, or sufficient end loading held to induce enough tension in the wall to prohibit collapse of the sidewalls.

In the application of an insulation system such as this to a boost vehicle, it would be a serious disadvantage if the tank could not be depressurized with the insulation in place. There is frequently a need to depressurize in order to remove fill and drain lines or instrumentation or to have access to the inside of the tank.

At the time the insulation was installed on the tank there was some uncertainty as to whether the constrictive load of the wrap would cause the tank to buckle if the tank were depressurized. After completion of the heat-transfer tests, the tank was placed in stretch and was completely depressurized to determine if buckling would occur. It was found that there was no tendency to buckle from the constrictive wrap. This depressurization took place approximately 158 days after the constrictive wrap was installed with a prestrain of 0.84 percent. This prestrain corresponded to a 2-pound-per-square-inch compressive load from the constrictive wrap. Prior to depressurization, several strands of fiber-glass wrap were marked off in 100-inch lengths on the tank.

They were then cut, removed from the tank, and remeasured. It was found that the remaining strain in the winding while on the tank was 0.5 percent, which resulted in a compressive pressure load of approximately 1.2 pounds per square inch at the time of depressurization. The resulting compressive stress in the tank wall would be 1800 pounds per square inch if it were assumed that all of the load from the constrictive wrap were transferred through the insulation to the tank wall.

Subsequently, buckling tests have been made on smaller steel cylinders having a diameter to thickness ratio of about 250 to 1. In these tests a constrictive wrap of nylon with a prestrain of about 12 percent was continuously applied to the cylinders until they buckled. It was found that compressive yield in the cylinders occurred before buckling. It now appears that a bonded insulation system plus a constrictive wrap such as installed on the full-scale tank actually increases, rather than decreases, the buckling resistance of the tank. In fact, if a constrictive wrap is bonded to the tank, the tank cannot buckle from the constrictive load until the bond fails.

CONCLUDING REMARKS

The results of a long-time ground-hold investigation of a fiber-glass constrictive-wrap, hermetically sealed foam insulation system as applied to a full-scale Centaur tank filled with liquid hydrogen can be summarized as follows:

1. The average thermal conductivity of the insulation system installed on the full-scale Centaur tank was found to be approximately 0.10 (Btu)(in.)/(hr)(sq ft)($^{\circ}$R) at a mean temperature of about 200° R during ground-hold tests. This thermal conductivity is smaller than can be obtained by helium-purged insulation or internal insulation in which hydrogen leaks into the foam. This conductivity is consistent with the published values for 2-pound-per-cubic-foot polyurethane foam.

2. Several blisters in the insulation were caused by small leaks that permitted air to be cryopumped into or behind the insulation during the ground-hold tests. These small leaks apparently had no measurable effect on the thermal performance of the system.

3. The leaks that occurred in the hermetically sealed insulation system generally occurred in cutouts of the insulation panels for the protuberances. Although these leaks had no serious consequences on the insulation system, they should be minimized. More careful attention to sealing in these areas and better support from the filament wrap, as discussed in chapter VI, should significantly reduce the problem.

4. Experimental tests on both the full-scale tank and on small cylindrical models have indicated that there is little danger of a depressurized tank buckling from a bonded constrictive wrap. It appears that a bonded insulation system plus a constrictive wrap actually increases rather than decreases the buckling resistance of the tank.

5. From the overall results of the ground-hold tests on this insulation system, it appears that the system is satisfactory for hydrogen-fueled boost vehicles.

APPENDIX - EXAMINATION OF INSULATION AFTER TEST

Figure VIII-8, a developed view of the lightweight insulation system, shows how the panels were positioned with respect to the many protuberances and the blistered areas observed during the first and second tests. The cross-hatched areas occurred with the first run, whereas the dotted areas occurred during the second run. It should be noted that four panels were affected during the first test, and an additional four panels were affected during the second test. A total of 11 areas were observed, panel 13 having three areas. Five of the areas were observed during the first test, whereas the remaining six were observed in the second test. In four of the areas, a piece of foam was cracked free from the large panel. Three of the cracked areas occurred during the first test. The MAM laminate and the glass-cloth covering were deformed during warmup (fig. VIII-9) and showed the outline of the piece of foam that cracked loose. This damage was caused by a local pressure buildup between the panel and the tank. In other areas the adhesive bond between the MAM laminate and the foam was broken, and the covering was bulged or pushed away from the foam by a pressure buildup within the hermetically sealed panel. This pressure buildup was caused by the air that was cryopumped into the system during the long periods of time the tank contained liquid hydrogen. If a small leak occurs in the insulation seal, the outside air will be pulled in and condensed at the cryogenic temperature. In this investigation, this process occurred over several hours. At warmup, however, the gas within the sealed volume

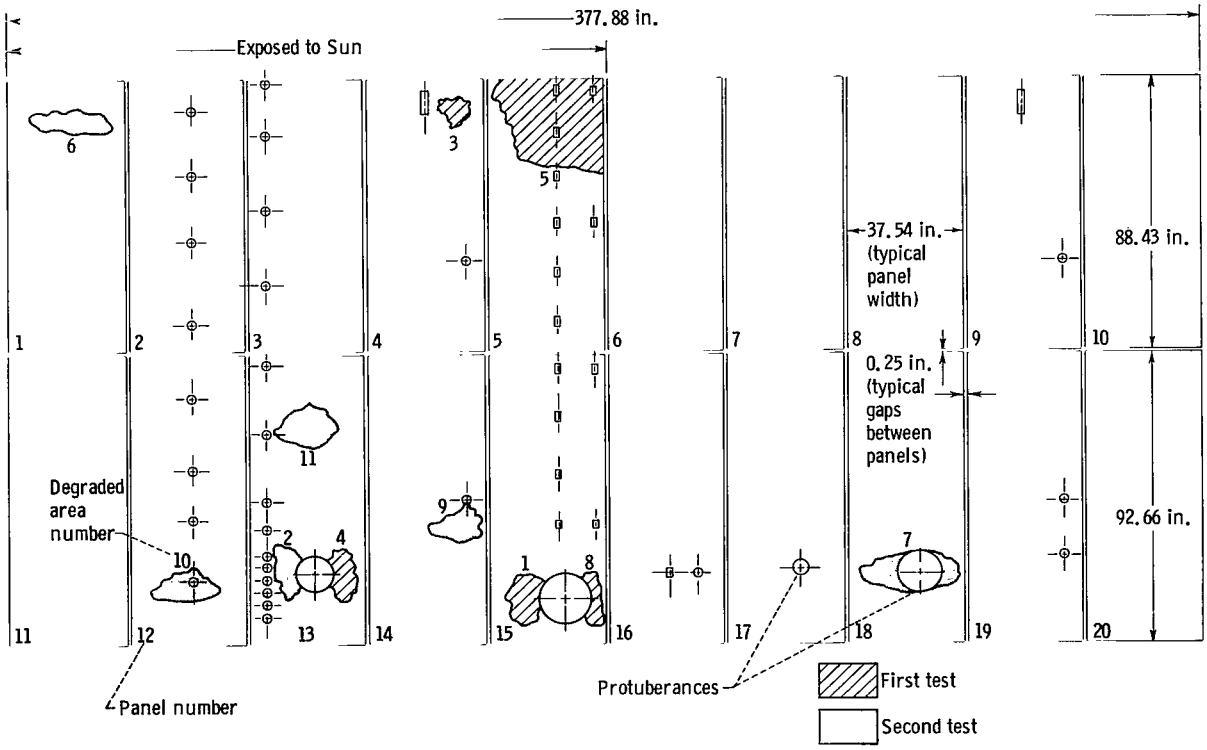

Figure VIII-8. - Developed view of lightweight insulation system showing panels and locations of blistered areas.

vaporized and expanded rapidly, and an increase in pressure resulted. It was this increase in pressure that caused the damage to the insulation system.

Figure VIII-9 shows detailed photographs of area 1 (fig. VIII-8). Figure VIII-9(a) shows the pattern of the filament winding around a large protuberance and the outline of the broken piece of panel foam. It should be noted that the unsupported area was much larger than the broken piece of foam. The MAM laminate and the glass cloth were permanently stretched around the cracked foam as a result of this buildup of pressure from the warming of the cryopumped air. Figure VIII-9(b) shows the cracked foam, and figure VIII-9(c) shows that the broken piece was over a section of the inside layer of MAM laminate that was without adhesive. Chapter VII of this report describes how the adhesive was applied on the panels before their application to the tank. Figure VIII-9(d) clearly shows the adhesive pattern. The beads of adhesive were applied in a square grid pattern with an approximate 6-inch spacing. When the panels were applied to the tank, the beads were flattened and spread as shown. Therefore, the MAM laminate within this adhesive-free area was unsupported. These free areas showed signs of permanent set from the pressure buildup where leaks permitted air to cryopump behind the insulation panels. Close examination indicated the path of the cryopumped air leading from the large protuberance and following the edges of the double reinforcement around the protuberance from one unsupported section to another.

The constrictive wrap was applied with a pretension, which provided a compressive load to the panels (ch. VII). The four local areas where the foam was cracked were not covered by a constrictive wrap (fig. VIII-9(a)). The foam was brittle at cryogenic temperatures, and therefore, the pressure buildup under these areas without adhesive caused the foam to crack out.

Figures VIII-10 and VIII-11 are photographs of areas 2 and 3, respectively. The characteristics of these areas were the same as those described for area 1, except that the MAM laminate in area 2 (fig. VIII-10(b)) was definitely under pressure. The test had been completed 54 days before the picture was taken. Figure VIII-10(c) shows that again the failure was over an area without adhesive and over a doubler or step in the tank wall. Area 3 (fig. VIII-11) was not located over a doubler as were the other two areas.

Area 4 (fig. VIII-12) was cut open during warmup after the first test. The outer layer of MAM laminate and glass cloth appeared to be excessively bulged, and therefore, the pressure was relieved to prevent any permanent damage. The crack that shows in the foam in figure VIII-12(b) was sealed, and a MAM-laminate patch was installed to seal the panel again. Throughout the second test, the patched areas showed no indication of cryopumping or permanent damage.

In seven of the reference areas, the only permanent damage to the system was the breaking of the bond between the foam panel and the outside layer of MAM laminate. This was caused by the buildup of internal pressure within the sealed panel. The constrictive wrap prevented any serious damage. The outside layer of MAM laminate and glass cloth in area 10 was expanded so that this covering was bulged out between the filament winding to form a gap similar to

the gap shown below the scale in figure VIII-9(a). During the second run, this area did not show the results of cryopumping, and hence, the small leak appeared to have sealed itself.

Many of the areas examined showed that little or no adhesive was bonding the MAM laminate to the foam. For example, in area 3 (fig. VIII-11(b)) there appeared to be no adhesive on the inside of the piece of broken foam. Close examination of figure VIII-11(b) shows that the piece of MAM laminate bent back is covered with particles of foam, and this indicates that a good bond existed between the foam and the outside layer of MAM laminate. The inside of all the MAM laminate should have this appearance. Figure VIII-9(c) shows that the inside of the area 1 MAM laminate was clean and had not adhered to the foam. This absence of a bond between the foam and MAM laminate made it much easier for the insulation to blister.

A close examination of the foam, for example, the piece broken out of area 1 revealed that the foam contained some holes completely through the material and some that were almost through. These holes would not only reduce the thermal efficiency of the foam, but would also serve as a storage for cryopumped air. The holes would also provide a path for the cryopumped air to seek the weakest side of the foam and exert its resultant pressure to cause blisters. A foam free of these defects should be used for the lightweight insulation system.

Ten of the eleven areas were located on the side of the tank exposed to the Sun (fig. VIII-8). This suggests the possibility that the MAM laminate and/or the adhesive bond were susceptible to the detrimental effects of sunlight.

REFERENCE

1. Moeller, Calvin E., Loser, John B., Snyder, Warren E., and Hopkins, Vern: Thermophysical Properties on Thermal Insulating Materials. Final Rep. Feb. 1, 1961-Jan 19, 1962 (ASD TDR-62-215), Midwest Res. Inst., July 1962.

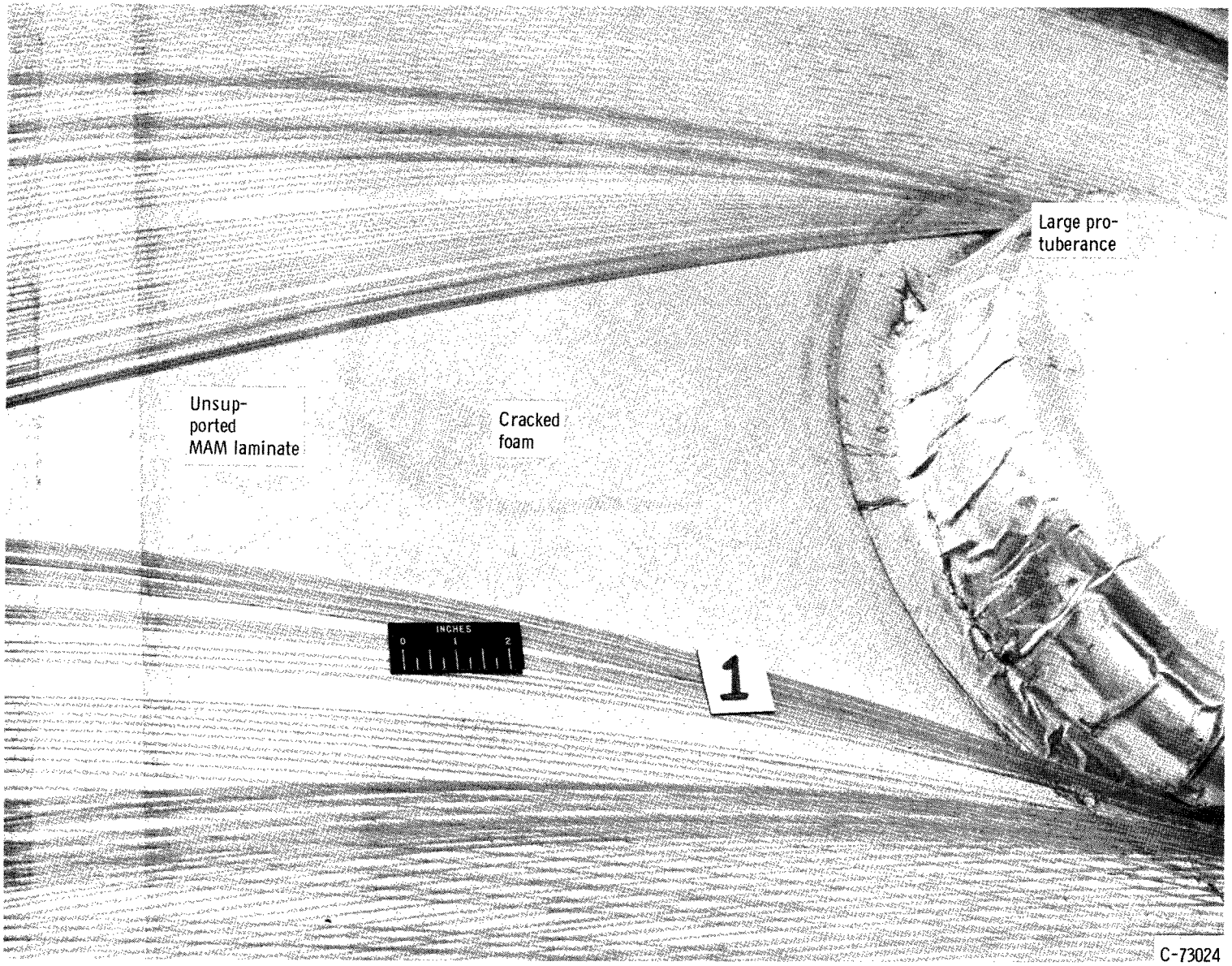

(a) Before examination.

Figure VIII-9. - Blistered area 1.

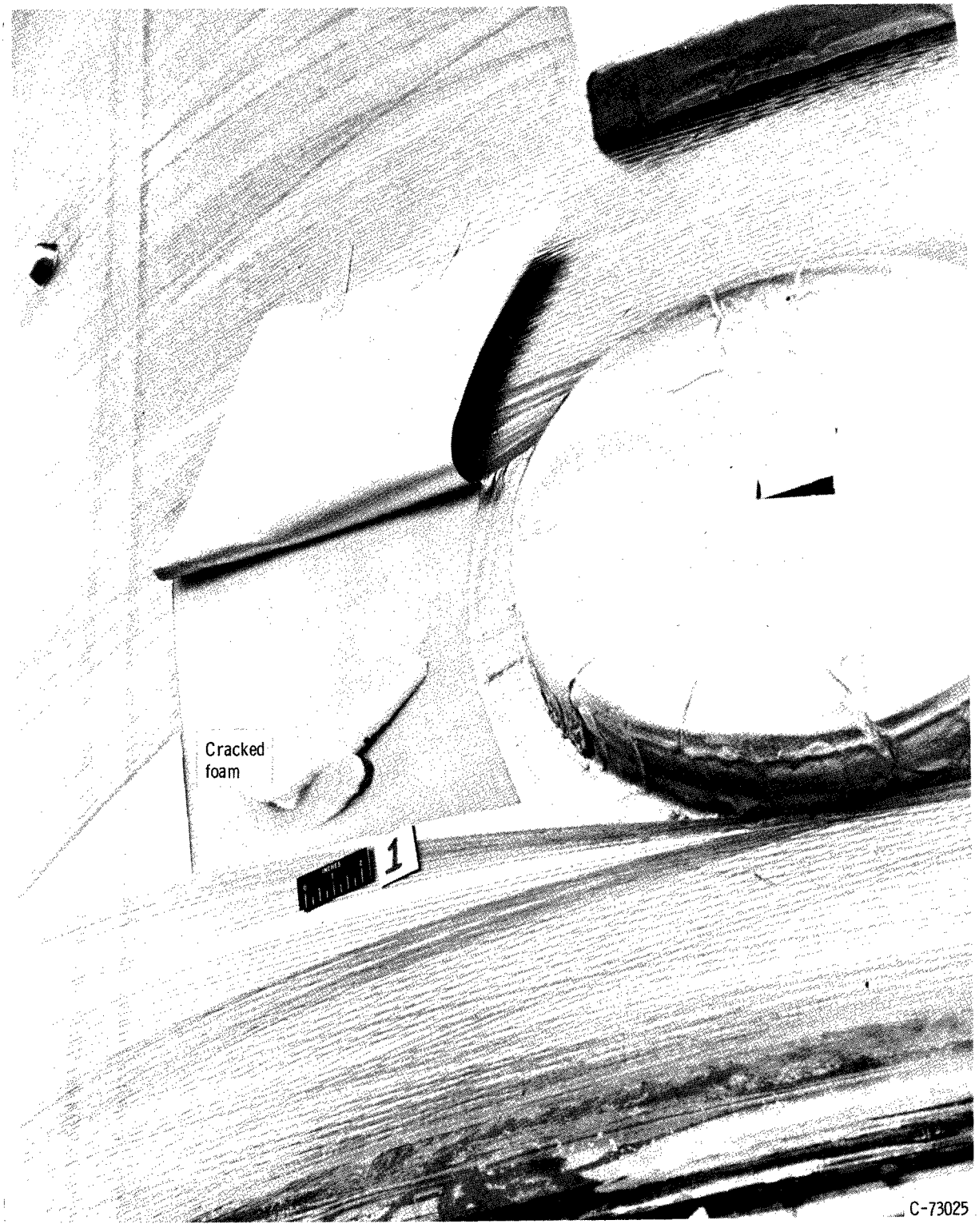

(b) MAM laminate folded back exposing cracked foam.

Figure VIII-9. Continued. Blistered area 1.

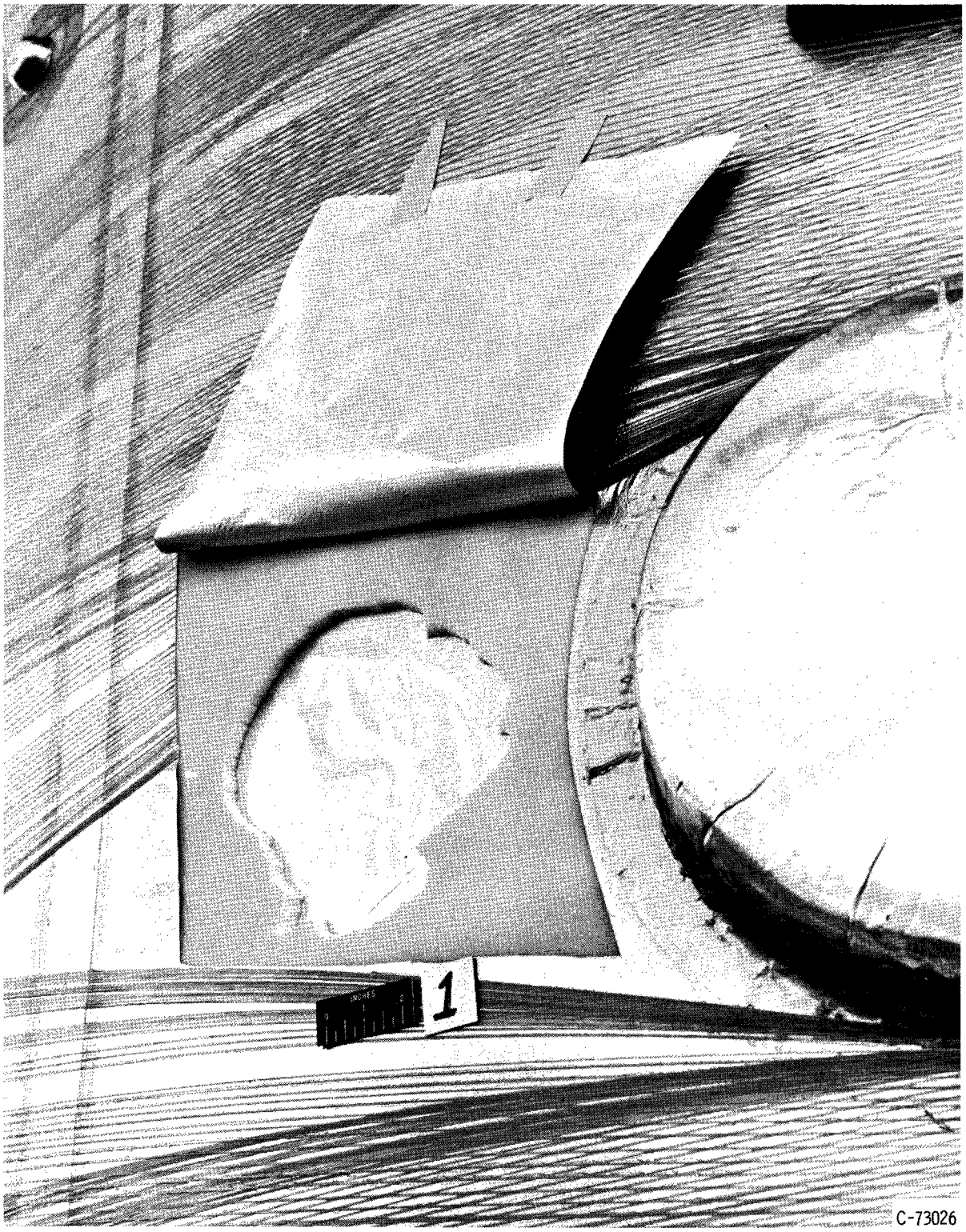

(c) Cracked foam removed.

Figure VIII-9. - Continued. Blistered area 1.

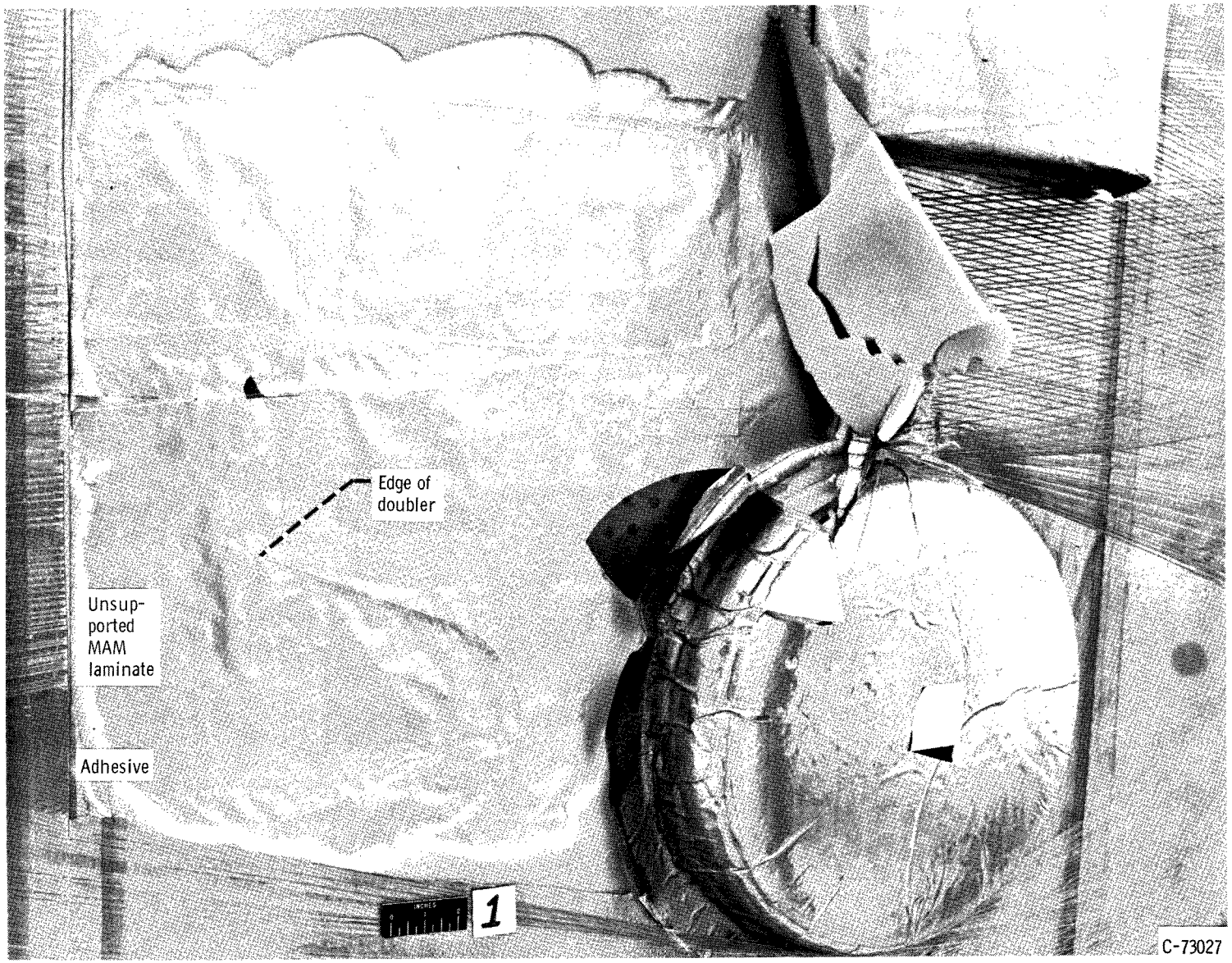

(d) Inside layer of MAM laminate exposed showing impression of doubler.

Figure VIII-9. - Concluded. Blistered area 1.

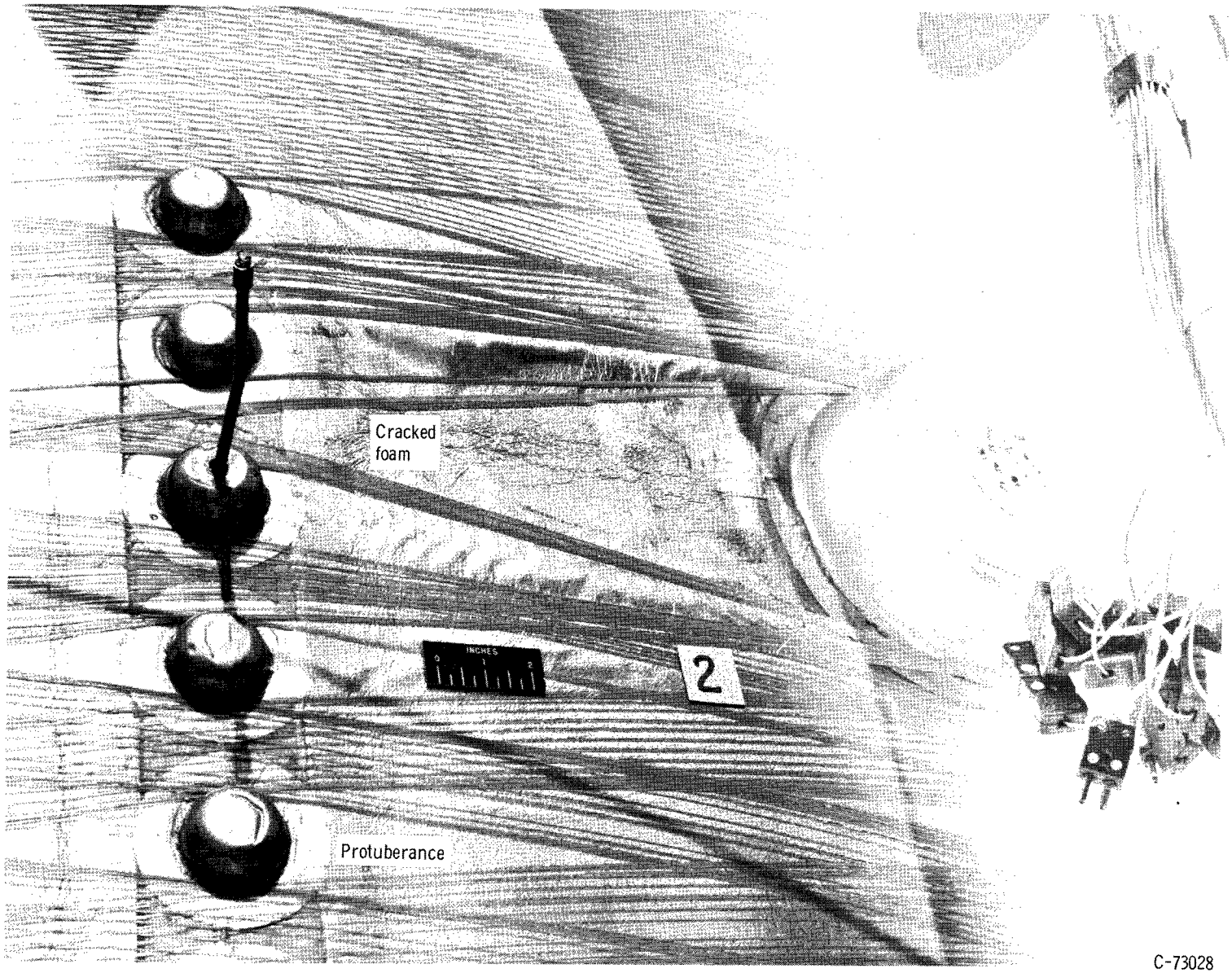

(a) Before examination.

Figure VIII-10. - Blistered area 2.

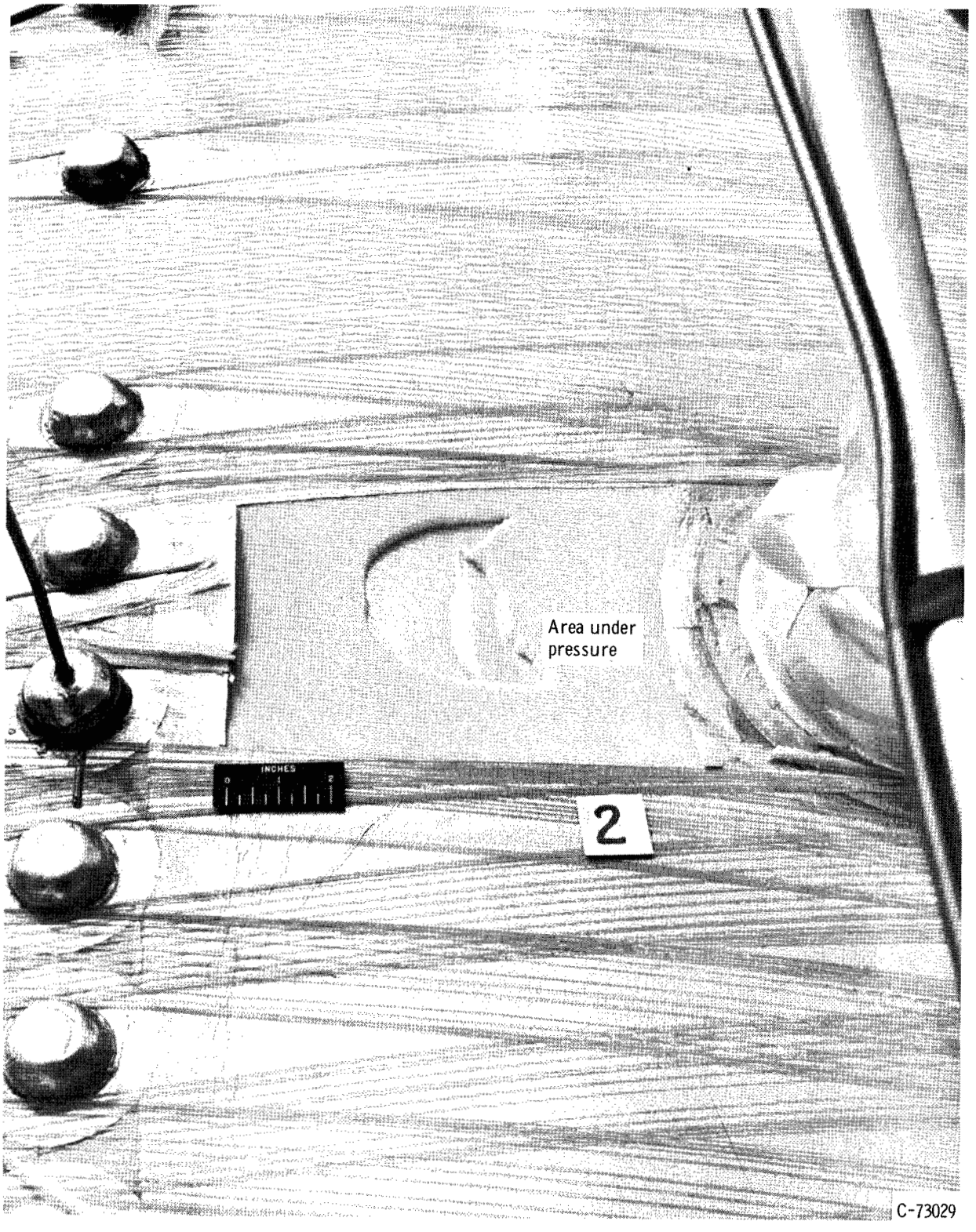

(b) Broken foam removed.

Figure VIII-10. - Continued. Blistered area 2.

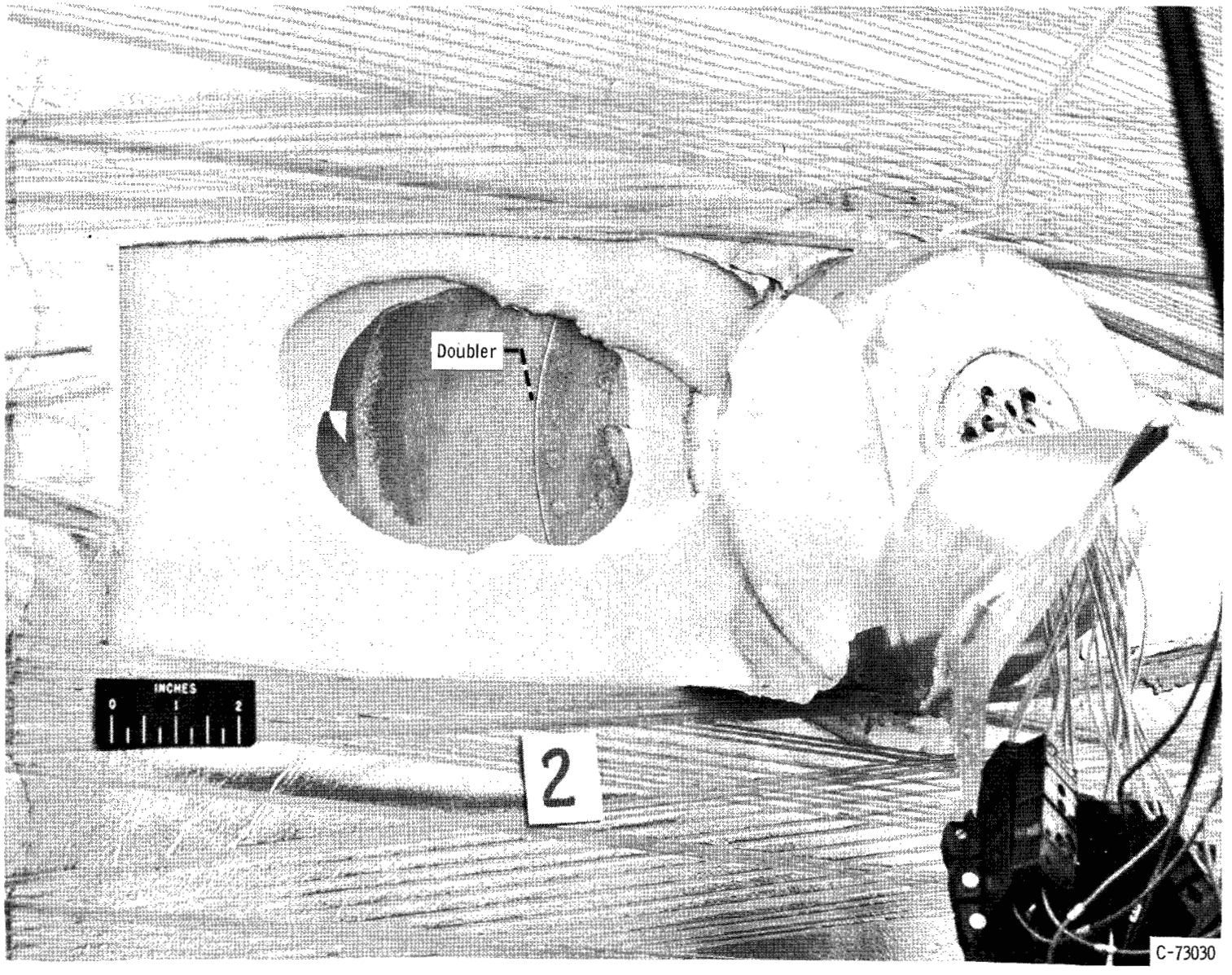

(c) Tank surface exposed showing doubler.

Figure VIII-10. - Concluded. Blistered area 2.

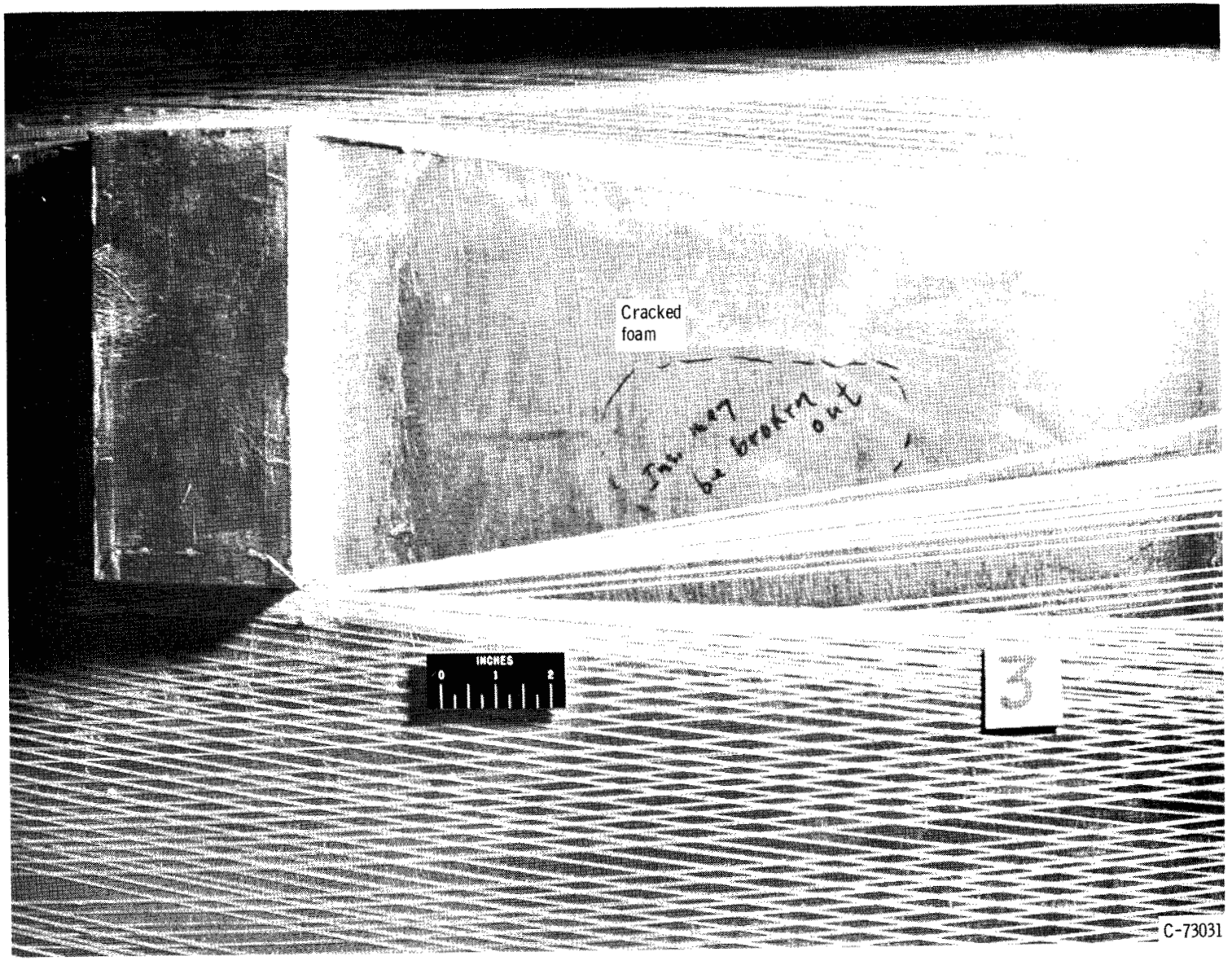

(a) Before examination.

Figure VIII-11. - Blistered area 3.

(b) MAM laminate and cracked foam folded back.

Figure VIII-11. - Continued. Blistered area 3.

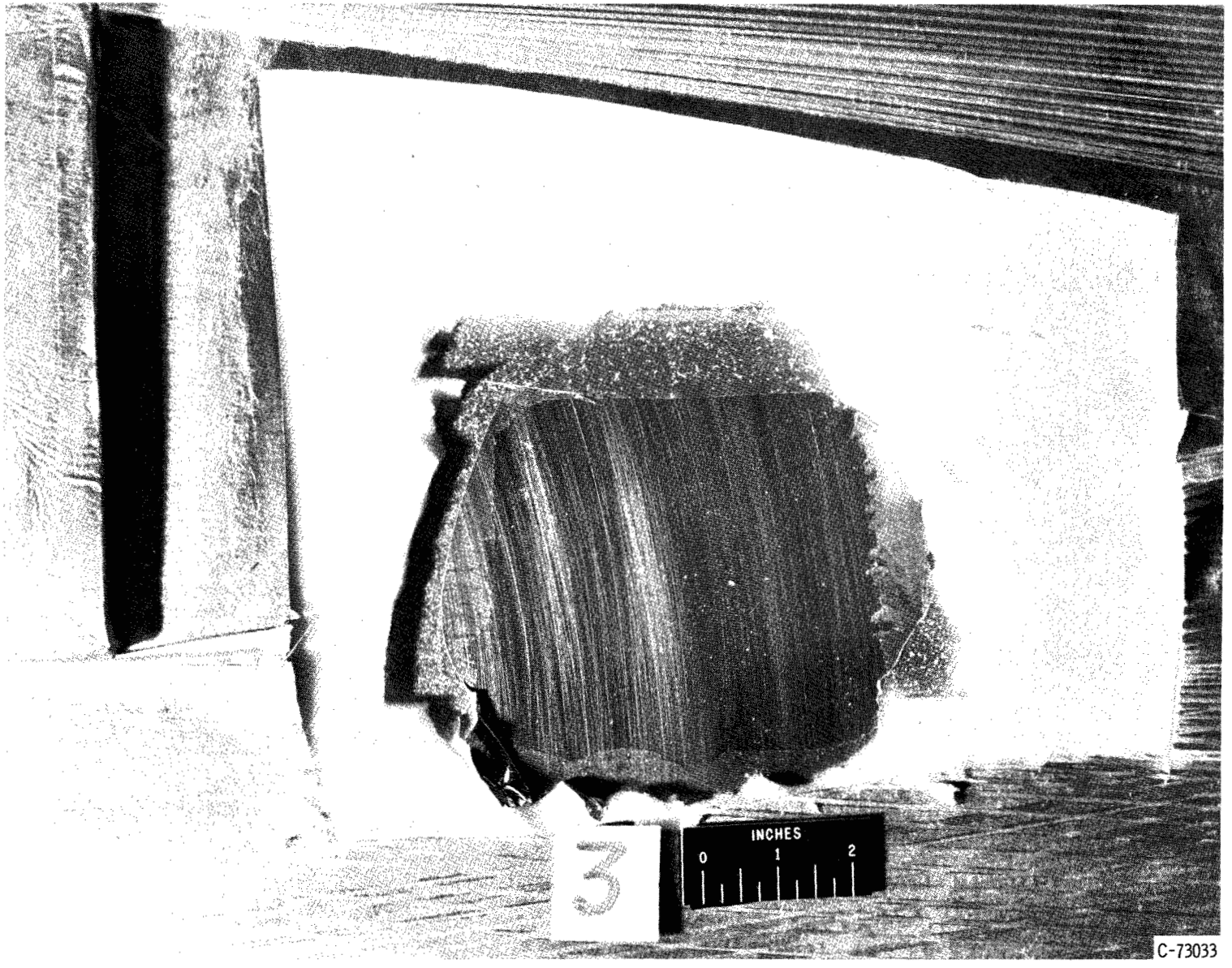

(c) Inside layer of MAM laminate removed.

Figure VIII-11. - Concluded. Blistered area 3.

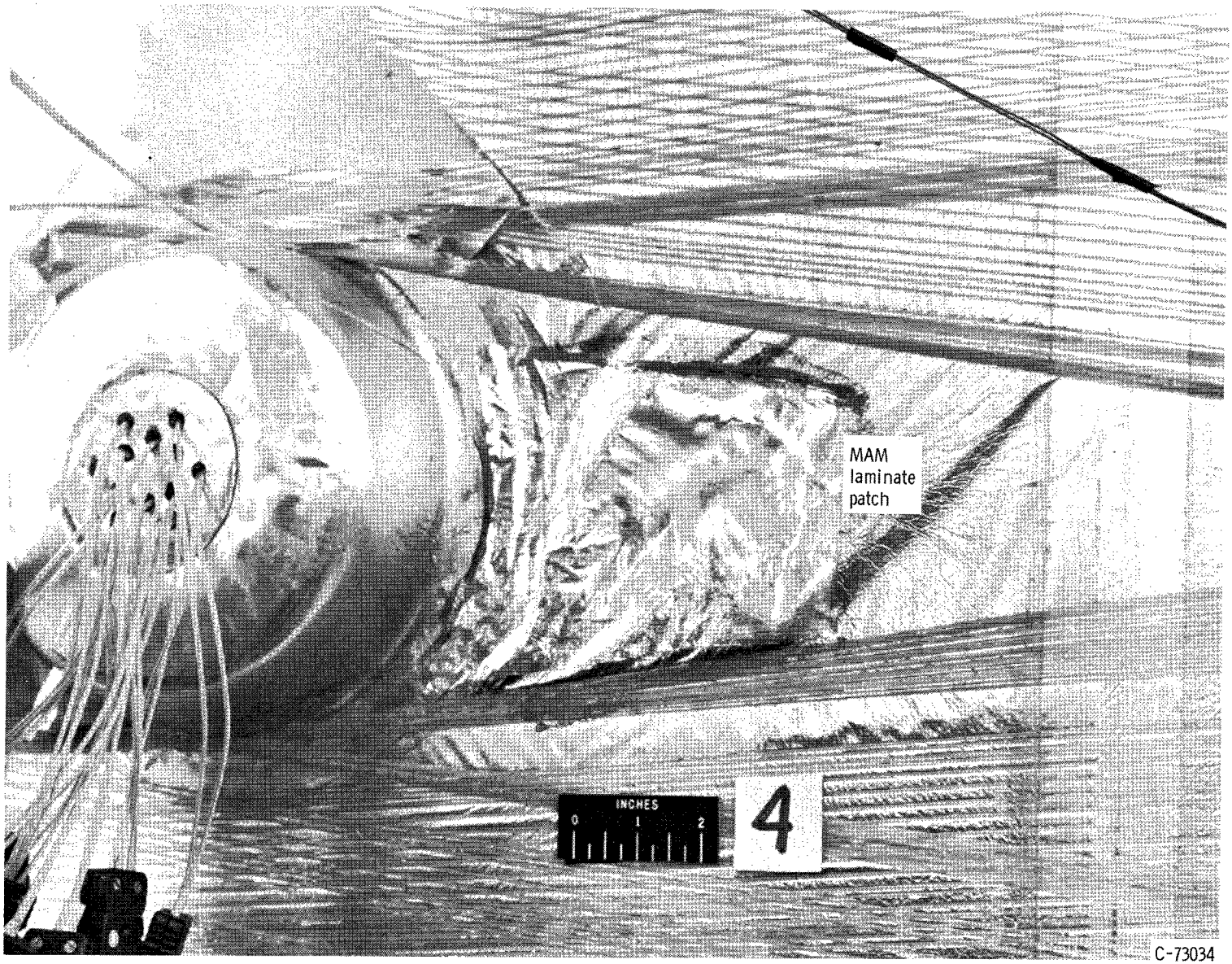

(a) Before examination.

Figure VIII-12. - Blistered area 4.

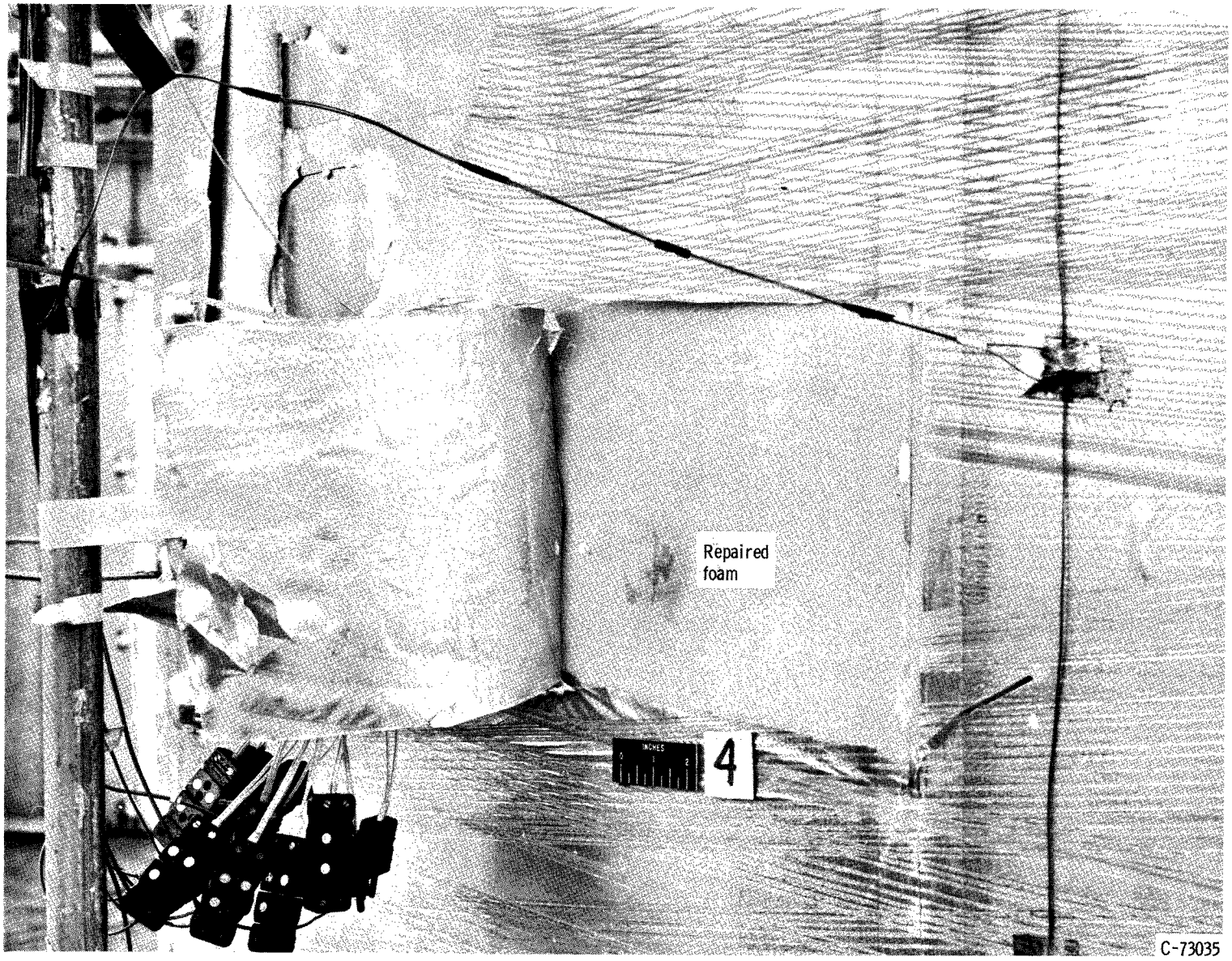

(b) Outside layer of MAM laminate folded back.

Figure VIII-12. - Continued. Blistered area 4.

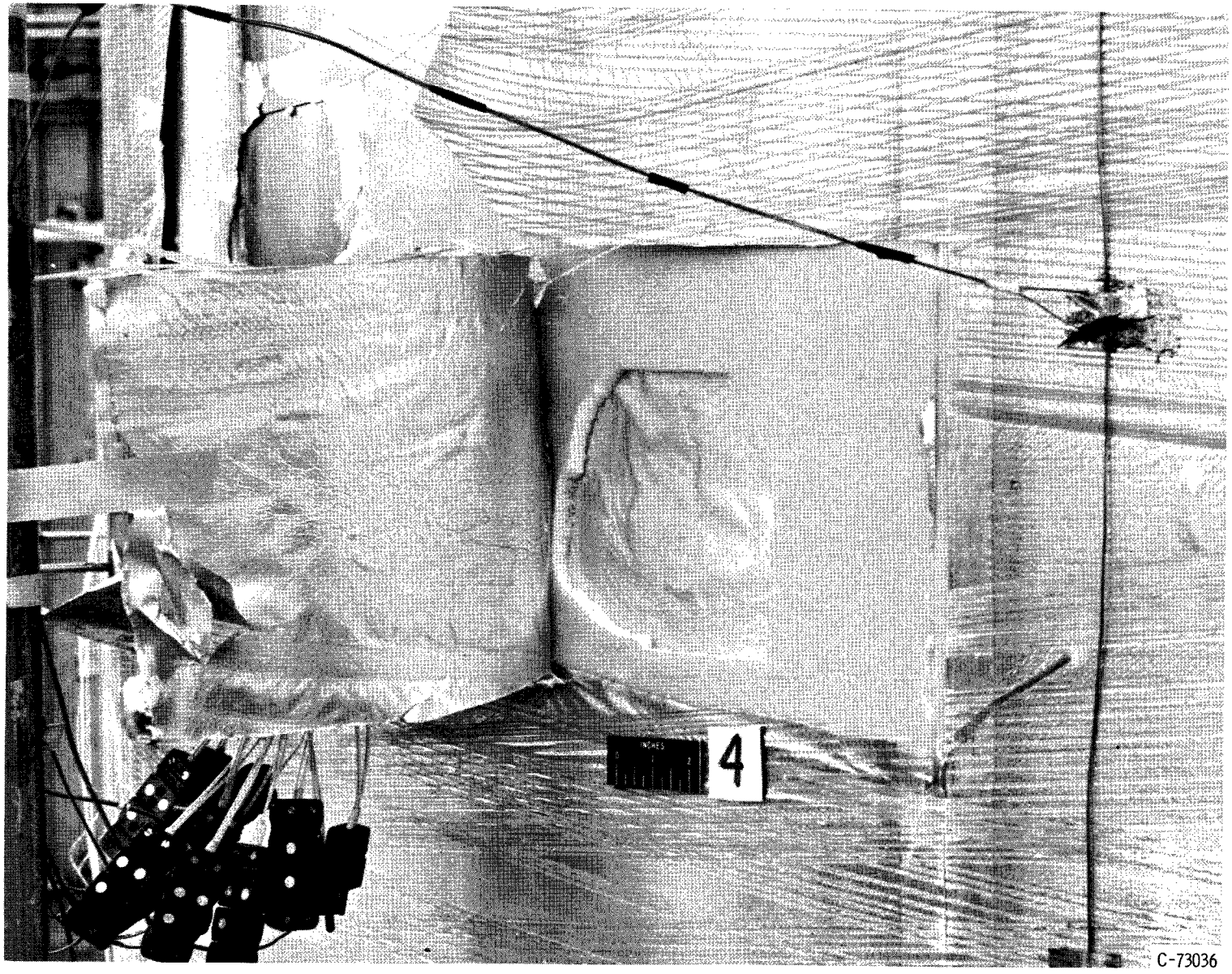

(c) Foam removed.

Figure VIII-12. - Continued. Blistered area 4.

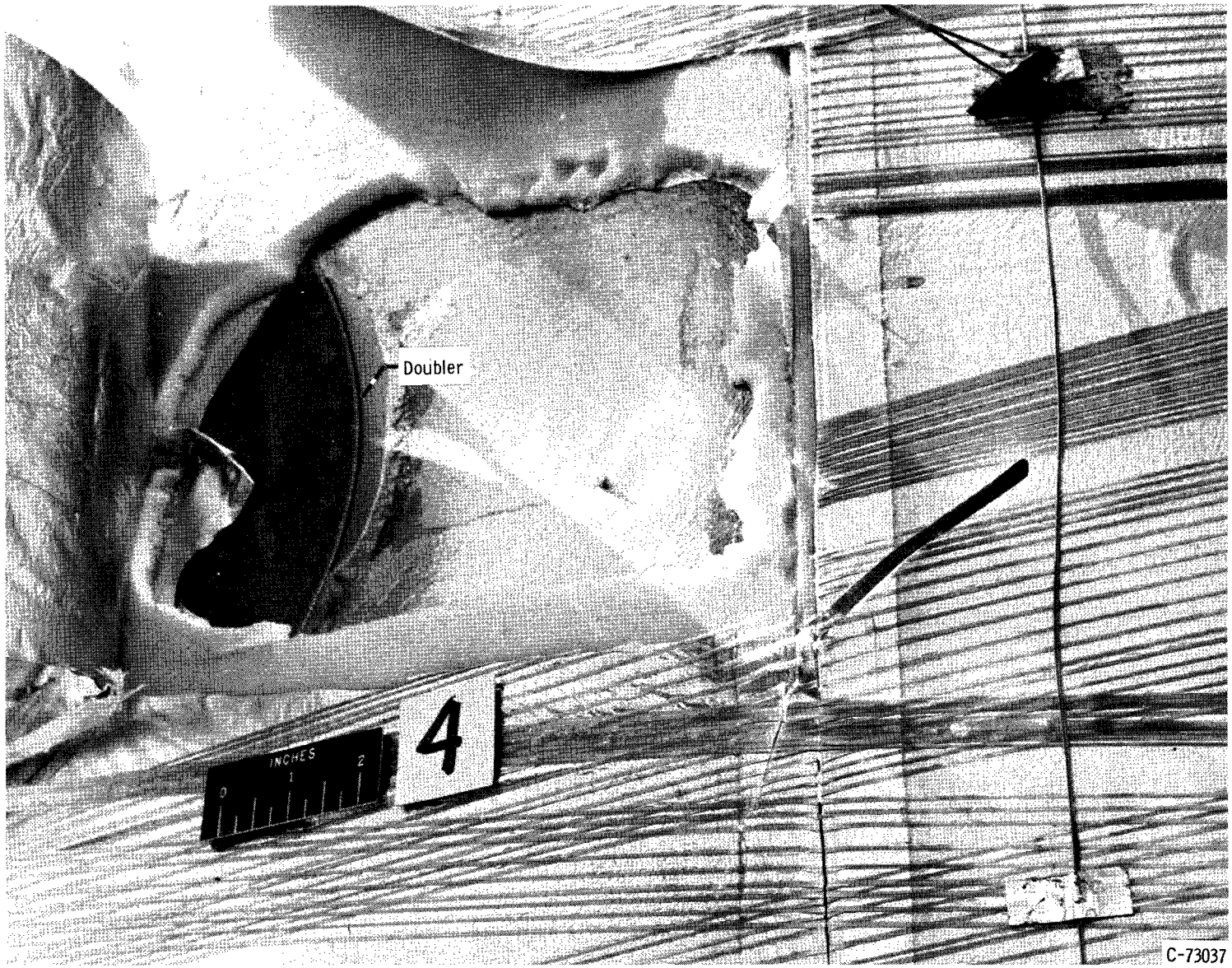

(d) Doubler exposed.

Figure VIII-12. - Concluded. Blistered area 4.

CHAPTER IX

SUMMARY OF INVESTIGATION

by Jack B. Esgar and Paul T. Hacker

Lewis Research Center

The concept of a sealed-foam, constrictive-wrapped, external insulation system for liquid-hydrogen tanks of boost vehicles as described in chapter I was thoroughly investigated to evaluate its feasibility and practicality. The investigation included (1) an analytical study to establish pertinent launch environment parameters for use in design and testing, (2) the selection and evaluation of insulation materials, (3) insulation of subscale tanks for development of fabrication and application techniques and for thermal and mechanical testing in various environmental conditions, and (4) insulation of a full-scale Centaur vehicle liquid-hydrogen tank that was tested under ground-hold conditions. Details of the various phases of the investigation are presented in chapters II to VIII. This final chapter summarizes the design and pertinent findings of the investigation, and, in addition, presents a comparison between the payload weight penalties imposed by this lightweight nonjettisonable insulation system and a heavy jettisonable insulation system that has been test flown on a Centaur vehicle.

DESIGN OF INSULATION SYSTEM

The insulation system, as finally developed and applied to a full-scale Centaur tank, consisted of lightweight polyurethane foam panels that were encapsulated in a vapor-tight foil laminate to prohibit air from being cryopumped into the insulation. The insulation panels were bonded to the Centaur hydrogen tank to stop air from cryopumping in between the tank wall and the insulation panels. The panels were then covered with a lightweight glass cloth to provide protection from the erosive action of aerodynamic forces during the launch trajectory. The anchoring method that ensured that the insulation panels were held firmly in place during ground hold and launch was a constrictive wrap of prestressed fiber-glass roving that was applied in a large filament winding machine.

Insulation Panel Construction

Polyurethane foam was selected for the insulation system because of its superior insulating qualities. It is available in a range of densities using either carbon dioxide or Freon as blowing agents. The selection of the foam density for this insulation system was based on considerations of system weight, thermal conductivity, and compressive strength. Thermal conductivity and compressive strength both decrease with decreasing density. A foam density of

2 pounds per cubic foot provided a reasonable compromise between thermal conductivity and strength. It was, therefore, selected for use in this investigation. Freon-blown foam was selected over carbon-dioxide-blown foam because it possesses a lower thermal conductivity (ch. V). The published thermal conductivity of Freon-blown polyurethane foam at a mean temperature of 250° R is about 0.11 (Btu)(in.)/(hr)(sq ft)(°R). A foam thickness of 0.4 inch was selected so that the total heat flux to a full-scale Centaur tank for this insulation system based on the aforementioned thermal conductivity would be equivalent to the total heat flux with an existing helium-purged heavy jettisonable insulation system during a ground-hold condition.

The foam panels were hermetically sealed on the two faces by a thin Mylar-aluminum-Mylar (MAM) laminate and on the edges by preformed channels of Mylar film. The MAM laminate face sheets were made of 0.0005-inch-thick Mylar film bonded to each side of 0.0005-inch-thick aluminum foil. The Mylar edge channels were 0.002-inch thick. The MAM laminate is better for sealing the foam than either aluminum foil or Mylar film. Aluminum foil is less permeable than Mylar, but Mylar is tougher and resists damage such as tearing and puncturing in normal handling. Lamination thus combines the desirable features of the individual materials while diminishing the undesirable characteristics. The laminate can be thinner and thus weigh less than one of the materials by itself since the probability of lining up the holes in the individual materials is low. Mylar instead of MAM laminate was used to seal the panel edges to reduce the thermal short effect. The use of a more permeable material in this area was permissible because the panel joints were protected by a MAM laminate cover strip. The MAM laminate and the Mylar face and edge seals were bonded to the foam with a polyester adhesive (Goodyear Tire and Rubber Co. Vitel PE 207). The panels were contoured to the tank radius of curvature by holding flat panels of foam in a mold while bonding the face seals to the foam.

The maximum panel size as applied to the full-scale Centaur tanks was approximately 37 by 92 inches. The insulation was divided into many individually sealed panels so that the individual panels could be checked for vapor tightness before installation on the tank wall (ch. VII), and the effect of the leak could not spread throughout the entire insulation if a panel leaked after installation. The panel size was made as large as practical to provide ease in handling during fabrication and yet minimize the total length of edge seals and joints on the insulated tank. The edge seals result in heat shorts, and leaks into and behind the panels usually occur around edge seals and joints. The panels were approximately one half as long as the insulated tank. The width was selected on the basis of the width of available MAM laminate (38 in.) so that splices would not have to be made in the panel faces.

Installation on Tank

The fabricated panels were bonded to the tank wall with Narmco 7343/7139 adhesive applied in a perimeter and grid pattern (ch. VII). The panels were held under vacuum bag pressure at room temperature until the adhesive had cured. The primary function of this adhesive bond was to seal the space between the tank and panels to prevent cryopumping of air. The bond also held the panels in place until the constrictive wrap was applied. Spaces between

panels were filled with strips of foam and sealed by a cover strip of MAM laminate. At each end of the insulated section of the tank, seal strips were also used between the panel edge and the metal wall of the tank to provide an additional barrier to air that might cryopump in between the panels and the tank wall.

After bonding and sealing the panels to the tank, the entire exterior surface of the insulation was covered with a very lightweight glass cloth (style 106). The glass cloth was impregnated with Dow Corning Silicone A-4000 resin that bonded it to the panels. From simulated aerodynamic heating tests, it was found that the glass cloth was necessary to protect the insulation panels from aerodynamic erosion under the high temperatures experienced during launch. An analytical study of a typical launch trajectory (ch. II) indicated a maximum temperature of about 650° F and a maximum dynamic pressure of 860 pounds per square foot would be encountered on the outer insulation surface. The two maximums, however, do not occur simultaneously. The pressure maximum occurs at an altitude of about 50,000 feet and a temperature of about 140° F, while the temperature maximum occurs at about 140,000 feet and a dynamic pressure of 120 pounds per square foot.

Both S/HTS Fiberglas and HT-1 Nylon were evaluated for use as the constrictive-wrap material (ch. VII). Fiber glass was selected for the final system because it has a higher operating temperature capability and the resulting system was lighter in weight. An eight-strand fiber-glass roving preimpregnated with epoxy resin was applied to the tank under a tension of 2 pounds per strand to provide a 0.84-percent strain in the roving. The wrap was bonded to itself at crossover points and to the underlying glass cloth with Dow Corning Silicone A-4000 resin that was cured at room temperature. The wrap was applied by a filament winding machine at a helix angle of 6° and a strand density of 60 per inch. This spacing produced an average compressive load of 2 pounds per square inch on the insulation panels. The wrapping strain of 0.84 percent was sufficient to keep a positive compression load on the panels for all conditions encountered during ground hold and launch. Factors considered in establishing this strain were (1) thermal contraction of tank when filled with liquid hydrogen, (2) deformation of the foam panels by the constrictive-wrap load, (3) possible foam shrinkage during aerodynamic heating, (4) thermal expansion of the wrap material when heated, and (5) pressure histories inside and outside the tank during ground hold and launch.

The Centaur test tank contained a number of protuberances on the cylindrical surface that required alterations in the basic panel design and the constrictive-wrap pattern. The tank contained two basic types of protuberances, those that could be covered with insulation and sealed and those that could not be completely covered and provided a direct heat short to the tank (ch. VII). In both cases, holes were cut through the panel to accommodate the protuberance. The foam edges along the perimeter of these holes were sealed with Mylar film in a manner similar to that used for the panel edges. Adhesive was applied around these holes on the back side of the panel when the panels were bonded to the tank surface. The presence of protuberances interrupts the normal winding pattern and results in areas where the insulation panels are unsupported on each side of the protuberance. These unsupported areas can be damaged by aerodynamic forces (ch. VI). To eliminate this problem a special

wrapping technique was developed. In this technique a row of short pins, normal to the tank surface and spaced to match the wrapping pattern, was placed on opposite sides of the protuberance. The pins were mounted on a sheet metal saddle placed around the protuberance. Rovings that would normally pass over the protuberance were routed around it but were held by the pins in a normal winding pattern much closer to the protuberance than was possible without the special wrapping technique (ch. VI). This method of wrapping around the protuberances was employed on aerodynamic test models but not on the full-scale Centaur tank, which was not subjected to aerodynamic tests in this investigation.

The total weight of the insulation system as applied to the Centaur test tank was 78.7 pounds, which gives an average unit weight of 0.16 pound per square foot. Of the total weight, about 64 percent is the sealed foam panels and about 19 percent is the constrictive fiber-glass wrap and its adhesive.

TEST RESULTS

During the development of the insulation system, a wide variety of tests were conducted to evaluate its performance. Results of these tests pertinent to the finally developed insulation system are summarized in the following paragraphs.

The overall thermal conductivity of the insulation system was determined (1) in a thermal-conductivity apparatus (ch. III), (2) by insulated subscale tanks (ch. V), and (3) for an insulated full-scale Centaur tank (ch. VIII). The overall thermal-conductivity value measured by the thermal-conductivity apparatus was about 0.14 (Btu)(in.)/(hr)(sq ft)($^{\circ}$R) at a mean temperature of 282° R. The use of a lightweight, low-thermal-conductivity, open-mesh material as a separator between sealed panels and cold wall designed to increase thermal contact resistance did not lower the thermal conductivity appreciably. Changes in the compressive load on the panels in the conductivity apparatus from 2 to 15 pounds per square inch did not appreciably change the overall thermal conductivity either.

Subscale tank tests for ground-hold conditions gave similar thermal-conductivity results to those obtained in the thermal-conductivity apparatus. Two tests of the full-scale Centaur tank at ground-hold conditions gave about 0.10 (Btu)(in.)/(hr)(sq ft)($^{\circ}$R). The mean temperatures of the insulation for the full-scale tests (about 200° R) were lower than those for the other tests (about 282° R) because of very cold atmospheric temperatures. The thermal-conductivity values obtained in these insulation tests approximated the published data for 2-pound-per-cubic-foot-density polyurethane foam.

The ground-hold tests, subscale and full scale, revealed that the seal on some of the panels did leak and allowed some air to be cryopumped into the foam as was indicated by blistering of the panels during warmup of insulation after a test. The affected areas were localized and did not spread throughout a panel. The constrictive wrap was effective in preventing the outer MAM sealing laminate from rupturing in the blistered areas. Panel blistering did not affect the overall thermal performance as evidenced by the results of

repeated tests.

The insulated subscale tanks used in ground-hold tests were subjected to quasi-simulated launch tests in a vacuum chamber to determine the combined effect of pressure change and heat on the insulation system (ch. V). The applied rates of change of pressure and temperature simulated launch conditions. Heat was supplied by infrared lamps on one side of the tanks. The constrictive wrap of fiber glass withstood temperatures as high as 835° F without any obvious damage, while the nylon wrap began to fail at a temperature of about 675° F. The outer MAM sealing laminate, which was not protected on the subscale tanks by the glass cloth, showed some damage at a temperature of 620° F. On the unheated side, depressurization by itself did not produce any obvious damage, even in areas that had blistered during previous ground-hold tests.

Aerodynamic heating and erosion tests were conducted with insulated subscale tanks in a subsonic exhaust jet of a turbojet engine and in a wind tunnel at transonic and supersonic velocities (ch. VI). In a jet engine test, the final insulation design (consisting of foam panels, a fiber-glass constrictive wrap, a glass-cloth heat-protection layer, and a protuberance) was subjected simultaneously to a maximum insulation surface temperature of 615° F and a maximum dynamic pressure of 952 pounds per square foot. These maximum conditions lasted about 17 seconds. The total time of the test was 82 seconds which was consistent with the time at high temperature and high dynamic pressure during launch. The fiber-glass wrap and the glass cloth were all intact at the end of the test.

In wind tunnel tests of the final insulation system on subscale tanks, the insulation was subjected to a maximum insulation temperature of 212° F and a maximum dynamic pressure of about 1300 pounds per square foot. Total test time at airflow conditions between Mach 0.5 and 2 was about 3 hours. The insulation was in excellent condition at the end of the test; only a slight local shrinkage of foam was noted. The buffet loads associated with transonic flow conditions did not have any apparent adverse effect on the insulation.

Organic materials such as foam can be impact sensitive in the presence of high oxygen concentrations. Since there is a possibility of a seal leak on the insulation panel that would allow air to be cryopumped into the foam and become liquified to produce a high concentration of oxygen, impact tests of insulation samples immersed in liquid oxygen were conducted to determine whether a danger of uncontrolled reactions existed (ch. IV). The tests showed that reactions in the form of light flashes and audible detonations occurred in only about 25 percent of the tests, while sustained reactions occurred in only one out of 40 tests. The impact energy of 88 foot-pounds utilized in these tests is sufficient to severely damage or puncture typical propellant tanks. The probability of a sustained reaction occurring from an impact of the insulation on a rocket propellant tank is very low because

(1) An accidental impact of the magnitude utilized is very unlikely.

(2) Areas affected by leaks in seals were observed in tank tests to be limited to relatively small areas.

(3) The affected area would be saturated with liquid air and thus would have a lower concentration of oxygen than was present in the test specimens.

From the results of this series of tests, it was concluded that the insulation system developed could satisfactorily withstand the ground-hold and launch conditions experienced by a typical boost vehicle. The overall installed weight of 0.16 pound per square foot is the lightest weight for an insulation system known to the authors that is suitable for a hydrogen-fueled boost vehicle.

WEIGHT COMPARISON OF JETTISONABLE AND NONJETTISONABLE INSULATION SYSTEMS

In making a weight comparison of jettisonable and nonjettisonable insulation systems for a boost vehicle, the most important weight consideration is the effect of insulation weight on payload capacity. On intermediate boost stages, insulation weight would have only a small effect on payload weight capacity. The largest effect occurs, of course, when the final stage is insulated, such as for the Centaur vehicle. If the insulation is not jettisoned, each pound of insulation weight reduces the payload capability by a pound. If, however, all or part of the insulation can be jettisoned prior to stage burnout, only part of the insulation weight is chargeable against payload. Hydrogen fuel losses from boiloff also reduce payload capacity, but in a more drastic manner than jettisoned weight if the fuel capacity (volume) of the vehicle is limited. When fuel is lost through boiloff, less is available for burning and thus burning time is reduced. To achieve the same burnout velocity with less fuel available, less payload weight can be accelerated to the required velocity.

A complete trajectory analysis is required for any particular vehicle to determine total payload loss resulting from hydrogen boiloff and from weight that is carried through part of the trajectory and then jettisoned. Payload loss factors supplied by the Centaur vehicle manufacturer, insulation weight data from chapter VII, and boiloff loss data from chapter II can be used to calculate payload losses (as a result of insulation system weight) for the lightweight nonjettisonable foam insulation described in this report and the heavier jettisonable insulation that has been used on Centaur vehicles. These weights are compared in table IX-I.

Comparison of the weights in table IX-I reveals that, even though the insulation weight of the jettisonable system is approximately 15 times as heavy as that of the nonjettisonable insulation system, the payload capability of the vehicle with the nonjettisonable insulation is 14.6 pounds less than that of Centaur. Inasmuch as there are far greater unknowns in the weights in fuel loading and utilization than this difference in insulation weight, the effect on payload for the two systems can probably be considered comparable. The greater inherent reliability of a nonjettisonable system could probably compensate for the small difference in weights.

TABLE IX-I. - COMPARISON OF JETTISONABLE

AND NONJETTISONABLE INSULATION SYSTEMS

	Weight, lb	Payload loss factor	Payload loss, lb
Sealed foam, constrictive-wrapped, nonjettisonable insulation system			
Insulation	[a]81.3	1.0	81.3
Jettisonable fairings[b]	30	.058	1.7
Maximum fuel boiloff at 0 to 173 sec[c]	37.0	.23	8.5
Maximum fuel boiloff at 173 to 250 sec[d]	16.0	.42	6.7
Maximum fuel boiloff at 250 to 675 sec[e]	15.3	.66	10.1
Total payload loss, lb	----	-----	108.3
Typical jettisonable insulation system			
Insulation	1200	0.058	69.6
Nonjettisonable weight[f]	9.0	1.0	9.0
Maximum fuel boiloff at 0 to 173 sec[c]	11.3	.23	2.6
Maximum fuel boiloff at 173 to 250 sec[d]	7.7	.42	3.2
Maximum fuel boiloff at 250 to 675 sec[e]	14.1	.66	9.3
Total payload loss, lb	----	----	93.7

[a]Includes 2.6-lb allowance for foam fairing to cover wiring harness required on Centaur vehicle.

[b]Fairing to provide aerodynamic shield over fuel boost pump required during atmospheric portion of boost trajectory. It can then be jettisoned.

[c]Jettisonable insulation jettisoned at 173 sec.

[d]First-stage sustainer engine cut off at 250 sec.

[e]Centaur engines burning.

[f]Part of helium-purge system and equipment for jettisoning insulation system cannot be jettisoned.

CONCLUDING REMARKS

A lightweight insulation system was developed for liquid-hydrogen propellant tanks that utilized (1) a hermetic seal to ensure that its thermal effectiveness was not degraded by cryopumped gases, (2) a lightweight fiber-glass cover for protection from aerodynamic forces, and (3) an external constrictive wrap to hold the insulation in place during ground hold and launch. This nonjettisonable system, which weighs only 0.16 pound per square foot, is competitive with a heavy jettisonable system on the basis of payload penalty, can have a thermal effectiveness as good as that of evacuated foam, and can withstand the environmental conditions expected during ground hold and launch.

Lewis Research Center,
National Aeronautics and Space Administration,
Cleveland, Ohio, November 25, 1964.

"The aeronautical and space activities of the United States shall be conducted so as to contribute . . . to the expansion of human knowledge of phenomena in the atmosphere and space. The Administration shall provide for the widest practicable and appropriate dissemination of information concerning its activities and the results thereof."

—NATIONAL AERONAUTICS AND SPACE ACT OF 1958

NASA SCIENTIFIC AND TECHNICAL PUBLICATIONS

TECHNICAL REPORTS: Scientific and technical information considered important, complete, and a lasting contribution to existing knowledge.

TECHNICAL NOTES: Information less broad in scope but nevertheless of importance as a contribution to existing knowledge.

TECHNICAL MEMORANDUMS: Information receiving limited distribution because of preliminary data, security classification, or other reasons.

CONTRACTOR REPORTS: Technical information generated in connection with a NASA contract or grant and released under NASA auspices.

TECHNICAL TRANSLATIONS: Information published in a foreign language considered to merit NASA distribution in English.

TECHNICAL REPRINTS: Information derived from NASA activities and initially published in the form of journal articles.

SPECIAL PUBLICATIONS: Information derived from or of value to NASA activities but not necessarily reporting the results of individual NASA-programmed scientific efforts. Publications include conference proceedings, monographs, data compilations, handbooks, sourcebooks, and special bibliographies.

Details on the availability of these publications may be obtained from:

SCIENTIFIC AND TECHNICAL INFORMATION DIVISION

NATIONAL AERONAUTICS AND SPACE ADMINISTRATION

Washington, D.C. 20546